ISSN 0021-9673

VOL. 502 NO. 2 MARCH 2, 1990

THIS ISSUE COMPLETES VOL. 502

JOURNAL OF CHROMATOGRAPHY

INTERNATIONAL JOURNAL ON CHROMATOGRAPHY, ELECTROPHORESIS AND RELATED METHODS

ELSEVIER

JOURNAL OF CHROMATOGRAPHY

Scope. The *Journal of Chromatography* publishes papers on all aspects of chromatography, electrophoresis and related methods. Contributions consist mainly of research papers dealing with chromatographic theory, instrumental development and their applications. The section *Biomedical Applications*, which is under separate editorship, deals with the following aspects: developments in and applications of chromatographic and electrophoretic techniques related to clinical diagnosis or alterations during medical treatment; screening and profiling of body fluids or tissues with special reference to metabolic disorders; results from basic medical research with direct consequences in clinical practice; drug level monitoring and pharmacokinetic studies; clinical toxicology; analytical studies in occupational medicine.

Submission of Papers. Papers in English, French and German may be submitted, in three copies. Manuscripts should be submitted to: The Editor of *Journal of Chromatography*, P.O. Box 681, 1000 AR Amsterdam, The Netherlands, or to: The Editor of *Journal of Chromatography, Biomedical Applications*, P.O. Box 681, 1000 AR Amsterdam, The Netherlands. Review articles are invited or proposed by letter to the Editors. An outline of the proposed review should first be forwarded to the Editors for preliminary discussion prior to preparation. Submission of an article is understood to imply that the article is original and unpublished and is not being considered for publication elsewhere. For copyright regulations, see below.

Subscription Orders. Subscription orders should be sent to: Elsevier Science Publishers B.V., P.O. Box 211, 1000 AE Amsterdam, The Netherlands, Tel. 5803 911, Telex 18582 ESPA NL. The *Journal of Chromatography* and the *Biomedical Applications* section can be subscribed to separately.

Publication. The *Journal of Chromatography* (incl. *Biomedical Applications*) has 37 volumes in 1990. The subscription prices for 1990 are:

J. Chromatogr. (incl. *Cum. Indexes, Vols. 451–500*) + *Biomed. Appl.* (Vols. 498–534):
Dfl. 6734.00 plus Dfl. 1036.00 (p.p.h.) (total *ca.* US$ 3564.25)

J. Chromatogr. (incl. *Cum. Indexes, Vols. 451–500*) only (Vols. 498–524):
Dfl. 5616.00 plus Dfl. 756.00 (p.p.h.) (total *ca.* US$ 2923.00)

Biomed. Appl. only (Vols. 525–534):
Dfl. 2080.00 plus Dfl. 280.00 (p.p.h.) (total *ca.* US$ 1082.50).

Our p.p.h. (postage, package and handling) charge includes surface delivery of all issues, except to subscribers in Argentina, Australia, Brasil, Canada, China, Hong Kong, India, Israel, Malaysia, Mexico, New Zealand, Pakistan, Singapore, South Africa, South Korea, Taiwan, Thailand and the U.S.A. who receive all issues by air delivery (S.A.L. — Surface Air Lifted) at no extra cost. For Japan, air delivery requires 50% additional charge; for all other countries airmail and S.A.L. charges are available upon request. Back volumes of the *Journal of Chromatography* (Vols. 1–497) are available at Dfl. 195.00 (plus postage). Claims for missing issues will be honoured, free of charge, within three months after publication of the issue. Customers in the U.S.A. and Canada wishing information on this and other Elsevier journals, please contact Journal Information Center, Elsevier Science Publishing Co. Inc., 655 Avenue of the Americas, New York, NY 10010. Tel. (212) 633-3750.

Abstracts/Contents Lists published in Analytical Abstracts, ASCA, Biochemical Abstracts, Biological Abstracts, Chemical Abstracts, Chemical Titles, Chromatography Abstracts, Clinical Chemistry Lookout, Current Contents/Physical, Chemical & Earth Sciences, Current Contents/Life Sciences, Deep-Sea Research/Part B: Oceanographic Literature Review, Excerpta Medica, Index Medicus, Mass Spectrometry Bulletin, PASCAL-CNRS, Pharmaceutical Abstracts, Referativnyi Zhurnal, Science Citation Index and Trends in Biotechnology.

See inside back cover for Publication Schedule, Information for Authors and information on Advertisements.

0021-9673/90/$03.50

Printed in The Netherlands

CONTENTS

(Abstracts/Contents Lists published in Analytical Abstracts, ASCA, Biochemical Abstracts, Biological Abstracts, Chemical Abstracts, Chemical Titles, Chromatography Abstracts, Current Contents/Physical, Chemical & Earth Sciences, Current Contents/Life Sciences, Deep-Sea Research/Part B: Oceanographic Literature Review, Excerpta Medica, Index Medicus, Mass Spectrometry Bulletin, PASCAL-CNRS, Referativnyi Zhurnal and Science Citation Index)

(Continued overleaf)

In articles with more than one author, the name of the author to whom correspondence should be addressed is indicated in the article heading by a 6-pointed asterisk (*)

Determination of Beta-Blockers in Biological Material

edited by **V. Marko**, *Institute of Experimental Pharmacology, Centre of Physiological Sciences, Slovak Academy of Sciences, Bratislava, Czechoslovakia*

(Techniques and Instrumentation in Analytical Chemistry, 4C)

This is the third volume of a sub-series entitled *Evaluation of Analytical Methods in Biological Systems*. (The first two were *Analysis of Biogenic Amines* edited by G.B. Baker and R.T. Coutts and *Hazardous Metals in Human Toxicology* edited by A. Vercruysse). This new volume addresses beta-blockers - an area of research for which a Nobel Prize in Medicine was awarded in 1988. It provides an up-to-date and comprehensive coverage of the theory and practice of the determination of beta-blockers in biological material. Two main fields of research are dealt with in this book: analytical chemistry and pharmacology, and, as it deals with drugs used in clinical practice, it is also related to a third area: therapy. Thus, it offers relevant information to workers in all three fields.

Some 50 beta-blockers and nine methods of analysis are discussed. The methods are divided into three groups: optical, chromatographic, and saturation methods. In addition to the analytical methods themselves, sample handling problems are also covered in detail, as is the information content of the analytical results obtained. Special chapters are directed to those working in pharmacology and pharmacokinetics. Finally, as recent evidence points to the increased importance of distinguishing optical isomers of drugs, a chapter on the determination of optical isomers of beta-blockers in biological material is also included. An extensive subject index and two supplements giving retention indices and structures of beta-blockers complete the book.

This is the first book to treat beta-blockers from the point of view of their determination and to discuss in detail the use of analytical methods for beta-blockers. It will thus appeal to a wide-ranging readership.

1989 xiv + 334 pages
US$ 152.75 / Dfl. 290.00
ISBN 0-444-87305-8

ELSEVIER SCIENCE PUBLISHERS

P.O. Box 211, 1000 AE Amsterdam, The Netherlands
P.O. Box 882, Madison Square Station, New York, NY 10159, USA

One capillary electrophoresis system may not be right for everyone.

So picture a choice of three.

1. An automated system for QA and other high-throughput jobs.
   - Large capacity: 40 samples and 4 different buffers
   - Includes data management and method programming
2. A compact, integrated research unit with multimode injection
   - 30-kV dual-polarity power
   - Reproducible analyses with as little as 2 µl of sample
3. A versatile on-column UV detector
   - Ideal for low-cost modular systems and special applications

All three give you femtomole sensitivity with samples you can't easily separate any other way. And affordability that may surprise you.

Ask today for details.

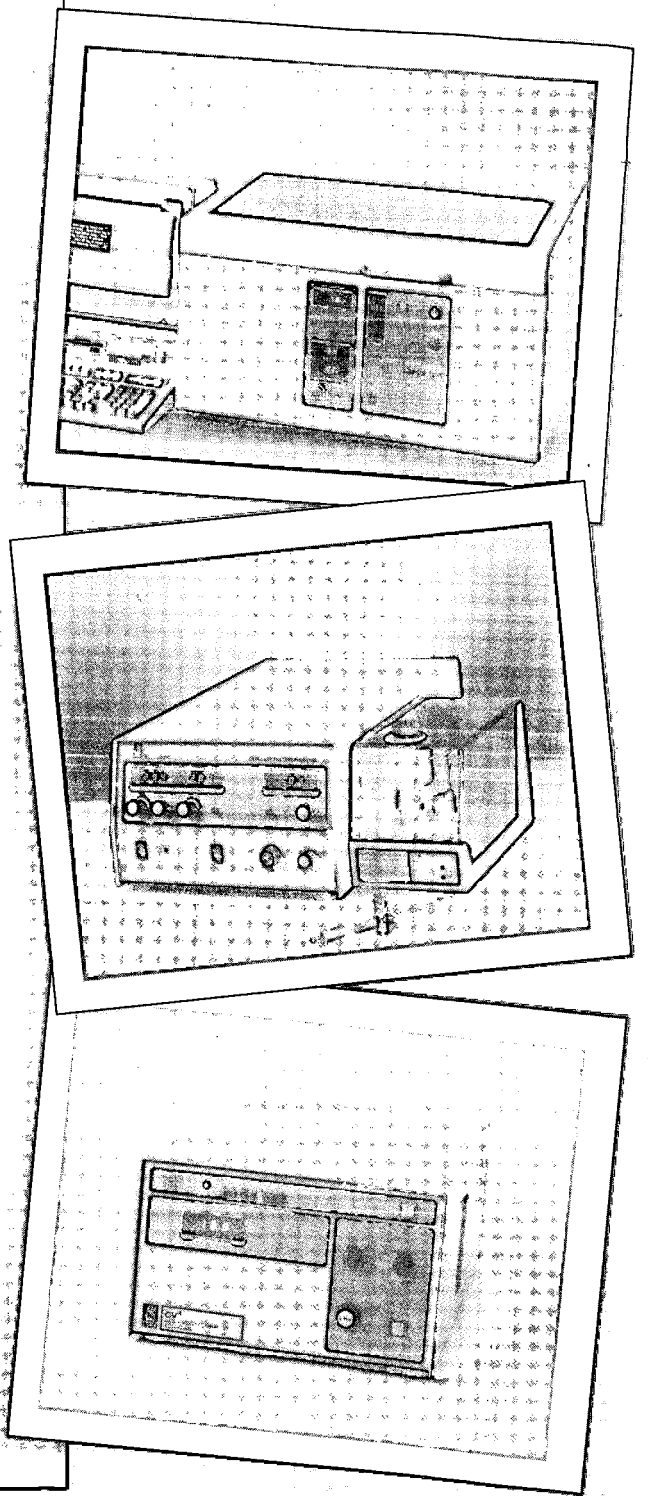

ISCO

Isco, Inc., P.O. Box 5347,
Lincoln NE 68505 U.S.A.
Tel. **(800)228-4250**

Isco Europe AG, Brüschstr. 17
CH8708 Männedorf, Switzerland
Fax **(41-1)920 62 08**

Distributors • **Australia:** Australian Chromatography Co. • **Austria:** INULA • **Belgium:** SA HVL NV • **Canada:** Canberra Packard Canada, Ltd. • **Denmark:** Mikrolab Aarhus • **Finland:** ETEK OY • **France:** Ets. Roucaire, S.A. • **Germany:** Colora Messtechnik GmbH • **Hungary:** Lasis Handelsges. mbH • **Italy:** Analytical Control Italia S.p.A. • **Japan:** JSI Co. Ltd. • **Korea:** Sang Chung, Ltd. • **The Netherlands:** Beun-de Ronde B.V. • **Norway:** Dipl. Ing. Houm A.S. • **Spain:** CHEMICONTROL, S.L. • **Sweden:** SAVEN AB • **Switzerland:** IG Instrumenten-Gesellschaft AG • **U.K.:** Life Science Laboratories, Ltd. •

Journal of Chromatography, 502 (1990) 247–255
Elsevier Science Publishers B.V., Amsterdam — Printed in The Netherlands

CHROM. 22 120

Detection and quantification of capillary electrophoresis zones by fluorescence microscopy[a]

LUIS HERNANDEZ*, RAFAEL MARQUINA and JOSE ESCALONA
Laboratory of Behavioral Physiology, School of Medicine, Los Andes University, Merida 5101-A (Venezuela)
and
NORBERTO A. GUZMAN[b]
Princeton Biochemicals Inc., Princeton, NJ 08543 (U.S.A.)
(First received april 10th, 1989; revised manuscript received September 19th, 1989)

SUMMARY

A fluorescence detector for capillary electrophoresis was built using an epillumination fluorescence microscope equipped with a 50-W mercury lamp and a photodiode. The performance of the detector was tested with riboflavin and fluorescamine-derivatized amino acids and amphetamine. We compared fluorite and conventional glass objectives and found that, by using a 25-μm I.D. capillary and a fluorite objective, an improvement in fluorescence detection by a factor of 56 can be achieved. A detection level of 500 amol for riboflavin was reached (using on-column detection). This sensitivity was at least comparable to that reported for other capillary electrophoresis systems using on-column non-coherent light fluorescence detectors. The potential and advantages of using a fluorescence microscope for capillary electrophoresis applications are discussed.

INTRODUCTION

Capillary electrophoresis (CE) is a powerful separation technique that resolves analytes into zones of a few nanoliters[1–5]. These features require the ability to detect subpicomole masses, usually dissolved in nanoliter volumes. Several types of detection mode have been used with CE, but fluorescence detection has emerged as one of the most sensitive[1–5]. Laboratory-made on-column fluorescence detectors, equipped with non-coherent light sources, have been specially designed for CE[6–8]. In these detectors, either a mercury or a mercury–xenon arc lamp provides the source of excitation.

[a] Presented at the *1st International Symposium on High-Performance Capillary Electrophoresis, Boston, MA, April 10–12, 1989*. The majority of the papers presented at this symposium have been published in *J. Chromatogr.*, Vol. 480 (1989).

[b] Present address: Roche Diagnostic Systems, Inc., a subsidiary of Hoffmann-La Roche Inc., 340 Kinsland Street, Nutley, NJ 07110-1199, U.S.A.

0021-9673/90/$03.50

Lenses located at a distance of 1 cm from the capillary are used to focus the excitation radiation on the capillary and to focus the emitted light on the photodetector. Similar designs have been incorporated into commercially available fluorescence detectors for CE[9]. In all these instruments, the fluorescence is collected at right-angles to the main axis of the capillary and the excitation beam. The detection limit for fluorescamine derivatized compounds is about 10 pg of fluorophore for these kinds of detectors[7].

On the other hand, fluorescence microscopes have been optimized to detect fluorescence in small samples. This is due to their large numerical aperture (NA) objectives and high-quality optical components. For this reason, the fluorescence microscope might be a good CE fluorescence detector. Particularly interesting in this regard is the epillumination fluorescence microscope. In this type of instrument, the excitation and the detection of fluorescence occur at the same side of the capillary (colinear arrangement), and the focusing and alignment of the capillary can be guided visually to obtain the optimum response. This paper describes a procedure for adapting a fluorescence microscope to CE, and presents the results of several tests that were conducted to elucidate the optimum optical conditions needed to detect fluorescence in a small capillary.

EXPERIMENTAL

Instrumentation

The microscope was a Zeiss Standard 14 IFD epillumination fluorescence microscope (Carl Zeiss, Thornwood, NY, U.S.A.). The excitation lamp was a 50-W, high-pressure mercury lamp. The following combination of filters was adapted to the microscope: a band-pass excitation filter to cut radiation above 405 nm; a chromatic beam splitter to reflect radiation below 420 nm and to refract radiation above 420 nm; and a long-pass filter (located between the eyepiece and the dichroic mirror) to suppress radiation under 418 nm. A direct current high-voltage power supply was used (Spellman High Voltage Electronics, Plainview, NY, U.S.A.). High-voltage was applied through platinum–iridium electrodes for both electrokinetic injections and sample separations. For recording the signals, a Model L-6512 strip-chart recorder was used (Linseis, Princeton Junction, NJ, U.S.A.) at 20 cm/h and 1 mV output.

Reagents

Sodium tetraborate was obtained from EM Science (Gibbtown, NJ, U.S.A.). Riboflavin, leucine, isoleucine, threonine, valine, serine and amphetamine were purchased from Sigma (St. Louis, MO, U.S.A.). Fluorescamine was obtained from Roche Diagnostic Systems (Nutley, NJ, U.S.A.). Hydrochloric acid and acetone were of HPLC grade from J. T. Baker (Phillipsburg, NJ, U.S.A.). All buffer and sample solutions were prepared with deionized water with 18 MΩ resistance from a Milli-Q system (Millipore, Bedford, MA, U.S.A.).

Procedure

The principles of adaptation of fluorescence microscopy to CE are shown in Figs. 1 and 2. Fig. 1 shows the excitation of the sample and Fig. 2 shows the emission and measurement of fluorescence.

Excitation (Fig. 1). The excitation lamp emits a mixed beam of visible and

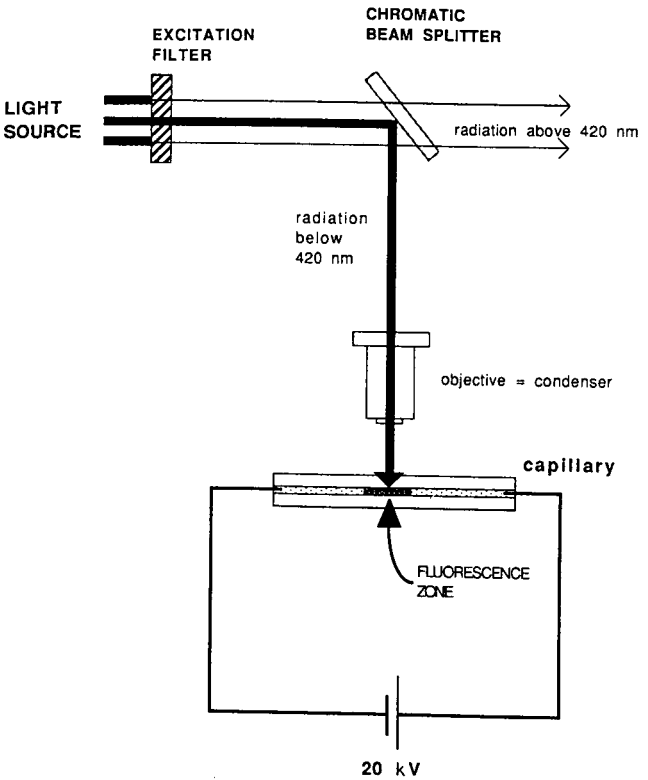

Fig. 1. Excitation of the sample with an epillumination fluorescence microscope. The UV beam is shown as the thick black line reflected at right-angles by the chromatic beam splitter. The fluorescence zone is indicated by the dark dotted area in the center of the capillary.

ultraviolet (UV) light. The excitation filter suppresses a substantial amount of radiation above 405 nm. The beam then reaches a chromatic beam splitter which reflects radiation below 420 nm. Therefore, only the UV is reflected toward the objective of the microscope. Three different fluorite objectives (Neofluar, Carl Zeiss) were used to determine the optimum magnification and numerical aperture: (1) 0.16 NA, 6.3×; (2) 0.32 NA, 16×; and (3) 0.75 NA, 40×. They were compared by electrokinetically injecting the same amount of riboflavin and measuring the relative fluorescence emitted. The same procedure was repeated for ordinary glass objectives using the same combination of magnification and numerical aperture. The generated data were fitted to polynomial equations of the second order. The statistical significance of the fittings was tested by *t*-tests on the correlation coefficients.

Emission and measurement of fluorescence (Fig. 2). The emitted light crosses the objective, the chromatic beam splitter and the long-pass filter that suppresses radiation under 418 nm. The beam is finally focused on a photodiode that transforms the light into an electrical signal which is recorded on a strip-chart recorder. In order to set the capillary on the microscope correctly, a carrier was made of Plexiglas, stainless-steel tubing and Teflon tubing (see Fig. 3). The carrier with the capillary was placed on the

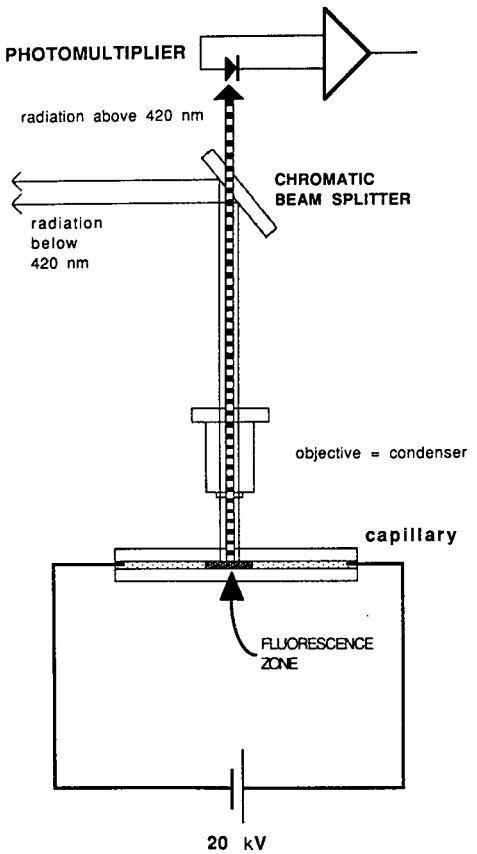

Fig. 2. Emission and measurement of fluorescence. The emitted light is indicated by the thick dashed line that crosses the chromatic beam splitter and is detected by the photodiode.

platina of the microscope and centered. The objective combined with a 10 × ocular was focused to obtain a sharp image of the capillary. The capillary used was fused silica (Scientific Glass Engineering, Austin, TX, U.S.A.), 25 μm I.D., 100 cm long, and primed with 0.05 *M* sodium tetraborate buffer (pH 6.0). The length of the capillary between the injection end and the objective of the microscope was 40 cm. The internal volume of this segment was 196 nl. Each end of the capillary was immersed in a 400-μl conical microcentrifuge vial containing the same buffer solution.

The electroosmotic flow was measured by electrokinetically injecting a $0.5 \cdot 10^{-3}$ *M* solution of riboflavin in borate buffer solution (pH 6.0) ten times. The injection parameters were 10 kV over a 7.5-s period. The ten different injections were run at 4, 6, 8, 10, 12, 14, 16, 18, 20 and 22 kV and the flow was calculated for each voltage. For this purpose, 196 nl were divided by the migration time (expressed in minutes) of the riboflavin peak. The data were fitted to a straight line. The statistical significance of the fitting was tested by a *t*-test on the correlation coefficient.

The detection limit for riboflavin was measured by injecting solutions of

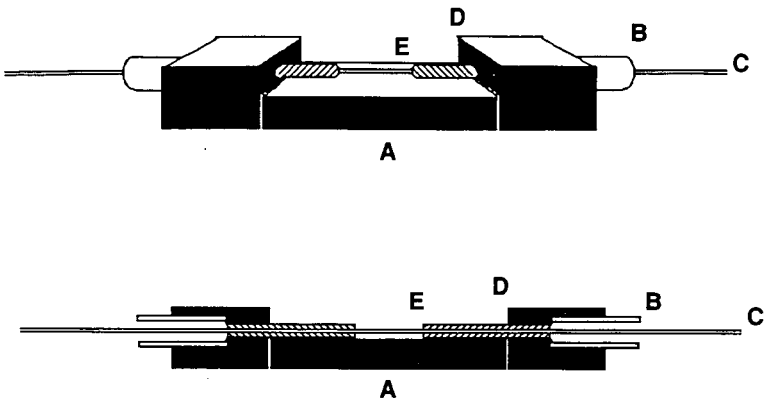

Fig. 3. Top, capillary carrier; bottom, cross section. A 50 × 25 × 5 mm parallelepiped (A) is the basis of the carrier. Two other 20 × 14 × 9 mm parallelepipeds (D) make the support for the capillary holders (E). Each of these holders is made of a 30 mm × 0.45 mm O.D. × 0.25 mm I.D. stainless-steel tube inside a 30 mm × 0.57 mm O.D. × 0.50 mm I.D. stainless-steel tube soldered together. Two holes are drilled at the main axis of D. One is of 9.5 mm bore and receives a 30 mm long piece of Teflon tubing (B). The other is of 0.60 mm bore for the capillary holder. Pieces D and A are glued with epoxy. All the Plexiglas pieces are coated with black paint to enhance the contrast between the fluorescence and the background. A section of 10 mm of the cover of the capillary (C) is burned to clear the glass surface of the capillary. Then the capillary is inserted until the uncovered section is located between the two capillary holders. The whole piece is mounted on the platina of the microscope and the uncovered section of the capillary is centered and focused.

decreasing concentration. The injection parameters were again 10 kV over a 7.5-s period. The detection limit was defined as the concentration that yields a 3:1 signal-to-noise ratio. The samples used were fluorescamine-derivatized amino acids and the drug amphetamine. To accomplish derivatization, 1 mg of fluorescamine was totally dissolved in 1 ml of acetone. This solution was then mixed with 1 ml of the sample which consisted of several amino acids or amphetamine dissolved in borate buffer (pH 8.3). The capillary column was primed with this borate buffer. The samples were electrokinetically loaded into the capillary by applying 10 kV for a period of 15 s. The samples were then separated by applying 20 kV for 40 min.

RESULTS

As shown in Fig. 4, a linear regression analysis for the ten riboflavin injections was obtained. The equation that best fitted the data was $y = 0.831x - 0.067$, and the correlation coefficient squared was 0.984. This fit was statistically significant ($t = 22.76, p < 0.001$). Based on this equation, injection volumes of 2.07 nl and 1.014 nl at 10 kV during 15 s and 7.5 s, respectively, were calculated.

Fig. 5 shows the impact of magnification and numerical aperture on the relative fluorescence of the same amount of riboflavin injected into the capillary. For the fluorite objectives, both variables (magnification and numerical aperture) were quadratically related to the relative fluorescence. These relationships were statistically significant [magnification (x) *vs.* relative fluorescence (y), $t = 31.8, p < 0.001$, best fit equation $y = 3.2 - 0.3x + 0.3x^2$; and numerical aperture (x) *vs.* relative fluorescence

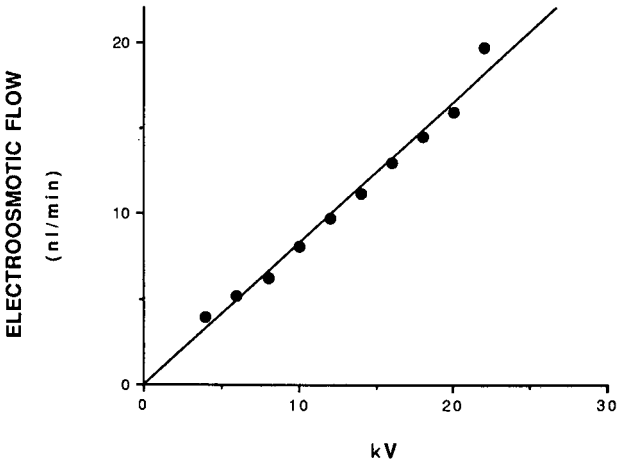

Fig. 4. Relationship between the applied voltage and the electroosmotic flow as measured by electrokinetically injecting riboflavin at 10 kV in 7.5 s and running at ten different voltages. $y = -0.064 + 0.831x$; $R^2 = 0.984$.

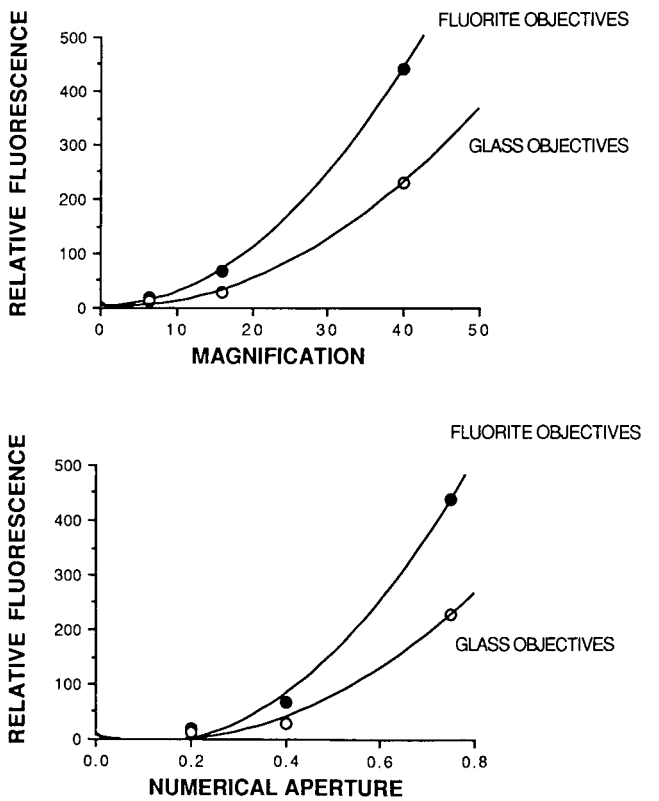

Fig. 5. Relationship between magnification and relative fluorescence (top) and numerical aperture and relative fluorescence (bottom) for fluorite objectives (●) and conventional glass objectives (○). The best fitting equations were quadratics. The fluorite objectives yielded more fluorescence particularly at the highest magnification and numerical aperture. Equations: top, ●: $y = 3.2 - 0.3x + 0.3x^2$; ○: $y = 3.4 - 0.7x + 0.16x^2$; bottom, ●: $y = 6.9 - 254.4x + 1104.1x^2$; ○: $y = 5.0 - 153.6x + 601.1x^2$.

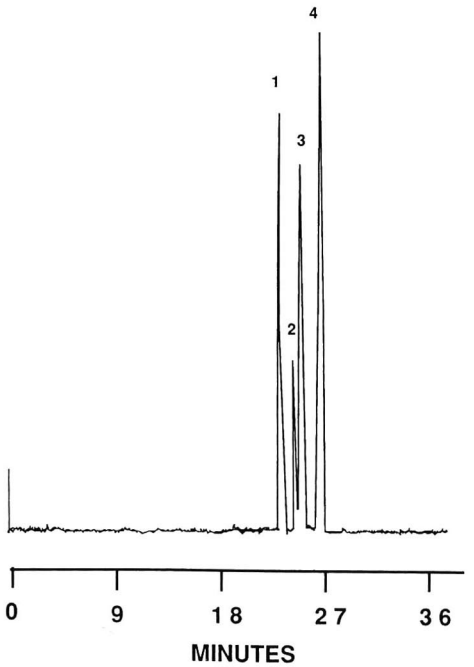

Fig. 6. Electropherogram of a 1 m*M* solution of fluorescamine-derivatized leucine and isoleucine (1), valine (2), threonine (3) and serine (4).

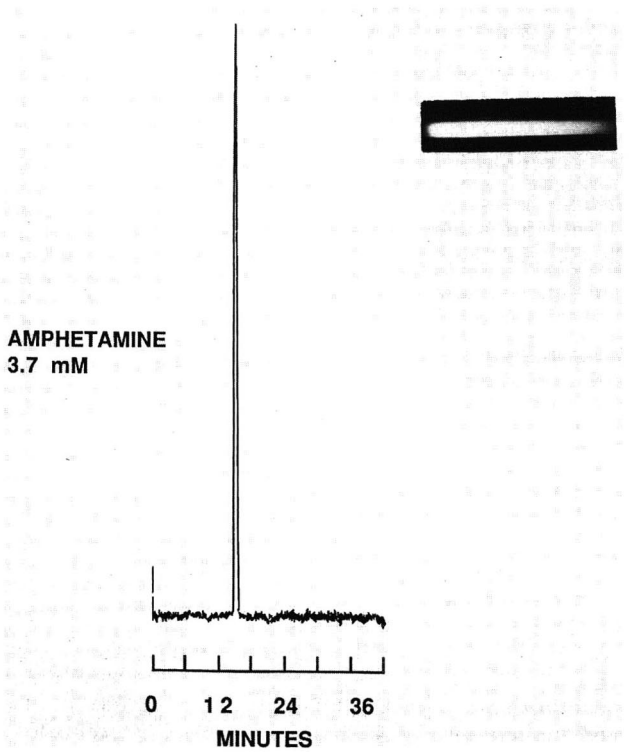

Fig. 7. Electropherogram of a 3.7 m*M* solution of fluorescamine-derivatized amphetamine. The inset shows the actual band of amphetamine detected by the microscope.

(y), $t = 22.68$, $p < 0.02$, best fit equation $y = 6.9 - 254.4 + 1104.1x^2$]. The glass objectives also showed a quadratic relationship between magnification, numerical aperture and relative fluorescence. However, the parameters for the best fit equations were different (see equations in Fig. 5). The correlation coefficients squared for the fluorite objective were double those for the glass objectives. The detection limit for riboflavin was $0.5 \cdot 10^{-6}$ *M*.

Fig. 6 shows the electropherogram of a mixture of five derivatized amino acids. Two of them, leucine and isoleucine, coeluted at the same migration time. Fig. 7 shows the electropherogram of derivatized *d*-amphetamine and the actual fluorescent zone running under the objective of the microscope.

DISCUSSION

The results show that a conventional fluorescence microscope can easily be converted into a fluorescence detector for capillary zone electrophoresis. As the pH of the buffer in the riboflavin experiment was 6.0, the riboflavin molecules were at their isoelectric point and therefore neutral[10]. In the electroosmotic flow measurement experiment, the straight line that best fitted the ten riboflavin injections did not intersect the coordinate system at the origin, but at -0.06, which represents a reasonable deviation. Among the fluorite objectives tested, the 0.75 NA and 40× objective gave the best results. In the tested range, the fluorescence increased quadratically with the numerical aperture and the magnification. This result shows that fluorescence on-column detection (using fused-silica capillaries) can be improved by a factor of 56 just by using a 40×, 0.75 NA fluorite objective instead of the conventional 6×, 0.16 NA glass objective. The minimum riboflavin concentration detected on-column was $0.5 \cdot 10^{-6}$ *M*. Considering that bias during electrokinetic injection was minimized by the pH of the buffer, and that a volume of 1 nl was injected, this indicates that 0.5 fmol of riboflavin (injected) was detected. For other CE detectors, lower detectable concentrations have been reported[7]. This point deserves further consideration.

In other experiments, 65 and 75 μm I.D. capillaries were used. Therefore, the injected amount was larger. In addition, a 100-W lamp, photomultiplier tubes and electronic circuits for noise supression were used. These devices improve the sensitivity of the detection system by 2–3 orders of magnitude in comparison with a 50-W lamp, photodiodes and no noise supression. In this work the concentration detected was not as low as those with other detectors[7,8]. Nevertheless, the total amount of analyte injected was smaller than that reported for other detectors. This suggests that the combination of fluorescence microscopy, a high-power UV lamp, a photomultiplier tube, and noise supression should improve the detection limit for the detector reported here by 2–3 orders of magnitude. As the microscope magnifies the capillary, only a 100-μm section (equivalent to 0.05 nl) is available for measurement. This indicates that the minimum amount detected is 0.025 fmol and represents an improvement over fluorimetric on-column detection, using non-coherent excitation, for capillary electrophoresis.

The microscope offers several additional features that make it particularly useful for CE. The epillumination method focuses the UV beam on the capillary, providing a very concentrated excitation of the sample. The colinear arrangement prevents loss

of fluorescence by self-absorption, especially at high analyte concentrations[11]. The objective and the ocular of the microscope concentrate the emitted light on the photodetector, thereby improving the efficiency of the measuring device. The objective is kept at 0.33 mm from the capillary, compared with 1 cm or more for other detectors. This feature allows the recovery of more light by reducing the wastage due to light scattering. The platina of the microscope is displaced by precision micrometer screws. Therefore, alignment of the capillaty and the UV beam is very simple. This is an advantage when changing one capillary for another of different outside diameter.

Dramatic improvements in sensitivity for CE fluorescence detection have been obtained by laser-induced fluorescence[12–15]. We have conducted preliminary tests with the fluorescence miroscope, an air-cooled argon-ion laser, a water-cooled gallium arsenide photomultiplier tube and a photon counter for statistical signal processing. Low milliattomole amounts of fluorescein-derivatized amino acids have been detected using on-column fluorescence detection[16]. We conclude that a fluorescence microscope can be used as an optical fluorescence device for CE.

REFERENCES

1 J. W. Jorgenson and K. D. Lukacs, *Science (Washington, D.C.)*, 222 (1983) 266.
2 M. J. Gordon, X. Huang, S. L. Pentoney, Jr. and R. N. Zare, *Science (Washington, D.C.)*, 242 (1988) 224.
3 A. G. Ewing, R. A. Wallingford and T. M. Olefirowicz, *Anal. Chem.*, 61 (1989) 292A.
4 N. A. Guzman, L. Hernandez and B. G. Hoebel, *Biopharm. Manuf.*, 2 (1989) 22.
5 N. A. Guzman, L. Hernandez and S. Terabe, in J. Nickelly and C. Horvath (Editors), *Separations in Analytical Biotechnology*, ACS Symposium Series, American Chemical Society, Washington, DC, 1990, in press.
6 J. W. Jorgenson and K. D. Lukacs, *Anal. Chem.*, 53 (1981) 1298.
7 E. J. Guthrie and J. W. Jorgenson, *Anal. Chem.*, 56 (1984) 483.
8 J. S. Green and J. W. Jorgenson, *J. Chromatogr.*, 352 (1986) 337.
9 R. G. Brownlee and S. W. Compton, *Am. Biotechnol. Lab.*, 6 (1988) 10.
10 W. H. Sebrell and R. S. Harris (Editors), *The Vitamins*, Vol. 5, Academic Press, New York, 1972, Ch. II, p. 9.
11 E. J. Bowen and F. Wokes in *Fluorescence of Solutions*, Longmans, Green, London, 1953, p. 20.
12 E. Gassmann, J. E. Kuo and R. N. Zare, *Science (Washington, D.C.)*, 230 (1985) 813.
13 M. C. Roach, P. Gozel and R. N. Zare, *J. Chromatogr.*, 426 (1988) 129.
14 E. Yeung, *Liq. Chromatogr. Gas Chromatogr.*, 7 (1989) 118.
15 Y.-F. Cheng and N. J. Dovichi, *Science (Washington, D.C.)*, 242 (1988) 562.
16 L. Hernandez, N. Joshi, J. Escalona and N. A. Guzman, to be presented at the *2nd International Symposium on High-Performance Capillary Electrophoresis, San Francisco, CA, January 29–31, 1990.*

Journal of Chromatography, 502 (1990) 257–264
Elsevier Science Publishers B.V., Amsterdam — Printed in The Netherlands

CHROM. 22 095

Simultaneous gas chromatographic determination of cyanide, iodide, nitrite, sulphide and thiocyanate anions by derivatization with pentafluorobenzyl bromide and using a kryptand as phase-transfer catalyst

SU-HWEI CHEN and HSIN-LUNG WU*
School of Pharmacy, Kaoshiung Medical College, Kaohsiung 80708 (Taiwan)
MINORU TANAKA and TOSHIYUKI SHONO
Department of Applied Chemistry, Faculty of Engineering, Osaka University, Yamada-oka, Suita, Osaka 565 (Japan)
and
KOICHI FUNAZO
Department of Chemistry, Osaka Prefectural Technical College, Saiwai-cho 26-12, Neyagawa, Osaka 572 (Japan)
(First received June 14th, 1989; revised manuscript received October 17th, 1989)

SUMMARY

An improved gas chromatographic method has been established for the simultaneous determination of cyanide, iodide, nitrite, sulphide and thiocyanate anions as their volatile pentafluorobenzyl derivatives. The method is based on kryptate formation using Kryptofix 222 B polymer as complexing agent and phase-transfer catalyst to transfer the anions from aqueous alkaline solution to the dichloromethane organic phase for derivatization with pentafluorobenzyl bromide to be effected. Structural identification and correction of the cyanide derivative was studied. The parameters affecting the partition and/or derivatization of the anions were investigated, including the concentrations of acid and base in the aqueous phase. Individual and simultaneous determinations of the anions are attainable at sub-micromole levels with flame ionization detection.

INTRODUCTION

In a previous paper[1], a gas chromatographic (GC) method was described for the determination of anions by derivatization with pentafluorobenzyl bromide (PFBBr) and using *n*-hexadecyltrimethylammonium bromide as phase-transfer catalyst (PTC). The disadvantages of using quaternary ammonium PTC without additional treatment include the formation of emulsions from derivatization based on biphasic reactions and the unavoidable introduction of various amounts of PTC onto the separation column. This could result in baseline drift and, worse, contamination of the highly sensitive detector.

0021-9673/90/$03.50

To solve these problems, we applied a polymeric and bonded kryptand instead of quaternary ammonium compounds as PTC for the simultaneous determination of anions including cyanide, iodide, nitrite, sulphide and thiocyanate at sub-micromole levels. This led to emulsion-free reactions, easy layer separation and injection of the sample without PTC as to it is in the form of a bonded solid particle. The problems of baseline drift, detector contamination and emultion formation were overcome. Several parameters that affecting the partition and derivatization of the anions were studied and are discussed in this paper.

EXPERIMENTAL

GC conditions

A Shimadzu (Kyoto, Japan) GC-8A gas chromatograph equipped with dual flame ionization detectors was used. The separation columns and the temperatures for individual and simultaneous determinations of inorganic anions are indicated in Table I. Nitrogen was used as the carrier gas at a flow-rate of 40 ml/min. A Shimadzu R-111 recorder and Shimadzu Chromatopac C-E1B integrator were used.

Materials

Kryptofix 222 B polymer (250–300 μm) (E. Merck, Darmstadt, F.R.G.) α-bromo-2,3,4,5,6-pentafluorotoluene (PFBBr) (Aldrich, Milwaukee, WI, U.S.A.), bibenzyl and *p*-dibromobenzene (Wako, Osaka, Japan), *p*-bromoiodobenzene and 2,3,5,6-tetrachloronitrobenzene (Tokyo Kasei, Tokyo, Japan), 10% OV-17 on Uniport HP (60–80 mesh) (Gasukuro, Tokyo, Japan), 4% OV-101 + 6% OV-210 on Chromosorb W HP (60–80 mesh) (Shimadzu) and 5% silicone DC QF-1 Chromosorb W AW DMCS (60–80 mesh) (Wako) were used without further treatment. Potassium hydroxide, potassium nitrate, potassium nitrite and potassium thiocyanate (E. Merck), potassium cyanide, potassium iodide and sodium sulphide (Wako), dichloro-

TABLE I

GC CONDITIONS

Detector and injector temperatures, 280°C.

Anion	*Stationary phase*	*Column temperature (°C)*
CN^-	4% OV-101 + 6% OV-210[a]	170
NO_2^-	4% OV-101 + 6% OV-210	160
SCN^-	4% OV-101 + 6% OV-210	200
I^-	10% OV-17[b]	140
S^{2-}	10% OV-17	200
Simultaneous determination	5% silicone DC QF-1[c]	Programmed (see Fig. 2)

[a] Coated on Chromosorb W HP (60–80 mesh) and packed in a stainless-steel column (3.0 m × 3 mm I.D.).

[b] Coated on Uniport HP (60–80 mesh) and packed in a stainless-steel column (2.0 m × 3 mm I.D.).

[c] Coated on Chromosorb W AW DMCS (60–80 mesh) and packed in a stainless-steel column (5.0 m × 3 mm I.D.).

methane and other reagents were of analytical-reagent grade. Solutions of inorganic anions were prepared by dissolving appropriate compounds in distilled, deionized water.

Derivatization procedures

Procedure for individual determination. As shown in Table II, a 0.2-ml volume of a solution of various inorganic anions was added to a 10-ml glass-stoppered test-tube containing a suitable amount of Kryptofix 222 B polymer and 0.1 ml of $2 \cdot 10^{-3}$ *M* potassium hydroxide solution, then 0.4 ml of the internal standard (I.S.) in dichloromethane and 0.1 ml of PFBBr solution containing various amounts of neat PFBBr in dichloromethane was added. The reaction mixture was shaken mechanically at 30°C for a fixed time, then an aliquot of the dichloromethane layer was injected for GC analysis with flame ionization detection (FID).

Procedure for simultaneous determination. Also as indicated in Table II, 0.2 ml of a solution of five anions was added to a 10 ml glass-stoppered test-tube containing 15 mg of Kryptofix 222 B polymer and 0.1 ml of $2 \cdot 10^{-3}$ *M* potassium hydroxide solution, then, 0.3 ml of I.S. (2,3,5,6-tetrachloronitrobenzene) solution and 0.2 ml of PFBBr solution were added. The reaction mixture was shaken mechanically at 30°C for 2.0 h, then an aliquot of the dichloromethane layer was subjected to GC–FID.

RESULTS AND DISCUSSION

The analytical derivatization of biologically important inorganic anions with PFBBr in a heterogeneous reaction system using immobilized PTC was studied. The PTC used is a polymeric and bound kryptand, Kryptofix 222 B polymer; its basic functional unit is similar to 4,7,13,16,21,24-hexaoxy-1,10-diazabicyclo[8.8.8]hexacosane (Kryptofix 222), which is highly selective for complexing potassium ion from the aqueous phase and formation of related kryptates with various anions. Therefore, the anion in the kryptate could partition to the organic phase, where derivatization with a suitable reagent proceeds. Based on this mechanism, only a few methods have been reported for the individual derivatization of thiocyanate anion with benzyl chloride[2] or ethyl iodide[3]. We have investigated the conditions for the individual and simultaneous derivatization of several biologically active anions with PFBBr, using Kryptofix 222 B polymer as PTC.

Derivatization conditions

The anions and the amounts used for study of the optimum conditions for derivatization were as follows: cyanide (3.85 μmol), iodide (1.58 μmol), nitrite (4.35 μmol), sulphide (1.56 μmol) and thiocyanate (3.45 μmol). The parameters that affect the formation of the anion derivatives were evaluated by procedures similar to those described previously[1], except that the PTC used was Kryptofix 222 B polymer.

The effects of the addition of 0.1 ml of base or acid at various concentrations to the reaction system as indicated under *Derivatization procedures* are illustrated in Fig. 1. The results indicate that the simultaneous determination of the anions is most favourable when using 0.1 ml of aqueous base at a concentration of *ca.* $2 \cdot 10^{-3}$ *M*; for individual determinations, a wider concentration range of aqueous base or acid can be adopted.

TABLE II

DERIVATIZATION CONDITIONS

Anion	*Amount of anion (μmol)*	*Kryptofix 222 B polymer (mg)*	*Reaction time (h)*	*Neat PFBBr (μl)*	*Internal standard (mM)*
For individual determinations:					
CN^-	3.85	10	1.0	2	*p*-Bromoiodobenzene (4.2)
NO_2^-	4.35	12	1.5	4	*p*-Bromoiodobenzene (5.3)
SCN^-	3.45	8	0.5	2	Bibenzyl (13.7)
I^-	1.58	8	0.5	2	*p*-Dibromobenzene (3.4)
S^{2-}	1.56	8	0.5	4	2,3,5,6-Tetrachloronitrobenzene (9.6)
For simultaneous determinations[a]		15	2.0	8	2,3,5,6-Tetrachloronitrobenzene (9.6)

[a] The amounts of anions used for simultaneous study were as follows: CN^-, 3.85; NO_2^-, 4.35; SCN^-, 3.45; I^-, 1.58; and S^{2-}, 1.56 μmol, in 0.2 ml of $2 \cdot 10^{-3}$ *M* KOH solution.

As shown in Fig. 1, the partition of the anions (iodide, thiocyanate and nitrate) from the aqueous to the dichloromethane phase for derivatization is also favourable in neutral or dilute acidic media. This could be due to the available anions in the aqueous media forming various kryptates with the complexed PTC (the potassium ion here for complexation is from the sample solution of potassium salts of the anions); the ready availability of the above-mentioned anions in diluted acidic media, especially iodide and thiocyanate, could probably be explained in part by their physical and chemical properties, as it is reported[4] that HI and HSCN are freely soluble in water, revealing the good dissociation characteristics of these acids. However, with cyanide and sulphide, the HCN and H_2S formed from acidic media are volatile and difficult to dissociate, which unfavourably affects their transfer for derivatization. Discontinuation of the study of cyanide derivatized in acidic media was partly due to the high toxicity of the volatile HCN. In addition, the low derivatization yields of the anions at high concentrations of base or acid are generally assumed from the competition of excess OH^- with the anions and the protonation of the anions, respectively, which unfavourably results in poor phase transfer and derivatization.

Studies of the effects of organic solvents (dichloromethane, acetophenone, cyclohexanone, 1-pentanol, 2-octanol and methyl isobutyl ketone), the reaction time at 30°C for dichloromethane and at 50°C for the other solvents, and the amount of PFBBr on the derivatization of the anions at a constant aqueous base level ($2 \cdot 10^{-3}$ *M*, 0.1 ml) led the adoption of dichloromethane as the best solvent for derivatization at 30°C; other optimum parameters including reaction time and the amount of PFBBr needed to reach an equilibrium reaction are summarized in Table II for individual and simultaneous determinations.

The amount of Kryptofix 222 B polymer used is also indicated in Table II; an attempt to reduce the reaction time for nitrite, which is assumed to be strongly solvated in water, by increasing the amount of the PTC failed, probably because the amount (12 mg) of immobilized and insoluble PTC used already overloaded the interface between dichloromethane and the aqueous phase under present conditions. Therefore, by the conventional mechanism of increasing the soluble PTC concentration to increase

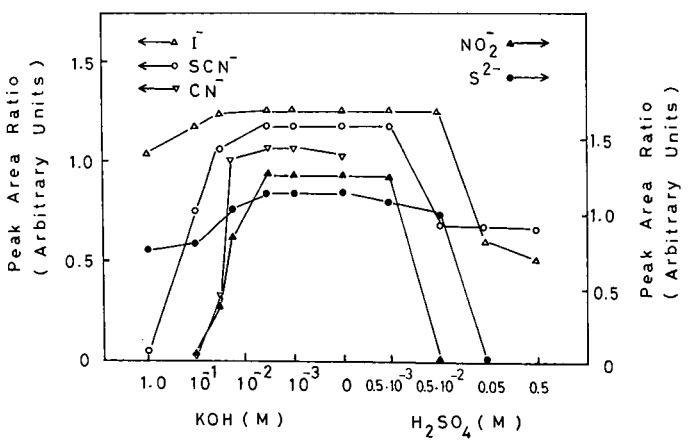

Fig. 1. Effect of added base or acid on the formation of the derivatives. ○, SCN^-; △, I^-; ▲, NO_2^-; ●, S^{2-}; ▽, CN^-; each point represents the average of three measurements.

ion-pair formation for better partition of anions to the organic layer for derivatization does not work here for the immobilized and insoluble PTC.

Based on the optimum conditions established, the derivatization procedures for the individual and simultaneous determinations of the anions were formulated as described under Experimental.

Quantitative determinations

To evaluate the quantitative applicability of the methods, six different concentrations of each anion down to submicromole levels were studied for individual and simultaneous determinations. The results in Table III indicate good linearity for quantification over the range tested, reflected in the high correlation coefficient ($r > 0.998$) derived from both determinations. The lower determination limits are similar to those obtained by the previous method[1]. Simultaneous determination of anions including nitrate is impractical because the equilibrium for the derivatization of nitrate cannot be attained in 24 h, probably owing to its high water solvation resulting in poor phase partition and derivatization.

Gas chromatography and structural identification of the derivatives

A typical gas chromatogram is presented in Fig. 2 and demonstrates good resolution of the anion derivatives using simultaneous determination with temperature-programmed elution. No drift of the baseline was observed in this method, but drift did occur in the previous study[1] using tetraalkylammonium compound as PTC for individual and simultaneous determinations of anions, owing to contamination of the column; therefore, additional treatment of the reacted solution with water to remove the PTC was necessary in the derivatization procedures in the previous work. The structures of the peaks equivalent to the derivatives of iodide (peak 1), nitrite (2), thiocyanate (4) and sulphide (6) are identical with pentafluorobenzyl iodide, α-nitro-2,3,4,5,6-pentafluorotoluene, pentafluorobenzyl thiocyanate and bis(pentafluorobenzyl)sulphide, respectively, reported in the previous paper[1] with similar identification techniques.

It should be noted that the structure of the cyanide derivative equivalent to peak 3 in Fig. 2 is identical with pentafluorobenzyl cyanide as obtained previously[5] by mass spectrometry, but it is different from the derivative of cyanide[6,7] obtained by its derivatization in a homogeneous system (cyanide in 0.015 *M* aqueous KOH reacted with PFBBr in acetone). The derivative from the homogeneous reaction was identified as 2,3-bis(pentafluorophenyl)propionitrile by electron-impact mass spectrometry (20 eV), with a molecular ion at m/z 387, and infrared spectrometry, with a characteristic cyano absorption at 2250 cm^{-1}, and by acceptable results of elemental analysis. The derivative of cyanide from the homogeneous reaction could be speculated from the following mechanism: the initial nucleophilic substitution between CN^- and PFBBr ($C_6F_5CH_2Br$) results in the formation of $C_6F_5CH_2CN$, which then deprotonates one of its active methylene hydrogens in strongly alkaline homogeneous media; the resulting anion species, $C_6F_5\bar{C}HCN$ as a new nucleophile further attacks the PFBBr and proceeds via a second nucleophilic substitution to the formation of the final derivative, 2,3-bis(pentafluoropheny)propionitrile. Therefore, a correction should be made to previous reports[6,7] of the cyanide derivative being incorrectly depicted as pentafluorobenzyl cyanide from homogeneous derivatization; the retention time of

TABLE III

REGRESSION ANALYSES FOR THE DETERMINATION OF ANIONS

y = Peak-area ratio of the anion derivative to the internal standard; x = amount of anions (μmol).

Anion	*Amount (range) (μmol)*	*Regression equation*	*Correlation coefficient (r)*
Individual determinations			
CN^-	0.0385–3.85	$y = 0.7358x - 0.00995$	0.999
I^-	0.0158–1.58	$y = 2.121x + 0.00504$	0.999
NO_2^-	0.0217–4.35	$y = 0.6302x - 0.00253$	0.998
S^{2-}	0.0156–1.56	$y = 1.654x + 0.00984$	0.998
SCN^-	0.00345–3.45	$y = 0.8352x - 0.00956$	0.999
Simultaneous determinations			
CN^-	0.0385–3.85	$y = 0.9802x + 0.0270$	0.999
I^-	0.0158–1.58	$y = 1.727x + 0.0128$	0.999
NO_2^-	0.0435–4.35	$y = 0.7222x + 0.0141$	0.998
S^{2-}	0.0156–1.56	$y = 2.688x + 0.0177$	0.998
SCN^-	0.0172–3.45	$y = 1.607x + 0,0142$	0.999

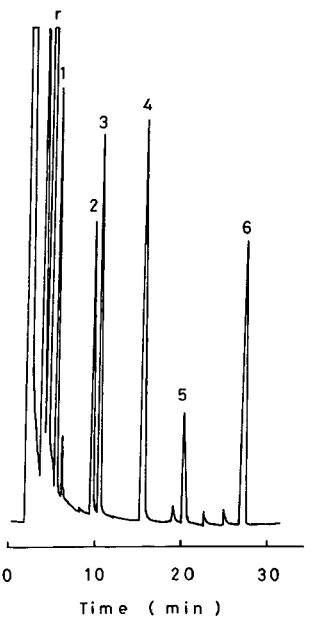

Fig. 2. Gas chromatogram for the simultaneous determination of five inorganic anions in 0.2 ml of solution containing 1.58 μmol I^-, 4.35 μmol NO_2^-, 3.85 μmol CN^-, 3.45 μmol SCN^- and 1.56 μmol S^{2-}. Peaks: 1 = derivative of I^-; 2 = derivative of NO_2^-; 3 = derivative of CN^-; 4 = derivative of SCN^-; 5 = tetrachloronitrobenzene (I.S.); 6 = derivative of S^{2-}; and r = PFBBr reagent blank. Conditions: stainless-steel column, 5.0 m × 3 mm I.D., 5% silicone DC QF-1 on Chromosorb W AW DMCS (60–80 mesh); nitrogen flow-rate, 25 ml/min; column temperature, initially 150°C, programmed at 2°C/min to 200°C, then held there for 5 min; flame ionization detection.

2,3-bis(pentafluorophenyl)propionitrile is significantly longer than that of pentafluorobenzyl cyanide obtained from the present method.

CONCLUSION

A study of the determination of inorganic anions at sub-micromole levels by derivatization GC using Kryptofix 222 B polymer as immobilized PTC resulted in simple procedures for the individual and simultaneous determinations of cyanide, iodide, nitrite, sulphide and thiocyanate anions. One of the advantages is that the PTC used for derivatization is immobilized as solid particles; also, the introduction of the sample solution of anion derivatives for GC determination will never contaminate the column and the detector by the PTC. This is especially important for the trace analysis of inorganic anions in biological samples by GC with a highly sensitive detector such as an electron-capture detector. Development of the method for the trace determination of nitrite and thiocyanate anions in biological specimens is in progress.

ACKNOWLEDGEMENT

H.-L. W. and S.-H. C. are grateful to the National Science Council, Republic of China, for financial support of part of this work (NSC 77-0208-M037-02).

REFERENCES

1 S.-H. Chen, H.-L. Wu, M. Tanaka, T. Shono and K. Funazo, *J. Chromatogr.*, 396 (1987) 129.
2 *Merck's Reagents, Kryptofix (Polyoxadiazamacrobicycles)*, E. Merck, Darmstadt, p. 10.
3 T. Chikamoto and T. Maitani, *Anal. Sci.*, 2 (1986) 161.
4 *The Merck Index*, Merck, Rahway, NJ, 10th ed., 1983, pp. 4701 and 9168.
5 K. Funazo, M. Tanaka, K. Morita, M. Kamino, T. Shono and H.L. Wu, *J. Chromatogr.*, 346 (1985) 215.
6 H.L. Wu, S.-H. Chen, S.-J. Lin, W.-R. Hwang, K. Funazo, M. Tanaka and T. Shono, *J. Chromatogr.*, 269 (1983) 183.
7 H.-L. Wu, W.-R. Hwang, K. Funazo, M. Tanaka and T. Shono, *J. Chromatogr.*, 284 (1984) 193.

Journal of Chromatography, 502 (1990) 265–274
Elsevier Science Publishers B.V., Amsterdam — Printed in The Netherlands

CHROM. 22 069

Enrichment and mass spectrometric analysis of trace impurity concentrations in gases

JÜRGEN HILLE
Central Institute of Physical Chemistry, Academy of Sciences, Rudower Chaussee 5, Berlin 1199 (G.D.R.)
(First received March 15th, 1989; revised manuscript received October 3rd, 1989)

SUMMARY

An apparatus for enrichment of trace impurity components in gases employing mass spectrometry for analysis is described. The main component is a zeolite-packed chromatographic column. The analytical procedure is carried out step by step: first the trace components are trapped on the adsorbent employing the frontal analysis technique, then the pressure in the column is decreased to a high vacuum by cryopumping and finally the adsorbed trace components are desorbed directly into a mass spectrometer for analysis. The analytical efficiency of the method is demonstrated. Detection limits are in the low-ng/l range.

INTRODUCTION

In certain fields of gas analysis (pollution control, semiconductor industry), analytical methods with very low detection limits (ppm, ppb[a]) are necessary. Conventional mass spectrometers are useful devices for trace gas analysis but their dynamic range (10^6) reduces the possibility of detecting concentrations below 1 ppm[1–8]. In many instances the chemical noise, the variety of contaminants and the fragmentation by electron impact lead to mass interferences that may frustate the analysis. To overcome these problems, various methods[9–11] have been used for enrichment of volatile trace components in gaseous matrices. Cryogenic, adsorptive[12–17] and permeative[18–22] methods for enrichment of trace components in gases are known.

Permeative enrichment is very selective, but using membrane separators enrichment factors of only 10–1000 can be achieved. Gas chromatography–mass spectrometry (GC–MS) has been used in combination with cryogenic or adsorptive enrichment methods[23–27]. This method allows one to separate or discriminate the matrix. In addition, the trapped trace components are fractionated before entering the mass spectrometer. The disadvantage of this procedure is the long and complicated passage of samples into the mass spectrometer. The samples can be contaminated by foreign

[a] Throughout this article, the American billion (10^9) is meant.

0021-9673/90/$03.50

substances, *e.g.*, from the laboratory atmosphere and from the apparatus itself. Moreover, considerable amounts of the sample are adsorbed and therefore lost.

In this paper, a procedure is described for enriching and sampling volatile trace components in gases to improve their MS analysis. The main advantages of the apparatus used are the minimal dead volume, the minimal leak rate and the prevention of dilution of trapped trace components by purging. All steps of the applied procedure (enrichment of trace components, fractionation of the enriched trace components and sampling into the mass spectrometer) were carried out using the same packed column[28,29].

The basic principles of the presented analytical procedure are (1) adsorptive enrichment of trace components in gases using a packed column employing the frontal analysis technique; (2) decreasing the pressure in the column by cryopumping to allow sample transfer into the ion source kept under high vacuum; and (3) fractional desorption of trace components from the adsorbent and their MS analysis.

EXPERIMENTAL

Apparatus

A prototype of the enrichment apparatus (Fig. 1) was attached to the direct inlet (sample rod) of a mass spectrometer (MAT 212) linked to a PDP-11-based data system (SS 188). The apparatus consists of a zeolite-packed chromatographic column 200 mm × 0.6 mm I.D.; Wolfen-Zeosorb 4A, VEB Laborchemie Apolda, G.D.R.; 0.08 g; particle size 0.1–0.15 mm), which is closable at both sides by valves. The inlet side of the column is connected to a sample reservoir and the other end is connected to a sample lock (via the sample rod) of the ion source housing. The column (Cr–Ni steel) may be heated (resistance heating) to 670 K or cooled to 80 K by means of liquid nitrogen.

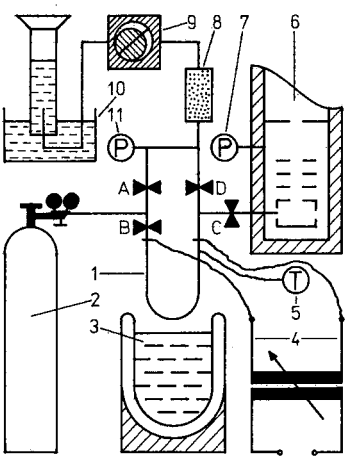

Fig. 1. Schematic diagram of apparatus suitable for the determination of volatile trace components in gases. 1, Packed column; 2, sample reservoir with pressure regulator; 3, cooling bath; 4, adjustable electric heating; 5, thermocouple; 6, mass spectrometer (ion source); 7, high-vacuum pressure control; 8, sorption trap for rotary pump oil vapour; 9, rotary pump; 10, flow meter and chemical trapping of hazardous gases; 11, forevacuum pressure control. A–D, valves.

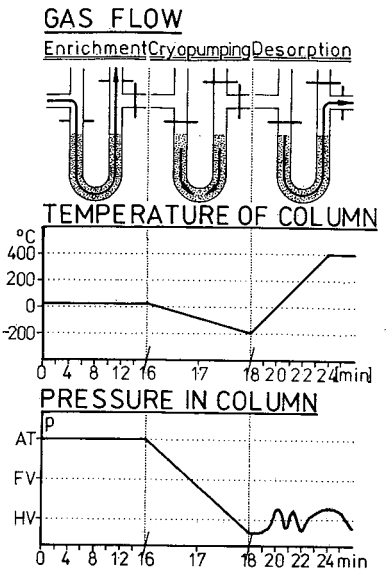

Fig. 2. Schematic diagram of sample line, temperature and pressure in column during enrichment, cryo-pumping and desorption. Enrichment of gaseous impurities in a matrix is carried out at room temperature and atmospheric pressure. Subsequently, the closed column is cryo-pumped, the temperature decreases to 80 K and the column pressure is adjusted to high vacuum. Than the adsorbed impurities are desorbed into the mass spectrometer. During annealing, fractional desorption occurs. For the arrangement of the column (here presented schematically) within the whole system, see Fig. 1.

Procedure

The analytical procedure was carried out in three steps, as shown in Fig. 2. First, volatile trace components in a gaseous matrix to be analysed were enriched in the activated (annealing at 670 K under high-vacuum conditions) zeolite-packed column by adsorption (frontal analysis technique). During the enrichment procedure the sample flows through the column by pumping via the waste line by a rotary oil pump (*cf.*, Fig. 1). The gas flow is adjustable by means of valve B and can be measured. The column temperature depends on the gas matrix to be analysed. The column has to be warm enough to allow the matrix to pass through, but on the other hand it must be cold enough to collect trace components almost completely (*cf.*, Fig. 2). The balance between the gas phase and adsorbed phase leads to the development of a system of adsorption zones.

The pressure in the column roughly equals atmospheric pressure at the end of the enrichment step. To transfer the sample into the ion source of the mass spectrometer, this pressure must be strongly reduced. To achieve this pressure decrease, valve B (*cf.*, Fig. 1) has to be closed at first. Subsequently, the pressure in the column decreases owing to the pumping effect of the rotary oil pump. At this stage it is necesary to take care of losses of adsorbed trace components. Only the matrix component characterized by small interaction forces should principally be pumped off. Therefore, the time required for pumping down has to be very brief. This pressure reduction contributes additionally to the preconcentration of trace components in the column. Subsequently, the whole enrichment step ceases, closing valve D.

The direct coupling of the packed column to the mass spectrometer requires a further pressure reduction in the column. Cryopumping is the most efficient pressure reduction step to allow a sample transfer process without losses. To adjust the pressure to high vacuum, the whole column is cooled to 80 K by immersing it in liquid nitrogen. The movement of impurity zones in the column stops because the gas phase is cryo-adsorbed. Now valve C can be opened without increasing the pressure within the ion source (*cf.*, Fig. 2).

Immediately after opening valve C (*cf.*, Fig. 1), the mass spectrometric analysis must be started. The following parameters have been found to be advantageous: residual gas pressure 10 μPa; maximum pressure during desorption, 1 mPa; temperature of ion source, 370–520 K; optimization of ion source, pressure linear; electron emission current, 0.5 mA; electron energy, 70 eV; investigated mass range 12–200 u; resolution (5% valley): 200–1000 m/Δm; scanning rate, 5–10 s per decade; interscan time, 0.5 s; and SEM factor, 10^6.

At the beginning of the desorption step the cold column warms to 220 K due to the environment. Therefore, the residuum of the matrix is desorbed in addition to very volatile trace components.

Subsequently the column is heated electrically to 670 K at 30–80 K/min. A copper–constantan thermocouple mounted at the column is used to check the temperature. Finally, the column is kept at constant temperature (670 K) for 10 min. Thus the column is activated for the next analysis.

RESULTS

Analysis of hydrogen

For the determination of trace components in hydrogen, trap temperatures between 170 and 300 K are advantageous. A 5-l volume of technical hydrogen (99%) was led through the column at room temperature. Fig. 3A shows the desorption profile of enriched fractionated trace components (total ion current and traces of ions of m/z 43, 57, 78 and 91 depending on time and scan number). MS analysis shows that most of the trace components are hydrocarbons of increasing carbon number. Fig. 3B–E shows mass spectra taken at the respective maxima of the total desorption profile indicated in Fig. 3A. The first two maxima of desorption (scans 17 and 33; Fig. 3B and C was identified to be characteristic of saturated hydrocarbons, especially propane and butane. The last desorption maximum is due to unsaturated hydrocarbons. Fig. 3D (scan 87) shows the occurrence of benzene and Fig. 3E (scan 88) toluene.

The analysis of pure hydrogen (99.999%) was carried out at a lower temperature (170 K) because the intention of this analysis was to detect more volatile trace components (*e.g.*, oxygen, nitrogen and carbon dioxide). The fractional desorption is represented in Fig. 4A. The spectra of oxygen (scan 12; Fig. 4B), nitrogen (scan 14; Fig. 4C), carbon dioxide (scan 37; Fig. 4D), benzene (scan 83, Fig. 4E) and toluene (scan 85, Fig. 4F) were recorded. A blank run without hydrogen but no calibration was carried out. Contamination originating from leaks or other sources was not observed.

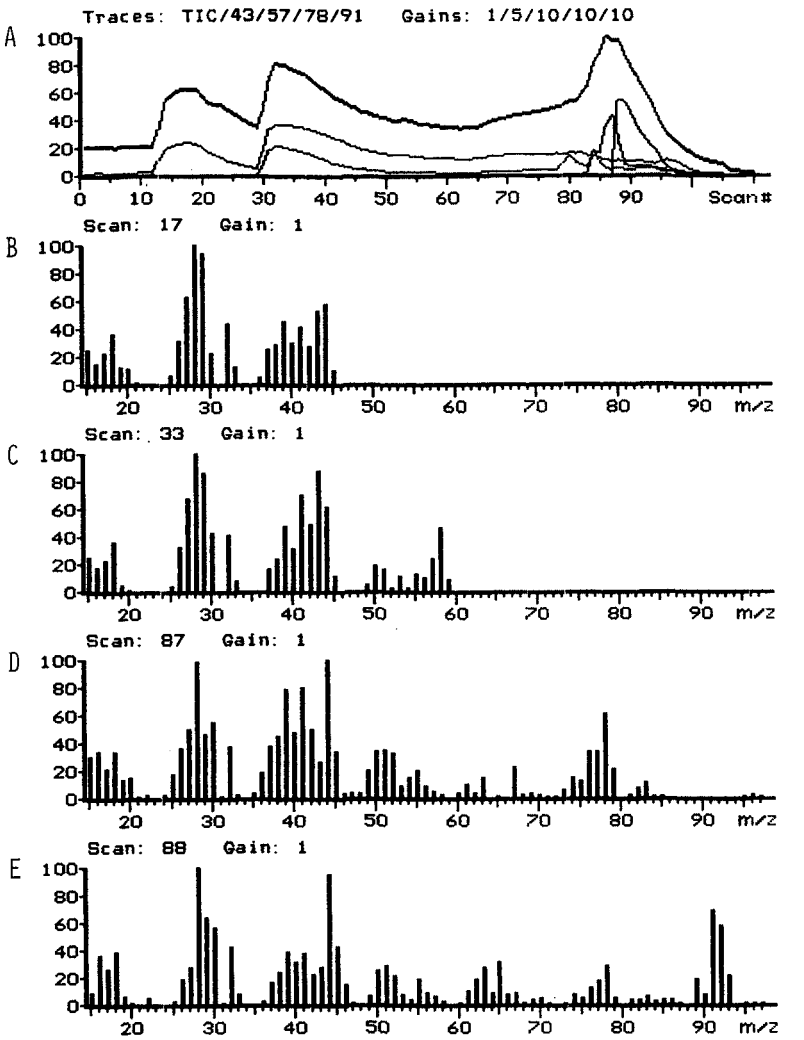

Fig. 3. (A) Desorption profile (total ion current and traces of ions depending on time and scan number) of trace components in technical hydrogen. (B) Scan 17 of the desorption profile: saturated hydrocarbons; main component, propane. (C) Scan 33 of the desorption profile: identified to be characteristic of saturated hydrocarbons; main components, butane. (D) Scan 87 of the desorption profile: identified to be characteristic of unsaturated hydrocarbons; main component, benzene. (E) Scan 88 of the desorption profile: identified to be characteristic of unsaturated hydrocarbons; main component, toluene.

Analysis of silane and phosphine

Phosphine is very toxic and silane is spontaneously flamable in air. Fortunately, our apparatus has the advantage of being a closed system. Dangerous gases may be rendered into a safe form in the waste line without problems (*cf.*, Fig. 1). The leak test and the determination of the gas flow-rate were carried out with a non-hazardous gas, *e.g.*, hydrogen or argon.

The determination of trace components in phosphine or silane is practicable at

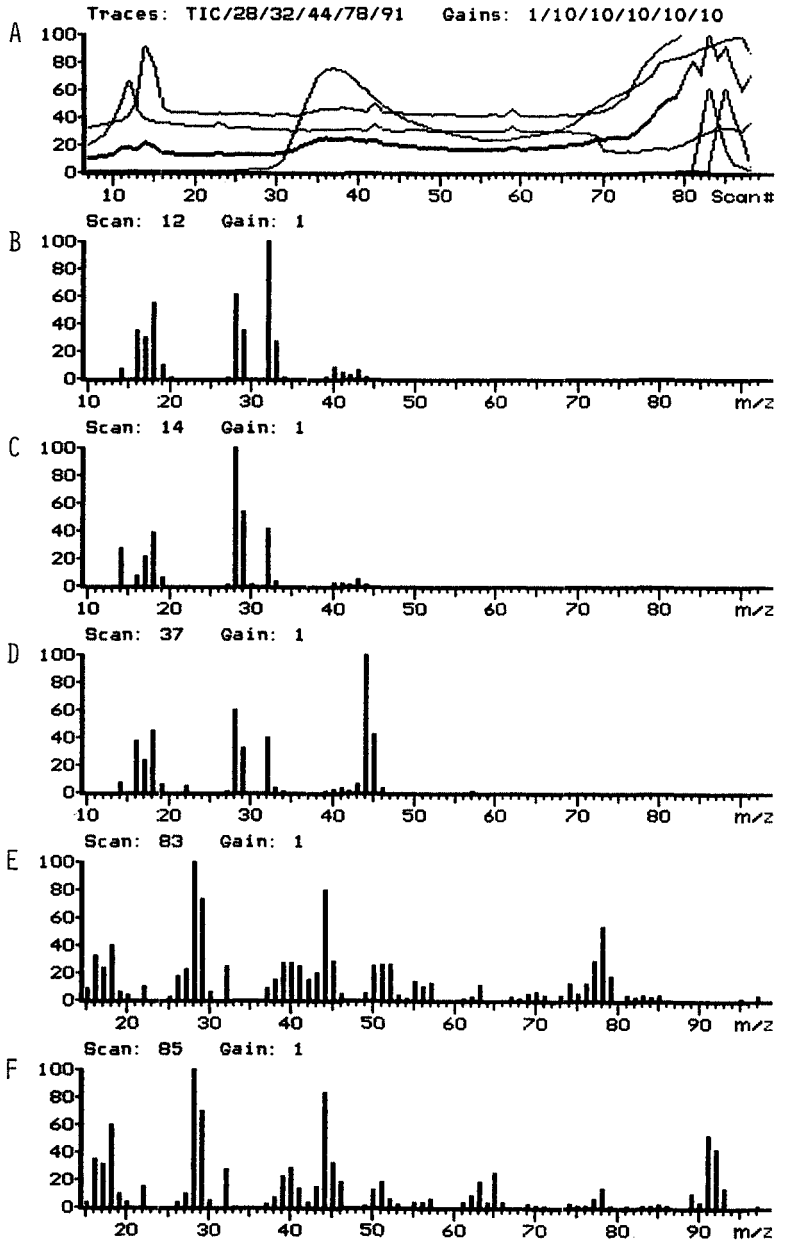

Fig. 4. (A) Desorption profile of trace components in pure hydrogen. (B) Scan 12 of the desorption profile: identified to be characteristic of oxygen. (C) Scan 14 of the desorption profile: identified to be characteristic of nitrogen. (D) Scan 37 of the desorption profile: identified to be characteristic of carbon dioxide. (E) Scan 83 of the desorption profile: identified to be characteristic of butadiene and benzene. (F) Scan 85 of the desorption profile: identified to be characteristic of toluene.

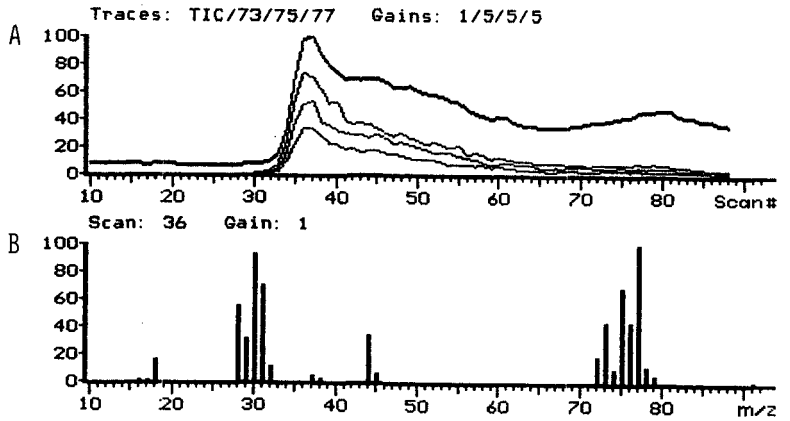

Fig. 5. (A) Desorption profile of trace components in a mixture of 10% silane in hydrogen. (B) Scan 36 of the desorption profile: identified to be characteristic of disiloxane.

room temperature, but the enrichment of, *e.g.*, oxygen or nitrogen at this temperature is not possible. In Fig. 5A the fractional desorption of enriched trace components of a mixture of 10% silane in hydrogen is shown. The maximum of desorption (scan 36) was identified to be disiloxane (Fig. 5B). A concentration of 8.7 ppm was determined without enrichment, but in analysis with enrichment the signal-to-noise ratio was 2000 times higher. In other samples of gas mixtures containing silane, disilane, chlorsilane, hexamethyldisiloxane and saturated or chlorinated hydrocarbons were found.

Mixtures of phosphine in hydrogen were analysed. Diethyl ether was identified to be an impurity (Fig. 6A). For the determination of quantitative data, a liquid mixture (5 μl) of benzene, dissolved in pentane (0.1 vol.-%), was dosed into the gas stream at the beginning of the enrichment. The mixture was exponentially diluted in this gas

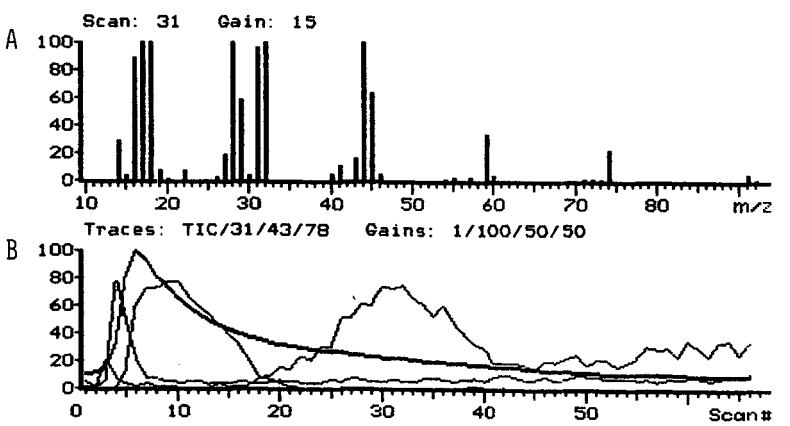

Fig. 6. (A) Determination of diethyl ether in the desorption profile of an enriched sample of 10% phosphine in hydrogen. (B) Desorption profile of enriched trace components: total ion current and traces of ions of pentane*(solvent), benzene (standard) and diethyl ether (trace) for quantitative determination; diethyl ether concentration, 5 ppm.

stream and carried into the column. Whereas pentane was not enriched effectively (maximum at scan 4 in Fig. 6B), benzene was enriched almost completely (maximum at scan 10 in Fig. 6B), allowing quantitative determination. Considering the fractionation pattern of both substances, a result of 5 ppm of diethyl ether was obtained by relating the areas of the desorption profiles of benzene and diethyl ether (*cf.*, Fig. 6A).

Other trace components occurring in phosphine–hydrogen or phosphine–argon mixtures were identified to be toluene, ethylbenzene, ethanol, tetrahydrofuran, dichloroethene or trichloroethene.

Analysis of air

Traces of dichloromethane in laboratory air, resulting from cleaning of laboratory glassware, were determined. A 150-ml volume of contaminated laboratory air was passed through the zeolite-filled column at room temperature. As a result a content of 40 ppb of dichloromethane was calculated from MS analysis (*cf.*, Fig. 7A). Remarkably, a concentration of 0.9 ppb was determined 8 h later. In the analysis of air, it is not necessary to use an external standard. The carbon dioxide in air (about 0.03%), which is enriched almost completely, may be used as an internal standard (*cf.*, Fig. 7B, scan 30, maximum of dichloromethane; scan 39, maximum of carbon dioxide). Because the intensity of the molecular peak at *m/z* 44 exceeds the dynamic range of the mass spectrometer, the isotopic peak at *m/z* 45 was used for quantification of data in the ppb range.

Optimization of parameters

Using the described apparatus for enrichment and sampling of volatile trace components in gases, various samples in our laboratory were routinely mass analysed. In normal situations unknown trace components in the ppm or ppb range should be detected. The standard addition method or external calibration should be used for accurate quantitative determination. Using microlitre sampling syringes, minimum concentrations of standards, diluted with inert solvents, were prepared and

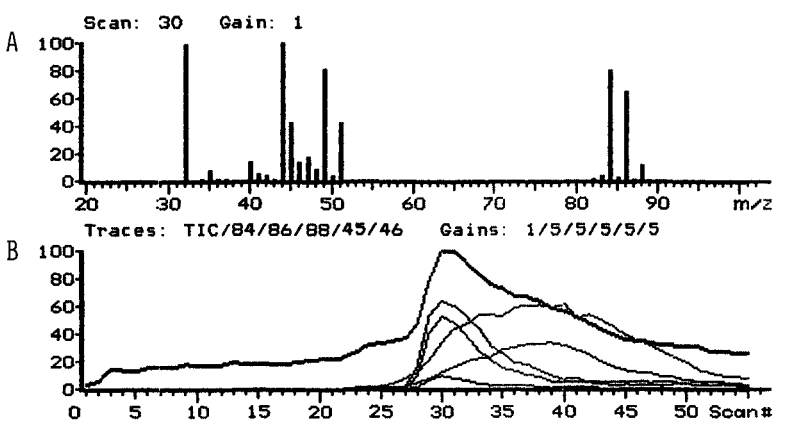

Fig. 7. (A) Determination of dichloromethane in laboratory air. (B) Desorption profile of the total ion current and traces of the ions of dichloromethane (40 ppb) and of the isotopic peaks of carbon dioxide of *m/z* 45 as standard.

dosed for quantitative analysis. The following parameters were varied to achieve an optimum enrichment: the adsorbent, the sample flow-rate, the maximum sample volume and the geometry of the packed column.

Molecular sieves (3A, 4A and 13X) and microporous carbon black were used as adsorbents. Optimum enrichment and fractionation by desorption were achieved using zeolite 4A. Owing to its polarity, hydrocarbons containing heteroatoms, *e.g.*, chlorinated hydrocarbons, alcohols or ethers, are effectively enriched.

The shape of the desorption profile of various substances is determined by diffusion processes in the pore system. Impurities with a larger effective molecular diameter than that of pores of the molecular sieve (*e.g.*, aromatic hydrocarbons) were enriched in its secondary pore structure. Their desorption is faster and their desorption profile is smaller.

For enrichment of non-polar trace components, a non-polar adsorbent should be used. Microporous carbon black was tested for the determination of trace components in hydrogen. Detection limits below 1 ppm cannot be achieved, because high blank values of hydrocarbons falsify the analysis.

The sample flow-rate by frontal analysis determines the formation of impurity adsorption zones in the packed column. The adsorption of trace components is incomplete at very high flow-rates while the diffusion in the column disturbs the sharp adsorption zones at very low flow-rate. Small adsorption zones allow small desorption profiles during fractional desorption with high signal-to-noise ratios. In our experiments sample flow-rates between 10 and 100 ml/min were used.

The maximum sample volume that can be used for an analysis depends on the kind of matrix and adsorbent, the amounts of adsorbent and trace components and the temperature at which the enrichment procedure was carried out. The typical sample volume is between 50 and 1000 ml and is limited by the adsorptive capacity of the column.

Packed columns of various length and diameter were tested. To guarantee a desorption peak of an intensity that does not exceed the dynamic range of the mass spectrometer, the amount of adsorbent must be minimized. Columns packed with 0.05–0.8 g of zeolite were used. A compromise between the length and the diameter of the columns used on the one hand and the optimum sample flow-rate during enrichment on the other must be found. Columns of diameter 0.7–2.0 mm and of length 40–200 mm were tested.

Analysis was carried out recording repeatedly single mass spectra during the desorption. Blank runs without the sample or runs with comparable samples are ususally carried out before and after the analysis to monitor contamination effects. The detection limit of the method was determined using dynamically mixed test gases composed of cryogenically cleaned pure hydrogen and benzene. To dose the minimum amount of benzene it was strongly diluted in pentane. A detection limit of 0.5 ppb of benzene in hydrogen was attained.

CONCLUSIONS

A packed chromatographic column was directly coupled to a mass spectrometer and was used for the adsorptive enrichment of trace components in gases and for fractional desorption of the enriched trace components. Cryopumping was used for

splitless adjustment of the partial pressure of the trace components between enrichment and analysis. This method, based on thermal desorption under high vacuum, is more sensitive than conventional purging methods. Detection limits in the lower ppb range were achieved. Sample handling operations are simpler than in coupling of adsorptive enrichment with GC–MS.

ACKNOWLEDGEMENT

The author expresses his appreciation to Mr. W. Unger for manuscript correction.

REFERENCES

1 Yu. A. Zolotov and M. Grasserbauer, *Pure Appl. Chem.*, 57 (1985) 1133.
2 W. Kroll, *Solid State Technol.*, (1984) 220.
3 W. Genuit, Ch. He-Neng, A. J. H. Boerboom and J. Los, *Int. J. Mass Spectrom. Ion Phys.*, 51 (1983) 207.
4 H. J. Christ, D. Schwanke, Th. Uihlein and H. G. Sockel, *J. Phys. E*, 19 (1986) 793.
5 D. Murphy and K. Mauersberger, *Int. J. Mass Spectrom. Ion Processes*, 76 (1987) 85.
6 K.-C. Lin and J. D. Burden, *J. Vac. Sci. Technol.*, 15 (1987) 373.
7 R. R. Corderman and P. E. Vanier, *J. Appl. Phys.*, 54 (1983) 3987.
8 J. A. Koprio, H. Gaug and H. Eppler, *Int. J. Mass Spectrom. Ion Phys.*, 48 (1983) 23.
9 A. Mizuike, *Fresenius Z. Anal. Chem.*, 319 (1984) 415.
10 K. Ballschmiter, *Pure Appl. Chem.*, 55 (1983) 1943.
11 F. W. Karasek, R. E. Clement and J. A. Sweetman, *Anal. Chem.*, 53 (1981) 1050A.
12 C. A. M. Brenninkmeijer, *Anal. Chem.*, 54 (1982) 2622.
13 T. Noy, P. Fabian, R. Borchers, F. Janssen, C. Cramers and J. Rijks, *J. Chromatogr.*, 393 (1987) 343.
14 W. A. McClenny, J. D. Pleil, M. W. Holdren and R. N. Smith, *Anal. Chem.*, 56 (1984) 2947.
15 R. W. Coutant, R. G. Lewis and J. Mulik, *Anal. Chem.*, 57 (1985) 219.
16 P. A. Steudler and W. Kijowski, *Anal. Chem.*, 56 (1984) 1432.
17 U. Müller and R. Schöllner, *Chem. Tech.*, 37 (1985) 473.
18 G. E. Spangler, *Membrane Technology in Trace Gas Detection*, Report 2083, U.S. Army Mobility Equipment Research and Development Center, Fort Belvoir, VA, 1973.
19 U. Eickmann and U. Werner, *Chem.-Ing.-Tech.*, 56 (1984) 720.
20 Ch. Jonas, *Chem. Tech.*, 31 (1979) 191.
21 G. E. Spangler and J. P. Carrico, *Int. J. Mass Spectrom. Ion Phys.*, 52 (1983) 267.
22 R. D. Blanchard and J. K. Hardy, *Anal. Chem.*, 56 (1984) 1621.
23 I. Morisako, T. Kato, Y. Ino and K. Schaefer, *Int. J. Mass Spectrom. Ion Phys.*, 48 (1983) 19.
24 F. Andrawes, G. Holzer, E. Roedder, E. K. Gibson and J. Oro, *J. Chromatogr.*, 302 (1984) 181.
25 T. G. Andronikashvili and G. V. Tsitsishvili, *J. Chromatogr.*, 292 (1984) 3.
26 M. A. Grayson, *J. Chromatogr. Sci.*, 24 (1986) 529.
27 W. Ecknig, D. Glöckl, B. Schulz and H. Schön, *Chem. Techn.*, 37 (1985) 214.
28 J. Hille, DD 242 127, (1985).
29 J. Hille, *Thesis*, Akademie der Wissenschaften der DDR, Zentralinstitut für Physikalische Chemie, Berlin, 1988.

Journal of Chromatography, 502 (1990) 275–286
Elsevier Science Publishers B.V., Amsterdam — Printed in The Netherlands

CHROM. 22 103

Determination of chlorotriazines and their photolysis products by liquid chromatography with photodiode-array and thermospray mass spectrometric detection

G. DURAND and D. BARCELÓ*
Environmental Chemistry Department, CID–CSIC, c/ Jordi Girona 18, 08034 Barcelona (Spain)
(First received June 21st, 1989; revised manuscript received September 6th, 1989)

SUMMARY

Liquid chromatography with diode-array (LC–DA) and positive ion (PI) mode thermospray LC–mass spectrometry (LC–MS) were used for the determination of atrazine, cyanazine, simazine, deethylatrazine and deisopropylatrazine and their photolysis products. The LC analyses were performed on RP-18 columns using methanol–water (70:30) or methanol–water (70:30) + 0.05 *M* ammonium formate for LC–DA or LC–MS, respectively. The main degradation products observed after photolysis experiments with the suntest apparatus at 44°C were the corresponding hydroxytriazines, which could easily be differentiated from their parent compounds by the structured and distinctive UV spectral information given by LC–DA. The degradation rates after 5 h of irradiation varied from atrazine, deethylatrazine and deisopropylatrazine, which rapidily disappeared, to cyanazine and simazine, with 22 and 36%, respectively, remaining. Special emphasis was devoted to the characterization of the different photolysis products. By employing PI mode thermospray LC–MS, the identification of several photodegradation products such as the hydroxy, 2-H and 2-methoxy analogues was feasible, showing the $[M + H]^+$ ion as the base peak and a second abundant ion corresponding to $[M + CH_3OH + H]^+$. The combined approach allows the identification directly after the photolysis experiments of the different solutions containing chlorotriazines, which is a clear advantage over current methods that require isolation of the photolysis products and elimination of water prior to MS characterization.

INTRODUCTION

Chlorotriazine herbicides are of interest owing to their wide use as herbicides for pre- and post-emergence weed control and as algicides[1,2]. The potential for contamination of water and sediment samples with pesticides is high owing to their physico-chemical properties such as water solubility >30 mg/l, adsorptivity K_{oc} (partition coefficient between soil organic carbon and water) <300–500 and hydrolysis

0021-9673/90/$03.50

half-life >25 weeks[2], and residue levels between 0.01 and 30 ppb[a] have been reported[2–6]. The degradation of these pesticides after application depends on several factors such as hydrolysis, photolysis and microbial activity. The influence of photolysis in different aquatic systems has been widely studied under laboratory conditions as one of these main degradation processes of different chlorotriazines[7–9].

It is of environmental interest, in these photodegradation processes, to establish the photodegradation pathways and to determine the different photodegradation products obtained. In this sense, most of the methods reported in the literature have used gas chromatography (GC) in combination with nitrogen–phosphorus (NPD) and mass spectrometric (MS) detection, and these are the most extensively used methods for the analysis of chlorotriazines[1,9–13].

Considering that some of the photodegradation products of the chlorotriazines are the corresponding hydroxy metabolites, it is of interest to directly determine the photodegraded samples by liquid chromatography (LC). Advantages claimed for LC, with UV detection, are its suitability for the analysis of thermally labile compounds such as cyanazine[14] and polar herbicides and their degradation products[15–19]. Other detection methods such as electrochemical[19] and MS[20–22] have also been employed with LC.

In the work described here, LC with diode-array detection (LC–DA) and thermospray LC–MS have been applied for the first time to the characterization of atrazine, cyanazine, deethylatrazine, deisopropylatrazine and simazine breakdown products obtained under photolysis using the suntest. Solutions of the decomposed analytes in distilled water were directly injected into the LC–DA and LC–MS systems, which is a clear advantage over GC methods that require evaporation of water and derivatization of the polar degradation products prior to injection into the GC system. The use of LC–DA and LC–MS offers good selectivity and sensitivity and the possibility of differentiating between the chlorotriazines and their degradation products. In this sense and in previous papers we have demonstrated the utility of LC–DA[23] and thermospray LC–MS[21,22] for characterizing the different chlorotriazines.

EXPERIMENTAL

Chemicals

HPLC-grade water from Riedel-de-Haën (Seelze-Hannover, F.R.G.) and methanol from Merck (Darmstadt, F.R.G.) were passed through a 0.45-μm filter (Scharlau, Barcelona, Spain) before use. Analytical-reagent grade ammonium formate was obtained from Fluka (Buchs, Switzerland), cyanazine (CYAN) from Riedel-de-Haën, atrazine (ATRZ) and symazine (SIM) from Polyscience (Niles, IL, U.S.A.), hydroxyatrazine (HA) and chlorodiamino-*s*-triazine (CAAT) from Promochem (Wesel, F.R.G.). Deethylatrazine (DEA), deisopropylatrazine (DIA), deethylhydroxyatrazine (DEHA) and deisopropylhydroxyatrazine (DIHA) were gifts from Ciba-Geigy (Basle, Switzerland).

Chromatographic conditions

An eluent flow-rate of 1.0 ml/min was delivered by a Model 64 high-pressure

[a] Throughout this article, the American billion (10^9) is meant.

pump from Knauer (Bad-Homburg, F.R.G.) coupled with a Chrom-A-Scope rapid-scanning UV–VIS detector from Barspec (Rehovot, Israel). Samples were injected via a 20-μl loop from Rheodyne (Cotati, CA, U.S.A.). Cartridge columns (22 cm × 4.6 mm I.D.) from BrownLee, Applied Biosystems (Santa Clara, CA, U.S.A.) and LiChroCART cartridge columns (12.5 cm × 4.0 mm I.D.) from Merck (Darmstadt, F.R.G.), were packed with 5-μm Spherisorb ODS and 5-μm LiChrospher 100 RP-18, respectively, from Merck.

The LC–DA and LC–MS experiments were performed separately. For LC–DA analysis the eluent was methanol–water (70:30) with DA detection at 220 nm and for the LC–MS experiments 0.05 *M* ammonium formate was added to the eluent as an ionizing additive.

Mass spectrometric analysis

A Hewlett-Packard (Palo Alto, CA, U.S.A.) Model 5988A thermospray (TSP) LC–MS quadrupole mass spectrometer and a Hewlett-Packard Model 35741B instrument for data acquisition and processing were employed. The TSP temperatures were stem 100°C, tip 178°C, vapour 194°C and ion source 296°C. In all the experiments the "filament-on" mode was used, in which conventional positive ion chemical ionization can be carried out by using the vaporized LC solvent, which is ionized by an electron beam, as the chemical ionization reagent gas.

Photolysis apparatus

In order to obtain stable and reproducible results in the photodegradation studies, a suntest apparatus from Heraeus (Hanau, F.R.G.) equipped with a xenon lamp was used. The wavelength range varies from 300 to 800 nm, which represents radiation very close to natural sunlight, and the temperature was set at 44°C.

Distilled water samples were spiked with 0.1 ppm of the different chlorotriazine pesticides in methanolic solution and kept in a quartz reaction reservoir and subsequently introduced into the suntest apparatus. At different periods of time, an unknown amount of the solution was analysed by LC–DA and thermospray LC–MS. Although most of the experiments were performed using distilled water containing 3–4% of methanol for solubility reasons, additional experiments with artificial sea water containing humic acids were also carried out. These experiments, closer to real environmental situations, were undertaken in order to examine the enhancement of photodegradation by using this matrix, as previously reported by Fukuda *et al.*[24].

RESULTS AND DISCUSSION

Photodegradation studies by LC with diode-array detection

The photolysis studies of the chlorotriazine herbicides in water samples containing 3–4% methanol were performed as described under Experimental by using the suntest apparatus. The degradation of DIA, DEA, CYAN, SIM and ATRZ was followed by LC–DA. The results obtained after degradation of solutions containing between 111 and 232 μg/l of the chlorotriazine herbicides at different times are shown in Table I.

After 180 min, the proportions of pesticides remaining were 3, 15, 18, 22 and 36% for ATRZ, DIA, DEA, CYAN and SIM, respectively, indicating that ATRZ

TABLE I

PHOTODEGRADATION OF ATRAZINE, CYANAZINE, SIMAZINE, DEISOPROPYLATRAZINE AND DEETHYLATRAZINE AS A FUNCTION OF TIME

Suntest apparatus at 44°C. Results given are concentrations of pesticides in distilled water in μg/l.

Pesticide	*Time (min)*						
	0	*30*	*45*	*60*	*120*	*180*	*300*
Atrazine	166	158	117	112	52	5	0
Cyanazine	232	210	188	166	139	51	30
Simazine	134	66	56	52	50	49	49
Deisopropylatrazine	116	114	89	78	40	18	2
Deethylatrazine	111	101	89	86	42	20	0

degrades the faster and SIM the slowest. When the concentrations of the parent compounds were measured at 300 min it was observed that ATRZ, DIA and DEA had completely disappeared and 12 and 36% of CYAN and SIM, respectively, remained. The fact that ATRZ can be easily degraded by UV radiation has been proposed as a safe means of disposal to avoid groundwater contamination[8].

The main degradation products observed for the different chlorotriazines are their corresponding hydroxy metabolites, the concentrations of which increase with time of UV irradiation. This is illustrated in Fig. 1, where the LC–DA chromatogram at 220 nm of degraded solutions of DIA, DEA, CYAN, SIM and ATRZ after 4, 4, 7, 5 and 3 h of UV irradiation are shown and the corresponding hydroxy metabolites are indicated by compounds 1–5, respectively. Fig. 2 shows the UV spectra of these hydroxychlorotriazines. The UV spectra of HA, DEHA and DIHA agree with those of the standard compounds and with previous spectra published by Vermeulen *et al.*[18]. The UV spectra of the hydroxy metabolites of CYAN and SIM (compounds 3 and 4, respectively, in Figs. 1 and 2) are reported here for the first time.

The hydroxy metabolites exhibit completely different spectra to the parent compounds. Thus, whereas the chlorotriazines generally exhibit a λ_{max} at 220 nm and second maximum with lower absorption at 260–270 nm, for the hydroxychlorotriazines a much broader maximum at 220 nm is observed and the second lower absorption maximum has completely disappeared[18,23]. For DEHA and DIHA (compounds 1 and 2 in Fig. 2), their λ_{max} values tend to shift to shorter wavelengths by 5–10 nm in comparison with HA (compound 5 in Fig. 2), which is to be expected because either ethyl or isopropyl groups have been lost.

In order to obtain a better approach to real environmental situations, preliminary experiments with the chlorotriazines added to artificial sea-water samples containing 1 mg per 600 ml of humic acids were carried out. The preliminary results indicated that the photodegradation rates are faster in the presence of salts, as previously shown for alkylated naphthalenes[24] and that the corresponding hydroxy metabolites do not exhibit an increase with time of UV irratiation; in contrast, they are easily degraded and their concentration decreases after 30–45 min of UV irradiation.

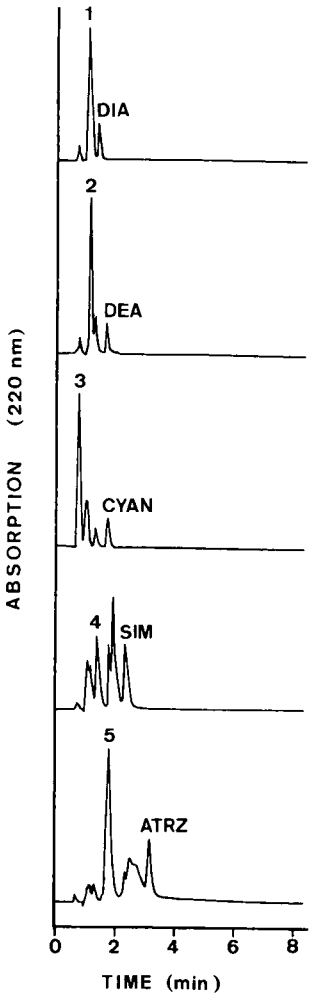

Fig. 1. LC of degraded solutions of deisopropylatrazine (DIA), deethylatrazine (DEA), cyanazine (CYAN), simazine (SIM) and atrazine (ATRZ) after 4, 4, 7, 5 and 3 h of photodegradation with the suntest apparatus. Peaks 1–5 correspond to the different hydroxy metabolites. Mobile phase: methanol–water (70:30) at 1 ml/min; diode-array detection at 220 nm; LC column, LiChroCART; loop volume, 20 μl.

Thermospray LC–MS of chlorotriazines and their photolysis products

By employing the thermospray LC–MS technique, the characterization of the hydroxy metabolites of the chlorotriazines was confirmed and other possible photodegradation products could also be identified.

The characterization of different chlorotriazine herbicides using ammonium formate as ionizing additive in PI mode thermospray LC–MS showed an $[M + H]^+$ ion as the base peak, which can be attributed to a higher proton affinity of the chlorotriazines than ammonia[25]. When methanol–water solutions containing 0.05 *M* ammonium formate were used as the LC eluent, a second abundant ion with a lower

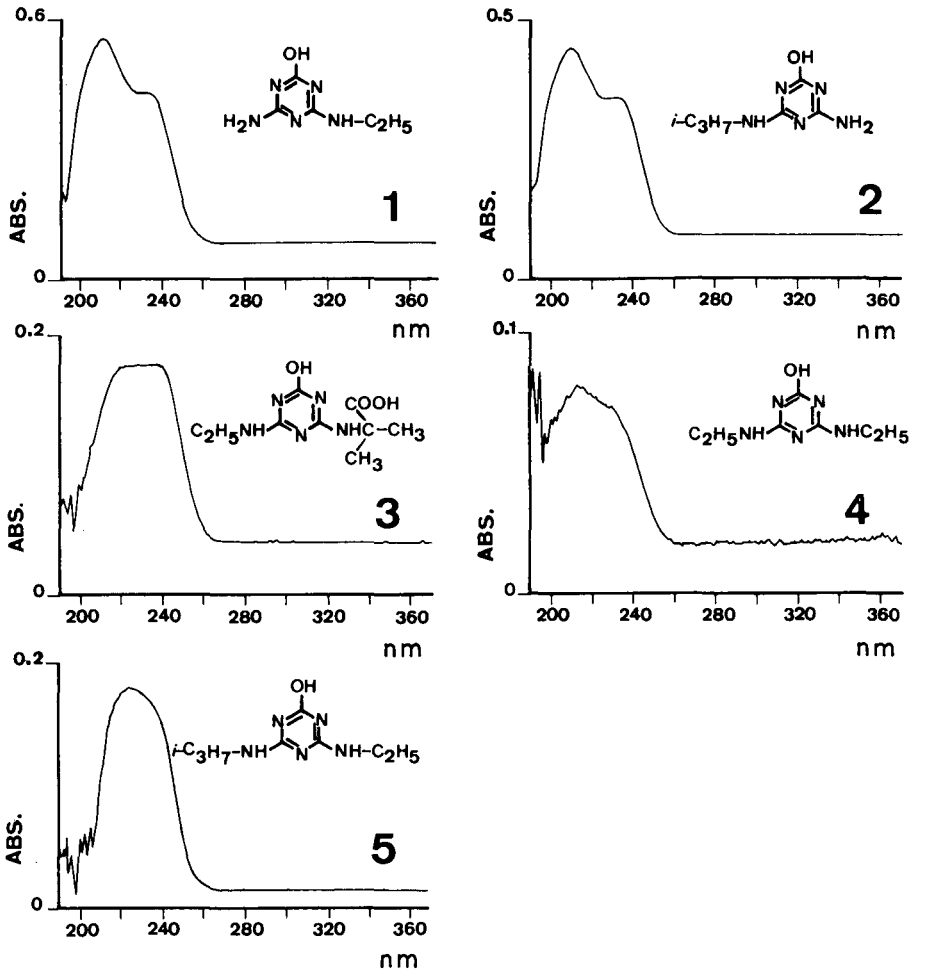

Fig. 2. UV spectra of peaks 1–5 in Fig. 1 corresponding to the hydroxy metabolites of the chlorotriazines. Abs. = Absorption.

relative intensity was formed which corresponds to $[M + CH_3OH + H]^+$, which has previously been explained by the gas-phase equilibrium between $[M + H]^+$ and CH_3OH, strongly dependent on pressure and temperature[22]. The formation of $[M + CH_3OH + H]^+$ is unique to the Hewlett-Packard thermospray system in comparison with the use of the Finnigan thermospray system[20], where the abundance of adduct ions with the LC eluent is generally less than 10%. An extensive comparison of these two thermospray LC–MS interfaces for chlorinated organic pollutants, which will be published elsewhere[26], showed that the Hewlett-Packard interface has higher tendency than the Finnigan interface to form eluent adduct ions.

For the hydroxychlorotriazines, in which a chlorine atom has been replaced with a hydroxy group, the rest of the triazine molecule remaining identical, a similar behaviour to the corresponding parent compounds is to be expected. In Fig. 3, the PI

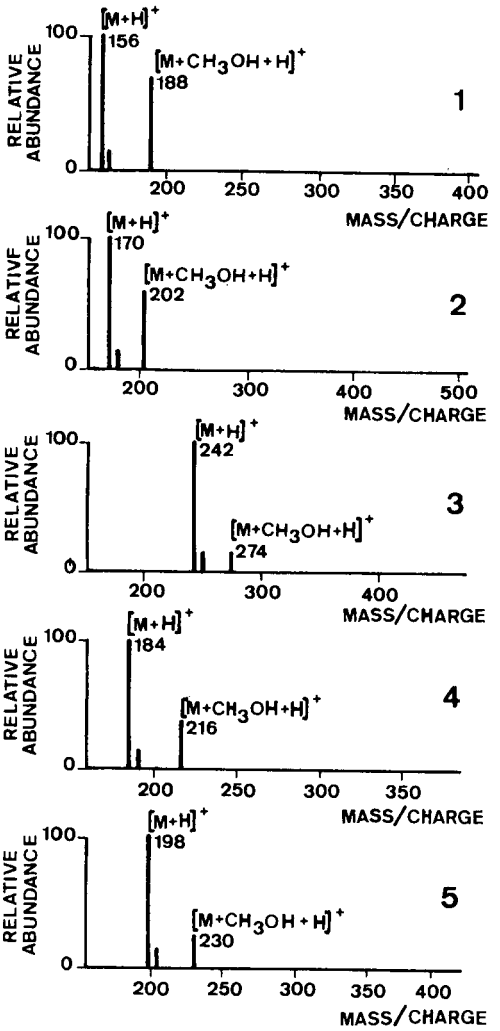

Fig. 3. PI mode thermospray LC–MS spectra of compounds 1–5 in Figs. 1 and 2. Mobile phase, methanol–water (70:30) containing 0.05 *M* ammonium formate at 1 ml/min; loop volume, 20 μl.

mode thermospray LC–MS spectra of the compounds 1–5 in Figs. 1 and 2 are shown. As mentioned, they correspond to the different hydroxychlorotriazines and exhibit the typical behaviour observed with the chlorotriazines, with $[M + H]^+$ as base peak and a second abundant ion corresponding to $[M + CH_3OH + H]^+$. Isotope peaks are virtually unobserved because the thermospray LC–MS spectra, obtained under full scan conditions, correspond to low nanogram levels (*ca.* 1–2 ng) of hydroxytriazines, which are very close to the detection limits of the chlorotriazines[22].

Although the hydroxychlorotriazines were the most abundant degradation products formed, other products have been detected, as can be observed in Fig. 1. A solution of ATRZ degraded after 3 h (Fig. 1) was injected into the thermospray LC–MS system and the total ion current and selected ion chromatograms obtained

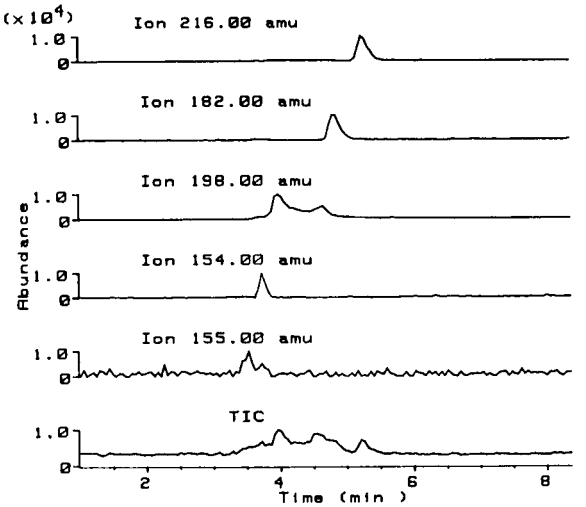

Fig. 4. Total ion current and selected ion chromatograms in PI mode thermospray LC–MS of a 166 μg/l degraded solution of atrazine (ATRZ) after 3 h of photodegradation with the suntest apparatus. The ions identified correspond to $[M + H]^+$ and their structures are given in Fig. 5. LC column, BrownLee. Other experimental conditions as in Fig. 3.

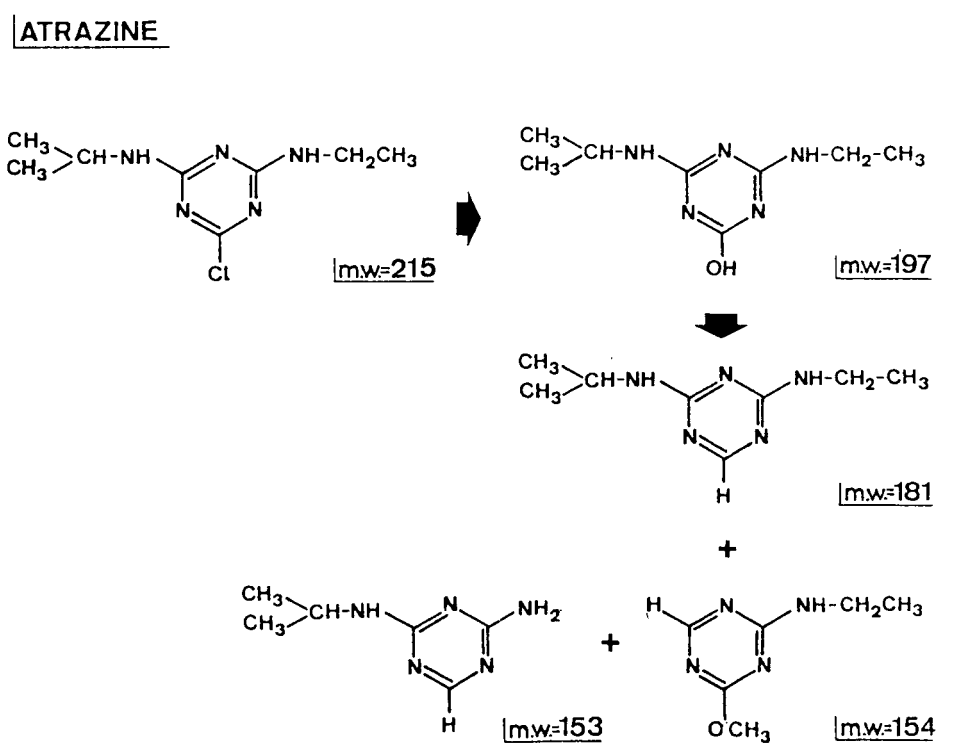

Fig. 5. Tentative photodegradation pathway of atrazine (molecular weight, m.w. = 215) in aqueous solution containing 3–4% of methanol.

are shown in Fig. 4. Here the HA and ATRZ $[M + H]^+$ ions correspond to m/z = 198 and 216, respectively. The other three ions, corresponding to m/z = 154, 155 and 182, can be attributed to three different degradation products of ATRZ of MW 153, 154 and 181, respectively. The tentative identification these photodegration products is shown in Fig. 5. They correspond to the 2-H (MW = 181), 2-H deethyl (MW) = 153) and 2-methoxy deisopropyl (MW = 154) analogues due to the photolysis in the presence of a small amount of methanol.

In the case of SIM, other analogues were detected following a similar photodegradation pathway. In Fig. 6 the total ion current and selected ion chromatograms of SIM after 5 h of photodegradation (see Fig. 1) can be seen with m/z values at 156, 170, 184, 168 and 198 for the different degradation products and at m/z = 202 for SIM. The tentative identification of these photodegradation products is shown in Fig. 7; the structures corresponding to MW of 183, 167, 197, 155 and 169 have been attributed to the hydroxy SIM, 2-H, 2-methoxy, DIHA and 2-methoxy deisopropyl analogues. The identification of these different degradation products agrees with the general scheme of the phtodegradation pathway for SIM in the presence of a methanolic solution, which has been described elsewhere[27].

A similar photodegradation process was observed for the other chlorinated triazines. For CYAN, in addition to the hydroxy metabolite, the 2-methoxy and DIHA analogues at m/z 256 and 156 were also identified. The 2-methoxy analogues were also observed for DEA and DIA at m/z 184 and 170, respectively. The 2-H analogue

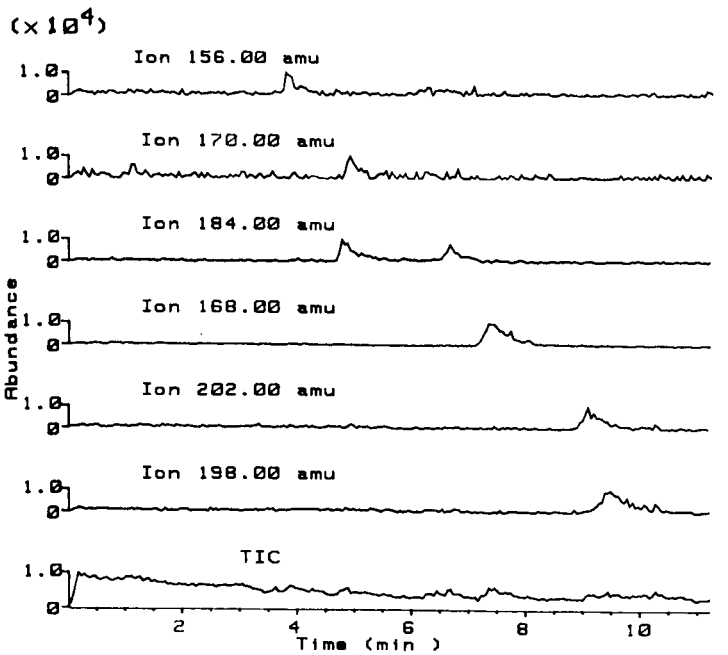

Fig. 6. Total ion current and selected ion chromatograms in PI mode thermospray LC–MS of a 134 μg/l degraded solution of simazine (SIM) after 5 h of photodegradation with the suntest apparatus. The ions idenfitied correspond to $[M + H]^+$ and their structures are given in Fig. 7. LC column, BrownLee. Other experimental conditions as in Fig. 3.

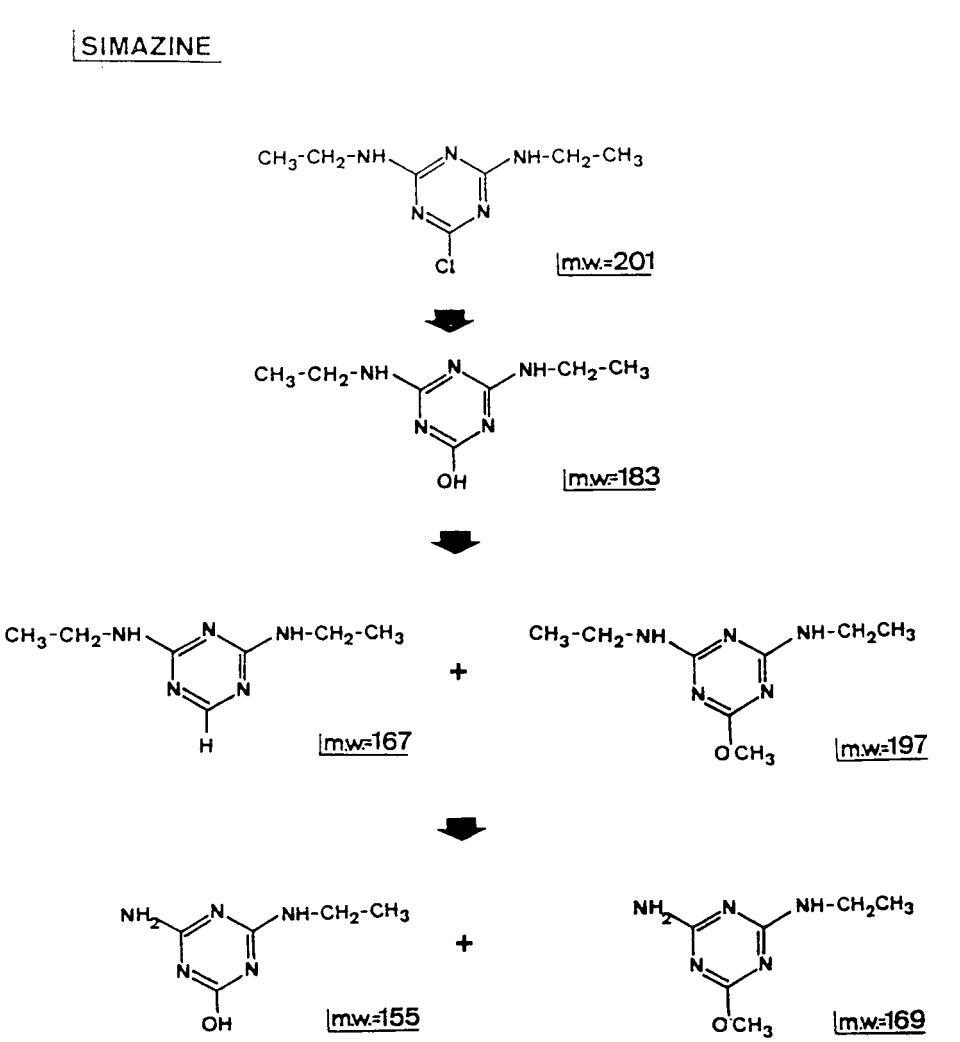

Fig. 7. Tentative photodegradation pathway of simazine (molecular weight, m.w. = 201) in aqueous solution containing 3–4% of methanol.

of DEA at *m/z* 154 was identified, whereas the 2-H analogue for DIA could not be determined because scanning was restricted to *m/z* values higher than 150[22].

CONCLUSIONS

The combination of LC–DA and TSP LC–MS has allowed the identification of different photolysis products of chlorotriazine herbicides in water by direct injection of the photodegradation solutions into the LC system. The method is much simpler than these currently used that require isolation of the different photodegradation products and off-line GC–MS characterization. The different polar degradation

products identified correspond to the hydroxy, 2-H and 2-methoxy analogues. Atrazine degraded faster the other chlorotriazines and simazine was the slowest under the experimental conditions of the suntest apparatus. Preliminary experiments using artificial sea-water containing humic acids indicated that less hydroxy metabolites are formed than when distilled water is used, together with a much faster and a different photodegradation pathway.

Future experiments will include the use of on-line precolumn techniques in LC[15], thus allowing the preconcentration and determination of the different polar photodegradation products by increasing the detection limits and consequently the possibility of detecting other degradation products.

ACKNOWLEDGEMENTS

G. D. is the recipient of a fellowship from the Commission of the European Communities (contract No. ST2*-0488). We thank Scharlau (Barcelona, Spain) for the loan of a Chrom-A-Scope rapid scanning UV–VIS detector from Barspec. This work was partly supported by the Community Bureau of Reference (Commission of the European Communities), the Ministerio de Educación y Ciencia and the BMFT through the Spanish-German cooperation programme (Acciones Integradas). Dr. M. Mansour (GSF, Munich, F.R.G.) is thanked for stimulating discussions. Dr. W. D. Hörmann and M. K. Huber (Ciba-Geigy, Basle, Switzerland) are thanked for kindly providing deethylhydroxyatrazine and deisopropylhydroxyatrazine. R. Alonso (CSIC) is thanked for laboratory assistance.

REFERENCES

1 A. E. Smith, D. C. G. Muir and R. Grover, in A. S. Y. Chau and B. K. Afghan (Editors), *Analysis of Pesticides in Water*, Vol. III, CRC Press, Boca Raton, FL, 1982, Ch. 3.
2 H. B. Pionke, D. E. Glotfelty, A. D. Lucas and J. B. Urban, *J. Environ. Qual.*, 17 (1988) 76.
3 S. Galassi, C. Battaglia and L. Viganó, *Chemosphere*, 17 (1988) 783.
4 D. C. G. Muir and B. E. Baker, *Weed Res.*, 18 (1978) 111.
5 Ch. S. Helling, W. Zhuang, T. J. Gish, C. B. Coffman, A. R. Isensee, Ph. C. Kearney, D. R. Hoagland and M. D. Woodward, *Chemosphere*, 17 (1988) 175.
6 D. C. Muir and B. E. Baker, *J. Agric. Food Chem.*, 24 (1978) 122.
7 H. Burkhard, D. O. Eberle and J. A. Guth, in F. Coulston and F. Korte (Editors), *Pesticides, IUPAC Third International Congress of Pesticide Chemistry*, Georg Thieme, Stuttgart, 1975, pp. 203–213.
8 P. C. Kearney, M. T. Muldoon, C. J. Somich, J. M. Ruth and D. J. Voaden, *J. Agric. Food. Chem.*, 36 (1988) 1301.
9 M. Mansour, K. Hustert and R. Müller, *Int. J. Environ. Anal. Chem.*, 37 (1989) 83.
10 T. A. Steinheimer and M. G. Brooks, *Int. J. Environ. Anal. Chem.*, 17 (1984) 97.
11 H. B. Lee and Y. D. Stokker, *J. Assoc. Off. Anal. Chem.*, 69 (1988) 568.
12 C. E. Rostad, W. E. Pereira and T. J. Leiker, *Proceedings of the 36th ASMS Conference on Mass Spectrometry and Allied Topics, June 5–10, 1988, San Francisco, CA*, pp. 248–249.
13 R. Bagnati, E. Benfenati, E. Davoli and R. Fanelli, *Chemosphere*, 17 (1988) 59.
14 F. Sanchez-Rasero and G. C. Dios, *J. Chromatogr.*, 447 (1988) 426.
15 P. Subra, M. C. Henion, R. Rosset and R. W. Frei, *J. Chromatogr.*, 456 (1988) 121.
16 I. G. Ferris and B. M. Haigh, *J. Chromatogr. Sci.*, 25 (1987) 170.
17 D. Barceló, *Chromatographia*, 25 (1988) 928.
18 N. M. J. Vermeulen, Z. Apostolides, D. J. J. Potgieter, P. C. Nel and N. S. H. Smit, *J. Chromatogr.*, 240 (1982) 247.
19 V. Pacakova, K. Stulik and M. Prihoda, *J. Chromatogr.*, 442 (1988) 147.

20 R. D. Voyksner and C. A. Haney, *Anal. Chem.*, 57 (1985) 991.
21 D. Barceló, *Chromatographia*, 25 (1988) 295.
22 D. Barceló, *Org. Mass Spectrom.*, 24 (1989) 219.
23 G. Durand and D. Barceló, *Toxicol. Environ. Chem.*, 25 (1989) 1.
24 K. Fukuda, Y. Inagaki, T. Maruyama, H. I. Kojima and T. Yoshida, *Chemosphere*, 17 (1988) 651.
25 A. G. Harrison, *Chemical Ionization Mass Spectrometry*, CRC Press, Boca Raton, FL, 1983, p. 33.
26 R. J. Vreeken, U. A. Th. Brinkman, G. J. de Jong and D. Barceló, *Biomed. Environ. Mass Spectrom.*, in press.
27 H. O. Esser, G. Dupuis, E. Ebert, C. Vogel and G. J. Marco in P. C. Kearney and D. D. Kauffman (Editors), *Herbicides, Chemistry, Degradation and Mode of Action*, Vol. I, Marcel Dekker, New York, 1975, Ch. 2.

Journal of Chromatography, 502 (1990) 287–296
Elsevier Science Publishers B.V., Amsterdam — Printed in The Netherlands

CHROM. 22 085

Improved chiral stationary phase based on cellulose triacetate supported on non-macroporous silica gel diol for the high-performance liquid chromatographic separation of racemic flavanones and diastereomeric flavanone glycosides[a]

MARTIN KRAUSE and RUDOLF GALENSA*
Institut für Lebensmittelchemie der Technischen Universität Braunschweig, Pockelsstrasse 4, 3300 Braunschweig (F.R.G.)

(First received July 13th, 1989; revised manuscript received October 11th, 1989)

SUMMARY

Microcrystalline cellulose triacetate (MCCTA) and depolymerized MCCTA were dissolved and coated on non-macroporous silica gel diol. The chiral stationary phases obtained were found to be superior to a commercially available column based on cellulose triacetate for the enantiomeric separation of polyhydroxylated flavanones. Diastereomeric flavanone glycosides could also be resolved, together with the aglycones in a mixture. As an example of the analysis of a complex matrix, the separation of naringenin enantiomers in a tomato skin extract is presented.

INTRODUCTION

Since the work of Hesse and Hagel[1], many papers have dealt with the enantiomeric separation of racemic compounds on microcrystalline cellulose triacetate (MCCTA) as a chiral stationary phase (CSP) (*e.g.*, refs. 2–7). With the preparation of 10-μm particles, MCCTA became suitable as a packing material for high-performance liquid chromatography (HPLC), and columns packed with MCCTA are commercially available (Merck, Daicel, Macherey & Nagel). Although MCCTA shows excellent enantioselectivity towards many enantiomers, the efficiency (number of theoretical plates) of such columns for analytical purposes is poor. Further, the choice of eluents and the flow-rate (compressibility) are limited. Consequently, many papers describe separations of single racemates and not of complex mixtures.

Okamoto and co-workers[8–12], Shibata and co-workers[13,14] and Ichida *et al.*[15] supported cellulose triacetate (CTA) and other polysaccharide derivatives on macroporous silica gel and obtained CSPs for HPLC. Coated CTA has different enantio-

[a] Dedicated to Prof. Dr. H. Thaler on the occasion of his 85th birthday.

0021-9673/90/$03.50

selective properties towards racemic compounds owing to an altered structure. MCCTA has a crystalline form which is referred to as CTA I[a] and which is lost on dissolution. Reprecipitation usually yields the modification CTA II[a,16]. The elution order of enantiomers is often reversed on CTA II, a phenomenon that has been investigated by several research groups[15,17,18]. It is interesting that the coating solvents play an important role in chiral recognition[14,15]. Recently, it was reported that CTA I can also be obtained from solution[19,20].

Optical resolution of flavanones has been achieved on various cellulose-based and other polymeric CSPs. Recently, we reported the enantiomeric HPLC separation of several hydroxylated flavanones on MCCTA as a chiral stationary phase[21]. Flavanones occur naturally in immense variety[22] and many others have been synthesized. Various monomethyoxylated flavanones were successfully separated by our group on a poly-N-acryloyl-S-phenylalanine ethyl ester CSP (ChiraSpher, Merck)[23,24] and on a poly(diphenyl-2-pyridylmethyl methacrylate) CSP [Chiralpak OP(+), Daicel][24].

Many cellulose and amylose phenylcarbamate derivatives have shown high separation factors for the parent compound flavanone[8,9,12]. With Cellulose tris-3,5-dimethylphenylcarbamate (Chiralcel OD, Daicel), flavanone, methoxylated and some hydroxylated flavanones were resolved, but the group of the polyhydroxylated flavanones could not be separated without derivatization[23,24].

Some racemic 3-hydroxyflavanones, which are also classified as flavanonols or dihydroflavonols[25], were resolved on a poly(triphenylmethyl methacrylate) stationary phase [Chiralpak OT(+), Daicel] by HPLC[26]. It should be mentioned additionally that on the same type of column the separation of a racemic biflavanone has been reported[27].

Although the enantioselectivity for hydroxylated flavanones using MCCTA (CTA I) as a CSP is very good (separation factors up to 2)[21], the efficiency of such columns is low, which makes it difficult to determine racemic flavanones in complex matrices such as plant extracts.

CTA II has also been evaluated as a CSP for flavanones, but with a commercially available column packed with CTA II coated on macroporous silica gel (Chiralcel OA, Daicel) hydroxylated flavanones such as naringenin were only partially resolved. However, the column efficiency for CTA coated on silica gel was usually much better compared with MCCTA[13,18]. As far as we can ascertain, no efficient CPS for the direct enantiomeric separation of polyhydroxylated flavanones is commercially available. Therefore, we tried to improve this type of CSP for the analysis of racemic flavanones. We found that CTA coated on non-macroporous silica gel diol (pore size 10 nm) resulted in improved and cheap HPLC columns.

EXPERIMENTAL

Materials

Homoeriodictyol was synthesized by Wagner (Munich, F.R.G.) and pinocembrin was a gift from Wollenweber (Darmstadt, F.R.G.). Taxifolin was obtained from

---

[a] In a previous paper[21], the abbreviations CTA I, CTA II, CTA III and CTA IV were not related to a modification as here, but were used for the consecutive numbering of the CSPs used in that study.

Sigma (Deisenhofen, F.R.G.); all other flavanones (Table I) were from Roth (Karlsruhe, F.R.G.).

Methanol and 2-propanol were of HPLC grade and dichloromethane, 2-propanol, isooctane, *n*-hexane and ethoxyethanol were of analytical-reagent grade, all purchased from Baker (Gross-Gerau, F.R.G.).

LiChrosorb diol (7 μm) (pore size 10 nm) and microcrystalline CTA were obtained from Merck (Darmstadt, F.R.G.) and Nucleosil diol (7 μm) (pore size 10 nm) from Macherey & Nagel (Düren, F.R.G.).

High-performance liquid chromatography

HPLC was performed using a gradient system from Beckman (Munich, F.R.G.) with two 114 M pumps and a high-pressure mixing chamber, an Altex 210 A sampling valve (Beckman) equipped with a 20-μl sample loop and a Pye Unicam variable-wavelength UV detector (Philips, Kassel, F.R.G.) set at either 254 or 280 nm. The results were recorded with Model 3390 A integrator (Hewlett-Packard, Waldbronn, F.R.G.) and a Pye Unicam PU 4850 video chromatography control centre, respectively.

Enantiomeric separation was verified by co-chromatography of the (−)- and (+)-enantiomers collected by chromatography on MCCTA[21].

TABLE I

SUBSTITUTION PATTERN OF FLAVANONES

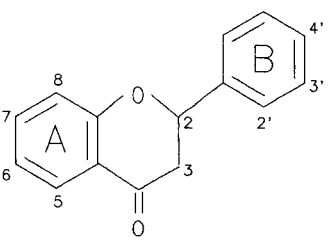

Compound	*Name*
1	5,7-Dihydroxyflavanone (pinocembrin)
2	5,7-Dihydroxy-4′-methoxyflavanone (isosakuranetin)
3	5,7,4′-Trihydroxyflavanone (naringenin)
4	5,7,4′,3′-Tetrahydroxyflavanone (eriodictyol)
5	5,7,4′-Trihydroxy-3′-methoxyflavanone (homoeriodictyol)
6	5,7,3′-Trihydroxy-4′-methoxyflavanone (hesperetin)
7	5,4′-Dihydroxy-7-methoxyflavanone (sakuranetin)
8	5-Hydroxy-7-methoxyflavanone (pinostobin)
9	Flavanone
10	5-Methoxyflavanone
11	6-Hydroxyflavanone
12	6-Methoxyflavanone
13	4′-Hydroxyflavanone
14	4′-Methoxyflavanone
15	2′-Hydroxyflavanone
16	3,5,7,3′,4′-Pentahydroxyflavanone (dihydroquercetin, taxifolin)
17	Naringenin-7-O-glucoside (prunin)
18	Naringenin-7-O-neohesperidoside (naringin)

Chromatography was performed at ambient temperature unless specified otherwise. The column temperatures were adjusted, if necessary, with a column oven from Techlab (Erkerode, F.R.G.).

The following gradients were applied using solvent A [*n*-hexane–2-propanol (9:1, v/v)] and solvent B [methanol–2-propanol (2:1, v/v)]: (I) 10 min 10% B, 15 min 10–15% B, 7 min 15–25% B (Fig. 2); (II) 1 min 5% B, 22 min 5–15% B, 30 min 15–100% B (Fig. 3); (III) 1 min 20% B, 20 min 20–60% B (Fig. 5).

Preparation of the CTA–diol CSPs

CSP I is the commercially available CSP.

CSP II (method 1). MCCTA (0.8 g) was dissolved in 15 ml of dichloromethane, 3 ml of *n*-hexane were added and the solution was stirred until precipitated CTA was redissolved. A 3-g amount of the silica gel diol was added and the suspension was cooled to −70°C while stirring, then 25 ml of *n*-hexane were added while still stirring. The stationary phase was separated with a glas filter, washed three times with 20 ml of *n*-hexane and dried.

CSP III (method 2). MCCTA was depolymerized with a mixture of acetic acid, anhydrous acetic acid and sulphuric acid as described[28] for 30 min. The resulting material was dried and reprecipitated from dichloromethane with 2-propanol. A 0.8-g amount of depolymerized CTA was dissolved in 20 ml of dichloromethane, 9 ml of isooctane were added and the solution was stirred until precipitated CTA was redissolved. Then 3 g of the silica gel diol were added and the solvents were slowly evaporated under vacuum.

Columns

The commercially available column (CSP I) was made of stainless-steel (250 × 4.6 mm I.D.), packed with CTA supported on macroporous silica gel (10 μm) [Chiralcel OA; Baker (Daicel)].

Other columns were made of stainless-steel, packed with the stationary phase by a conventional slurry method (2-propanol as slurry solvent and methanol as packing solvent) at a pressure of 44 MPa (440 bar). The column dimensions were 250 × 4.0 mm I.D. for CSP II and 125 × 4.6 mm I.D. for CSP III.

Sample clean-up for qualitative analysis

Dried tomato skins (0.5 g) were extracted with 30 ml of methanol–water (70:30, v/v) at 70°C for 1 h and the filtered extracts were evaporated under vacuum to about 4–5 ml. This solution was added to a polyamide cartridge (Chromabond PA; Macherey & Nagel), the cartridge was washed with 8 ml of water and the flavonoids were eluted with 6 ml of methanol. The methanolic solution was evaporated to dryness and the residue was dissolved in 1 ml of methanol–2-propanol (2:1, v/v). *n*-Hexane (1 ml) was added and the solution was filtered.

RESULTS AND DISCUSSION

Fig. 1A shows the enantiomeric separation of naringenin (compound 3) on a commercially available column (CSP I) packed with CTA coated on macroporous silica gel (Chiralcel OA, Daicel). The peak shape is not symmetrical (asymmetry factor

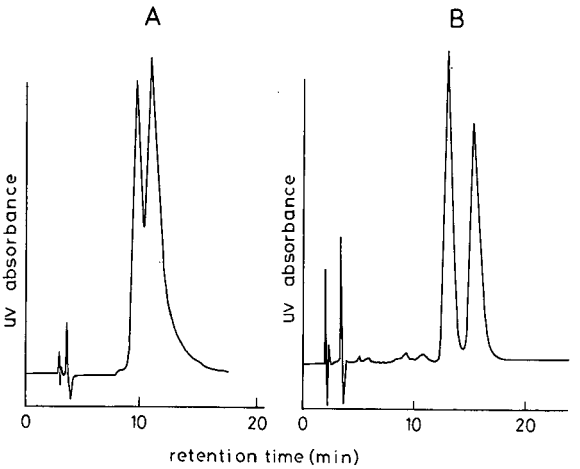

Fig. 1. Enantiomeric separation of naringenin (*cf.*, Table I) on two CSPs based on cellulose triacetate. (A) CTA coated on 10-μm macroporous silica gel (CSP I; Chiralcel OA, Daicel), *n*-hexane–methanol–2-propanol (72:20:8, v/v/v), 1 ml/min; (B) dissolved MCCTA coated on 7-μm Nucleosil diol (CSP II), *n*-hexane–methanol–2-propanol (75:16.3:8.7, v/v/v), 1 ml/min.

2.5–3) and the resolution (R_s = 0.6) is incomplete. The reason for the tailing in the chromatogram may be non-specific adsorption on the silica gel support, which as far as we know consists of macroporous silica gel treated with diphenyldimethoxysilane and N,N-bistrimethylsilylacetamide[28]. Rimböck *et al.*[18] suggested in their studies of CTA coated on silica gel that there are interactions with uncoated parts of this type of stationary phase, which contribute to the overall chromatographic properties of such columns.

There have been several publications describing the coating of cellulose derivatives on a silica gel support. In the first reports on this topic, the coating solvents were slowly evaporated under reduced pressure[10,14,18], whereas in subsequent work the solvents were partially evaporated and the wet material was added to *n*-hexane[11]. The support was usually a silica gel derivative of pore size 100 or 400 nm (macroporous silica gel).

During our investigations, we found that the use of a phase material consisting of a silica gel diol supported with CTA resulted in peak shapes (asymmetry factors 1.4–1.8) superior to those obtained with the commercial column, as illustrated, *e.g.*, in Figs. 1B and 5.

The silica gel diol was supported with (1) dissolved MCCTA (CSP II) and (2) dissolved depolymerized MCCTA (CSP III).

CSP II

Initial attempts to coat silica gel diol by dissolving MCCTA and evaporating the solvents failed, because no powdery material was obtained. The coating of MCCTA on silica gel has been described[10,18], but no details about the quality of the prepared stationary phase were given. Perhaps the molecular weight of MCCTA was different.

We therefore developed a new method in which dissolved MCCTA (in an almost

TABLE II

ENANTIOMERIC SEPARATION OF NARINGENIN: COMPARISON OF CSP I, II AND III

CSP	k'_1[a]	α[b]	R_s[c]	*HETP*[d]	*Mobile phase*[e]
I	2.4	1.20	0.60	0.59	A
II	6.0	1.21	1.16	0.21	B
III	8.2	1.21	1.41	0.13	B

[a] k'_1 = capacity factor of first-eluted enantiomer.

[b] $\alpha = k'_2/k'_1$.

[c] $R_s = 1.198 \cdot \frac{t_2 - t_1}{w_{1/2\,(1)} + w_{1/2\,(2)}}$, where t = retention time and $w_{1/2}$ = peak width at half-height.

[d] HETP = height equivalent to a theoretical plate (mm).

[e] A = *n*-hexane–methanol–2-propanol (72:20:8), 1 ml/min; B = *n*-hexane–methanol–2-propanol (75:16:9), 1 ml/min.

saturated solution) was precipitated at low temperatures (about −70°C) with *n*-hexane. The obtained stationary phases were powdery, but many particles were still agglomerated. This might be the reason why not all of the columns that we prepared where equally good. However, all of them had a better resolution than the commercial column (CSP I), and the separation factor, α, was in the same range (*e.g.*, Table II).

CSP III

Using depolymerized MCCTA (see Experimental), no agglomeration of particles occurred when the solvents (dichloromethane–isooctane, 10:4) were evaporated in vacuum. With these stationary phases the separation factor, α, for naringenin enantiomers was almost the same as with CSP II, but the height equivalent to a theoretical plate (HETP) was lower (Table II) and a better resolution was attained. The reproducibility was satisfactory. Because of the relative high back-pressure of the CTA–diol columns, CSP III was packed in short columns (125 × 4.6 mm I.D.).

Despite the relatively high back-pressure of the HPLC columns [4–6 MPa (40–60 bar) at a flow-rate of 1 ml/min and a mobile phase composed of *n*-hexane–methanol–2-propanol (75:17:8)] we found that non-macroporous silica gel diol is suitable as a support for CTA.

Because we have insufficient information about the commercially available column (CSP I), it is difficult to interpret the differences in resolution and peak symmetry. The decrease in HETP for CTA–diol may be also due to the smaller particle size of 7 μm. From the viewpoint of practical use, however, we can state that CTA–diol columns are better for the separation of polyhydroxylated flavanones.

We also tried to increase the efficiency further by using 5-μm particles. Although it was possible to pack columns with CTA-coated 5-μm silica gel diol, the reproducibility was not good and for most of the columns the HETP was not better than that for the 7-μm columns. The main problem may be the packing procedure itself, because using very short columns (60 × 4.6 mm I.D.) resulted for several columns in a decrease in HETP (about 0.06 mm). Fig. 2 demonstrates that a separation of naringenin enantiomers is possible on this very short column with 5-μm particles.

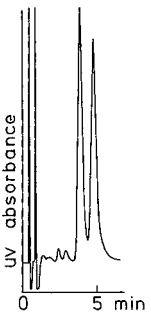

Fig. 2. Optical resolution of naringenin enantiomers on CTA–diol (CSP III type) with 5-μm particles (column 60 × 4.6 mm I.D.). Mobile phase, *n*-hexane–methanol–2-propanol (75:17:8); flow-rate, 1 ml/min; $\alpha = 1.27$; $R_s = 1.4$; pressure = 8 bar.

There are still many problems to be solved, but these results may encourage further investigations in this direction in order to produce efficient cellulose-derived HPLC columns.

The chromatographic data for flavanones with different substitution patterns on a CTA–diol column (CSP III) with an apolar mobile phase are listed in Table III. With

TABLE III

CHROMATOGRAPHIC DATA OF FLAVANONES ON A CTA-COATED DIOL STATIONARY PHASE (CSP III, SHORT COLUMN)

Compound	*Normal-phase mode*			*Reversed-phase mode*[d]	
	k'_1[a]	α[b]	*Mobile phase*[c]	k'_1[a]	α[b]
1	3.75 (−)	1.19	A	2.13 (−)	1.15
2	5.44 (−)	1.13	A	2.55 (−)	1.10
3	11.18 (−)	1.17	A	1.75 (−)	1.22
4	20.84 (−)	1.14	A	1.48 (−)	1.18
5	14.97 (−)	1.15	A	1.67 (−)	1.17
6	13.60 (−)	1.14	A	1.68 (−)	1.18
7	7.22	1.00	A	3.26	1.00
8	4.56	1.00	B	4.12	1.00
9	2.20	1.00	B	1.62	1.00
10	5.87	1.00	B	1.24	1.00
11	3.24	1.00	A	1.31	1.00
12	2.41	1.00	B	2.05	1.00
13	4.54	1.00	B	1.38	1.00
14	3.59	1.00	B	2.07	1.00
15	9.03	1.00	B	1.23	1.00
16	12.10	1.00	C	0.97	1.00

[a] k'_1 = capacity factor of first-eluted enantiomer; the calculation is based on 1,3,5-tri-*tert.*-butylbenzene as non-retained compound[4].

[b] α = separation factor, k'_2/k'_1.

[c] Mobile phase (1 ml/min): (A) *n*-hexane–methanol–2-propanol (80:13.4:6.6); (B) *n*-hexane–methanol–2-propanol (95:3.3:1.7); (C) *n*-hexane–methanol–2-propanol (70:20:10).

[d] Mobile phase: methanol–water (70:30), 0.5 ml/min.

CTA coated on silica gel diol (CTA–diol), only flavanones with 5,7-dihydroxy substitution (phloroglucinol type at ring A) (compounds 1–6, Table I) were resolved. The (−)-enantiomers were eluted before the (+)-enantiomers. These flavanones were also resolved on an MCCTA column (CTA I)[22]. It is interesting to note that (±)-taxifolin (compound 16), a polyhydroxylated 3-hydroxyflavanone, was not resolved on CTA–diol (CSP III), whereas the analogous racemate without the hydroxyl group in position 3 (eriodictyol, compound 4) was separated.

Several eluents were tested with regard to chromatographic behaviour and chiral recognition of naringenin (Table IV). The best resolution was achieved with *n*-hexane–2-propanol–methanol (R_s = 1.5). On substituting *tert.*-butyl methyl ether for 2-propanol the separation factor, α, and the resolution decreased slightly. With *n*-hexane–methanol–ethoxyethanol and *n*-hexane–2-propanol the resolution (R_s = 0.8) was worse. Although naringenin was eluted very fast with methanol (k'_1 = 0.4), a partial resolution was observed. A methanol–water mobile phase resulted in a high separation factor (α = 1.36) and a resolution of R_s = 1.1. None of these mobile phases damaged the stationary phase and the retention times were constant.

Not recommended are acetonitrile-containing mobile phases such as *n*-hexane–*tert.*-butyl methyl ether–acetonitrile (60:30:10) or isooctane–diethyl ether–acetonitrile (150:80:20). The columns were irreversibly damaged by loss of phase material.

Similar to the situation of MCCTA (CTA I)[21] is the influence of temperature on the separation factor, α: decreasing the temperature increases the α values. For example, for naringenin α = 1.16 at 30°C and 1.37 at 5°C with a mobile phase composition of *n*-hexane–2-propanol–methanol (75:8.5:16.5) at a flow-rate of 1 ml/min (measured with a CSP II-type column).

Regarding the separability of different flavanones, the normal-phase mode (apolar eluents) is better than the reversed-phase mode (polar eluents). Fig. 3 illustrates the separation and optical resolution of a mixture of six racemic flavanones (compounds 1–6, Table I) applying gradient I (see Experimental). Except for hesperetin and homoeriodictyol (positional isomers at 3′ and 4′), where two peaks are overlapping, all other flavanones were at least partially resolved. In contrast, in the reversed-phase mode the flavanones are eluted in a narrow retention zone (Table III).

TABLE IV

OPTICAL RESOLUTION OF NARINGENIN ENANTIOMERS ON CSP III: EVALUATION OF MOBILE PHASES

Mobile phase	k'_1 [a]	α [b]	R_s [c]
n-Hexane–methanol–2-propanol (75:17:8)	5.5	1.23	1.5
n-Hexane–methanol–*tert.*-butyl methyl ether (75:17:8)	5.4	1.19	1.4
n-Hexane–methanol–ethoxyethanol (75:17:8)	4.0	1.14	0.8
n-Hexane–2-propanol (75:25)	8.6	1.19	0.8
Methanol	0.4	1.30	—[d]
Methanol–water (70:30)	1.4	1.36	1.1

[a] k'_1 = capacity factor based on a void volume of 1.15 ml as determined with tri-*tert.*-butylbenzene[4].
[b] $\alpha = k'_2/k'_1$.
[c] See Table II.
[d] Partial resolution, R_s not calculated.

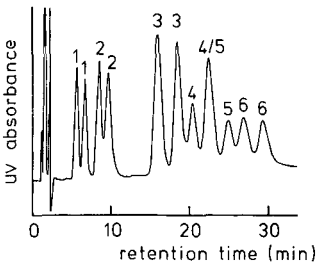

Fig. 3. Gradient elution (I) in the normal-phase mode of a mixture of six flavanones on CSP III (125 × 4.6 mm I.D.). For details, see Experimental. Peaks: 1 = pinocembrin; 2 = isosakuranetin; 3 = naringenin; 4 = hesperetin; 5 = homoeriodictyol; 6 = eriodictyol (*cf.*, Table I). (−)-Enantiomers are eluted before (+)-enantiomers.

Another example of the separation of complex mixtures is the analysis of a tomato skin extract on a short column (125 × 4.6 mm I.D.) applying gradient II in the normal-phase mode (Fig. 4). Naringenin enantiomers are separated from the matrix substances. Peak identification was performed by co-chromatography of naringenin enantiomers and by recording the UV spectra with a diode-array detector. Most naturally occurring flavanones were isolated in an optically active form[29]. The observation that in tomato skins both enantiomers were present may be due to racemization or spontaneous cyclization of naringenin–chalcone during sample preparation. This point is now under investigation.

Flavanone glycosides, which are diastereomers due to the chiral sugar moiety, were separated from the aglycones and were also resolved on CTA–diol (CSP III), as demonstrated in Fig. 5. The elution order with respect to C_2 stereochemistry was confirmed by enzymatic hydrolysis of the enriched fractions of the diastereomers and determination of the enantiomeric aglycone. Flavanone glycosides have been separated as their acetates[30] or benzoates[31] on a silica gel column previously, but direct separation by HPLC has not yet been reported.

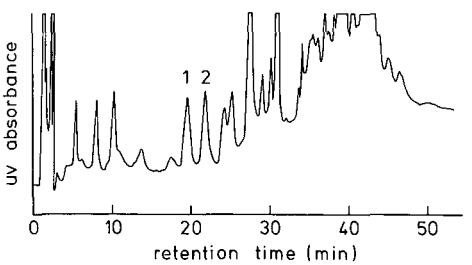

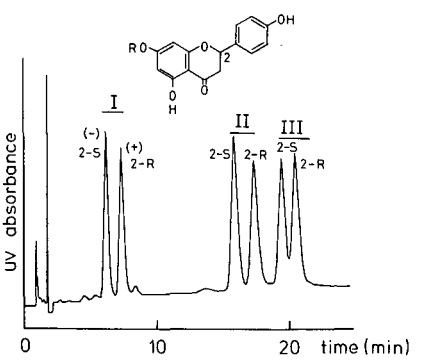

Fig. 4. Naringenin enantiomers in a tomato skin extract on CSP III (CTA–diol) by gradient elution (II) in the normal-phase mode. For details, see Experimental. Peaks: 1 = (−)(2*S*)-naringenin; 2 = (+)(2*R*)-naringenin.

Fig. 5. Separation of naringenin enantiomers and diastereomeric naringenin glycosides in a single chromatographic run on CTA III by gradient elution. For details, see text. Peaks: I = naringenin, R = H; II = naringenin-7-O-glucoside, R = β-D-glucopyranose; III = naringenin-7-O-neohesperidoside, R = α-L-rhamnopyranosyl-β-D-(1,2)-glucopyranose.

CONCLUSION

Although the resolving power (separation factor) of a chiral stationary phase of silica gel diol coated with CTA (CTA–diol) is lower than that of MCCTA[21], the former is superior to MCCTA and to a commercial CTA-coated silica gel column (Chiralcel OA) for the enantiomeric separation of polyhydroxylated flavanones owing to its higher efficiency. With gradient elution the analysis of complex mixtures is possible. The described chiral stationary phase can be easily prepared and may also be an alternative to the very expensive commercially available column for the solution of other problems.

REFERENCES

1 G. Hesse and R. Hagel, *Chromatographia*, 6 (1973) 277.
2 G. Blaschke, *J. Liq. Chromatogr.*, 9 (1986) 341.
3 A. Hussenius, R. Isaksson and O. Matson, *J. Chromatogr.*, 405 (1987) 155.
4 H. Koller, K.-H. Rimböck and A. Mannschreck, *J. Chromatogr.*, 282 (1983) 89.
5 K. R. Lindner and A. Mannschreck, *J. Chromatogr.*, 193 (1980) 308.
6 K.-H. Rimböck, F. Kastner and A. Mannschreck, *J. Chromatogr.*, 329 (1985) 307.
7 A. Mannschreck, H. Koller and R. Wernike, *Kontakte (Darmstadt)*, 1 (1985) 40.
8 Y. Okamoto, M. Kawashima and K. Hatada, *J. Chromatogr.*, 363 (1986) 173.
9 Y. Okamoto, R. Aburatani, T. Fukumoto and K. Hatada, *Chem. Lett.*, (1987) 1857.
10 Y. Okamoto, M. Kawashima, K. Yamamoto and K. Hatada, *Chem. Lett.*, (1984) 739.
11 Y. Okamoto, R. Aburatani and K. Hatada, *J. Chromatogr.*, 389 (1987) 95.
12 Y. Okamoto, H. Sakamoto, K. Hatada and M. Irie, *Chem. Lett.*, (1986) 983.
13 T. Shibata, I. Okamoto and K. Ishii, *J. Liq. Chromatogr.*, 9 (1986) 313.
14 T. Shibata, T. Sei, H. Nishimura and K. Deguchi, *Chromatographia*, 24 (1987) 552.
15 A. Ichida, T. Shibata, I. Okamoto, Y. Yuki, H. Namikoshi and Y. Toga, *Chromatographia*, 19 (1984) 280.
16 R. H. Marchessault and P. R. Sundararjan, in G. O. Aspinall (Editor), *The Polysaccharides*, Vol. 2, Academic Press, London, 1983, pp. 82–89.
17 E. Francotte, R. M. Wolf, D. Lohmann and R. Müller, *J. Chromatogr.*, 347 (1985) 25.
18 K.-H. Rimböck, M. A. Cuyegkeng and A. Mannschreck, *Chromatographia*, 21 (1986) 223.
19 Daicel Chemicals Industries, *Jpn. Pat.*, 63 117 001 (1988); *C.A.*, 109 (1988) 131 104d.
20 E. J. Roche, J. P. O'Brien and S. R. Allen, *Polym. Commun.*, 27 (1986) 138.
21 M. Krause and R. Galensa, *J. Chromatogr.*, 441 (1988) 417.
22 B. A. Bohm, in J. B. Harborne (Editor), *The Flavonoids, Advances in Research*, Chapman and Hall, London, New York, 1988, pp. 348–372.
23 M. Krause and R. Galensa, *Lebensmittelchem. Gerichtl. Chem.*, 43 (1989) 12.
24 M. Krause and R. Galensa, *J. Chromatogr.*, submitted for publication.
25 B. A. Bohm, in J. B. Harborne (Editor), *The Flavonoids, Advances in Research*, Chapman and Hall, London, New York, 1988, pp. 372–379.
26 H. Takahashi, S. Li, Y. Harigaya and M. Onda, *Heterocycles*, 26 (1987) 3239.
27 M. Niwa, S. Otsuji, H. Tatamatsu, G.-Q. Liu, X.-F. Chen and Y. Hirata, *Chem. Pharm. Bull.*, 34 (1986) 3249.
28 Daicel Chemical Industries, *Eur. Pat. Appl.*, 0 121 776 A1 (1984); *C.A.*, 102 (1985) 26 690z.
29 H. Arakawa and M. Nakazaki, *Justus Liebigs Ann. Chem.*, 636 (1960) 111.
30 R. Galensa and K. Herrmann, *J. Chromatogr.*, 198 (1980) 217.
31 D. Treutter, R. Galensa, W. Feucht and P. P. S. Schmid, *Physiol. Plant.*, 65 (1985) 95.

Journal of Chromatography, 502 (1990) 297–304
Elsevier Science Publishers B.V., Amsterdam — Printed in The Netherlands

CHROM. 22 109

Effect of chain length of oligosaccharide in high-performance affinity chromatography of a lectin on oligosaccharide-immobilized columns

KAZUAKI KAKEHI, YOSHIKAZU KOJIMA, SHIGEO SUZUKI and SUSUMU HONDA*
Faculty of Pharmaceutical Sciences, Kinki University, 3-4-1 Kowakae, Higashi-osaka 577 (Japan)
(First received July 27th, 1989; revised manuscript received October 20th, 1989)

SUMMARY

Homologous oligosaccharides ranging from bioses to tetraoses were immobilized to 3-(β-aminoethoxy)propylsilica by reductive amination, and the chromatographic behaviour of concanavalin A (Con A) with the resultant gels was examined. Con A showed a strong affinity to immobilized mannose oligomers having mainly α1→2 interglycosidic linkages, giving broadened peaks when phosphate buffers containing glucose as a displacing sugar were employed as eluents. The association constant (K_a) calculated from elution volume increased with increasing degree of polymerization, implying that not only the non-reducing monosaccharide residue but also the interior portion of the sugar chain took part in complexation. Con A showed a similar tendency to glucose oligomers linked through α1 →6 bonds, although the K_a values were much smaller than those of the corresponding mannose oligomers.

INTRODUCTION

Affinity chromatography based on specific interactions between proteins and carbohydrates has been widely applied to the isolation and purification of the biological substances involved. Especially chromatography on protein-[1] or carbohydrate-immobilized[2] agarose gels is convenient and is capable of affording highly purified components on a preparative scale by a simple procedure of specific adsorption followed by desorption. However, the use of such soft gels is inappropriate for analytical purposes, because of the low reproducibility of analysis and the poor durability of the matrices. In a previous paper[3] we reported the attempted immobilization of a few popular disaccharides to a methacrylate polymer and demonstrated the usefulness of the resulting resins for high-performance affinity chromatography (HPAC) of lectins. In a subsequent paper[4] we reported the efficient separation of proteins on a resin carrying a number of oligosaccharides derived from a glycoprotein, by stepwise elution with buffers containing various displacing sugars. Such HPAC techniques are valuable for the separation and determination of specific proteins of biological interest in minute amounts. They are also useful for the investigation of

0021-9673/90/$03.50

structure–affinity correlations. In continuation of such HPAC studies, we have now examined the effect of the chain length of homologous oligosaccharides on their affinity to protein. This paper reports investigations of the interactions of mannose and glucose oligomers immobilized to silica with concanavalin A (Con A) as a specific protein.

EXPERIMENTAL

Chemicals

Con A from *Canavalia ensiformis* was obtained from Hohnen Seiyu (Tokyo, Japan) and used as a $1.0 \cdot 10^{-3}$% solution in the eluent used for HPAC. Homogeneity of Con A was confirmed by electrophoresis on polyacrylamide gel containing $1.0 \cdot 10^{-2}$% sodium dodecyl sulphate (SDS) according to the procedure of Laemmli[5]. Yeast α-glucosidase was purchased from Sigma (St. Louis, MO, U.S.A.) and used after dialysis against 120 m*M* phosphate buffer (pH 6.8).

Glucose oligomers (isomaltooligosaccharides) were obtained by partial acid hydrolysis of dextran, followed by separation on a column of Bio-Gel P-4, by the method of Yamashita *et al.*[6]. The peracetates of mannose oligomers were obtained by acetolysis of yeast mannan, followed by fractionation of the product on a silica gel column by stepwise elution with benzene–ethyl acetate. Each of the purified acetates was dissolved in 100 m*M* sodium methoxide in methanol[7], and the reaction mixture was deionized by passing it through a column of Amberlite CG-120 (H^+). Evaporation of the combined eluate and the water washings to dryness gave a pure sample of a mannose oligomer. Based on ^{1}H NMR analysis, the deacetylated products were concluded to have the structures Manα1 → 2Man, Manα1 → 2Manα1 → 2Man and Manα1 → 3Manα1 → 2Manα1 → 2Man.

Dihydroxysilica gel (LiChrosorb DIOL, 5 μm, pore size 6 nm), which has a 3-(β,γ-dihydroxypropoxy)propyl group on a polysilicate base, was obtained from Merck (Darmstadt, F.R.G.). Other reagents and solvents were of the highest grade commercially available.

Immobilization of oligosaccharides to dihydroxysilica gel

Dihydroxysilica gel (3 g) and sodium metaperiodate (3 g) were added to 90% aqueous acetic acid (60 ml) and the mixture was gently swirled for 2 h at room temperature. The gel was collected by centrifugation at 1800 *g*, washed thoroughly with water and suspended in methanol (20 ml). Sodium cyanoborohydride (0.63 g) and ammonium acetate (1.0 g) were added to the suspension and the mixture was kept overnight at room temperature with swirling. By this series of treatments the 3-(β,γ-dihydroxypropoxy)propyl group was converted, via the aldehyde form, to a 3-(β-aminoethoxy)propyl group. The resulting aminosilica gel was collected and washed thoroughly with water.

The aminosilica gel was stirred in an aqueous solution containing an oligosaccharide sample (0.10 g), sodium cyanoborohydride (0.63 g) and acetic acid (0.10 ml) in methanol (10 ml) for 24 h at 37°C. The oligosaccharide-immobilized silica gel thus obtained was further treated with glutaraldehyde (0.10 ml), to block the remaining free amino group. The gel finally obtained was collected and washed thoroughly with water.

HPAC

A sample of oligosaccharide-immobilized silica gel was packed in a stainless-steel column (100 mm × 4 mm I.D.) by the slurry method using water as a packing solvent. The column temperature was maintained at 29°C throughout the work. Elution of HPAC was performed with 50 m*M* phosphate buffer (pH 6.8) containing sodium chloride at a concentration of 200 m*M* at a flow-rate of 0.50 ml/min. Con A (200 ng per 20 μl) was injected via a Rheodyne 7125 injector. Con A in the eluates was monitored by measuring the fluorescence at 340 nm, generated from the tryptophan residue in the polypeptide core, with irradiation at 300 nm.

Determination of the total amounts of immobilized oligosaccharides

The total amounts of immobilized oligosaccharides were determined spectrophotometrically by the direct phenol–sulphuric acid method as follows. A sample of oligosaccharide-immobilized silica (*ca.* 10 mg), weighed accurately, was suspended in distilled water (0.50 ml). A 5.0% aqueous solution (0.50 ml) of phenol was added and the mixture was shaken vigorously. Concentrated sulphuric acid (5.0 ml) was added in one portion and the mixture was vortexed. The developed colour was measured at 490 nm and the total amount of the immobilized oligosaccharide was calculated using a calibration graph constructed using standard solutions of mannose or glucose.

The absorbance obtained for the isomaltose-immobilized gel by this method was almost the same as that for the acid hydrolysate (2 *M* trifluoroacetic acid, 100°C, 5 h) of the same amount of the isomaltose-immobilized gel. This result provided evidence that hydrolysis was complete during the above operation. The values obtained (m*M* in the gel) were as follows: glucobiose (isomaltose), 25.7; glucotriose (isomaltotriose), 21.1; glucotetraose (isomaltotetraose), 7.93; mannobiose, 25.0; mannotriose, 10.4; and mannotetraose, 5.51. The concentration of the 3-(β-aminoethoxy)propyl group in the gel, as calculated from elemental analysis of carbon (3.2%), was 0.10 *M*. Based on this value, the efficiencies of immobilization of oligosaccharides ranged from 6.3 to 17%.

Determination of the molar fractions of the oligosaccharides immobilized to the particle surface

A 50-mg portion of maltose-immobilized silica gel, prepared as described above for other oligosaccharides, was incubated for 24 h at 37°C, with constant stirring, with yeast α-glucosidase (*ca.* 10 mU) in 120 m*M* phosphate buffer (pH 6.8). The reaction mixture was centrifuged at 1800 *g* and the combined supernatant and water washings were desalted by passage through a small column of Amberlite CG-120 (H^+) and Amberlite CG-400 (CH_3COO^-). The combined eluate and water washings were evaporated to dryness and the residue was reconstituted with water (100 μl). High-performance liquid chromatography (HPLC) of a 20-μl aliquot on a column of Interaction CHO-620 (300 mm × 7.8 mm I.D., 80°C) with water as eluent (0.5 ml/min), with UV detection at 280 nm after post-column labeling with 2-cyanoacetamide by the method of Honda *et al.*[8], gave a glucose peak equivalent to 2.79 nmol. From this value the amount of maltose immobilized to the particle surface was calculated to be 270 nmol/g.

The total amount of immobilized maltose was determined by acid hydrolysis with 2 *M* trifluoroacetic acid for 6 h at 100°C, followed by HPLC of the liberated glucose as described above. The value obtained was 43.0 μmol/g.

From the foregoing two values of the enzyme- and acid-released glucose, the molar fraction was calculated to be 0.0063. This value is considered to be universally applicable to all oligosaccharide-immobilized gels, as immobilization was assumed to have occurred at an equal rate to both the particle surface and the inner walls of the pores. The values obtained for the effective concentration of oligosaccharides were as follows: glucobiose (isomaltose), $162 \cdot 10^{-6}$ *M*; glucotriose (isomaltotriose), $132 \cdot 10^{-6}$ *M*; glucotetraose (isomaltotetraose), $50.0 \cdot 10^{-6}$ *M*; mannobiose, $158 \cdot 10^{-6}$ *M*; mannotriose, $65.8 \cdot 10^{-6}$ *M*; and mannotetraose, $34.8 \cdot 10^{-6}$ *M*.

RESULTS AND DISCUSSION

Among various methods for the determination of the magnitude of protein–carbohydrate interactions, HPAC is one of the most convenient and provides reproducible data. In HPAC methods, either protein- or carbohydrate-immobilized gels may be used. Immobilization of protein involves coupling of the free amino group in a protein sample to a supporting gel. During this chemical reaction, care must be taken to avoid three-dimensional structural changes of the protein molecule, and to leave the amino groups at and near the binding site of the protein intact. In addition, protein-immobilized gels are generally unstable to heat and prolonged storage. In contrast, immobilization of carbohydrate eliminates the problem of denaturation, and the stability of immobilized carbohydrate is greater than that of immobilized protein. For this reason the latter mode was adopted in this work.

The oligosaccharides used were of homologous glucose or mannose series, ranging from biose to tetraose. All glucosyl residues in the glucose oligomers were $\alpha 1 \rightarrow 6$ linked, and all mannosyl residues in the mannobiose and mannotriose were $\alpha 1 \rightarrow 2$ linked. The mannosyl residue at the non-reducing end of the mannotetraose was exceptionally $\alpha 1 \rightarrow 3$ linked. All reducing monosaccharide residues in these oligosaccharides were derivatized, on immobilization, to the glycamines having open-chain structures which served as spacers. As a result, every oligosaccharide immobilized to silica gel functioned as a saccharide having a degree of polymerization (DP) one less than that of the starting oligosaccharide.

Fig. 1 shows the changes in the efficiency and shape of the Con A peak for each column packed with an oligosaccharide-immobilized silica gel, with varying concentrations of glucose as a displacing sugar in the mobile phase.

With both series of oligosaccharides, the number of theoretical plates (N) increased with increase in DP and with increase in the concentration of glucose (Fig. 1a and b for glucose and mannose oligomers, respectively). The increment of N corresponding to the change in DP from 2 to 3 was small, whereas that for the change in DP from 3 to 4 was large, especially in the mannose series. The mannose oligomers gave broader peaks than the corresponding glucose oligomers with all DP values, giving N values approximately one fifth (DP 2–3) or half (DP 4) of those of the corresponding glucose oligomers. These results indicate that mannose oligomer-immobilized gels showed a stronger affinity to Con A, giving broadened peaks, and accordingly smaller values of N. Fig. 1c and d show the changes in the tailing factor (T) of the Con A peak. All columns showed large T values, gradually increasing with increasing glucose concentration, but the variation was not large in either series. The T values became slightly larger as DP increased. In every system Con A interacts with both immobilized

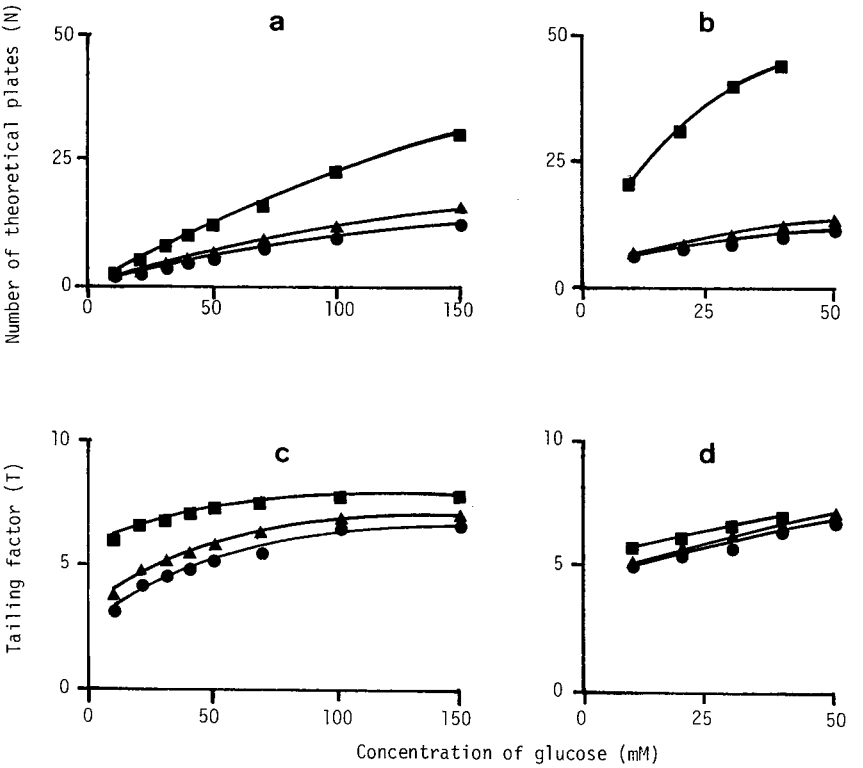

Fig. 1. Effects of glucose concentration on the number of theoretical plates [N; (a) glucose oligomer-immobilized silica; (b) mannose oligomer-immobilized silica] and the tailing factor [T; (c) glucose oligomer-immobilized silica; (d) mannose oligomer-immobilized silica] of the Con A peak. Column, 100 mm × 4 mm I.D.; column temperature, 29°C; eluent, 50 mM phosphate buffer (pH 6.8) containing sodium chloride at a concentration of 200 mM and glucose at a concentration of either 10, 20, 30, 40, 50, 70, 100 or 150 mM; flow-rate, 0.5 ml/min; detection, fluorescence at 340 nm with irradiation at 300 nm. Amount of sample (Con A) injected: 200 ng per 20 μl. ● = Biose; ▲ = triose; ■ = tetraose.

oligosaccharide and glucose in the eluent. If Con A interacts in the monovalent mode, the equation proposed by Swaisgood and Chaiken[9] can be applied:

$$\frac{1}{V - V_0} = \frac{K_d}{(V_0 - V_m)\,[M]} + \frac{[L]\,K'_d}{(V_0 - V_m)\,[M]\,K'_d} \quad (1)$$

where V, V_m and V_0 are elution volume of Con A, the volume of mobile phase in the column and the elution volume of unretained species, respectively. The values of V_m and V_0 could be obtained as the peak volumes of injected water (detected as a solvent shock by UV absorption at 254 nm) and Con A eluted with a sufficiently high concentration (500 mM) of glucose. At this concentration, the binding of Con A to glucose was so strong that its binding to the immobilized oligosaccharide was almost negligible, hence Con A was not retained at all. [L] and [M] designate the concentration of glucose as a displacing sugar and the effective concentration of immobilized oligosaccharide, respectively. The pores in the supporting gel were too small (average

diameter 10 nm) for the Con A molecule to enter them. In order to obtain the effective concentration of oligosaccharide immobilized to the particle surface, ready to interact with Con A, we determined the amounts of enzyme- and acid-released glucose from maltose-immobilized silica gel. The ratio of these amounts (0.0063) can be regarded as the molar fraction of oligosaccharides on the particle surface. Thus [M] was obtained by multiplying the total number of moles of immobilized oligosaccharides by a factor of 0.0063 and dividing the product by the volume of stationary phase, which was obtained by subtraction of V_m from the column volume. K_d and K'_d are the equilibrium dissociation constants of immobilized oligosaccharide–Con A and glucose–Con A complexes, respectively.

Eqn. 1 indicates that the relationship between [L] and $(V - V_0)^{-1}$ is first order. However, the plot of [L] *vs.* $(V - V_0)^{-1}$ in the range 10–100 m*M* gave concave curves for all oligosaccharide-immobilized gels, as exemplified by Figs. 2 and 3. On the other hand, non-linear least-squares regression analysis by using the MULTI system[10] showed an excellent fit to the equation applied to bivalent system also proposed by Swaisgood and Chaiken[9]:

$$\frac{1}{V - V_0} = \frac{1 + 2 \cdot \frac{[L]}{K'_d} + \left(\frac{[L]}{K'_d}\right)^2}{(V_0 - V_m)\left[2 \cdot \frac{[M]}{K_d} + \left(\frac{[M]}{K_d}\right)^2 + 2 \cdot \frac{[L]\,[M]}{K_d K'_d}\right]} \qquad (2)$$

The association constant (K_a) of an immobilized oligosaccharide to Con A could be calculated as the reciprocal of K_d. The values of K_a obtained are summarized in Table I. The results indicate that K_a became larger as DP increased, and the rate of increase accelerated with increase in DP. The K_a value for tetraose was by

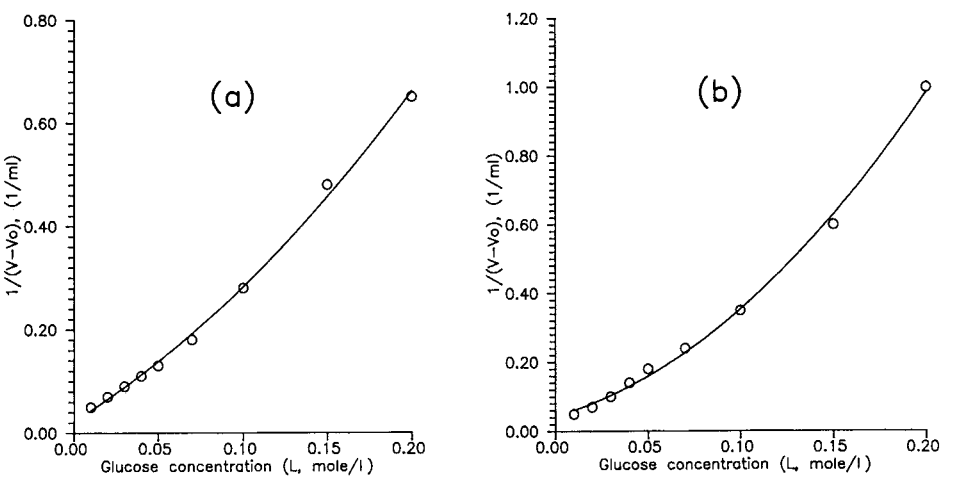

Fig. 2. Relationship between glucose concentration (L) and $(V - V_0)^{-1}$ for (a) glucobiose-immobilized and (b) glucotriose-immobilized columns. Analytical conditions as in Fig. 1.

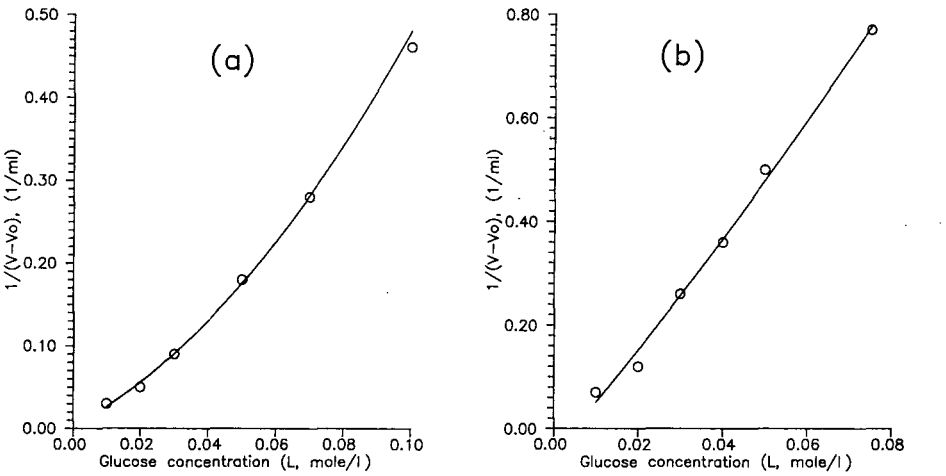

Fig. 3. Relationship between glucose concentration (L) and $(V - V_0)^{-1}$ for (a) mannobiose-immobilized and (b) mannotriose-immobilized columns. Analytical conditions as in Fig. 1.

approximately one order of magnitude higher than that of biose in both series of oligosaccharides. Also, the K_a values for the immobilized mannose oligomers were several times larger than those of the corresponding glucose oligomers having the same DP values.

The K_a value for mannobiose ($4.82 \cdot 10^5$ l mol^{-1}) is approximately 60 times larger than the literature value for methyl α-mannopyranoside ($8.3 \cdot 10^3$ l mol^{-1} at 27°C), obtained by a spectrophotometric method based on displacement of Con A-bound *p*-nitrophenyl α-mannopyranoside with methyl α-mannopyranoside in

TABLE I

ASSOCIATION CONSTANTS OF CON A TO VARIOUS IMMOBILIZED OLIGOSACCHARIDES

Immobilized oligosaccharide	*Association constant (K_a, 10^5 l mol^{-1})*	*Square of decision coefficient (r^2)*[a]
Glucose oligomer:		
Biose	1.30	0.92
Triose	2.04	0.97
Tetraose	14.4	0.94
Mannose oligomer:		
Biose	4.82	0.90
Triose	5.33	0.91
Tetraose	41.0	0.89

[a] $r^2 = \dfrac{[\Sigma(\overline{\text{obs}} - \text{obs}_i)^2 - \Sigma(\text{cal}_i - \text{obs}_i)^2]}{\Sigma(\overline{\text{obs}} - \text{obs}_i)^2}$, where

$\overline{\text{obs}}$ = average of observed values; obs_i = the *i*th observed value and cal_i = the *i*th calculated value.

solution[11]. The immobilized saccharide in this work had mannamine as aglycone, which is bound to silica via the ethoxypropyl group. The variation of the aglycone from the small methyl group in methyl α-mannopyranoside to the bulky aglycone in the immobilized saccharides may be the main cause of the observed difference in the K_a values, although the difference in assay method should also be taken into account.

Although HPAC may not give genuine association constants of free oligosaccharides to proteins, comparison of K_a values among immobilized saccharides obtained under identical conditions offers useful information on structure–affinity relationships. The increase in K_a with increasing DP implies that elongation of the carbohydrate chain increases the binding sites to Con A, *i.e.*, the binding site is not only at the non-reducing monosaccharide residue but also in the interior portion of the carbohydrate chain. It is plausible to assume that the hydroxyl groups in the non-reducing and interior monosaccharide residues were bound to the specific amino acid residue(s) in Con A, and elongation of the oligosaccharide chain resulted in an increase in the number of such bonds, by which Con A–oligosaccharide complexes were stabilized. The effect of the disposition of hydroxyl groups on the affinity to Con A is a problem to be investigated further. A comparative study by using positional isomers of oligosaccharides is now in progress. Considering the Con A part, it is well known that Con A exists as a tetramer of α-subunits under physiological conditions[10]. It may be considered that there are two pairs of subunits and the two subunits of each pair behave identically on binding to an oligosaccharide. However, further structural studies of Con A are necessary before unequivocal conclusions can be drawn.

REFERENCES

1 H. Lis and N. Sharon, in I. E. Liener, N. Sharon and I. J. Goldstein (Editors), *The Lectins*, Academic Press, New York, 1986, p. 293.
2 H. Lis, R. Lotan and N. Sharon, *Methods Enzymol.*, 34 (1974) 341.
3 S. Honda, S. Suzuki and K. Kakehi, *J. Chromatogr.*, 396 (1987) 93.
4 S. Honda, K. Suzuki, S. Suzuki and K. Kakehi, *Anal. Biochem.*, 169 (1988) 239.
5 U. A. Laemmli, *Nature (London)*, 227 (1970) 680.
6 K. Yamashita, T. Mizuochi and A. Kobata, *Methods Enzymol.*, 83 (1982) 105.
7 P. A. J. Gorin, J. F. T. Spencer and S. S. Bhattacharjee, *Can. J. Chem.*, 47 (1969) 1499.
8 S. Honda, M. Takahashi, Y. Nishimura, K. Kakehi and S. Ganno, *Anal. Biochem.*, 118 (1981) 162.
9 H. E. Swaisgood and I. M. Chaiken, in I. M. Chaiken (Editor), *Analytical Affinity Chromatography*, CRC Press, Boca Raton, FL, 1987, p. 65.
10 K. Yamaoka, Y. Tanigawara, T. Nakagawa and T. Uno, *J. Pharmacobio Dyn.*, 4 (1981) 879.
11 W. Bessler, J. A. Shafer and I. J. Goldstein, *J. Biol. Chem.*, 249 (1974) 2819.

Journal of Chromatography, 502 (1990) 305–315
Elsevier Science Publishers B.V., Amsterdam — Printed in The Netherlands

CHROM. 22 052

Sensitive, indirect photometric detector for high-performance liquid chromatography using a light-emitting diode

ALAIN BERTHOD[a], MARK GLICK and JAMES D. WINEFORDNER*
University of Florida, Department of Chemistry, Gainesville, FL 32611 (U.S.A.)
(First received June 15th, 1989; revised manuscript received October 3rd, 1989)

SUMMARY

A low-noise detector for indirect photometric detection has been constructed using a highly stable source —a light-emitting diode (LED). Use of the detector is demonstrated for reversed-phase liquid chromatography by adding methylene blue to the mobile phase to make a background signal. The indirect determination of alcohols by their effect on methylene blue concentration distribution is demonstrated, and an investigation is made into the conditions for high sensitivity. Because the source exhibits low noise, the detection limits for alcohols are as low as more complex and expensive detection methods, despite the lower radiant power of the LED. Detection limits for nine alcohols are below μg injected amounts.

INTRODUCTION

The main problem in liquid chromatography (LC) is detection. In gas chromatography there are different universal detectors such as the flame ionization detector, the electron-capture detector or the mass spectrometer. In LC the column effluent contains trace amounts of solutes of interest that can be difficult to detect. Pre- or post-column derivatization can solve some specific problems, but these techniques are time consuming and are not universal. Another approach is to use a mobile phase containing an additive with an inherent detector response. Analytes can be indirectly detected by their displacement of the additive. This approach is often referred to as indirect detection, and has been demonstrated for a wide variety of chromatographic systems[1]. The most successful use of indirect detection, and one of the earliest, has been for ionic compound LC detection. An absorbing ion is paired with transparent ionic solutes of the opposite charge. The ion pairs can be detected by the counter-ion absorbance[2]. Indirect detection was later extended to non-charged solutes.

There are several problems associated with indirect detection. All chromatograms obtained using indirect methods contain one or more extraneous peaks, called

[a] Permanent address: Laboratoire des Sciences Analytiques, UA CNRS 435 (J. M. Mermet), Université de Lyon 1, 69622 Villeurbanne Cedex, France.

0021-9673/90/$03.50

system peaks[3]. These peaks may result in incorrect peak identification, or coelution with solutes and erroneous quantitation. Baseline instability is another inherent drawback of indirect detection methods.

In previous papers we demonstrated methods for indirect fluorescence detection and proposed a possible mechanism of response[4–6]. We also recently showed that it is possible to construct a high-precision fluorimeter by using a light-emitting diode (LED)[7]. In this work we describe an inexpensive, sensitive indirect photometric detector using an LED. By monitoring the absorbance of a colored additive in the mobile phase, non-absorbing solutes could be indirectly detected. The separation of aliphatic alcohols, using methylene blue as the additive, was chosen as a test system for evaluation of the detector performance. This chromatographic system was first studied by Gnanasambandan and Freiser[8,9].

EXPERIMENTAL

Chemicals

Methylene blue ($C_{16}H_{18}N_3SCl$, mol.wt. 319.9) was purchased from Kodak. The purity was listed as 84%, and it was used as received. Methanol, ethanol, 1-propanol, 2-propanol, 2-methyl-2-propanol, 1-butanol, 2-butanol, 2-methyl-1-butanol, 1-pentanol, 3-pentanol, 1-hexanol, 1-heptanol, 1-octanol and 1-decanol were obtained from Burdick and Jackson, Fisher, Aldrich and Kodak. All were analytical grade and were used as received. Water was deionized and filtered to a resistivity greater than 14 MΩ with a Barnstead Ultrapure system.

Chromatography

An Altex high-performance liquid chromatograph was used to pump the methylene blue–methanol–water mobile phase through a 25 cm × 4.6 mm I.D. Altex Ultrasphere column. The packing material was 5 μm particle size bonded with octadecyl chains and end-capped with trimethyl chlorosilane. The silica pore size was 8 nm mean diameter. The surface area was approximately 200 m^2/g. The carbon loading was approximately 12% (w/w), and the calculated surface coverage is about 2.96 $\mu mol/m^2$. The dry stationary phase column content was estimated to be 2.5 g (column surface area: 620 m^2, column organic stationary phase content: 1.2 mmole). A pulse dampener (Alltech Free-Flow) was used to improve baseline stability. The column was immersed in a water bath for temperature stability. All measurements were made at 30 ± 0.5°C.

Detection system

The LC detector was a modification of the LED fluorometer described in an earlier paper[7]. A diagram of the detection system is shown in Fig. 1.

The peak wavelength of the LED (Hewlett-Packard, HLMP-3950) was 565 nm. Rather than use lenses to transfer the light through the cell, the LED was placed directly on the face of the flow cell. A 12-V motorcycle battery in series with a variable resistance (100–500 Ω) was used to power the LED for long periods of time without recharging. To reduce long-term intensity drift of the LED, the LED was "aged" by operating at high current (>20 mA) for about a week. Urethane foam was used throughout the detector to keep out stray light and to thermostat the LED. A photodiode (EG & G, UV-100BG) was placed next to the LED to monitor the intensity.

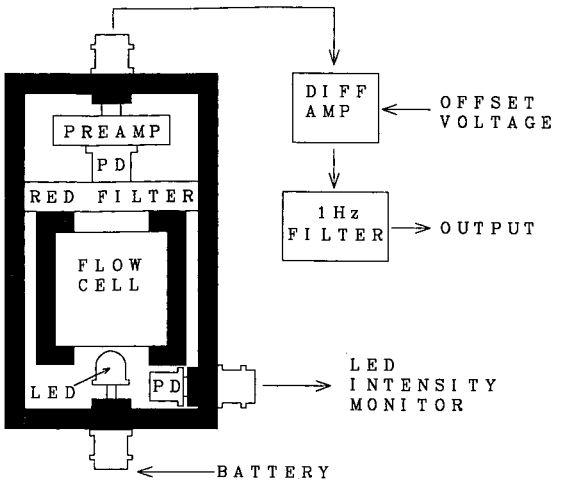

Fig. 1. Diagram of the LED detector. A photodiode (PD) was used to monitor the LED light intensity. A second integral photodiode/preamplifier (PREAMP) detected the transmitted light.

The flow cell was a 1-cm cuvette with an internal volume of 8 μl (Hellma, 176.753). A red glass filter was used to reduce stray light. A combination photodiode/preamplifier (EG & G, TCN 1000-93) was used to detect the light transmitted through the flow cell and the filter. Several 9-V batteries were used to power the detector.

The voltage output of the detector was amplified by a differential amplifier (Princeton Applied Research, 113) with respect to a constant-voltage source (laboratory constructed). The voltage source could be varied to negate the large offset that occurs with indirect photometry. All chromatograms were obtained with an instrumental bandwidth of 1 Hz.

RESULTS

Methylene blue adsorption

The column was conditioned with all of the mobile phases including the dye additive according to the procedure described by Gnanasambandan and Freiser[8,9]. The mobile phase was passed through the column until the effluent absorbance was equivalent to that of the original mobile phase. The mobile phase volume was measured and used to calculate the amount of adsorbed dye (break-through method).

To remove the dye, the column was flushed with 20 internal volumes of pure methanol (1 ml/min for 30 min) and 20 internal volumes of chloroform–methanol (20:80, v/v)[8]. The column was then rinsed overnight with pure methanol (0.5 ml/min for 12 h). All effluents were collected and the dye concentration was spectrophotometrically determined, corresponding to a desorbed quantity of dye. After this treatment, the dye was considered to be removed, although it was still possible to see a very pale blue color in the eluting methanol mobile phase. A maximum dye concentration of $1.2 \cdot 10^{-6} M$ was measured in the case of the water–methanol (95:5) mobile phase after the desorption treatment. The adsorbed amount of dye obtained with the

TABLE I

METHYLENE BLUE ADSORPTION ON ULTRASPHERE ODS

Mobile phase water–methanol (%,v/v)	*Methylene blue concentration* (M)	*Adsorbed amount* mass (g)	*Adsorbed amount* mole (μmole)	*Stationary phase*[a] *concentration* (molar ratio)
95:5	$6.7 \cdot 10^{-4}$	14.8	46	0.035
95:5	$1 \cdot 10^{-4}$	8.3	26	0.020
95:5	$3 \cdot 10^{-5}$	4.0	12.5	0.0096
90:10	$1 \cdot 10^{-4}$	3.5	11	0.0085
40:60	$1 \cdot 10^{-4}$	0.54	1.7	0.0013
30:70	$1 \cdot 10^{-4}$	0.51	1.6	0.0012

[a] The active stationary phase is the ODS layer estimated to be 1.3 mmoles inside the column. The stationary phase concentration is the molar ratio of the adsorbed moles of dye over the ODS moles (1.3) in the column.

break-through method was in agreement within 10% with the corresponding desorbed amount. The average values are listed in Table I.

Separation of aliphatic alcohols

Fig. 2 presents the chromatogram obtained after injecting a mixture of six alcohols. Table II lists the chromatographic parameters and analytical figures of merit for the mobile phases studied. Fig. 3 shows a chromatogram obtained after injecting a mixture of nine alcohols. Peak heights were used for quantitation. The detector response was linear over three orders of magnitude of injected concentration

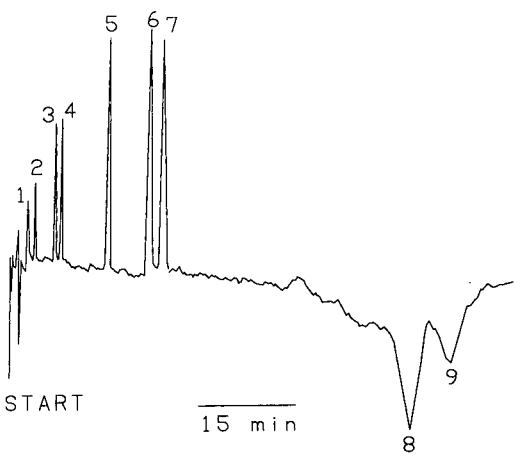

Fig. 2. Indirect chromatogram of six alcohols. Mobile phase water–methanol (95:5, v/v) with methylene blue 10^{-4} *M*, 1 ml/min, 30°C. Peaks: 1 = methanol; 2 = ethanol; 3 = 2-propanol; 4 = 1-propanol; 5 = 2-methyl-2-propanol; 6 = 2-butanol; 7 = 1-butanol; 8, 9 = system peaks. Injection: 8 μg of each alcohol but methanol (injection of a 20 μl 0.05%, v/v, solution).

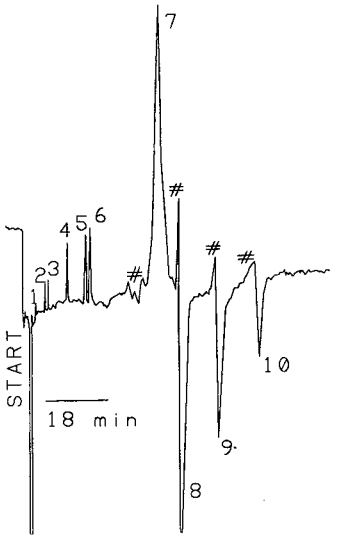

Fig. 3. Indirect chromatogram of nine alcohols. Mobile phase water–methanol (90:10, v/v) with methylene blue $10^{-4}M$, 1 ml/min, 30°C. Peaks: 1 = ethanol (6 μg); 2 = 2-propanol (6 μg); 3 = 1-propanol (6 μg); 4 = 2-methyl-2-propanol (6 μg); 5 = 2-butanol (6 μg); 6 = 1-butanol (6 μg); 7 = 3-pentanol (16 μg); 8 = system peak; 9 = 2-methyl-1-butanol (16 μg); 10 = 1-pentanol (16 μg); # = shoulder peaks, see text.

(0.005% to 5%, v/v, injected solution) for the water–methanol (95:5) mobile phase. The linearity was only two orders of magnitude for the other mobile phases.

Peak efficiencies, N, were determined using the classical plate count equation for Gaussian peaks, $N = 4\,(V_R/w_{0.6h})^2$, in which V_R is the retention volume and $w_{0.6h}$ is the peak width, expressed in volume units, at 60% of the peak height.

DISCUSSION

LED detector

The capabilities of the simple LED detector presented in this paper are demonstrated by the low limits of detection (LOD) obtained for aliphatic alcohols (Table II). As described by Takeuchi and Yeung[10], the dynamic reserve, the concentration of the absorbing additive, and the displacement ratio play important roles in determining the sensitivity that can be achieved with indirect detection. The dynamic reserve of a detector is defined as the ratio of the background signal to its noise level[10]. Although the light power of an LED is low, in the 50 mW range, the emitted light is so stable, with root mean square noise fluctuation in the 0.0004% range[7], that the signal-to-noise ratio is better than many other light sources.

The concentration of the absorbing species —the mobile phase additive— is responsible for the background signal. However, it also has a strong influence on the amount of dye adsorbed on the stationary phase (Table II). In our case, we found that the amount of methylene blue adsorbed in the Ultrasphere ODS column followed a Langmuir isotherm, *i.e.* the ratio 1/(mobile phase dye concentration) is proportional

TABLE II

CHROMATOGRAPHIC RETENTION PARAMETERS AND ANALYTICAL FIGURES OF MERIT

Mobile phase water–methanol	*Methylene blue concentration (M)*	*Alcohol*	V_R *(ml)*	*k'*	*N (plates)*	*LOD*		*Response factor (a.u./mmol)*
						μg	*nmole*	
95:5	$1 \cdot 10^{-4}$	Ethanol	3.72	1.25	3900	1.6	29	130
		2-Propanol	6.84	3.15	5100	0.9	15	290
		1-Propanol	7.80	3.73	5200	0.9	15	310
		2-Methyl-2-propanol	15.2	8.20	6200	0.6	8	730
		2-Butanol	21.8	12.2	6800	0.5	6.8	750
		1-Butanol	23.9	13.5	6600	0.5	6.8	660
		System I	63.2[a]	37.3	2900	–	–	–
		System II	69.3[a]	41.0	2900	–	–	–
95:5	$3 \cdot 10^{-5}$	Ethanol	3.62	1.19	3500	2.0	44	51
		2-Propanol	6.75	3.09	4200	1.4	24	100
		1-Propanol	7.65	3.64	4200	1.3	12	110
		2-Methyl-2-propanol	15.0	8.09	4900	1.0	13.5	230
		2-Butanol	21.3	11.9	5700	0.9	12.2	240
		1-Butanol	23.2	13.1	6000	0.9	12.2	260
		System I	63.0[a]	37.1	2800	–	–	–
		System II	69.1[a]	40.8	2800	–	–	–

90:10	$1 \cdot 10^{-4}$	Ethanol	3.42	1.07	7000	3.0	65	29
		2-Propanol	5.88	2.56	9500	1.5	25	83
		1-Propanol	6.72	3.07	9500	1.5	25	84
		2-Methyl-2-propanol	12.4	6.49	11000	0.7	9.5	210
		2-Butanol	17.7	9.73	13000	0.7	9.5	210
		1-Butanol	19.3	10.7	11000	0.6	8.2	240
		3-Pentanol	38.1	22.1	2800	0.4	4.5	360
		2-Methyl-1-butanol	55.5[a]	32.6	11000	0.9	9.9	170
		1-Pentanol	72.1[a]	42.7	12000	1.1	12	140
		System peak	45.3[a]	26.4	–	–	–	–
40:60	$1 \cdot 10^{-4}$	1-Pentanol	4.82	1.91	–[b]	60	680	6.1
		1-Hexanol	7.41	3.45	4400	110	1080	3.9
		1-Heptanol	12.0	6.27	4200	30	260	13
		1-Octanol	21.6[a]	12.1	4000	30	230	13
		1-Decanol	76.5[a]	45.5	4300	100	630	2.2
		System peak I	5.1[a]	2.09	–[b]	–	–	–
		System peak II	15.0[a]	8.09	–[b]	–	–	–
		System peak III	17.1[a]	9.36	–[b]	–	–	–

[a] Negative peak
[b] Efficiency cannot be calculated due to peak overlap.

to the ratio 1/(stationary phase dye concentration) with a regression coefficient r = 0.9997. The same relationship was observed by Vigh and Leitold[11] with benzyl alcohol as the absorbing additive and a Merck RP-18 stationary phase.

The displacement ratio is the number of dye molecules displaced by one solute molecule. The higher the displacement number, the higher the detection sensitivity. Clearly the displacement ratio is dependent on the amount of adsorbed dye on the stationary phase. Table II shows that the response factors are lower when the adsorbed amount of dye is lower (Table I). The LOD values of the water–methanol (95:5) mobile phase containing only $3 \cdot 10^{-5}$ M of methylene blue were 50% higher than the corresponding value with the same mobile phase containing 10^{-4} M of dye (Table II). Decreasing the dye concentration in the mobile phase produced a decrease in background signal and noise, which should increase the sensitivity. However, a concurrent reduction in the amount of adsorbed dye produced a decrease in the displacement ratio and in the response factor, which should decrease the sensitivity. The global effect was negative, producing higher LOD values with lower mobile phase dye concentrations.

The chromatograms of Figs. 2 and 3 and the analytical figures of merit listed in Table II compare quite well with those of similar studies found in the literature[2,8,9,12]. These figures of merit demonstrate the utility of the simple LED detector.

Chromatographic efficiency

The column efficiency was tested using a commercial UV LC detector with a classical mobile phase (methanol–water 70:30) and was found to be in the 12 000 plate range (height equivalent to a theoretical plate = 20 μm or 4 × particle diameter). The efficiencies measured with the LED detector and the water–methanol (95:5) mobile phase were 50% lower (Table II), while those obtained with the water–methanol (90:10) mobile phase were in the 12 000 plate range. We think that the high water content (95%) of the first mobile phase is responsible for the lower efficiency. It has been shown that water-rich mobile phase does not properly wet the monolayer ODS stationary phases. The C_{18} hydrocarbon chain of the "brush" type ODS phase can be agglomerated by water (hydrophobic repulsion)[13]. Such a water collapsed state is destroyed by about 10% methanol which can wet the C_{18} chains and restore the efficiency (Table II). A low efficiency was also obtained with a methanol-rich mobile phase, but the corresponding experiments were performed last and we suspected column aging. The detector flow cell volume (8 μl) was suitable for classical chromatographic analysis and did not induce excessive band broadening.

System peaks

Figs. 2 and 3 and Table II show system peaks. As stated already, such peaks always appear in indirect detection methods. System peaks have been intensively studied in the literature[3,11,14–16]. They are produced by a disruption of the adsorbed mobile phase components (dye additive, methanol and water) by the injected sample. It was found that system peaks carried much useful information about adsorption isotherms, void volumes and retention mechanisms[3,14]. In indirect detection chromatography, one of the system peaks corresponded to the retention of the absorbing additive. In our case, we observed two system peaks with the water–methanol (95:5) (Fig. 2) and only one with the water–methanol (90:10) mobile phase (Fig. 3). As

system peaks are not really useful for quantitative analysis, it is best to minimize them by dissolving all injected solutes in the mobile phase with the same amount of dye. In Fig. 3a symbol marks shoulders or associated peaks that appeared before each peak that was close to the system peak. Similar artifacts were observed by Parkin and Lau[17] who suggested that they were due to refractive index changes. We think the artifact peaks could be due to a local methylene blue concentration perturbation. They may also arise from an absorbing impurity in the methylene blue, which was only 84% pure. An impurity would explain the second system peak observed with some mobile phase compositions (Fig. 2).

Chromatographic mechanism

The alcohol–methylene blue complex formation advanced by Gnanasambandan and Freiser[8] was questioned by several authors[11,17,18]. The mechanistic interpretation of induced peaks described by Stranahan and Deming[16] more likely explains the alcohol–methylene blue induced peaks obtained in our case. The injection of a solute disturbs the steady-state concentration distribution of methylene blue in the injection zone and this disturbance travels through the column. This leads to an induced peak that coelutes with the solute and a peak in the reverse direction eluting at the dye retention time. For solutes with retention times shorter than the system peak, the local disturbance is a solubility enhancement of the dye in the mobile phase due to the presence of the alcohol. Conversely, if the alcohol retention time is greater than the system peak, then the disturbance is a decrease in the solubility of the dye in the mobile phase (Fig. 3).

Table III lists the slopes and intercepts and regression coefficients of the plots $\log k' = f(n_c)$, in which n_c is the carbon number of linear aliphatic alcohols. The logarithm of the capacity factor k' can be related to the free energy of phase transfer of the solute, ΔG^0, by:

$$\ln k' = \Delta G^0/RT + \ln \varphi$$

where R, T and φ are the gas constant, the absolute temperature and the phase ratio of the column[19]. For members of a homologous series of solutes, such as the linear primary alcohols, the previous equation can be written as:

$$\ln k' = \Delta G_e^0/RT + \ln \varphi + n_c \Delta G_i^0/RT$$

TABLE III

METHYLENE FREE ENERGY OF TRANSFER FOR LINEAR ALCOHOLS

Mobile phase water–methanol	*log k' = f(n_c)*	*n_c*	*Correlation coefficient*	*$\Delta G^0_{CH_2}$ (kJ/mol)*
95:5	$-0.950 + 0.517\ n_c$	3	0.9989	3.0
95:5[a]	$-0.983 + 0.522\ n_c$	3	0.9993	3.0
90:10	$-1.238 + 0.571\ n_c$	4	0.9996	3.3
40:60	$-1.116 + 0.276\ n_c$	5	0.9996	1.6
30:70	$-0.985 + 0.209\ n_c$	5	0.9996	1.2

[a] Methylene blue concentration $3 \cdot 10^{-5}$ *M*, all other mobile phase contained $1 \cdot 10^{-4}$ *M* methylene blue.

in which the subscripts e and i refer to the retention energy contribution of the end group (OH) and the incremental (CH_2) group, respectively.

The first two entries listed in Table III show that there was no significant change in the retention mechanism when the methylene blue concentration was changed. The dye does not seem to interfere in the retention process. The methylene free energy increased from 3.0 to 3.3 kJ/mol when the methanol mobile phase content increased from 5 to 10%. This is evidence of the better wetting of the stationary phase by the 10% methanol mobile phase. Because the "collapsed" state is destroyed by the 10% methanol, the ODS chains have an enhanced mobility and they can interact more easily with the alcohol alkyl chains. At higher methanol content, the polarity difference between the stationary and the mobile phase decreased and so did the methylene blue free energy of transfer (Table III).

Some long-term noise was observed in all separations. Typically, the baseline fluctuated by 1% full scale with a period of several hours. Figs. 2 and 3 show chromatograms lasting more than an hour where the long term baseline drift can be seen. We found such baseline drifts in most papers showing indirect detection chromatograms lasting for more than one hour[1,2,8,12,17,18]. The short-term, peak–peak noise of the detection system was 0.004% —a factor of ten poorer than the noise of the LED. Pressure and temperature instabilities were believed to be responsible for this degradation. The steady-state dye distribution is very sensitive to any variation. The whole system must be carefully temperature regulated in order to minimize such noise. It is also possible that each injection induced "second order" or higher order systems peaks that would explain the long-term noise observed.

CONCLUSIONS

A simple, compact low-noise LED-filter-photodiode indirect photometric detector for reversed-phase high-performance LC using methylene blue in the mobile phase is shown to have use for non-absorbing solutes. Because of the low noise of both the LED source and the photodiode detector, the detection limits for alcohols are similar to more expensive, more complex commercial systems based on various spectrometric principles. The detector could easily be miniaturized further and operated in the field. The potential use of this detector in a mobile system appears considerable.

ACKNOWLEDGEMENT

This research was supported by NIH-RO1-GM11373-26.

REFERENCES

1 G. Schill and J. Crommen, *Trends Anal. Chem.*, 6 (1987) 111.
2 M. Denkert, L. Hackzell, G. Schill and E. Sjögren, *J. Chromatogr.*, 218 (1981) 31.
3 S. Levin and E. Grushka, *Anal. Chem.*, 58 (1986) 1602.
4 S. Y. Su, A. Jurgensen, A. Bolton and J. D. Winefordner, *Anal. Lett. Part A.*, 14 (1981) 1.
5 S. Y. Su, E. P. C. Lai and J. D. Winefordner, *Anal. Lett. Part A.*, 15 (1982) 439.
6 E. L. Torres, F. Van Geel and J. D. Winefordner, *Anal. Lett. Part A*, 16 (1983) 1207.
7 B. W. Smith, B. T. Jones and J. D. Winefordner, *Applied Spectrosc.*, 42 (1988) 1469.

8 T. Gnanasambandan and H. Freiser, *Anal. Chem.*, 54 (1982) 1282.
9 T. Gnanasambandan and H. Freiser, *Anal. Chem.*, 53 (1981) 909.
10 T. Takeuchi and E. S. Yeung, *J. Chromatogr.*, 366 (1986) 145.
11 G. Vigh and A. Leitold, *J. Chromatogr.*, 312 (1984) 345.
12 L. Hackzell, T. Rydberg and G. Schill, *J. Chromatogr.*, 282 (1983) 179.
13 R. K. Gilpin, *J. Chromatogr. Sci.*, 22 (1984) 371.
14 S. Levin and E. Grushka, *Anal. Chem.*, 59 (1987) 1157.
15 G. Brandt, P. Vógler and A. Kettrup, *Fresenius Z. Anal. Chem.*, 325 (1986) 252.
16 J. J. Stranahan and S. N. Deming, *Anal. Chem.*, 54 (1982) 1540.
17 J. E. Parkin and H. T. Lau, *J. Chromatogr.*, 314 (1984) 488.
18 W. Kang, H. B. Oh and Y. J. Moon, *J. Korean Chem. Soc.*, 31 (1987) 184.
19 G. Guiochon, in Cs. Horváth (Editor), *High-Performance Liquid Chromatography —Advances and Perspectives*, Vol. 2 Academic Press, New York, 1980.

Journal of Chromatography, 502 (1990) 317–324
Elsevier Science Publishers B.V., Amsterdam — Printed in The Netherlands

CHROM. 22 101

Automated precolumn derivatization of amino acids with *ortho*-phthalaldehyde using a hollow-fibre membrane reactor

JUN HAGINAKA* and JUNKO WAKAI
Faculty of Pharmaceutical Sciences, Mukogawa Women's University, 11-68, Koshien Kyuban-cho, Nishinomiya 663 (Japan)
(First received April 12th, 1989; revised manuscript received August 8th, 1989)

SUMMARY

An automated precolumn derivatization procedure was developed for the determination of amino acids, involving the reaction of amino acids with *o*-phthalaldehyde (OPA) and 2-mercaptoethanol using a cation-exchange hollow-fibre membrane reactor, which is immersed in the reagent solution, and a trap column. Column switching is used to transfer OPA–amino acid derivatives from the trap column to an analytical C_{18} column, and the derivatives are subjected to gradient elution and fluorimetric detection. The detection limit is 0.3–2 pmol for each amino acid. For 20 pmol of amino acids, the precision is 0.9–5.0% (relative standard deviation, $n = 5$). The determination of amino acids in a protein hydrolysate sample is described.

INTRODUCTION

In recent years, automated procedures for pre- and postcolumn derivatization have been developed for the high-performance liquid chromatographic (HPLC) determination of various compounds. For the trace determination of amino acids, precolumn derivatization with dansyl chloride[1], 4-fluoro-7-nitrobenzo-2-oxa-1,3-diazole[2], *o*-phthalaldehyde (OPA)[3,4] and 9-fluorenylmethyl chloroformate[5] and phenyl isothiocyanate[6] has been employed.

Although the precolumn derivatization method with OPA is sometimes applied to amino acids, the precision of the method is dependent on the control of the reaction time. Therefore, various automated procedures have been developed, such as those using a peristalic pump[7,8], a reciprocating pump[9], or pneumatic pressure[10] to mix the sample and reagent, those using an automatic injector and a glass bead column (the former for injecting the sample and reagent and the latter for performing the derivatization reaction)[11,12] and those using a modified automatic injector[13,14]. Recently, an automatic injector which can automate precolumn derivatization has become commercially available. The problem with most such automated procedures is that they require the delivery, injection or dispensing of two or three solutions (sample and reagent solutions or these two plus the derivatized solutions). Errors in any of

0021-9673/90/$03.50

these procedures would have a detrimental effect on the precision and accuracy of the assay.

In a previous paper[15], we reported an HPLC method for the determination of amino acids using cation-exchange and anion-exchange hollow-fibre membrane reactors (HFMRs) immersed in hypochlorite, and OPA and 2-mercaptoethanol (2-ME) reagents, which are introduced into the main flow-stream by a concentration differential. This paper deals with automated procedures for the precolumn derivatization of amino acids with OPA and 2-ME using a cation-exchange HFMR. The advantage of the proposed method is that only one injection of the sample solution is needed because of the continuous supply of a constant amount of the reagent through the HFMR. This method was successfully applied to the determination of amino acids in a protein hydrolysate sample.

EXPERIMENTAL

Reagents and materials

Amino acids (L-form) were purchased from the Protein Research Foundation (Minoh, Osaka, Japan). OPA, 2-ME, and bovine serum albumin (BSA) were obtained from Nacalai Tesque (Kyoto, Japan). Acetonitrile of HPLC grade and other chemicals of analytical-reagent grade were obtained from Wako (Osaka, Japan). A cation-exchange HFMR (AFS-2) was obtained from Dionex (Sunnyvale, CA, U.S.A.).

Water prepared with a NANOpure II unit (Barnstead, Boston, MA, U.S.A.) was used for the preparation of the eluent and the sample solution. The OPA–2-ME reagent solution was prepared by dissolving 300 mg of OPA in 3 ml of ethanol and, after addition of 120 μl of 2-ME, diluting the solution to 20 ml with 20 m*M* borate buffer solution (pH 9.3).

Chromatography

The experimental setup is illustrated in Fig. 1. The pumps were a Trirotar-V pump (pump A) (Japan Spectroscopic, Tokyo, Japan) equipped with a gradient

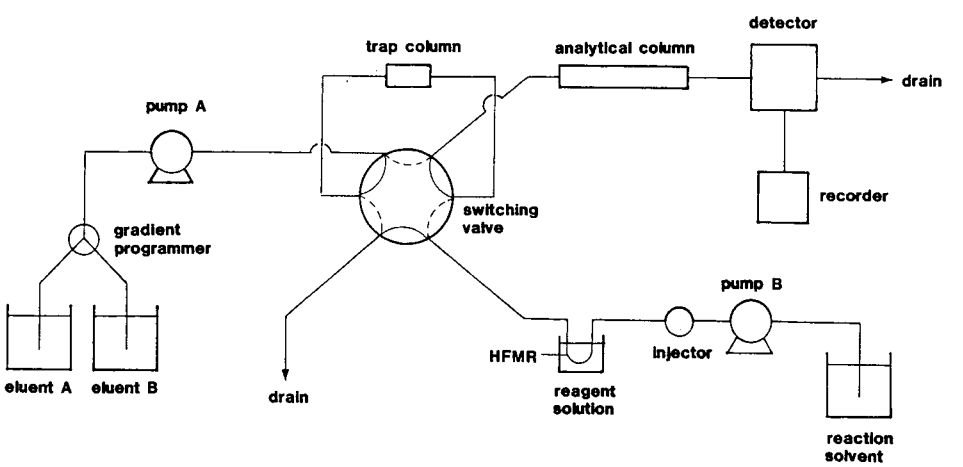

Fig. 1. Experimental setup. HFMR = hollow-fibre membrane reactor. Dashed lines, flow lines for the precolumn derivatization; solid lines, flow lines for separation and detection of the OPA–amino acid derivatives.

programmer (GP-A40; Japan Spectroscopic) and a degasser (KT-31, Showa Denko, Tokyo, Japan) for delivering the eluent and a Bip-I pump (pump B) (Japan Spectroscopic) for delivering the reaction solvent. The injector and automatic sampler were a Model 7125 loop injector (Rheodyne, Cotati, CA, U.S.A.) equipped with a 100-μl loop or a Sil-9A Auto Injector (Shimadzu, Kyoto, Japan), respectively. The columns were a 250 × 4.6 mm I.D. column packed with Develosil ODS-5 (5-μm particle size) (Nomura Chemicals, Seto, Aichi, Japan), a guard column (30 × 4.6 mm I.D.) packed with the same materials and a trap column (10 × 4.6 mm I.D.) packed with Capcell Pak C_{18} (10–25-μm particle size) (Shiseido, Tokyo, Japan), which is a silicone-coated silica gel modified with octadecyl groups and has excellent stability against alkaline mobile phases such as at pH 9–10[16]. Other equipment consisted of a cation-exchange HFMR, 15 cm in length, a PT-8000 six-port switching valve (Tosoh, Tokyo, Japan), an F1000 spectrofluorimeter detector (Hitachi, Tokyo, Japan) equipped with a 12-μl flow-through cell and a C-R3A recorder–integrator (Shimadzu).

The eluents used were as follows: eluent A, 5 m*M* sodium dihydrogenphosphate–5 m*M* disodium hydrogenphosphate–acetonitrile (4:4:1, v/v/v); eluent B, 5 m*M* sodium dihydrogenphosphate–5 m*M* disodium hydrogenphosphate–acetonitrile (1:1:2, v/v/v); linear gradient, 0–70 min, 80% eluent B. The flow-rate was maintained at 0.8 ml/min. The reaction solvent, with the flow-rate maintained at 0.1 ml/min, was 20 m*M* borate buffer solution (pH 9.3).

The HFMR inserted between the injector and the trap column was immersed in 20 ml of OPA and 2-ME reagent. The HFMR was inserted in a PTFE tube (*ca.* 2 cm × 0.8 mm I.D.) and was attached to the connecting fittings (Japan Spectroscopic), as reported previously[17]. Precolumn reaction and separation were carried out at ambient temperature. Detection was performed with excitation at 340 nm and emission at 450 nm.

Automated precolumn derivatization procedure

Automated precolumn derivatization of amino acids with OPA was accomplished by employing the HFMR, a trap column and a six-port switching valve. Amino acid samples were introduced via the injector or the automatic sampler for the semi-automated or fully automated procedure, respectively. The samples reacted both in the HFMR and in the trap column. The OPA and 2-ME were delivered through the passive HFMR immersed in the reagent solution, by a concentration differential. The six-port valve was switched 2 min after injection of the sample. The OPA–amino acid derivatives were transferred to the analytical column in the back-flush mode and separated by gradient elution.

Preparation of protein hydrolysate sample

The protein sample (*ca.* 1 mg) was dissolved in 1 ml of 6 *M* hydrochloric acid and transferred to a hydrolysis tube. The tube was flushed with nitrogen, sealed and left in an oven at 110°C for 24 h. The hydrolysate sample was neutralized with 6 *M* sodium hydroxide solution and diluted 50-fold with 5 m*M* sodium dihydrogenphosphate–5 m*M* disodium hydrogenphosphate–acetonitrile (4:4:1, v/v/v). A 20-μl aliquot of the sample was injected onto the system described above.

RESULTS AND DISCUSSION

Precolumn reaction conditions for HFMR

In a previous paper[15], we reported the successful postcolumn derivatization of primary and secondary amino acids with OPA and 2-ME and with hypochlorite using cation- and anion-exchange HFMRs immersed in the reagent solution. The negatively charged membrane matrices permitted transport of both the uncharged and positively charged spcies due to the concentration gradient[15]. In this study, we tried to automate the precolumn derivatization of amino acids with OPA and 2-ME by using cation-exchange HFMR and a trap column in a precedure that included column switching.

The precolumn reaction conditions for Asp, Asn, Thr, Arg and Ala as typical amino acids were examined with respect to the various factors affecting the precolumn reaction: pH of the reaction solution, length of HFMR, reaction time and concentrations of OPA and 2-ME. The pH of the reaction solution used for the precolumn derivatization of amino acids with OPA was 9–10[7–14]. Therefore, we selected 20 m*M* borate buffer (pH 9.3) as the reaction solvent. The length of the HFMR, which is an important factor for introducing the reagent into the sample flow stream, was varied from 7.5 to 30 cm. Under the assumption that the derivatization reaction occurred completely, the leakage of Arg (basic amino acid) from the negatively charged membrane matrices was about 40, 65, 80% at HFMR lengths of 7.5, 15 and 30 cm, respectively (leakage calculated by comparison with standard loop injection of the corresponding OPA–amino acid derivatives). No leakage of other amino acids, except Asp (about 30% at a length of 15 cm), was observed in spite of the length of the HFMR. Therefore, 15 cm was chosen as the length of the HFMR. Since the leakage of ammonia from the negatively charged membrane matrices occurs to a greater extent than that of Arg, the present precolumn derivatization method is almost free from the influence of any ammonia which may contaminate the sample solutions.

The instability of OPA–amino acid derivatives is known to affect the precision and accuracy of precolumn derivatization methods[9,10]. The factor that must be controlled most precisely is the reaction time. In our precolumn reaction system, the factors affecting the reaction time were the flow-rate of the reaction solvent and the column switching time.

Fig. 2A and B show the effects of the flow-rate of the reaction solvent and the column switching time, respectively, on the fluorescence intensity of the OPA–amino acid derivatives. At 0.2 ml/min (column switching time 2 min), the peak of Asp was not observed owing to elution of the OPA–Asp derivative from the trap column. The fluorescence intensity of Arg increased with increase in flow-rate, because Arg leakage decreased with decrease in residence time. Therefore, the flow-rate of the reaction solvent was fixed at 0.1 ml/min.

The column switching time was varied from 1 to 5 min. Asp was eluted from the trap column at a column switching time of later than 4 min. The fluorescence intensity of the other amino acid derivatives was almost constant at column switching times longer than 2 min. Therefore, the column switching time was selected as 2 min.

Fig. 3A and B illustrate the effects of the concentrations of OPA and 2-ME on the fluorescence intensity. The fluorescence intensities of Arg and Ala were almost unaffected by the concentrations of OPA and 2-ME, whereas those of the other amino

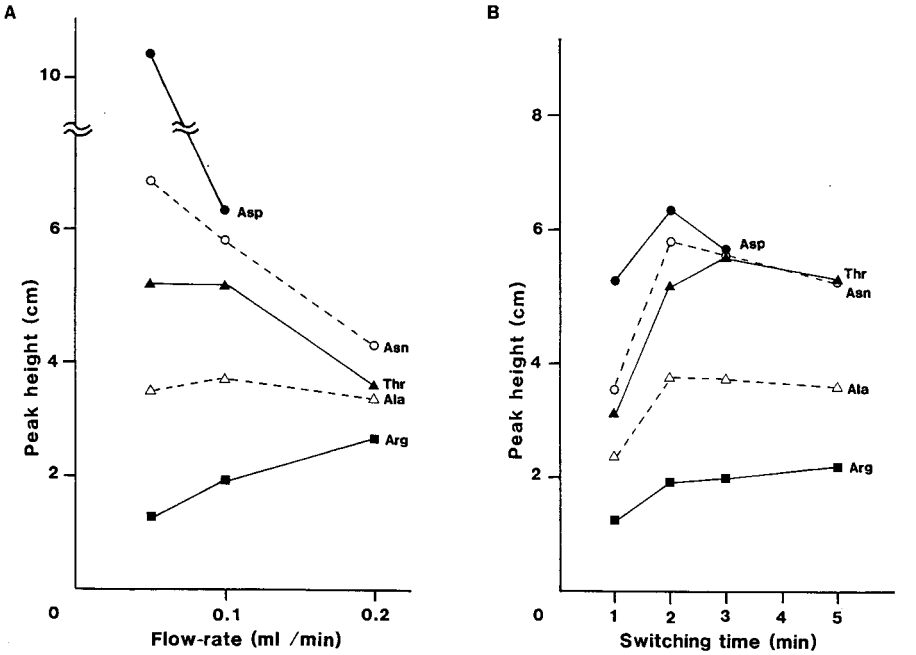

Fig. 2. Effects of (A) flow-rate of the reaction solvent and (B) column switching time on the fluorescence intensity of the OPA–amino acid derivatives. Amounts of 100 pmol of each amino acid were injected and the peak heights were measured. The concentrations of OPA and 2-ME were 15 mg/ml and 0.6%, respectively. (A) Switching time fixed at 2 min and (B) flow-rate of reaction solvent fixed at 0.1 ml/min.

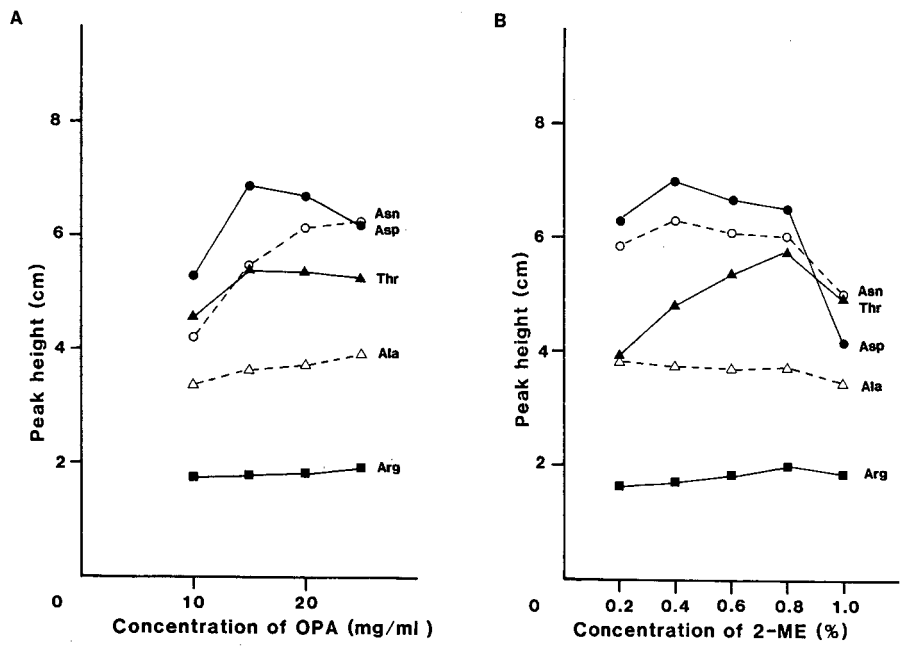

Fig. 3. Effects of concentrations of (A) OPA and (B) 2-ME on the fluorescence intensity of the OPA–amino acid derivatives. Amounts of 100 pmol of each amino acid were injected and the peak heights were measured. Flow-rate of reaction solvent, 0.1 ml/min; switching time, 2 min. (A) Concentration of 2-ME fixed at 0.6% and (B) concentration of OPA fixed at 15 mg/ml.

acids were considerably affected. The optimum concentrations of OPA and 2-ME were determined to be 15 mg/ml and 0.6%, respectively.

The precolumn reaction conditions described under Experimental were used for the assay of amino acids. The chromatogram of a standard mixture of amino acids, obtained under the optimum precolumn reaction conditions, is shown in Fig. 4.

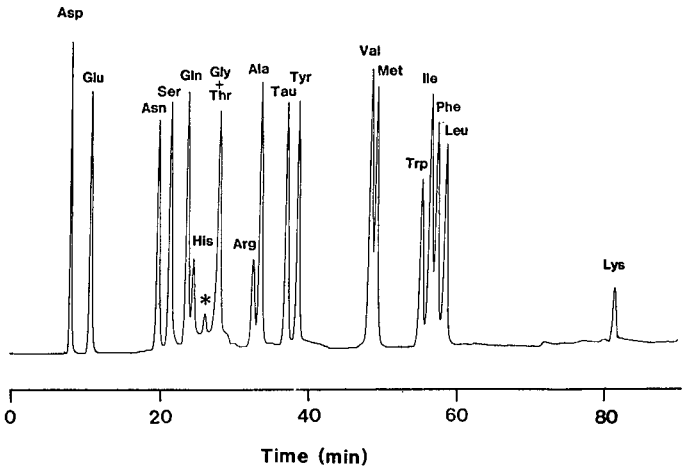

Fig. 4. Chromatogram of a standard mixture of amino acids. Amount injected, 100 pmol of each except for 50 pmol for Gly and Thr and 200 pmol for Lys. The asterisk indicates a system peak.

Reproducibility, linearity and detection limits

Table I lists the relative standard deviations (R.S.D.) ($n = 5$) for the measured peak heights of standard amino acids when 20 and 100 pmol were injected. The reproducibility was good for the amino acids studied. The measured peak heights were randomly scattered around a mean value, and there were no trends such as a constant decrease in peak height with time. This shows that at the reaction stage the optimum concentrations of OPA and 2-ME are maintained in spite of their continuous depletion. Although the OPA–2-ME reagent could still be used after a 24-h run, it was freshly prepared every day.

The calibration graph constructed from peak height *versus* absolute amount of each amino acid was linear over the range 2–500 pmol with a correaltion coefficient of 0.999 or above, and passed through the origin. The detection limits for amino acids with the proposed method are below 0.3–2 pmol and are determined by the purity of the reagent rather than by the signal-to-noise ratio, as reported previously[8].

Application to determination of protein amino acids

On the basis of the above findings, we applied the method to the determination of protein amino acids. Fig. 5 shows a chromatogram of a BSA hydrolysate sample. As the asparagine and glutamine residues were converted to aspartic acid and glutamic acids, respectively, during acid hydrolysis, they did not appear on the chromatogram. The composition of the amino acids agreed very well with that reported previously[15,18], as shown in Table II.

TABLE I

REPRODUCIBILITY OF AMINO ACID ASSAY

Relative standard deviations (R.S.D.) of five analyses. Amounts of Gly and Thr injected, 10 or 50 pmol of each.

Amino acid	*R.S.D. (%)*	
	20 pmol	*100 pmol*
Asp	5.0	4.0
Glu	2.9	2.9
Asn	2.1	2.6
Ser	4.7	2.3
His	1.6	3.1
Gly + Thr	4.0	3.3
Arg	4.6	3.6
Ala	2.0	1.8
Tau	1.1	0.6
Tyr	1.3	0.8
Met	0.9	1.0
Val	2.1	1.3
Trp	1.6	0.6
Ile	0.9	0.8
Phe	1.4	0.9
Leu	1.6	2.1
Lys	4.5	3.5

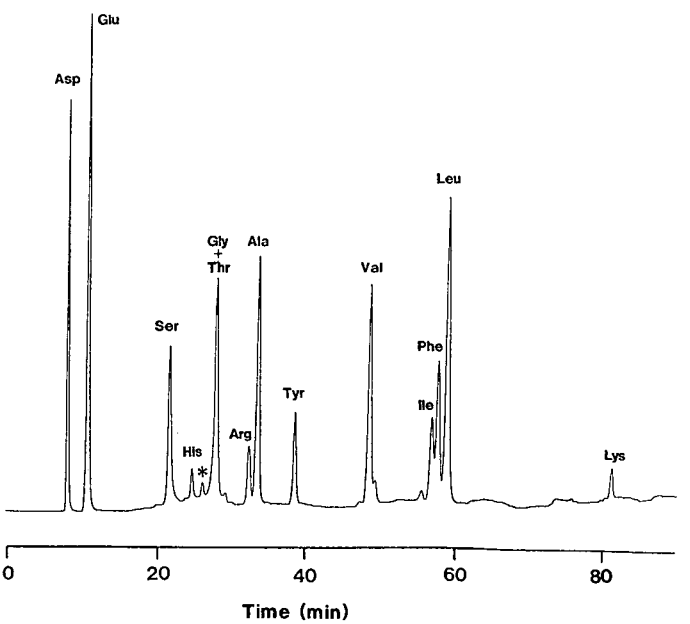

Fig. 5. Chromatogram of a BSA hydrolysate sample. The asterisk indicates a system peak.

TABLE II

AMINO ACID COMPOSITION OF BOVINE SERUM ALBUMIN

All values normalized to alanine = 1.00.

Amino acid	*Found*	*Known*
Asp + Asn	1.24	1.20
Glu + Gln	1.77	1.73
Ser	0.55	0.61
His	0.35	0.34
Arg	0.73	0.51
Ala	1.00	1.00
Tyr	0.37	0.37
Val	0.78	0.69
Ile	0.32	0.23
Phe	0.58	0.54
Leu	1.42	1.27
Lys	1.20	1.28

We are now investigating the application of this automated precolumn derivatization method to assays of biological substances and drugs in biological fluids followed by automated pretreatments such as deproteinization, extraction, and/or concentration.

ACKNOWLEDGEMENTS

The authors are grateful to T. Uno and H. Yasuda, Mukogawa Women's University, for their interest and support.

REFERENCES

1 J. M. Wilkinson, *J. Chromatogr. Sci.*, 16 (1978) 547.
2 Y. Watanabe and K. Imai, *J. Chromatogr.*, 309 (1984) 279.
3 P. Lindroth and K. Mopper, *Anal. Chem.*, 51 (1979) 1667.
4 D. W. Hill, F. H. Walters, T. D. Wilson and J. D. Stuart, *Anal. Chem.*, 51 (1979) 1338.
5 S. Einarsson, S. Folestad, B. Josefsson and S. Lagerkvist, *Anal. Chem.*, 58 (1986) 1638.
6 S. A. Cohen and D. J. Strydom, *Anal. Biochem.*, 174 (1988) 1, and references cited therein.
7 K. Venema, W. Leever, J. O. Bakker, G. Haayer and J. Korf, *J. Chromatogr.*, 260 (1983) 371.
8 R. H. Buck and K. Krummen, *J. Chromatogr.*, 303 (1984) 238.
9 M. J. Winspear and A. Oaks, *J. Chromatogr.*, 270 (1983) 378.
10 D. E. Willis, *J. Chromatogr.*, 408 (1987) 217.
11 M. O. Fleury and D. V. Ashley, *Anal. Biochem.*, 133 (1983) 330.
12 R. J. Smith and K. A. Panico, *J. Liq. Chromatogr.*, 8 (1985) 1783.
13 J. C. Hodgin, P. Y. Howard, D. M. Ball, C. Cloete, L. de Jager, *J. Chromatogr. Sci.*, 21 (1983) 503.
14 C. Cloete, *J. Liq. Chromatogr..*, 7 (1984) 1979.
15 J. Haginaka and J. Wakai, *Anal. Biochem.*, 171 (1988) 398.
16 Y. Ohtsu, H. Fukui, T. Kanda, K. Nakamura, M. Nakano, O. Nakata and Y. Fujiyama, *Chromatographia*, 24 (1987) 380.
17 J. Haginaka, J. Wakai and H. Yasuda, *Anal. Chem.*, 59 (1987) 324.
18 M. O. Dayhoff, *Atlas of Protein Sequence and Structure*, Vol. 5, Suppl. 2, National Biomedical Foundation, Washington, DC, 1976.

Journal of Chromatography, 502 (1990) 325–336
Elsevier Science Publishers B.V., Amsterdam — Printed in The Netherlands

CHROM. 22 076

High-performance liquid chromatography of insulin

Accessibility and flexibility

A. N. McLEOD*, A. AUF DER MAUER and S. P. WOOD
Laboratory of Molecular Biology, Department of Crystallography, Birkbeck College, University of London, Malet Street, London WC1E 7HX (U.K.)
(First received July 11th, 1989; revised manuscript received October 9th, 1989)

SUMMARY

Current ideas suggest that a conformational change in the insulin monomer may play an important part in its interaction with the insulin receptor. An investigation is reported in which analytical reversed-phase high-performance liquid chromatography of insulin analogues was used to investigate the solution conformation of the insulin monomer. The results are interpreted in terms of elution coefficients modified by the calculated surface accessibilities of individual residues. The results suggest a partial unfolding of the insulin monomer under the experimental conditions used, which is consistent with current ideas on the biologically active conformation of insulin.

INTRODUCTION

Recent reports of shortened insulin analogues with either normal or enhanced potency[1–6] have focused attention on the role of the C-terminal region of the insulin B-chain in hormone–receptor interactions. By amidating the terminal carboxylate of B26–B30 despentapeptide insulin (DPI), its biological activity is increased from approximately 20% of that of native insulin[7] to greater than 100%[2–4]. Studies with analogues containing substitutions at B24 and B25 which, in whole insulin, are known either to decrease or to increase biological activity, have demonstrated that the terminal pentapeptide may have an inhibitory or, in some instances, an enhancing role in the biological action of insulin[1–6].

A receptor binding region, centred on B25 Phe, was originally proposed in the 1970s[8,9] and, since then, the concept has been expanded to take account of a possible role for flexibility of the insulin monomer in the expression of its biological activity[10]. A model has been produced which assumes a specific role for conformational flexibility in the C-terminal region of the B-chain[3].

In the work reported here we used analytical reversed-phase high-performance liquid chromatography (HPLC) of a series of modified insulins to assess the possible

0021-9673/90/$03.50

effects of flexibility in the C-terminus of the B-chain on HPLC elution behaviour. The analogues used were DPI, B23–B30 desoctapeptide insulin (DOI), desAsn-A21, desAla-B30 (DAA) insulin and native bovine insulin. The methodology used is an extension of our earlier work on the use of analytical reversed-phase HPLC as a probe of the three-dimensional structure of insulin, where we were able to make a qualitative interpretation of the effects of chemical modification of surface amino acids in terms of insulin's known three-dimensional structure[11].

Earlier attempts to predict the elution of peptides in reversed-phase HPLC, on the basis of their composition, have relied on assigning to each amino acid an elution coefficient based on an experimentally derived estimate of its tendency to affect retention[12–14] and to assign an aggregate coefficient for a peptide based on the sum of the values for its constituent amino acids. This method works well for many short peptides but has been criticized for several reasons, the most important of which are that it assumed an equal contribution from all residues in the peptide and is therefore clearly inapplicable to folded proteins. In addition, the value of the elution coefficient for a particular amino acid has been shown to be affected by its position in a sequence[15].

Here we used the calculated surface accessibility of each residue to modify its elution coefficient, allowing the method to be applied to folded molecules and the experimental result to be interpreted in terms of several modelled conformations. By using analogues which share the same sequence, except where residues are deleted from the ends of chains, we have aimed to reduce sequence-dependent effects. In an earlier examination of the elution behaviour of chemical analogues of insulin, where we did not take account of the surface accessibility of individual residues, we found that it was not possible to explain our results quantitatively and our analysis was therefore based on a qualitative assessment of the chemical nature of the substituents combined with our knowledge of the refined crystal structure of two-zinc insulin[16]. The effects on elution of groups such as acetyl, succinyl and thiazolidine and amino acids such as Arg, Glu and Phe, attached to the N-terminus of the A-chain and, for acetyl, the B-chain, were assessed in terms of the assumption that their chemical environments were determined by the structure of the two-zinc insulin monomer; the experimental results were found to fit well with most of our theoretical predictions. In addition, an examination of the elution behaviour of DAA insulin allowed us to comment on the effects of pH on the solution conformation of this analogue which is considered to be significantly disturbed at neutral pH as compared with native insulin[17] but which, in our study, eluted close to native insulin at pH 2.

In this paper, we interpret our results in terms of several possible conformations of the insulin molecule. The use of analogues with residues deleted from ends of chains and an interpretation which uses the calculated surface accessibility of individual residues together with elution coefficients allow us to estimate how far the conformation of the C-terminus of the B-chain deviates in our system from the two-zinc crystal structure. Several sets of elution coefficients have been used, including three derived from work by Houghten and De Graw[15], who produced ranges of values for each residue type depending on its sequence position.

The basis of our calculations was the refined crystal structure for porcine insulin[16], with the necessary side-chain substitutions to make the sequence compatible with bovine insulin. Fig. 1 shows a stereo view of the insulin monomer. In addition to

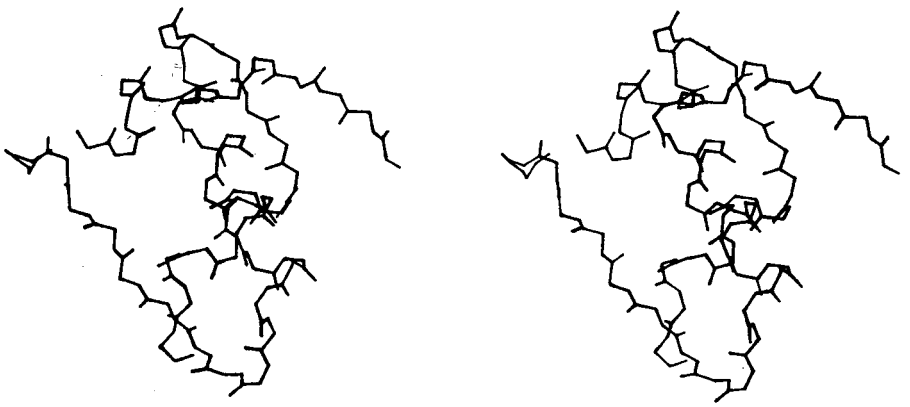

Fig. 1. Stereo view of the insulin monomer main chains (molecule 1, Chinese convention).

calculating accessibilities for the native monomer crystal structure, we have made the necessary deletions to allow us to model DOI, DPI and DAA insulin and have calculated accessibilities for modelled insulins with unfolded B-chain C-termini.

EXPERIMENTAL

Two series of experiments were carried out using a Varian 5000 Series liquid chromatograph equipped with an ODS Ultrasphere column supplied by Beckman. The mobile phase consisted of two components. Solution A was phosphate buffer which, for the first series of experiments, was made up by adjusting a 0.1 *M* solution of sodium dihydrogenphosphate to pH 2 with orthophosphoric acid and, for the second series, consisted of a solution of disodium hydrogenphosphate adjusted, as above, to pH 6.5. Solution B was acetonitrile. All reagents used for solution A were of AnalaR grade, supplied by BDH; water was distilled and deionized. Acetonitrile of HPLC grade 'S' was supplied by the Rathburn. Bovine insulin was supplied by Eli Lilly, DOI was prepared by the method of Bromer and Chance[18] and DPI by the method of Gattner[7]. DAA insulin was prepared by the method of Young and Carpenter[19].

Accessibility calculations and elution coefficients

Solvent contact surfaces for individual residues were calculated by the method of Richmond and Richards[20], which is a development of the method of Lee and Richards[21] for calculation of solvent-accessible surfaces, using computer programs written by S. Islam[a]. This method gives the surface area (Å^2) for each atom which can come in contact with a spherical probe of radius 1.4 Å, taken as being equivalent to a 'standard' solvent molecule. We used the sum of the accessible surfaces for all atoms within a residue as a measure of the contribution which that residue will make to the elution of the insulin molecule as a whole. Elution coefficients were derived from refs. 13–15. The solvent-accessible surface was calculated for each residue in the insulin

[a] Programs written in our laboratory using algorithms from ref. 21.

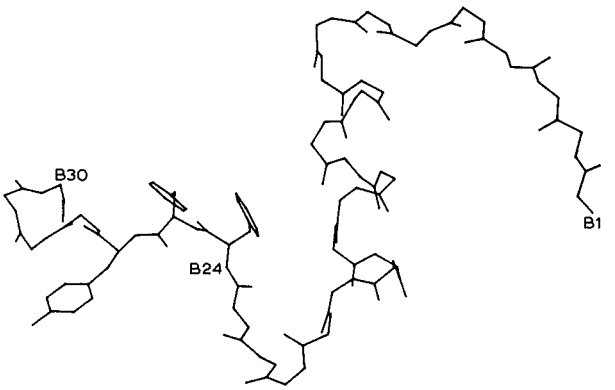

Fig. 2. Insulin B-chain with the C-terminal region unfolded from B24.

molecule. All residues where the surface accessibility of the side-chain alone was less than 7% of the maximum were considered to be buried, according to the criterion of Hubbard and Blundell[22], and eliminated from the calculation. Each of the remaining residues was then considered individually and its accessibility multiplied by its elution coefficient, producing a unique new coefficient for each exposed residue. These coefficients were then summed to give an overall coefficient for the whole molecule which could then be used to calculate its predicted relative elution time.

Coordinates for two-zinc porcine insulin refined at 1.5 Å resolution were extracted from the Brookhaven Protein Databank[16]. As bovine insulin and analogues were used in the HPLC experiments, the coordinates were modified by changing A8 Thr to Ala and A10 Ile to Val. Coordinate sets for DPI, DOI and DAA insulin were produced by deleting the appropriate residues. In addition, three modified coordinate sets were produced. For the first of these, the C-terminal region of the B-chain was unfolded at B23. B23 is a glycine which is conserved in all known insulin sequences and, in the known crystal structures, has main-chain dihedral angles which are inaccessible to L-amino acids with side-chains. It is one of the residues which forms part of the sharp turn which allows the B-chain to turn back upon itself between the

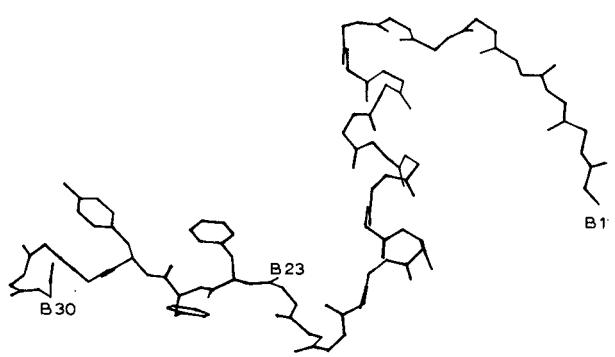

Fig. 3. Insulin B-chain with the C-terminal region unfolded from B23.

B-chain helix and the strand which participates in β-sheet formation across the dimer interface. B23 was seen as a point of significant flexibility and, in the monomer where the β-structure at B24–B26 is no longer present, it is possible that significant changes in dihedral angles may take place. The main-chain torsion angles for B23 are changed from $\varphi = 88.42°, \psi = 172.16°$ to $\varphi = 30.16°, \psi = -122.63°$, exploring a different area of the conformational space available to a glycine with a positive φ and allowing maximum separation between residues B24 and B25 and the core of the molecule. Fig. 2 shows the conformation of the B-chain in the resulting model. The second coordinate set was made by changing the main-chain torsion angles for B24 from $\varphi = -154.74°, \psi = 171.30°$ to $\varphi = -145.02°, \psi = -49.88°$, producing a conformation at B25 which is generally similar to that seen in the crystal structure for the monomeric insulin analogues DPI[23]; the B-chain conformation in this model is shown in Fig. 3. The third, which applied to coordinates for DOI only, was produced by changing the torsion angles of B20–B23 to $-140°, 140°$, maximising the accessibility of these residues. All modifications to the native crystal structure were carried out using the program FRODO[24], running on an Evans and Sutherland PS300 computer graphics system.

RESULTS AND DISCUSSION

Before discussing the results, we shall consider the expected conformation and aggregation state of insulin under our experimental conditions. In solution, insulin aggregates to dimers and, in the presence of zinc, to hexamers. In the experiments described here, all samples were made up at a concentration of 1 mg/ml in phosphate buffer at either pH 2 or 6.5. Under these conditions insulin exists as a monomer–dimer equilibrium with dimers predominating at pH 6.5 and monomers at pH 2 (ref. 8). During the chromatographic process itself, the presence of acetonitrile and/or interaction with the hydrophobic column packing would be expected to interfere with any hydrophobic interaction between monomers. It is known that various organic solvents, such as methanol, dimethylformamide, dioxane and butanol, are capable of causing dissociation of dimers to monomers[8]. The reactivity to iodination of the B-chain tyrosine residues, which is slow in aqueous solution where dimers predominate, is accelerated in the presence of butanol, suggesting that insulin is essentially monomeric under these conditions[8]. We have argued[11] that the general consistency of chromatographic results over a pH range, and the similar elution behaviour of insulins capable of dimerization and insulin analogues such as DOI, which lacks the B-chain residues essential for dimer formation and hence exists in solution as a monomer, suggest that all insulins are monomeric under the range of experimental conditions used in this study. Circular dichroism spectroscopy of native bovine insulin, carried out in 0.1 *M* phosphate containing 28% acetonitrile, also suggest that insulin is monomeric under these conditions[25].

We have previously considered the effects of the experimental conditions on the conformation of the monomer[11]. The most significant effects are likely to be low pH (in experiments carried out at low pH), the presence of organic solvent or the interaction of the insulin monomer with the hydrophobic stationary phase, and we have concluded that the basic conformational framework of the molecule is likely to be preserved under these conditions to the extent that it is possible to explain the effects

on elution behaviour of chemical modifications to insulin in terms of the known crystal structure of the monomer. Considering the effects of interaction between the insulin monomer and the stationary phase, it is accepted that the nature of the solvent-accessible surface determines retention characteristics[26], as it alone defines the variation of the observed partition coefficient. It is also possible that we are observing the relative reversibility of an unfolding process occurring at the hydrophobic surface. If we make the reasonable assumption that the unfolded states have a common framework consisting of the three insulin helices and the extended region of the A-chain whose relative orientations, in the native monomer, are determined by the three disulphide bridges, then the free energy of mass transfer between the phases must be a function of the solution conformation which, in turn, defines accessible surface area.

Conservation of the three-dimensional structure of the flexible ends of the B-chain is less certain, however. In this study, we examine the possible effects on insulin's HPLC elution behavior of conformational changes in the C-terminus of the B-chain.

In the crystal structure of the two-zinc insulin dimer, the major secondary structural elements are three helices in each monomer and the antiparallel β-sheet which is formed across the dimer interface between residues B24, B25 and B26 and their counterparts on the second monomer. This short area of sheet involves four hydrogen bonds which, in the dimer, play a major part in stabilizing the conformation of this part of the B-chain. The situation in the monomer is less clear. In the crystal structure of DPI[23], which is monomeric, there is a significant change in the main-chain dihedral angles of B24, which result in a displacement of B25 from its position in the two-zinc structure. We have, at present, no direct evidence for the conformation of this region of the B-chain in a native insulin monomer in solution.

B25 Phe has a significant place in both the proposed receptor binding region[9] and the region responsible for negative cooperativity in hormone–receptor interaction[27]. It also plays a crucial role in the receptor binding model proposed by Nagagawa and Tager[3], where a change in the conformation of the C-terminal region of the B-chain is a necessary part of the expression of biological activity. It is of great interest, therefore, to have a method for the investigation of the conformational stability of the C-terminal region of the B-chain.

TABLE I

EXPERIMENTALLY DETERMINED RELATIVE ELUTION TIMES WITH RESPECT TO BOVINE INSULIN, MEASURED AT pH 2 AND 6.5

Insulin[a]	*RET*	
	pH 2	*pH 6.5*
DOI	0.56	0.56
Bovine insulin	1.00	1.00
DAA insulin	1.20	2.00
DPI	1.09	0.88

[a] DOI = B23–B30 desoctapeptide insulin; DAA insulin = desAsn-A21,desAla-B30 insulin; DPI = B26–B30 despentapeptide insulin.

TABLE II

PREDICTED RELATIVE ELUTION TIMES FOR THE SAME ANALOGUES AS IN TABLE I, DETERMINED FROM ELUTION COEFFICIENTS[12,13,15] ALONE

Basis	*Insulin*	*RET*
Guo, pH 2	DOI	0.84
	Bovine insulin	1.00
	DAA insulin	0.99
	DPI	0.95
Guo, pH 7	DOI	0.83
	Bovine insulin	1.00
	DAA insulin	0.99
	DPI	0.94
Houghten high	DOI	0.82
	Bovine insulin	1.00
	DAA insulin	0.99
	DPI	0.93
Houghten mean	DOI	0.81
	Bovine insulin	1.00
	DAA insulin	1.00
	DPI	0.95
Houghten low	DOI	0.75
	Bovine insulin	1.00
	DAA insulin	1.07
	DPI	1.06

The elution times of bovine insulin, DAA insulin, DPI and DOI at pH 2 and 6.5 are presented in Table I and there are several significant features. Firstly, DAA insulin elutes close to both native bovine insulin and DPI at pH 2, but its relative elution time (RET) with respect to native insulin is increased from 1.20 to 2.00 at pH 6.5; none of the other analogues behave in this way. Second, DOI elutes significantly before native insulin at both pH values, suggesting that it is much more hydrophilic.

Table II shows the predicted RETs for the native bovine insulin monomer, DOI, DPI and DAA insulin, calculated from elution coefficients alone, with no correction for accessiblity. Five predictions are presented, two based on coefficients from Guo *et al.*[12] for pH 2 and 7, and three based on coefficients from work by Houghten and De Graw[15], where it was demonstrated that each residue type may have a range of elution coefficients based on its sequence environment. These are designated Houghten 'high', 'medium' and 'low', and are derived from the maximum, mean and minimum values for each amino acid type as specified in ref. 15. It can be seen that there is basic agreement between the predictions based on both of the Guo coefficient sets and all three Houghten sets. The Houghten low coefficient set generally gave more variable results than the others in all of our predictions and, for this reason, the following arguments are based on predictions calculated from the other four sets, although all predicted RETs are presented in the tables.

Comparing these predictions with the experimentally determined values, it can be seen that the prediction gives a general idea of the RETs observed experimentally in that the RETs for DPI, DAA insulin and native bovine insulin cluster together at pH 2 whereas DOI appears more hydrophilic. This method fails, however, to predict

TABLE III

PREDICTED RELATIVE ELUTION TIMES DETERMINED FROM ELUTION COEFFICIENTS AND RESIDUE ACCESSIBILITIES[21] CALCULATED FROM THE TWO-ZINC INSULIN MONOMER

Basis	*Insulin*	*RET*
Guo, pH 2	DOI	0.98
	Bovine insulin	1.00
	DAA insulin	1.02
	DPI	1.00
Guo, pH 7	DOI	0.94
	Bovine insulin	1.00
	DAA insulin	1.03
	DPI	1.08
Houghten high	DOI	0.93
	Bovine insulin	1.00
	DAA insulin	1.02
	DPI	1.05
Houghten medium	DOI	0.95
	Bovine insulin	1.00
	DAA insulin	1.03
	DPI	1.14
Houghten low	DOI	1.24
	Bovine insulin	1.00
	DAA insulin	1.26
	DPI	2.25

either the extent of the difference between the observed RET for DOI and the other analogues or the discrepancy between the RET for DAA insulin at pH 2 and 7.

Further predictions were therefore carried out using elution coefficients modified by calculated surface accessibilities of individual residues as described under Experimental. Table III shows the results obtained from accessibility calculations carried out on models based on the conformation of the two-zinc insulin monomer molecule 1 (Chinese convention). It can be seen that all of the RETs are clustered around 1.0, and the fit to the experimental data is worse than predictions based on elution coeffiecients alone. Accessibilities here are calculated for a globular monomer where buried residues make no contribution to the solvent-accessible surface and the remaining residues contribute to the surface, and hence the total chromatographic contact area, depending on their relative exposure. The use of elution coefficients alone assumes that all residues are equally accessible to the solvent, so these results appear to suggest that, under our experimental conditions, the molecules are partially unfolded.

As the region of the B-chain from B24 and B26 is stabilized in the two-zinc dimer by inter-monomer hydrogen bonding, it is probable that its conformation will be different in the monomer. Any unfolding in this region is likely to have a significant effect on the accessibility of the hydrophobic residues B24 Phe–B25 Phe and, therefore, their relative contributions to the overall hydrophobicity of the molecule, combined with an increase in the accessibility of A2 Ile, allowing it to contribute to the surface of the molecule. Modelled coordinate sets were therefore produced, as de-

TABLE IV

PREDICTED RELATIVE ELUTION TIMES DETERMINED FROM ELUTION COEFFICIENTS AND RESIDUE ACCESSIBILITIES CALCULATED FROM THE TWO-ZINC INSULIN MONOMER UNFOLDED AT B24

Basis	*Insulin*	*RET*
Guo, pH 2	DOI	0.82
	Bovine insulin	1.00
	DAA insulin	1.01
	DPI	0.99
Guo, pH 7	DOI	0.79
	Bovine insulin	1.00
	DAA insulin	1.02
	DPI	0.96
Houghten high	DOI	0.84
	Bovine insulin	1.00
	DAA insulin	1.07
	DPI	1.00
Houghten medium	DOI	0.79
	Bovine insulin	1.00
	DAA insulin	1.03
	DPI	1.00
Houghten low	DOI	0.75
	Bovine insulin	1.00
	DAA insulin	1.17
	DPI	1.53

TABLE V

PREDICTED RELATIVE ELUTION TIMES DETERMINED FROM ELUTION COEFFICIENTS AND RESIDUE ACCESSIBILITIES CALCULATED FROM THE TWO-ZINC INSULIN MONOMER UNFOLDED AT B23

Basis	*Insulin*	*RET*
Guo, pH 2	DOI	0.68
	Bovine insulin	1.00
	DAA insulin	1.23
	DPI	0.99
Guo, pH 7	DOI	0.66
	Bovine insulin	1.00
	DAA insulin	1.26
	DPI	0.96
Houghten high	DOI	0.67
	Bovine insulin	1.00
	DAA insulin	1.18
	DPI	0.95
Houghten medium	DOI	0.63
	Bovine insulin	1.00
	DAA insulin	1.20
	DPI	1.00
Houghten low	DOI	0.41
	Bovine insulin	1.00
	DAA insulin	1.30
	DPI	1.30

scribed under Experimental, with the B-chain unfolded from B24 and from B23. These models were then used as a basis for further accessibility calculations and RETs calculated as before. The results are shown in Tables IV and V. It can be seen that these results approach the experimental values more closely, with the B23 unfolded model giving the best fit. It is important to note that the accessibilities for DOI are the same in all instances, the B24 and B25 unfoldings being within the octapeptide which is deleted in this analogue. The hypothesis which best fits these results is that, under the experimental conditions adopted, unfoldings in DPI and native insulins increase their retention times, leading to a lower relative elution time for DOI. This is probably due to the consequent increase in the accessibility of the hydrophobic side-chains of B24 and B25 Phe, together with the partial exposure of core residues such as A2 Ile.

There is some evidence that a change in conformation in the insulin monomer from the two-zinc crystal structure may be a necessary part of receptor binding and expression of biological activity[1–6,10] and a model has been produced which implies a conformational change in the C-terminal region of the B-chain[3]. In addition, visual inspection of the crystal structure for both molecules 1 and 2 suggests that a change in the position of the pentapeptide B25–B30 would improve the accessibility of residues A3, A4 and A5, facilitating their ability to bind to the receptor. The crystal structure for DPI[23] shows a significant change in the main-chain dihedral angles of B24 Phe, allowing B25 Phe to fold outwards from the core of the molecule. If this change were repeated in the complete insulin monomer, the resulting conformational change would be consistent with current ideas of conformational change as a requirement for the expression of biological activity.

The results presented here are consistent with an unfolding of the B-chain from B23 to B30. This change, which involves disruption of the hydrogen bond between B23 carbonyl oxygen and A21 nitrogen and the hydrogen bond between B25 nitrogen and A19 oxygen, is a more radical conformational disturbance than is seen in DPI, where only the B25–A19 hydrogen bond is lost. Although these results do appear to give an indication of the extent to which the C-terminal region of the B-chain may be unfolded in the insulin monomer in solution, it is important to consider them in the light of the experimental conditions. The conditions used range from low pH to near physiological pH and, apart from the marked difference in the effects on DAA insulin, they are consistent within this pH range.The chromatographic process involves both the presence of organic solvent and interaction with the hydrophobic column packing. There is no analogue of these in solution under physiological conditions. It is probable, however, that binding of insulin to its receptor involves a hydrophobic interaction[28], and the behaviour of the B-chain under the hydrophobic experimental conditions may give some indication of its potential for flexibility in a hydrophobic environment *in vivo*.

The predictions for the B23 unfolded model give the best fit to the experimental results for DPI and DOI. The apparent hydrophilicity of DOI tends to be understated, however, and an additional model has been produced to examine the possibility that a further unfolding may take place at B20, as described under Experimental. Predictions based on this model are essentially indistinguishable from the B23 unfolded model, so no theoretical conclusions could be drawn.

The observed difference in the RET for DAA insulin is not predicted by any of the calculations. It has been suggested[17] that the removal of A21 Asn is likely to lead

to a disruption of the conformation of insulin by placing a negative charge close to the hydrophobic core of the molecule. In an earlier HPLC investigation of insulin analogues[11] we found, unexpectedly, that DAA insulin eluted before native bovine insulin in the shallow gradient system used. This finding was explained by the fact that, at pH 2, the carboxylate of A20 Cys is likely to be partially protonated, leading to a reduction in charge. In the current series of experiments, DAA elutes slightly after native insulin at pH 2, but still close to the position predicted by all methods. At pH 7, however, its RET is significantly greater than both the pH 2 results and all of the predictions for pH 7.

This result suggests that there is a significant conformational disturbance when the carboxylate of A20 becomes charged. Looking at the structure of the molecule, the residues closest to A20 are B24 and B25, the A20–B24 C-α to C-α distance being 4.17 Å and the A20–B25 distance being 6.61 Å in the crystal structure for molecule 1. If we assume, however, that the B-chain is unfolded from B23, the accesssibilities of B24 and B25 will be significantly increased so that any further increase due to the repulsive effect of the charge on B20 is likely to be small. Predictions at both pH 2 and 7 for B23 unfolded insulin, where the accessibilities of both B24 and B25 are maximized, give little indication of an RET for DAA insulin as large as the experimental value of 2.0 at pH 6.5, whilst the predicted result for B23 and B24 unfolded DAA is similar at both pH values. These results suggest a more drastic disturbance in the conformation of DAA insulin when the terminal carboxylate of A20 is charged; possibly the altered charge environment in the B19–B20 region acts to destabilize the conformation of the molecule as a whole, leading to great exposure of core residues.

CONCLUSION

It is clear that the approach adopted here has some value in interpreting the HPLC elution of closely related molecules. Regnier[26] proposed that the interaction of a folded protein with the stationary phase in a chromatographic system is dependent on a chromatographic contact area which, in reversed-phase chromatography, may occupy a significant proportion of the surface of the molecule. From our previous work[11], we have concluded that, with a small molecule such as insulin, the reversed-phase chromatographic contact area is effectively the whole surface of the molecule and that a change at any position on the surface is likely to affect the chromatographic behaviour. It has been possible, using this assumption, to combine experimentally derived HPLC elution coefficients with accessibility calculations in interpreting the elution behaviour of insulin analogues and to provide experimental evidence for the extent of flexibility of the C-terminal portion of the insulin B-chain.

REFERENCES

1 M. Casaretto, M. Spoden, C. Diaconescu, H.-G- Gattner, H. Zahn, D. Brandenburg and A. Wollmer, *Biol. Chem. Hoppe-Seyler*, 368 (1987) 709.
2 W. H. Fischer, D. Saunders, D. Brandenburg, A. Wollmer and H. Zahn, *Biol. Chem. Hoppe-Seyler*, 367 (1985) 999.
3 S. H. Nagagawa and H. S. Tager, *J. Biol. Chem.*, 262 (1987) 1254.
4 S. H. Nagagawa and H. S. Tager, *J. Biol. Chem.*, 261 (1986) 7332.
5 G. P. Schwartz, G. T. Burke and P. G. Katsoyannis, *Proc. Natl. Acad. Sci. U.S.A.*, 86 (1989) 458.

6 G. P. Schwartz, G. T. Burke and P. G. Katsoyannis, *Proc. Natl. Acad. Sci. U.S.A.*, 84 (1987) 6408.
7 H.-G. Gattner, *Hoppe-Seyler's Z. Physiol. Chem.*, 356 (1975) 1397.
8 T. Blundell, G. Dodson, D. Hodgkin and D. Mercola, *Adv. Protein Chem.*, 26 (1972) 279.
9 R. A. Pullen, D. G. Lindsay, S. P. Wood, I. J. Tickle, T. L. Blundell, A. Wollmer, G. Krail, D. Brandenburg, H. Zahn, J. Glieman and S. Gammeltoft, *Nature (London)*, 259 (1976) 369.
10 E. J. Dodson, G. G. Dodson, R. E. Hubbard and C. D. Reynolds, *Biopolymers*, 22 (1983) 281.
11 A. McLeod and S. P. Wood, *J. Chromatogr.*, 285 (1984) 319.
12 D. Guo, C. T. Mant, A. K. Taneja, J. M. R. Parker and R. S. Hodges, *J. Chromatogr.*, 359 (1985) 499.
13 J. M. R. Parker, D. Guo and R. S. Hodges, *Biochemistry*, 25 (1986) 5425.
14 J. L. Meek, *Proc. Natl. Acad. Sci. U.S.A.*, 77 (1980) 1632.
15 R. A. Houghten and S. T. De Graw, *J. Chromatogr.*, 386 (1987) 223.
16 E. N. Baker, T. L. Blundell, J. F. Cutfield, S. M. Cutfield, E. J. Dodson, G. G. Dodson, D. M. C. Hodgkin, R. E. Hubbard, N. W. Isaacs, C. D. Reynolds, K. Sakabe, N. Sakabe and N. M. Vijayan, *Philos. Trans. R. Soc. London*, 319 (1988) 369.
17 J. Goldman and F. H. Carpenter, *Biochemistry*, 13 (1974) 4566.
18 W. W. Bromer and R. E. Chance, *Biochim. Biophys. Acta*, 133 (1967) 219.
19 J. D. Young and F. H. Carpenter, *J. Biol. Chem.*, 236 (1961) 743.
20 T. J. Richmond and F. M. Richards, *J. Mol. Biol.*, 119 (1978) 537.
21 D. Lee and F. M. Richards, *J. Mol. Biol.*, 55 (1971) 379.
22 T. J. P. Hubbard and T. L. Blundell, *Prot. Eng.*, 1 (1987) 159.
23 R. C. Bi, Z. Dauter, E. Dodson, G. Dodson, F. Giardano and C. Reynolds, *Biopolymers*, 23 (1984) 391.
24 T. A. Jones, *J. Appl. Crystallogr.*, 11 (1978) 268.
25 A. Wollmer, personal communication.
26 F. E. Regnier, *Science*, 238 (1987) 319.
27 P. De Meyts, E. Van Obberghen, J. Roth, A. Wollmer and D. Brandenburg, *Nature (London)*, 273 (1978) 504.
28 M. Waelbroeck, E. Van Obberghen and P. De Meyts, *J. Biol. Chem.*, 254 (1979) 7736.

Journal of Chromatography, 502 (1990) 337–349
Elsevier Science Publishers B.V., Amsterdam — Printed in The Netherlands

CHROM. 22 083

Improvements in the separation and detection of acetylcholine and choline using liquid chromatography and electrochemical detection

NIKLAS TYREFORS*
Uppsala University, Institute of Chemistry, P.O. Box 531, S-751 21 Uppsala (Sweden)
and
ANDERS CARLSSON
Carnegie Medicin AB, Roslagsvägen 101, S-105 20 Stockholm (Sweden)
(First received May 26th, 1989; revised manuscript received October 11th, 1989)

SUMMARY

The liquid chromatoghraphic separation and enzymatic conversion of acetylcholine and choline have been improved by using monosized polymer particles, Dynospheres, for both the separation column and the enzyme reactor. Theoretical expressions for the behaviour and optimization of post-column enzyme reactors have been derived. Some plausible supports and immobilization methods have been tested. Several antimicrobial agents have also been briefly evaluated for use as additives to the mobile phase.

INTRODUCTION

The investigation of the cholinergic transmitter system has been hampered over the years by the lack of simple and reliable methods for the determination of acetylcholine (ACh) and choline (Ch) *in vivo*[1]. Several methods have been developed and tested, mainly bioassays[2] and a variety of chemical methods[3]. They all have more or less severe drawbacks, however, which have limited their use to specialized and dedicated laboratories. New hope arose when Potter *et al.*[4] presented a concept using liquid chromatographic (LC) separation, post-column enzyme reaction and electrochemical detection. Several workers have applied and improved the method, as reported by Tyrefors and Gillberg[5] and Damsma[6]. However, several problems remain to be solved before widespread routine use can be expected.

Microdialysis is a recently introduced and rapidly accepted sampling technique that is useful in a wide variety of *in vivo* sampling situations. The inherent properties of the method place high demands on the subsequent analysis, however[7]. Work is in progress in this laboratory aimed towards developing a useful and reliable method for the determination of ACh and Ch in microdialysis samples. This work necessitates the careful examination of the different components of the analytical system involved. We

0021-9673/90/$03.50

have recently developed a separation system based on Dynospheres, a polymeric packing material with unique properties[8]. Further, several enzyme immobilization techniques have been briefly evaluated. This resulted in two which were adjudged worthy of further investigation. These were also both based on Dynospheres. Microbiological growth has been a major, but rarely recognized, problem in the systems designed earlier. We have tested several plausible poisons and found Kathon CG to be a suitable choice.

THEORY

Several more or less elaborate theories have been developed in order to describe the behaviour of enzyme reactors in flow systems[9–12], but the special considerations needed for a post-column reactor in LC have rarely been addressed[13].

The total dispersion in a chromatographic system is considered to be equal to the sum of dispersions from the different system components[14]. The dispersion in the present system can be described as

$$\sigma^2 = \sigma^2_{\text{inj}} + \sigma^2_{\text{column}} + \sigma^2_{\text{enz}} + \sigma^2_{\text{det}} \tag{1}$$

where σ^2 is the total dispersion in the chromatographic system (μl^2) and σ^2_{inj}, σ^2_{column}, σ^2_{enz} and σ^2_{det} are contributions from the injector, separation column, enzyme reactor and detector, respectively. Within the Gaussian approximation, the peak height obtained when injecting a sample plug varies with dispersion (variance) according to

$$h = ck_1 \cdot \frac{1}{\sigma\sqrt{2\pi}} \cdot \exp[-(x-m)^2/2\sigma^2] \tag{2}$$

where h = peak height, c = sample concentration, k_1 = detector sensitivity and $x - m$ = distance from peak maximum. Since only the maximum peak height is considered, $x - m = 0$, the expression reduces to

$$h = ck_2(1/\sigma) \tag{3}$$

where $k_2 = k_1/\sqrt{2\pi}$.

If the reactor length (l) is used as a single variable, the expression for the total system dispersion can be rearranged to

$$\sigma^2 = \sigma^2_{\text{sys}} + \sigma^2_{\text{enz}} l \tag{4}$$

where σ^2_{sys} is the dispersion from all components except the enzyme reactor and σ^2_{enz} the specific dispersion from the enzyme reactor (μl^2 mm^{-1}). Combining eqns. 3 and 4 yields

$$h = ck_2 \cdot \frac{1}{\sqrt{\sigma^2_{\text{sys}} + \sigma^2_{\text{enz}} l}} \tag{5}$$

The degree of conversion of an enzyme reactor under pseudo-first-order conditions can be described as[10]

$$X = 1 - \exp(-K_{ps}^{app}\tau) \tag{6}$$

where $X = (S_0 - S)/S_0$, S_0 is the starting substrate concentration, S the instantaneous substrate concentration, K_{ps}^{app} the apparent pseudo-first-order rate constant (s^{-1}) and τ the residence time in the enzyme reactor (s). The reason for using an apparent pseudo-first-order rate constant, K_{ps}^{app}, is to account for mass-transfer limitations. The relationship between the pseudo-first-order, K_{ps}, and the apparent pseudo-first-order rate constant[12] is

$$\frac{1}{K_{ps}^{app}} = \frac{d_p^{3/2}}{B\sqrt{F}} + \frac{1}{K_{ps}} \tag{7}$$

where $B = 9.75(1 - \varepsilon_E)D_m^{3/2} - \nu^{-1/6}$, ε_E = external void fraction, D_m = molecular diffusion coefficient ($m^2\ s^{-1}$), ν = kinematic viscosity ($m^2\ s^{-1}$), F = linear flow velocity ($m\ s^{-1}$), d_p = particle diameter (m) and K_{ps} = pseudo-first-order rate constant (no external mass-transfer limitations).

When using a constant flow-rate and varying the reactor length, K_{ps}^{app} can be expressed in the unit mm^{-1}, and we obtain

$$X = 1 - \exp(-\kappa_{ps}^{app}l) \tag{8}$$

where κ_{ps}^{app} is the apparent pseudo-first-order rate constant (mm^{-1}) and l the reactor length (mm). Using $c = n(S_0 - S)$, where n is a stoichiometric coefficient, and inserting eqn. 8 in eqn. 5 results in

$$h = \frac{S_0 n k_2[1 - \exp(-\kappa_{ps}^{app}l)]}{\sqrt{\sigma_{sys}^2 + \sigma_{enz}^2 l}} \tag{9}$$

Eqn. 9 describes how the peak height varies with reactor length and enzyme kinetics. Fig. 1 shows a theoretical plot of peak height (h) *vs.* the degree of conversion (X), and Fig. 2 peak height as a function of reactor length.

The conditions assumed for the separation column are $N = 3000$, $l = 100$ mm, column I.D. = 2 mm and void fraction = 70%. For the enzyme reactor, K_{ps}^{app} is varied according to the figures and $\sigma_{enz}^2 = 6.6\ \mu l^2\ mm^{-1}$. The specific dispersion, σ_{enz}^2, is determined from Fig. 3.

Several interesting observations can be made in Figs. 1 and 2. From Fig. 1 and eqn. 9, we can conclude that 100% conversion efficiency imposes infinite reactor length and dispersion, resulting in zero height. Further, the degree of conversion required for maximum peak height is dependent on k', K_{ps}^{app} and N, and it cannot be determined on an intuitive basis or by rules of thumb.

In Fig. 2, the arrows represent the maximum allowable reactor length if $N >$ 2600, *i.e.*, the dispersion caused by the enzyme reactor should not result in a substantial

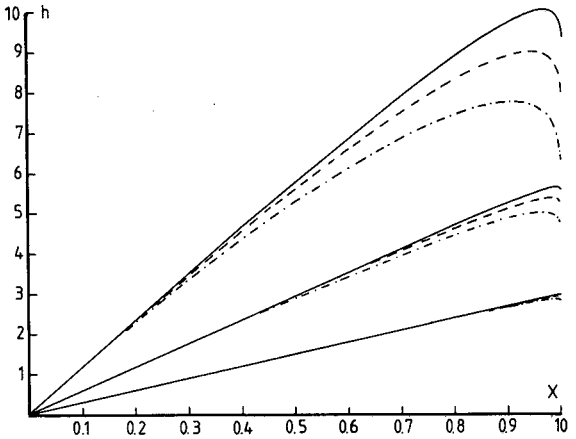

Fig. 1. Peak height as a function of degree of conversion under various conditions. The assumed k' values are 1, 3 and 7 from top to bottom. K_{ps}^{app}: ———, 1 mm^{-1}; – – – –, 0.5 mm^{-1}; – · – · –, 0.25 mm^{-1}. For other conditions, see text.

decrease in total system performance. We can conclude that a maximum peak height is not desirable under all conditions. When using slow enzyme preparations to convert early-eluting compounds, the reactor length required to obtain maximum peak height causes a severe decrease in the resolving power of the system.

In the opposite case, with late-eluting compounds passed through an efficient reactor, maximum peak height can be desirable. When neither sensitivity nor resolution is critical, the maximum degree of conversion can be desirable in order to achieve a long lifetime of the enzyme reactor and immunity to deactivation[12].

Thus, a post-column reactor of any kind needs to be carefully tailored to its application in order to deliver optimum performance.

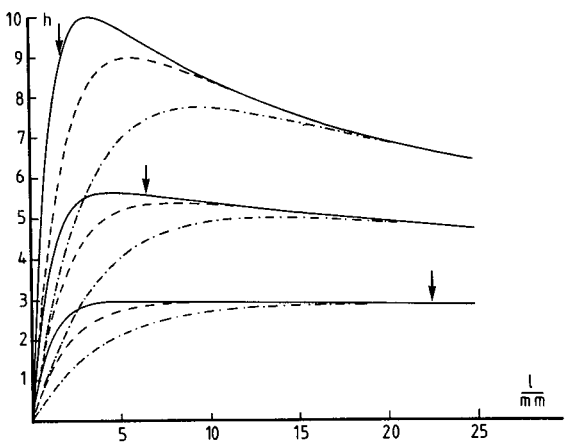

Fig. 2. Peak height as a function of reactor length under various conditions. K_{ps}^{app}: ———, 1 mm^{-1}; – – – –, 0.5 mm^{-1}; – · – · –, 0.25 mm^{-1}. The arrows indicate the maximum tolerable reactor length in order to keep the decrease in separation efficiency under 400 plates/m. For other conditions, see text.

Several factors not discussed here contribute to dispersion, making these assumptions approximate. Tailing peaks, for example, cannot be fully described in terms of σ^2. Further, if the substrate and products show different distributions between the stationary and mobile phases in the enzyme reactor, the dispersion will also be dependent on the degree of conversion.

EXPERIMENTAL

Chemicals

Acetylcholine chloride (AChCl), choline chloride (ChCl), acetylcholinesterase (AChE, EC 3.1.1.7) and cholineoxidase (ChO, EC 1.1.3.17) were obtained from Sigma (St. Louis, MO, U.S.A.). All activity units given refer to Sigma units. Superose 12 and Sephadex G-10 S were provided by Pharmacia (Uppsala, Sweden). Sodium dodecyl sulphate (SDS) with a guaranteed content of 98% C_{12} was obtained from Pierce (Rockford, IL, U.S.A.), 1,1,1-trifluoroethanesulphonyl chloride (tresyl chloride) from Fluka (Buchs, Switzerland) and Kathon CG from Rohm & Haas (Philadelphia, PA, U.S.A.). All other chemicals were from E. Merck (Darmstadt, F.R.G.) of analytical-reagent grade and used as received, unless stated otherwise. The water used for all solutions was distilled in glass and passed through a Milli-Q water purification system (Millipore, Bedford, MA, U.S.A.).

Chromatographic equipment

The chromatographic system consisted of a Knauer 364.00 high-performance liquid chromatographic (HPLC) pump fitted with a microbore pump head, a CMA/200 microsampler (Carnegie Medicin, Stockholm, Sweden) and an SP-4290 integrator (Spectra-Physics, San Jose, CA, U.S.A.). The column and enzyme reactor were thermostated using a block heater–cooler described elsewhere[15]. Briefly, the device is based on a Peltier element and operates between -5 and $+60$°C. This arrangement makes it possible to run the system at the optimum of 30–35°C and to store it at $+4$°C without removing the enzyme reactor.

For some flow-injection analysis (FIA) experiments and purity control of the enzymes, a Pharmacia FPLC system was used, consisting of two P-500 pumps an LCC-500 controller, two MV-7 injection valves and two MV-8 selector valves.

Mobile phase

The mobile phase used for the chromatographic and FIA experiments consisted of 6% (v/v) HPLC-grade acetone and 94% aqueous buffer containing 0.1 *M* NaH_2PO_4, 0.15 m*M* SDS, 0.2 m*M* EDTA and 0.1% Kathon CG. The pH of the aqueous buffer was adjusted to 7.5 with sodium hydroxide solution.

Detector system

The electronics of the electrochemical detector were constructed in-house according to commonly accepted principles[16] and the thin-layer flow cell closely resembled, with some exceptions, a commercially available model (BAS TL-5A).

The working electrode had an area of 0.79 mm^2 (1 mm diameter) and the thin-layer region was defined by a 23-μm thick Mylar gasket. An Ag/AgCl quasi-reference electrode was used, consisting of an Ag wire fitted downstream of the

Pt working electrode in the same Kel-F block, so the potential of the reference electrode was determined by the activity of Cl^- in the mobile phase.

Kathon CG contains 23% $MgCl_2$, which results in 4.8 m*M* Cl^- in the mobile phase; this concentration gives the reference electrode a potential of *ca.* 160 mV *vs.* Ag/AgCl (3 *M* KCl). All reported potentials were recalculated in order to refer to Ag/AgCl (3 *M* KCl).

Separation column

The separation column consisted of Dynospheres PD-051-R (Dyno Industrier, Lillestrøm, Norway) packed in a 60 × 2 mm I.D. or a 30 × 2 mm I.D. Knauer Vertex column. The particles are spherical with a diameter of 5 ± 0.2 μm and porous with a surface area of *ca.* 700 $m^2 g^{-1}$. The nominal pore size is 500 Å, but it can vary slightly from batch to batch. The particles can be made with a coefficient of variation of < 1% in particle size as measured with a Coulter Counter. This is equal to or better than the particles made by NASA under weightless conditions.

The columns were packed in accordance with the recommendations from Dyno; a 10% (v/v) slurry in methanol was packed at a constant pressure of 100 bar for 45 min. The resulting columns were only tested in the ACh system.

For comparison purposes, a 100 × 4.6 mm I.D. PLRP-S column (Polymer Labs., Shropshire, U.K.) was operated together with a silica-based enzyme reactor prepared according to Tyrefors and Gillberg[5].

Enzyme reactor

Both ChO and AChE were immobilized on 10-μm porous, hydrophilized Dynospheres (HD) using the aliphatic OH groups which are incorporated during the process of hydrophilization. The particles are an intermediate in the production of Pharmacia Mono-Q and Mono-S ion exchangers. The HD were suspended in a 40–50% (v/v) slurry in 4% acetic acid, from which aliquots were taken for activation. ChO was immobilized using tresyl coupling[17] and AChE by the carbonyldiimidazole (CDI) method[18]. The buffer used for all couplings was 0.1 *M* NaH_2PO_4–NaOH (pH 7.0) with 0.1% Kathon CG added as a preservative.

Solvents and reaction media were changed by trapping and rinsing the particles on 1/8-in. membrane filters, removing the filter with the thin cake of particles, suspending them in the new solvent and then picking up the filter. Three to four such transfers were easily performed without significant losses. The particles were thoroughly washed between each reaction step.

As both the ChO and AChE preparations contain Tris buffer salts, they were passed through a PD-10 desalting column (Pharmacia) in order to change to phosphate buffer before coupling.

Coupling of ChO was done by taking 80 μl of HD slurry and changing the solvent to 500 μl of acetone–pyridine (90:10), adding 40 μl of tresyl chloride and allowing reaction to proceed for 30 min at 4°C. The reaction medium was then changed to 500 μl of buffer with 3.5–4 mg of ChO added and allowed to couple for 1 h at +4°C.

The capacity of the enzyme reactor to bind protein was assessed by using a breakthrough technique similar to that described by Damsma *et al.*[19]. A 37 × 2 mm I.D. reactor packed with either tresyl chloride-activated HD or glutaraldehyde-activated silica was connected between the injector and a UV–VIS detector. The

detector was operated at 450 nm, and portions of ChO dissolved in buffer were injected until breakthrough was detected. The amount of ChO eluted was measured by integrating the resulting peaks.

AChE was coupled by taking 40 μl of HD, changing the solvent to 100 μl of dioxan, adding 6–7 mg of CDI and allowing reaction to proceed for 30 min at 22°C. The particles were then washed and suspended in 400 μl of buffer with 160–200 U of AChE and allowed to react for 1 h at 22°C.

The coupling of enzymes to silica was done for comparison purposes and has been described elsewhere[5].

RESULTS AND DISCUSSION

Comparison of immobilization supports

There are several reasons to doubt the choice of silica or porous glass as a support for the immobilization of AChE and ChO. Both hydrolyse at the optimum pH for enzyme activity (pH 7.0–8.5), and residual silanol activity causes tailing and band broadening in the absence of competing salts (*e.g.*, tetramethylammonium chloride).

We have tried some of the more plausible candidates as supports for immobilized enzymes. The requirements are mainly the same as those raised for use in high-performance liquid affinity chromatography applications[20], *i.e.*, small spherical particles with a narrow size distribution, large surface area and a narrow pore size distribution in a range where the protein has access to the pores. When this specification is applied to commercially available materials, we are left just a few possible candidates.

In addition to silica and Dynospheres, we also tried Pharmacia Superose 12 and Sephadex G-10 Superfine, but none of them was rigid enough to withstand the pressure at the applied flow-rates.

Fig. 3 shows peak profiles for a 14 × 2 mm I.D. silica-based ChO reactor and

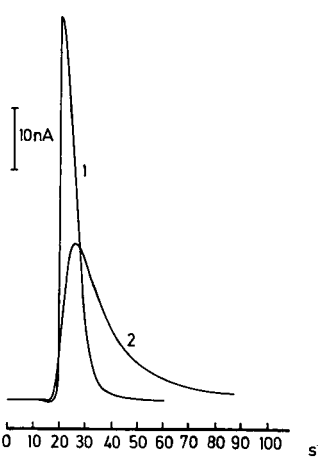

Fig. 3. Comparison of elution profiles for (1) polymer-based and (2) silica-based ChO reactors. The silica-based reactor shows severe tailing but gives approximately the same area as the polymer-based reactor. For details, see text.

a 15 × 2 mm I.D. polymer-based reactor operated at a flow-rate of 200 μl min^{-1} and a temperature of 35°C. The working electrode potential was 450 mV and the sample was 10 μl of 8 μM ChCl. It is observed that the dispersion (σ) in the silica-based reactor is 2.5 times that in the polymer-based reactor. However, the difference in conversion efficiency is negligible. The difference can be related to mass transport limitations, adsorption, or probably both, but the result remains that the polymer-based reactor is superior with respect to dispersion.

The tresyl chloride-activated HD showed a capacity of 140 mg protein per ml bed volume, and the glutaraldehyde-activated silica 100 mg/ml. This can be compared with the 10.4 mg/ml that is achieved using 5-μm particles with 120 Å pore size[19]. We did not observe any leakage of protein before the respective breakthrough, indicating fast coupling reactions.

Methods for immobilization

We tried several common methods for enzyme immobilization in order to find some suitable for our application.

Every attempt to use diazo linkage[11] of ChO to any support resulted in high protein binding, but a complete loss of activity. The CDI method refused to bind ChO at all, leading to complete elution of the enzyme from the reactor. Glutaraldehyde[21], cyanogen bromide[22] and tresyl coupling retained both ChO and its activity, but both cyanogen bromide and glutaraldehyde raise serious doubts according to the structure and stability of the binding[23–25]. Further, the use of glutaraldehyde necessitates the incorporation of a primary amine on the carrier particle surface. This obviously makes the process of coupling the enzymes more laborious and complex.

AChE, on the other hand, did not retain much of its activity either when tresyl or diazo coupling was used. Glutaraldehyde, cyanogen bromide and CDI couplings retained both enzyme and activity, but the same objections against glutaraldehyde and cyanogen bromide as raised for ChO are valid for AChE.

This screening leaves tresyl coupling for ChO and CDI coupling for AChE.

Characteristics of the enzyme reactor

Enzyme reactors can be characterized by their degree of conversion, but that is a limited measure, valid only under strictly defined conditions. If pseudo-first-order kinetics can be assumed (linear calibration graphs), the pseudo-first-order rate constant is a valuable measure of the reactor efficiency[12]. The rate constant is reasonably independent of flow-rate and can be corrected for temperature variations and different reactor lengths. In our case, the AChE have a much higher specific activity (1000–2000 U/mg) than ChO (10–15 U/mg), and therefore we only considered the kinetics of ChO.

The degree of conversion is more difficult to determine than it appears at first sight. The obvious way would be to inject a Ch standard and compare the area of the resulting peak with that obtained on injecting a hydrogen peroxide standard. We have not been able to achieve reproducible results from such experiments using stainless-steel components in an HPLC system.

When using the FPLC system where wetted parts are made of Kel-F, Tefzel or glass (and titanium in some pump parts), it was possible to inject hydrogen peroxide and obtain reproducible results. However, the pumps and tubing do not cover the range of pressures needed for studies of kinetics in these enzyme reactors.

One way to circumvent the problem is to measure the amount of Ch consumed by the reactor instead of the hydrogen peroxide produced. This was done by injecting a known amount of Ch and then collecting the mobile phase with the eluted peak in a weighed microvial and then weighing the vial again. Then a portion of the collected mobile phase was reinjected and the resulting peak area was determined. Finally, we calculated how much Ch was left after passage through the reactor. This is possible because injection of Ch gave reproducible results and straight calibration graphs, whereas injection of hydrogen peroxide did not.

Another fundamental complication is the reaction mechanism. The oxidation of Ch to hydrogen peroxide and betaine is a two-step reaction proceeding via betaine aldehyde[26]:

$$(CH_3)_3N^+CH_2CH_2OH + O_2 \rightarrow (CH_3)_3N^+CH_2COH + H_2O_2$$

$$(CH_3)_3N^+CH_2COH + O_2 + H_2O \rightarrow (CH_3)_3N^+CH_2COOH + H_2O_2$$

Despite this complication, the simplification involved when assuming first-order conditions has been shown to be valid to a useful extent.

Fig. 4 shows a chromatogram obtained with a 30 × 2 mm I.D. separation column and an 11.5 × 2 mm I.D. ChO reactor obtained when reinjecting a portion of a previously collected peak. As can be seen, betaine aldehyde is separated from Ch and is clearly visible. The conditions for the first passage were: flow-rate 400 μl min^{-1}, temperature 22°C and 10 μl of 60 μM ChCl injected.

Fig. 5 shows a plot of $-\ln(1 - X)$ *vs.* τ for an 11.5 × 2 mm I.D. ChO reactor operated at 22°C. The slope of the regression line gives $K_{ps}^{app} = 0.58\ s^{-1}$, indicating that a residence time of about 8 s will result in 99% conversion of Ch to hydrogen peroxide and betaine. When using a flow-rate of 200 μl min^{-1} and a 30 × 2 mm I.D. reactor, a residence time of about 20 s will result in 99.999% conversion.

The residence time was determined by comparing the time from injection to peak

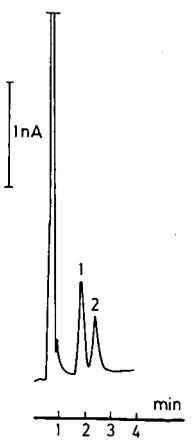

Fig. 4. Chromatogram obtained on reinjecting a portion of a previously injected ChCl sample. (1) Betaine aldehyde; (2) Ch. For details, see text.

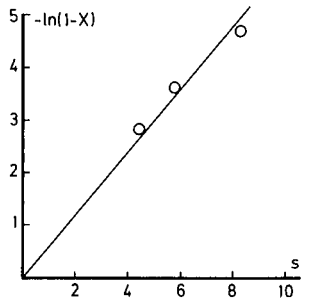

Fig. 5. Plot of $-\ln(1 - X)$ *vs.* residence time for an 11.5 × 2 mm I.D. polymer-based ChO reactor. The transformation is valid only under pseudo-fist-order conditions; under higher order conditions the plot would deviate from a straight line.

maximum with and without the reactor when injecting hydrogen peroxide. Changing the flow-rate instead of the reactor length is fully justified if eqn. 7 is evaluated in the range of flow-rates that we used.

Bacterial growth

It has been reported elsewhere[27] that bacterial growth in the mobile phase can cause severe problems with high background currents, noise and a rapid decline in reactor performance. The acetone that we use as an organic modifier in the mobile phase has some bacteriostatic properties, but not enough to eliminate completely the microbiological activity in the mobile phase.

We searched for a good poison to be used as additive to the mobile phase without disturbing any part of the chromatographic system. Sodium azide, ascorbic acid and the different Parabens are all readily oxidized by the Pt electrode at the potentials used and give rise to high and unstable background currents. Thiomersal rapidly reduces the ChO activity to zero, and chlorhexidine is strongly retained by the separation column, causing the retention times to shift. Formaldehyde reacts readily with primary amine residues of the immobilized enzymes, forming Schiff bases, and denatures the enzymes.

After some experimenting with these common bacteriostats, we found that Kathon CG was a suitable candidate that does not interfere with the separation or detection. The active component of Kathon CG is a mixture of two isothiazolines, stabilized with 23% magnesium chloride in aqueous solution. For further information, Rohm & Haas provide extensive documentation on request. So far we have not encountered any problem that can be associated either with the presence of 0.1% Kathon CG or with bacterial growth.

Chromatographic separation

Fig. 6 shows a chromatogram obtained on injecting 20 μl of 2 μM ChCl and AChCl onto a 100 × 4.6 mm I.D. PLRPS column followed by a 30 × 4 mm I.D. enzyme reactor as described previously[5]. The flow-rate was 1.0 ml min^{-1}, the temperature 35°C and the working electrode was 3 mm diameter and operated at 450 mV. The chromatogram is representative of what is achieved with this system; the main features are 3000–7000 plates/m and severe tailing.

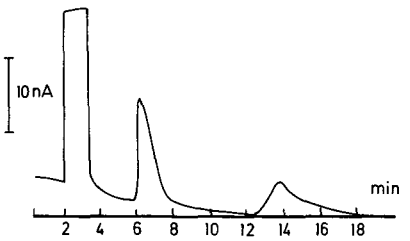

Fig. 6. Chromatogram obtained with a 100 × 4.6 mm I.D. PLRPS column and a 30 × 4 mm I.D. silica-based enzyme reactor.

Fig. 7 shows a chromatogram obtained with the polymer-based system using a 60 × 2 mm I.D. separation column and a 30 × 2 mm I.D. enzyme reactor operated at 35°C, using a flow-rate of 200 μl min^{-1}. The working electrode was a 1 mm diameter Pt electrode operated at 450 mV and 10 μl of an 8 μM ChCl and AChCl solution were injected.

A calculation of the number of theoretical plates[28] based on Fig. 7 results in 30 000–40 000 plates/m. The result can be corrected for the contribution from the enzyme reactor, assuming the variance (σ^2) to be additive, and using Fig. 1 to estimate the variance from the enzyme reactor the result is 40 000–50 000 plates/m for the separation column alone. The slight fronting observed is probably due to channels in an imperfectly packed column, the fronting becoming more pronounced at large k'.

Fig. 8 shows log k' *vs.* SDS concentration at 2% acetone and log k' *vs.* acetone concentration at 0.2 mM SDS for ACh and Ch. The reason for the non-linear behaviour of log k' *vs.* SDS concentration is probably micelle formation and the adsorption isotherm for adsorption of SDS to the stationary phase. The critical micellar concentration for SDS in water is found in this concentration region[29].

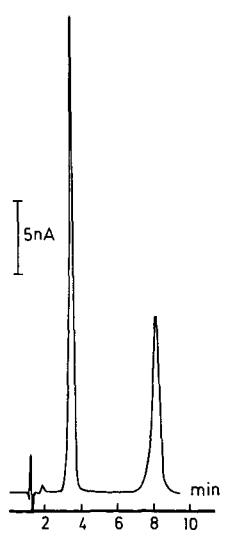

Fig. 7. Chromatogram obtained with a 60 × 2 mm I.D. separation column and a 30 × 2 mm I.D. enzyme reactor, both based on Dynospheres. For details, see text.

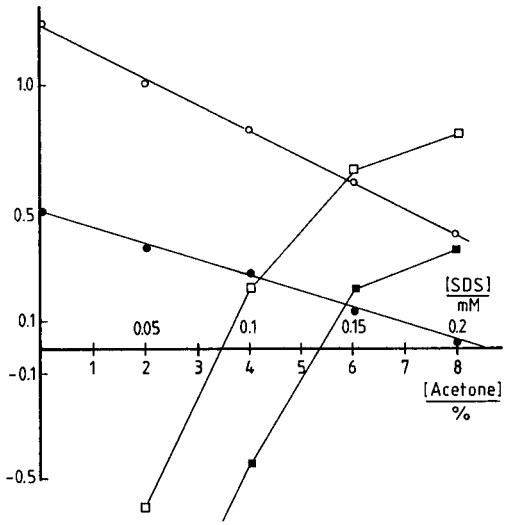

Fig. 8. Log k' *vs.* mobile phase composition. (●) ACh and (○) Ch *vs.* acetone concentration; (■) ACh and (□) Ch *vs.* SDS concentration.

CONCLUSIONS

The need for careful design of post-column enzyme reactors has been demonstrated. Useful relationships for performing such designs have been derived. The described application of monosized particles seems to be a valuable solution to some of the problems associated with efficient separation and enzymatic derivatization of Ch and ACh. Kathon CG is a suitable poison for use in conjunction with immobilized enzymes and electrochemical detectors.

ACKNOWLEDGEMENTS

We are greatly indebted to Bo-Lennart Johansson of Pharmacia for providing us with hydrophilized Dynospheres. Without the expert advice on electronics construction from Rolf Danielsson and the expert advice on thinking from Åke Olin it would have been impossible to conduct this study. We are also very grateful to Professor Bengt Nygård for his continuous support.

REFERENCES

1 B. Holmstedt, in P. G. Waser (Editor), *Cholinergic Mechanisms*, Raven Press, New York, 1975, pp. 1–21.
2 F. C. MacIntosh and W. L. M. Perry, *Methods Med. Res.*, 3 (1950) 78.
3 I. Hanin (Editor), *Acetylcholine and Choline: Handbook of Chemical Assay Methods*, Raven Press, New York, 1974.
4 P. E. Potter, J. L. Meek and N. H. Neff, *J. Neurochem.*, 41 (1983) 188.
5 N. Tyrefors and P. G. Gillberg, *J. Chromatogr.*, 423 (1987) 85.
6 G. Damsma, *Ph.D. Thesis*, Rijksuniversiteit Groningen, Groningen, 1987.
7 H. Karlsson and U. Ungerstedt, in preparation.
8 J. Ugelstad, P. C. Mørk, K. H. Kaggerud, T. Ellingsen and A. Berge, *Adv. Colloid Interface Sci.*, 13 (1980) 101.

9 P. W. Carr and L. D. Bowers, *Immobilized Enzymes in Analytical Chemistry*, Wiley, New York, 1980.
10 B. Olsson, *Ph.D. Thesis*, University of Lund, Lund, 1985.
11 B. Olsson and L. Ögren, *Anal. Chim. Acta*, 145 (1983) 87.
12 G. Johansson, L. Ögren and B. Olsson, *Anal. Chim. Acta*, 145 (1983) 71.
13 Y. T. Shih and P. W. Carr, *Anal. Chim. Acta*, 167 (1985) 137.
14 L. R. Snyder and J. J. Kirkland, *Introduction to Modern Liquid Chromatography*, Wiley, New York, 2nd ed., 1979, p. 33.
15 N. Tyrefors, in preparation.
16 D. Britz, *J. Electroanal. Chem.*, 88 (1978) 309.
17 K. Nilsson and K. Mosbach, *Methods Enzymol.*, 135 (1987) 78.
18 G. S. Bethell, J. S. Ayers, W. S. Hancock and M. T. W. Hearn, *J. Biol. Chem.*, 254 (1979) 2572.
19 G. Damsma, D. Lammerts van Buren, B. H. C. Westerink and A. S. Horn, *Chromatographia*, 24 (1987) 827.
20 P.-O. Larsson, M. Glad, L. Hansson, M.-O. Månsson, S. Ohlson and K. Mosbach, *Adv. Chromatogr.*, 21 (1983) 41.
21 Wetall, *Science*, 166 (1969) 615.
22 R. Axen, J. Porath and S. Erback, *Nature (London)*, 214 (1967) 1302.
23 G. S. Bethell, J. S. Ayers, M. T. W. Hearn and W. S. Hancock, *J. Chromatogr.*, 219 (1981) 361.
24 A. F. S. A. Habeeb and R. Hiramoto, *Arch. Biochem. Biophys.*, 126 (1968) 16.
25 O. R. Zaborsky, *Immobilized Enzymes*, CRC Press, Cleveland, OH, 1973.
26 W. J. Albery, P. N. Bartlett, M. Bycroft, D. H. Craston and B. J. Driscoll. *J. Electroanal. Chem.*, 218 (1987) 119.
27 *Curr. Sep.*, 8 (1987) 66.
28 C. F. Poole and S. A. Schuette, *Contemporary Practice of Chromatography*, Elsevier, Amsterdam, 1984, p. 8.
29 J. G. Dorsey, M. G. Khaledi, J. S. Landy and J. L. Lin, *J. Chromatogr.*, 316 (1984) 183.

Journal of Chromatography, 502 (1990) 351–358
Elsevier Science Publishers B.V., Amsterdam — Printed in The Netherlands

CHROM. 22 116

Impurity profiling of clarithromycin using high-performance liquid chromatography with ultraviolet detection

DANA MORGAN*, PHYLLIS CUGIER, BARBARA MARELLO, CHERYL SAROCKA, DAVID STROZ and ANDREW PLASZ

Analytical Research Department, Abbott Laboratories, Department 417 R1B, North Chicago, IL 60064 (U.S.A.)

(First received April 25th, 1989; revised manuscript received October 24th, 1989)

SUMMARY

Clarithromycin is a semi-synthetic antibiotic. High-performance liquid chromatography is used to identify and estimate both manufacturing and degradation impurities. The sample is chromatographed on a $YMCC_{18}$ column using an eluent of acetonitrile–0.033 *M* KH_2PO_4 (48:52) at an apparent pH of 5.4 and ultraviolet detection at 205 nm. Due to the limited availability of impurities, all related substances are referenced to a single impurity standard. A computing integrator is programmed to compensate for differences in detector responses and to identify and calculate the % (w/w) of all known impurities. The majority of all currently identified impurities are detectable at the 0.10% (w/w) level.

INTRODUCTION

During the synthesis of today's complex pharmaceutical drugs, many potential impurities can be produced. Some sources of these impurities are solvents, reagents, starting materials, inorganics, catalysts, reaction byproducts, reaction intermediates and degradation products. The latter three sources generally produce compounds which are structurally related to the drug substance and are commonly referred to as related substances. The identification and quantification of these related substances have become more important with the concern for the overall chemical purity of the drug substance[1–5]. Due to the similarity of these related substances, high-performance liquid chromatography (HPLC) is typically the method of choice.

Clarithromycin is a semi-synthetic antibiotic which was discovered by Taisho Co., Japan. A HPLC method has been developed for clarithromycin to monitor the levels of related substances. Preliminary identification is made based on retention time. Bulk drug purity has been estimated by many different methods[6–8]. The best approach is a direct identification and quantitation *versus* a reference standard of each impurity. However, for complex molecules like clarithromycin, it is not practical to produce and characterize reference standard quantities of all possible related substances. Therefore,

0021-9673/90/$03.50

most of the existing methods are based on the assumption that the detector response is identical for all compounds of interest. In some cases, the differences in detector response might be within the scientific error; however, using ultraviolet detection at 205 nm for compounds such as clarithromycin, this assumption can lead to errors of an order of magnitude. Thus, our approach is based on an indirect quantitation which compensates for differences in the molar extinction coefficient for each compound. This method should eliminate errors due to the variable detector response.

EXPERIMENTAL

Apparatus

Method development was performed on two different systems. The first system consisted of a ConstaMetric IIIG pump (LDC/Milton Roy, Riviera Beach, FL, U.S.A.), a Shimadzu SIL-6A autosampler, a CTO-6A column oven, and a CR-3A integrator (Shimadzu, Kyoto, Japan). The second system consisted of a SP-8700 solvent delivery system, a SP-4270 computing integrator (Spectra-Physics, San Jose, CA, U.S.A.), a CTO-6A column oven (Shimadzu, Kyoto, Japan) and a IBM LC/9505 autosampler (IBM, Danbury, CT, U.S.A.). Kratos Model 783 variable-wavelength detectors (ABI, Ramsey, NJ, U.S.A.) were used on both systems. The HPLC column used was a YMC A-303 5-μm 120-Å C_{18} column (YMC, Japan) 250 × 4.6 mm I.D.

Reagents and solvents

HPLC-grade acetonitrile and methanol were either purchased from Mallinckrodt (Paris, KY, U.S.A.) or J. T. Baker (Phillipsburgh, NJ, U.S.A.). The potassium phosphate, monobasic, reagent grade was also supplied by Mallinckrodt. The 6-O-methylerythromycin A and 6,11-di-O-methylerythromycin A reference standards were synthesized by Abbott Labs. (N. Chicago, IL, U.S.A.). All other related substances were either synthesized and/or isolated by either Abbott Labs. or Taisho (Tokyo, Japan).

Optimum chromatographic conditions

The mobile phase consisted of acetonitrile–0.033 *M* KH_2PO_4 (48:52, v/v). The apparent pH of the mobile phase was maintained between 5.3 and 5.5. A flow-rate of 1.0 ml/min was used at a column temperature of 50°C. A constant sample injection volume of 50 μl was maintained. The detector was operated at 205 nm with a rise time of 2.0 s and a range of 0.03 a.u./10 mV. The chromatograms were graphed at 1.0 cm/min with an attenuation of 4 mV full scale.

Standard and sample preparation

About 105 mg of clarithromycin reference standard was added to a 50-ml volumetric flask containing 25.0 ml of acetonitrile. After dissolution the solution was diluted with water to volume. This was the stock clarithromycin solution. A bulk 6,11-di-O-methylerythromycin A solution was prepared from 45 mg of 6,11-di-O--methylerythromycin A diluted with methanol to 100.0 ml. A 10-ml aliquot of this solution was further diluted with acetonitrile–water (1:3) to 100.0 ml to give a stock 6,11-di-O-methylerythromycin A solution. The working standard solution was prepared from 5.0 ml of the stock clarithromycin solution and 10.0 ml of the stock

6,11-di-O-methylerythromycin A solution diluted with acetonitrile–water (1:3) to 50.0 ml.

The sample solution was prepared from 105 mg of clarithromycin dissolved in 25.0 ml of acetonitrile and diluted with water to 50.0 ml. A 10-ml aliquot of this solution is further diluted with acetonitrile–water (1:3) to 50.0 ml.

RESULTS AND DISCUSSION

Clarithromycin is a semi-synthetic antibiotic which is a derivative of erythromycin A. The structures of clarithromycin and its related substances are given in Fig. 1. From the similarities in the structures it was obvious that column selectivity was an extremely important parameter in the column selection. Using a test mixture of clarithromycin and seven related substances, several different columns were investigated: (1) Nucleosil, C_{18} 5 μm, 150 × 4.6 mm I.D. and 250 × 4.6 mm I.D. (2) Zorbax Golden Series, C_8 3 μm, 80 × 6.2 mm I.D. (3) IBM, C_8 3 μm, 100 × 4.5 mm I.D. (4) YMC, C_{18} 5 μm, 150 × 4.6 mm I.D. and 250 × 4.6 mm I.D.

Of these columns both columns 2 and 3 did not have high enough efficiencies to provide the needed separation. The low efficiencies are due to tailing. Column 1 in the 250 × 4.6 mm I.D. configuration did provide a usable separation; however, the column life-time was unacceptable. Also comparing columns 1 and 4 for peak symmetry, the YMC offered the best performance. The 250 mm length was selected for a sight additional efficiency over the 150 mm. Since selection of the YMC column, several additional columns have been tested for equality. These columns were all 250 × 4.6 mm I.D. 5 μm with the following stationary phases: Phenomenex Carbosphere, Whatman ODS, TSK Gel ODS, and Regis ODS II. Of theses columns only the

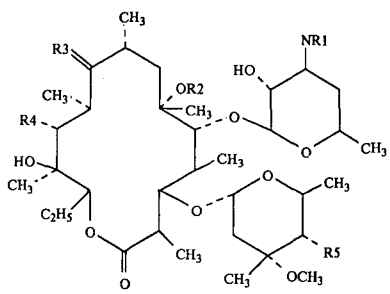

NAME	R1	R2	R3	R4	R5
Clarithromycin	$(CH_3)_2$	CH_3	O	OH	OH
EM=NOH	$(CH_3)_2$	H	NOH	OH	OH
=NOH	$(CH_3)_2$	CH_3	NOH	OH	OH
=NOH,NH	$H(CH_3)$	CH_3	NOH	OH	OH
-NH	$H(CH_3)$	CH_3	O	OH	OH
6,11-Di	$(CH_3)_2$	CH_3	O	CH_3	OH
6,4"-Di	$(CH_3)_2$	CH_3	O	OH	CH_3
=NOMe	$(CH_3)_2$	CH_3	$NOCH_3$	OH	OH
N-Formyl	$(COH)(CH_3)$	CH_3	O	OH	OH

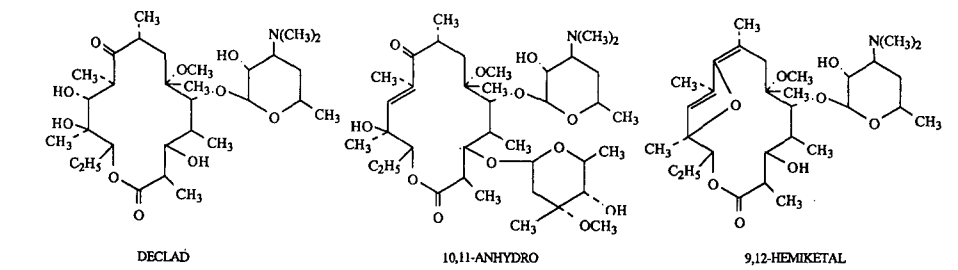

DECLAD 10,11-ANHYDRO 9,12-HEMIKETAL

Fig. 1. Structure of clarithromycin and related compounds. Definitions of abbreviations are found in Table I.

Phenomenex Carbosphere gave promising results; however, it was not totally equivalent.

During the column screening process, the effects of mobile phase variations were investigated. The effect of mobile phase pH was studied and found to be minimal; thus, the apparent pH is monitored only to verify the proper value. Also, the column temperature does not greatly affect the retention, but is necessary to maintain good peak symmetry and resolution. The organic–aqueous ratio however, has a dramatic effect on the separation. Fig. 2 illustrates this critical relationship. The test compounds in Fig. 2 include those related substances which most closely elute with clarithromycin. At the lower organic concentrations, the separation between most compounds increases; however, 6-O-methylerythromycin A-N-oxide and 6,11-di-O-methylerythromycin A coelute. These two compounds are separated at the higher organic concentration at the sacrifice of resolution of early eluting compounds. To compromise between detection limits and resolution, a mobile phase consisting of 0.033 *M* KH_2PO_4–acetonitrile (52:48) was selected. Typical chromatograms of the reference standard clarithromycin and the reference standard spiked with various different related substances at both the 0.2 and 1.0% (w/w) levels are presented in Figs. 3 and 4.

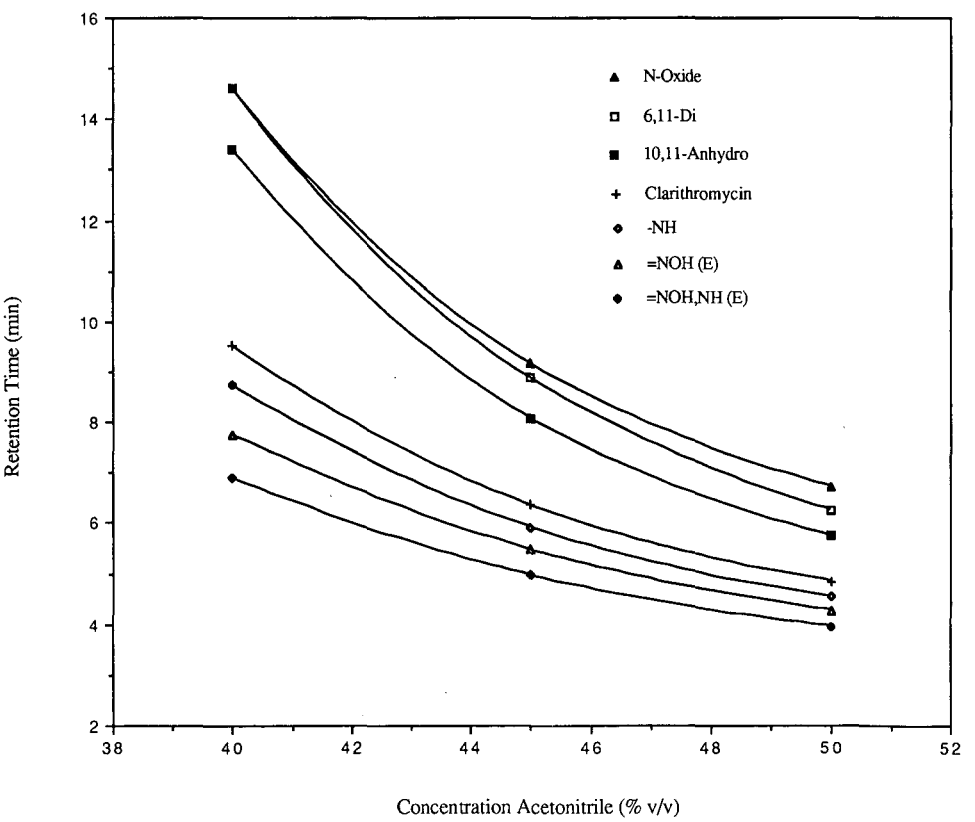

Fig. 2. Effect of acetonitrile concentration on retention time. 0.067 *M* KH_2PO_4 buffer was used to maintain a constant apparent pH of 5.4. Definitions of abbreviations are found in Table I.

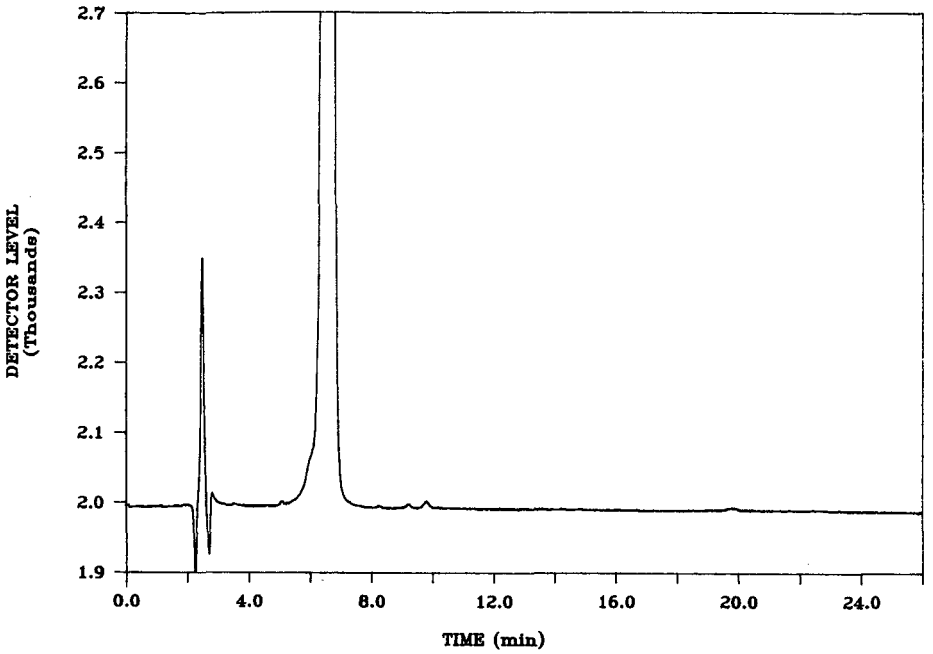

Fig. 3. Typical chromatogram of clarithromycin reference standard.

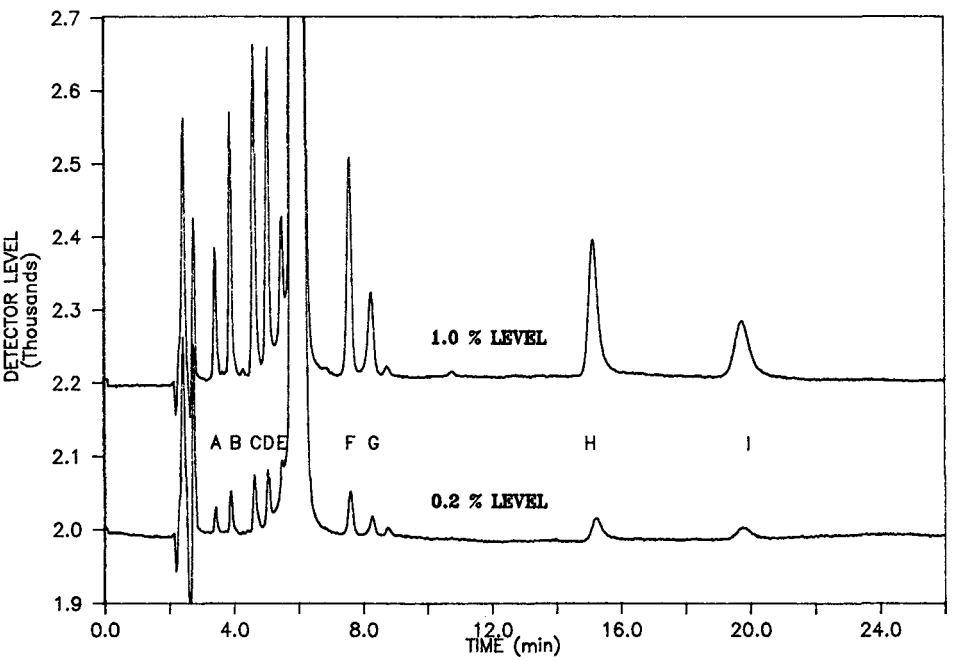

Fig. 4. Chromatograms of reference standard spiked with related substances at the 1.0 and 0.2% (w/w) level. A = Decladinosyl-6-O-Me-ery A; B = Ery A-9-oxime (E); C = N-De-Me-6-O-Me-ery A-9-oxime (E); D = 6-O-Me-ery A-9-oxime (E); E = N-De-Me-6-O-Me-ery A; F = 10,11-anhydro-6-O-Me-ery A; G = 6,11-Di-O-Me-ery A; H = 6-O-Me-ery A-9-Me-oxime (E); I = N-De-Me-N-formyl-6-O-Me-ery A.

Fig. 4 also illustrates the need to correct for the various detector responses. Even though all of the impurities are at the same concentration, the peak area of each impurity can differ dramatically. To correct for the different molar extinction characteristics, a normalization factor is determined for each impurity. The reference compound selected was 6,11-di-O-methylerythromycin A. This compound was selected for various reasons: it is the most likely produced impurity, it has very similar absorption properties to clarithromycin and it can easily be synthesized in good purity. The procedure for determination of the normalization factor is quite simple. First, the structure and purity of each compound was determined by using techniques such as HPLC, thin-layer chromatography, ^{1}H NMR, ^{13}C NMR and mass spectrometry. Then, binary mixtures of the impurity and the reference compound were made at six different concentrations ranging from approximately 0.6 to 20 μg/ml. The peak response calibration curve for each compound was obtained and the slope of the calibration curve was defined as the response factor of that compound. If the intercept of the calibration curve is essentially the origin, then the normalization factor can be obtained from the ratio of the response factor of the related substance to the response factor of 6,11-di-O-methylerythromycin A. This relationship is only true if the intercept of the calibration curve is zero. If the intercept is positive, then at low concentrations the concentration will be overestimated and at high concentrations, a low bias will result. If the intercept is negative then the reverse systematic error exists. The inability to accurately integrate the area of N-demethyl-6-O-methylerythromycin A, which is located on the front slope of the major peak, causes a positive intercept and thus peak heights were used to obtain a zero intercept that guarantees the accuracy of the quantitation. Table I summarizes the normalization factors and relative capacity factors of the most common impurities. The preliminary peak identifications are made

TABLE I

RELATIVE CAPACITY FACTOR AND NORMALIZATION FACTORS FOR CLARITHROMYCIN RELATED SUBSTANCES

Compound[a]	*Abbreviation*	*Rel. capacity factor*	*Normalization factor*
Decladinosyl-6-O-Me-ery A	DECLAD	0.21	1.12
Ery A-9-oxime (E)	EM=NOH (E)	0.30	1.39
6-O-Me-ery A 9-oxime (Z)	=NOH (Z)	0.37	2.00
N-De-Me-6-O-Me-ery A-9-oxime (E)	=NOH,NH (E)	0.44	2.48
6-O-Me-ery A-9-oxime (E)	=NOH (E)	0.50	2.41
N-De-Me-6-O-Me-ery A	-NH	0.56	1.72
10,11-Anhydro-6-O-Me-ery A	10,11-ANHYDRO	0.89	2.62
6,11-Di-O-Me-ery A	6,11-Di	1.00	1.00
Di-O-Me-ery A	Di-O-Me	1.10	1.00
6-O-Me-ery A-N-oxide	N-oxide	1.10	0.95
6,4″-Di-O-Me-ery A	6,4″-Di	1.15	0.88
6-O-Me-ery A-N-oxime (Z)	=NOMe (Z)	1.28	2.34
3-Decladinosyl-8,9;10,11-dianhydro--9,12-hemiketal	9,12-HEMIKETAL	1.70	4.50
6-O-Me-ery A-9-Me-oxime (E)	=NOMe (E)	2.02	2.74
N-De-Me-N-formyl-6-O-Me-ery A	N-formyl	2.15	5.47

[a] De-Me = Demethyl; Me = methyl; ery = erythromycin.

TABLE II

DIRECT *VERSUS* INDIRECT QUANTITATION FOR IDENTIFIED IMPURITIES IN A REPRESENTATIVE LOT

Compound	*Direct (%, w/w)*	*Indirect (%, w/w)*
=NOH,NH (E)	≪0.25	≪0.25
=NOH (E)	0.25	0.23
-NH	0.24	0.29
10,11-ANHYDRO	≪0.25	≪0.25
N-oxide	0.48	0.40

based on the relative capacity factor of each peak. The calculation of both the relative capacity factor and % (w/w) for each peak is performed by the integrator using in-house developed software which is based on the following equation:

$$\% \text{ (w/w)} = \frac{\text{(Response impurity) (concentration of 6,11-Di) (dilution factor)}}{\text{(Response 6,11-Di) (sample weight) (normalization factor)}}$$

All of the related substances were found to exhibit linearity from at least 1 to 10 μg/ml and had zero intercepts. The detection limit was obtained for 6,11-di-O-methyl-erythromycin A from a calibration curve of areas. The linear analysis of a range of 0.14 to 34 μg/ml gave an intercept of −967 counts, a slope of 3216 counts ml/μg, with a correlation coefficient of 0.9996. The detection limit for a peak with a signal-to-noise ratio of 3 was found to be 0.14 μg/ml which was approximately 0.04% (w/w). Due to the limited availability of all related substances and since almost all compounds have a normalization factor of greater than one, a minimal reportable value of 0.10% (w/w) was defined.

To prove that identification and quantitation *versus* a reference compound gives

TABLE III

REPRODUCIBILITY OF THE METHOD

A representative lot was assayed ten times (1–10), values are % (w/w).

Impurity	*1*	*2*	*3*	*4*	*5*	*6*	*7*	*8*	*9*	*10*	*Mean*	*S.D.*
DECLAD	0.04	0.01		0.04	0.04	0.02	0.05	0.04	0.04	0.02	0.04	±0.013
EM=NOH (E)	0.02	0.01	0.01	0.02	0.01			0.02	0.02		0.02	±0.005
=NOH (Z)	0.02	0.01		0.02	0.03	0.03	0.03	0.03	0.02	0.03	0.02	±0.007
=NOH, NH (E)			0.02								0.02	±0.000
=NOH (E)	0.12	0.17	0.08	0.12	0.12	0.12	0.10	0.27	0.12	0.12	0.13	±0.053
-NH	0.16	0.17	0.16	0.13	0.14	0.17	0.06	0.13	0.12	0.19	0.14	±0.037
6,11-Di	0.17	0.20	0.15	0.18	0.16	0.22	0.14	0.18	0.19	0.23	0.18	±0.029
Di-O-Me	0.21	0.23	0.19	0.20	0.33	0.22	0.20	0.21	0.30	0.24	0.23	±0.046
6,4″-Di	0.08	0.10	0.08	0.08	0.07	0.08	0.06	0.09	0.08	0.10	0.08	±0.012
=NOMe (Z)	0.04	0.05		0.03	0.03	0.04	0.03	0.04	0.04	0.04	0.04	±0.007
=NOMe (E)	0.37	0.39	0.29	0.32	0.37	0.38	0.34	0.32	0.36	0.36	0.35	±0.032
N-formyl	0.04			0.03	0.04	0.05	0.02	0.02	0.04	0.06	0.04	±0.014

compatible results with a direct quantitation using individual standards, a typical production intermediate sample was assayed against individual standards as well as indirectly *versus* 6,11-di-O-methylerythromycin A. For five selected impurities, individual calibration curves were obained and the representative lot was quantitated directly *versus* the individual standards curves. This direct value was compared with the concentrations obtained using the normalization factors and a single 6,11-di-O--methylerythromycin A reference standard. The results (Table II) indicate an excellent agreement between the two techniques.

Table III demonstrates the reproducibility of the method. A representative lot was assayed a total of ten times by two different analysts using entirely different HPLC systems. To better illustrate the reproducibility of the methodology, all values below 0.10% (w/w) were estimated to the nearest 0.01% and standard deviations (S.D.) to $\pm 0.001\%$. Considering the low levels of all of the related substances, the agreement between various analysts and chromatographic systems is very good.

CONCLUSIONS

Clarithromycin is a complex antibiotic and has several potential impurities. The related substances are structurally very similar to the parent compound and the separation is quite difficult. By compensating for differences in absorbance properties of different compounds, this method allows for an accurate, simple procedure using a single standard to identify and quantitate all related substances. Thus, this method provides identification and quantitation of most of the related substances at the 0.10% (w/w) level. When used with other techniques for the determination of moisture, residual solvents and inorganic material, a complete impurity profile of the bulk drug is possible. This type of normalization procedure can be adapted for any set of compounds and thus eliminates errors associated with techniques such as peak area percent.

REFERENCES

1 Pharmaceutical Manufactures Association, *Pharmacopeial Forum*, Sept.-Oct. (1987) 2972.
2 *Drug Purity-Where Are We Now? (APQ Symposium), Third Annual Meeting, American Association of Pharmaceutical Scientists, Orlando, FL, Oct. 30–Nov. 3, 1988.*
3 L. Chafetz, *Pharm. Technol.*, 8:10 (1984) 24.
4 R. J. Wolters, *Pharm. Technol.*, 8:10 (1984) 35.
5 C. A. Johnson, *Pharm. Technol.*, 8:10 (1984) 28.
6 E. L. Inman, *J. Chromatogr.*, 410 (1987) 363.
7 E. L. Inman, *J. Chromatogr. Sci.*, 26 (1988) 89.
8 N. Beaulieu, P. Lacroix, R. Sears and E. Lovering, *J. Pharm. Sci.*, 77 (1988) 889.

Journal of Chromatography, 502 (1990) 359–369
Elsevier Science Publishers B.V., Amsterdam — Printed in The Netherlands

CHROM. 22 106

Purification and characterization of hementin, a fibrinogenolytic protease from the leech *Haementeria ghilianii*

JOEL K. SWADESH*,[a] and I.-YIH HUANG
Smith Kline & French Laboratories, King of Prussia, PA 19406-0939 (U.S.A.)
and
ANDREI Z. BUDZYNSKI
Department of Biochemistry, Temple University School of Medicine, Philadelphia, PA 19140 (U.S.A.)
(First received April 3rd, 1989; revised manuscript received August 17th, 1989)

SUMMARY

The fibrinogenolytic enzyme hementin, present in extracts of the posterior salivary glands of the giant leech *Haementeria ghilianii*, was isolated by ultrafiltration, high-performance ion-exchange chromatography and subsequent reversed-phase liquid chromatography. Approximately 100 μg (1 nmol) of hementin, present at less than 0.5% in the crude leech salivary extract, was brought to about 90% purity in three steps. Hementin migrated at an M_r of about 73 000 on non-reducing sodium dodecyl sulfate polyacrylamide gel electrophoresis (SDS-PAGE) and at 82 000 on reducing SDS-PAGE. The amino terminal sequence was determined to be TTLTEPEPDL. The amino terminal sequences of two inactive proteins that partially coeluted with hementin in the first chromatographic step were also determined.

INTRODUCTION

Extracts of the salivary glands of the leech *Haementeria ghilianii* contain proteolytic activity. The enzyme present in the anterior gland is more abundant than that in the posterior gland, so the extract of the anterior gland has been the principal object of investigation. Fibrin strip zymography of electrophoretic separations of extracts of posterior and anterior glands indicated that the enzymatic activity may originate from the same protein resident in both glands[1,2]. Hementin is a fibrinogenolytic enzyme acting as a blood anticoagulant with properties substantially different than those found in other leech species. Unlike hirudin[3], an inhibitor of thrombin, hementin acts directly on fibrinogen, proteolyzing it such that it is rendered incoagu-

[a] Present address: Polymer Laboratories, Inc., Amherst Fields Research Park, 160 Old Farm Road, Amherst, MA 01002, U.S.A.

0021-9673/90/$03.50

lable. Only a few, discrete bands are observed on sodium dodecyl sulfate polyacrylamide gel electrophoresis (SDS-PAGE) of hementin-treated fibrinogen, indicating that the enzyme has a high degree of specificity. Hementin was previously observed to be inactivated by metal-chelating and disulfide-reducing reagents, but the proteolytic activity was found to be unaffected by typical inhibitors of serine protease activity[4]. In a previous attempt to isolate hementin[4], chromatography on diethylaminoethylcellulose (DEAE), followed by ammonium sulfate (AS) precipitation and chromatography on carboxymethylcellulose (CMC), did not afford a homogeneous preparation, so non-denaturing polyacrylamide gel electrophoresis was used to prepare sufficient material for a determination of molecular weight (M_r), which was reported to be 120 000 daltons.

The extract of the posterior salivary gland of *Haementeria ghilianii* is a complex mixture, containing many proteins. In this work, the proteins associated with activity of hementin were isolated. The amino terminal sequences of three proteins that co-eluted in ion-exchange chromatography during hementin purification were determined by automated Edman sequencing.

EXPERIMENTAL

Materials

Ammonium hydrogencarbonate was purchased from Sigma (St. Louis, MO, U.S.A.). Calcium chloride dihydrate, sodium chloride, 25% glutaraldehyde, ammonia solution, HPLC-grade 2-propanol (iPA) and gradient-tested trifluoroacetic acid (TFA) were obtained from J. T. Baker (Phillipsburg, NJ, U.S.A.). Bromphenol blue and N,N,N′,N′-tetramethylethylenediamine were purchased from LKB Instruments (Gaithesburg, MD, U.S.A.). The silver stain kit, which used ammoniacal silver[5], was from ICN Biochemicals (Irvine, CA, U.S.A.). Utrapure 4-(2-hydroxyethyl)-1-piperazineethanesulfonic acid (HEPES) was obtained from Boehringer Mannheim Biochemicals (Indianapolis, IN, U.S.A.). Molecular weight markers (composed of a mixture of proteins of M_r equivalent to 14 300, 18 400, 25 700, 43 000, 68 000, 97 400 and 200 000 daltons), ultrapure glycine and ultrapure Tris were from Bethesda Research Labs. (Gaithesburg, MD, U.S.A.). Ultrapure acrylamide, ultrapure N,N′-methylenebisacrylamide and Coomassie Brilliant Blue R250 (CBB) were obtained from Schwarz/Mann Biotech (Cleveland, OH, U.S.A.). Sodium dodecyl sulfate (SDS) and 2-mercaptoethanol (BME) were purchased from Pierce (Rockford, IL, U.S.A.). The fibrinogen used to test for hementin activity was of human origin (Grade L; Kabi Vitrum, Stockholm, Sweden). Solvent filters (0.2 μm) were from Rainin Instrument (Woburn, MA, U.S.A.). The preparation of the posterior gland extract has been described previously[4]. Briefly, dried posterior salivary glands, obtained from a breeding facility at the University of California (Berkeley, CA, U.S.A.). were homogenized with a cell disruptor in 20 m*M* HEPES buffer (pH 7.8) containing 10 m*M* calcium chloride. Cell debris was removed by centrifugation and the supernatant collected.

Instrumentation

Ultrafiltration was performed using an 8MC stirred cell (Amicon, Danvers, MA, U.S.A.) equipped with a YM-100 (Amicon) 100 000-dalton cutoff membrane. Some samples were concentrated using a Centricon 30 (Amicon) 30 000-dalton mi-

croconcentrator and a Model RC-5B Sorvall (DuPont, Wilmington, DE, U.S.A.) refrigerated centrifuge. The ion-exchange chromatograph consisted of Model 2150 pump, a Model 2152 controller and an injection valve from LKB Instruments. The ion-exchange system was equipped with a Mono Q high-performance anion-exchange column (Pharmacia, Piscataway, NJ, U.S.A.).

Reversed-phase liquid chromatography (RPLC) was performed on a Spectra-Physics (San Jose, CA, U.S.A.) 8700 system. This was equipped with a type 201-TP54 C_4 Vydac column (Separations Group, Hesperia, CA, U.S.A.). This column had a 5-μm particle size support with 300-Å pores, packed in a 15 cm × 4.6 mm I.D. stainless-steel column. Chromatographic detection was effected by measuring the absorbance at 220 or 280 nm, using a Model 116 detector (Gilson Medical Electronics, Middleton, WI, U.S.A.).

Densitometry of electrophoretic gels was performed on an LKB 2202 Ultrascan laser densitometer. Sequencing was performed on either an 890M-2 Sequencer (Beckman, Palo Alto, CA, U.S.A.) or on an Applied Biosystems (Foster City, CA, U.S.A.) 470A gas-phase sequencer. Separation and quantitation of the phenylthiohydantoin (PTH)-amino acids was performed using a previously described system[6]. Data were acquired and analyzed using a Beckman (Waldwick, NJ, U.S.A.) Computer Inquiry Systems Computer Automated Laboratory Systems (CALS) data system.

Buffer preparation

Buffers for all separation steps prior to RPLC contained 20 m*M* ammonium hydrogencarbonate adjusted to pH 8.0 ± 0.1 with ammonia solution. The ion-exchange starting buffer additionally contained 100 μM calcium chloride, and the elution buffer (IEC-B) additionally contained both 100 μM calcium chloride and 500 m*M* sodium chloride. The buffer used for transfer and concentration following ion-exchange chromatography was 250 m*M* in sodium chloride. All buffers and chromatographic eluents were filtered through 0.2-μm filters.

Ion-exchange chromatography (IEC)

A 600-μl portion of crude posterior gland extract was combined with 2.0 ml of 20 m*M* ammonium hydrogencarbonate buffer and ultrafiltered at 4°C and constant volume with 9 ml of the same buffer, using a YM-100 ultrafiltration membrane. The retentate was chromatographed by high-performance anion-exchange chromatography at 1 ml/min. The elution program was 0% IEC-B (5 min), to 8% (1 min), to 25% (19 min), to 40% (5 min), to 65% (15 min), to 100% (10 min). Detection was at 280 nm. Fractions of 1 ml were collected and assayed for fibrinogenolytic activity as described below. Portions of many of the fractions obtained by high-performance IEC were subjected to SDS-PAGE. Certain proteolytically active fractions were pooled and washed at 4°C using the Centricon 30 ultrafiltration apparatus.

Reversed-phase liquid chromatography

Portions of the enzymatically-active pooled IEC fractions were injected onto the RPLC column. Elution buffers were 0.1% aqueous TFA (buffer A) and 0.1% TFA–iPA (buffer B). Elution was accomplished by a programmed linear gradient at a flow-rate of 0.75 ml/min. The starting condition was 95% A, which was held for 2 min after injection, and the gradient proceeded to 70% B at 55 min. Detection was at 220 nm. Fractions were taken at 1-min intervals.

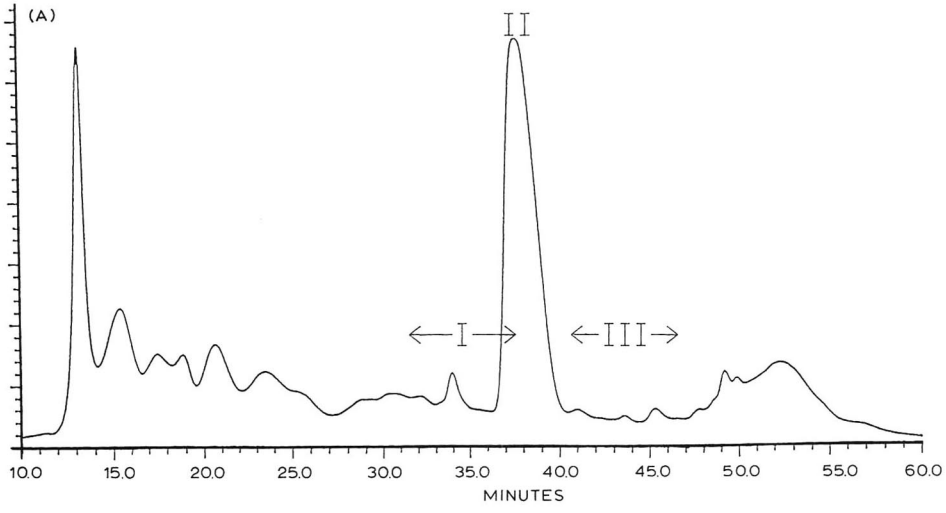
(A)
II
←I→
←III→
10.0
15.0
20.0
25.0
30.0
35.0
40.0
45.0
50.0
55.0
60.0
MINUTES

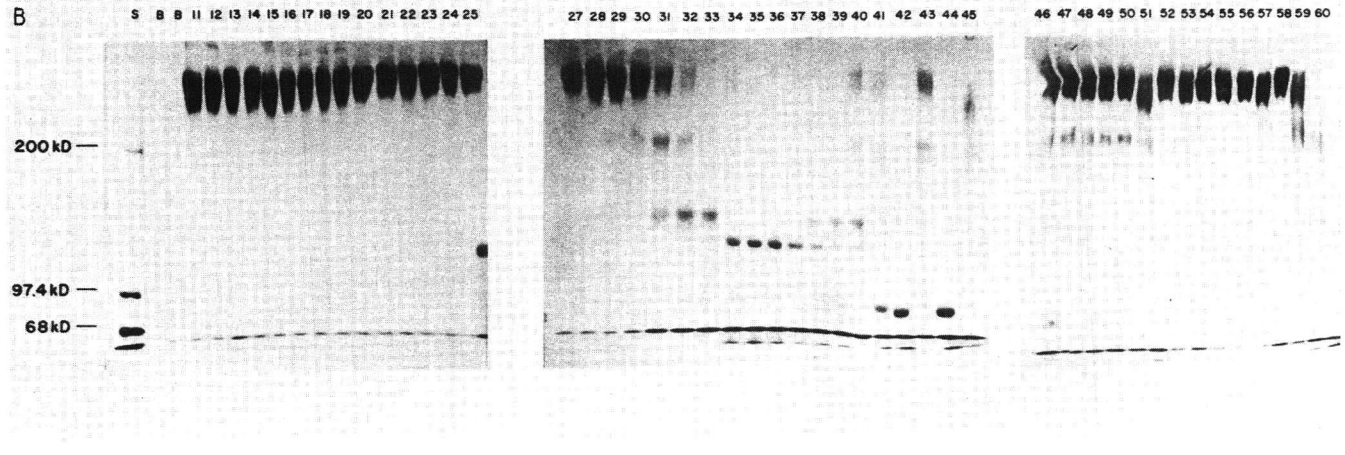
B
S 8 8 11 12 13 14 15 16 17 18 19 20 21 22 23 24 25
27 28 29 30 31 32 33 34 35 36 37 38 39 40 41 42 43 44 45
46 47 48 49 50 51 52 53 54 55 56 57 58 59 60
200kD
97.4kD
68kD

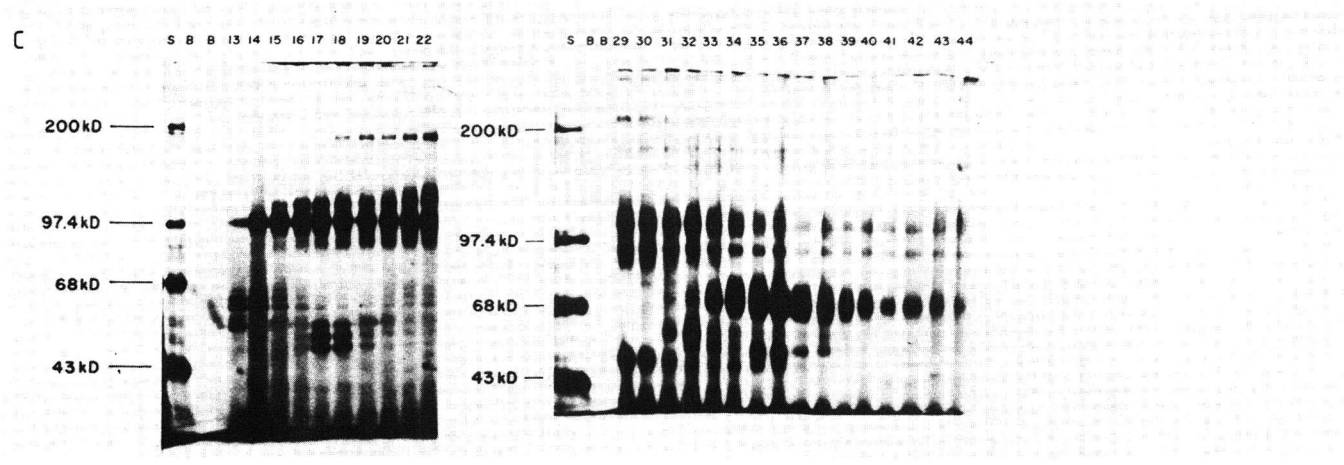

Fig. 1. High-performance anion-exchange chromatography of crude hementin. Leech salivary gland extract was ultrafiltered through a YM-100 membrane and the retentate applied on a Mono Q column. Elution was effected at a flow-rate of 1 ml/min with buffers containing 20 m*M* ammonium hydrogen-carbonate and 100 μM calcium chloride, pH 8.0; the elution buffer contained 0.5 *M* sodium chloride. Numerals along the horizontal axes are the chromatographic retention time in minutes. (A) Elution profile at 280 nm of retentate on IEC. (B) SDS-PAGE pattern (5% acrylamide, CBB stain) of fibrinogen incubated at 37°C with aliquots of column fractions from (A) (retentate). (C) Non-reducing SDS-PAGE (10% acrylamide, silver stain) of aliquots of column fractions from (A) (retentate). The symbols S and B in (B) and (C) indicate standards and blanks, respectively. Along the vertical axes of (B) and (C) are marked the electrophoretic migration positions of the protein standards in kilodaltons. Fractions 33–38 are designated peak I, the peak at 38 min is designated peak II and fractions 41–45 are designated peak III.

Activity assay

The column fractions were tested for fibrinogenolytic activity by incubation at 37°C with fibrinogen (1 mg/ml) in 150 m*M* HEPES (pH 7.9) containing 10 m*M* calcium chloride. To test the IEC fractions, 5 μl of sample were combined with 180 μl of fibrinogen solution. To test the RPLC fractions, 20 μl of sample were combined with 280 μl of fibrinogen solution. Aliquots of the digestion mixtures were taken at appropriate intervals, quenched with non-reducing electrophoresis sample loading buffer and electrophoresed by non-reducing SDS-PAGE.

Electrophoretic methods

Non-reducing sample buffer was prepared by combining 20 ml of glycerol, 8 ml of 1 *M* Tris–HCl (pH 6.8), 10 ml of 10% aqueous SDS, 0.5 ml of 0.4% aqueous bromphenol blue and 71 ml of water. Reducing sample buffer was prepared by combining non-reducing sample buffer with BME in the volume ratio 95:5. Samples were electrophoresed using the Laemmli system[7]. Up to twenty samples were simultaneously electrophoresed on 12.5 × 14 × 0.15 cm slab gels with 2.5-cm stacking gels. Activity assays were performed on 5% acrylamide gels using CBB staining. Individual IEC fractions were assayed on 7.5% acrylamide gels (non-reducing) with glutaraldehyde-enhanced silver staining[5]. A pool of IEC fractions 33–38 was assayed on 10% acrylamide (reducing and non-reducing) with CBB staining and silver stain overlay. RPLC fractions and the final preparation of hementin were assayed on 10% acrylamide gels with silver staining. Gels were scanned by laser densitometry, with the output being directed to the CALS system for analysis.

RESULTS

Ion-exchange chromatography

The retentate from ultrafiltration contained approximately 87% of the original hementin. It was injected onto a Mono Q IEC column and eluted with an ascending salt gradient. Fig. 1A shows the elution profile (280 nm) of the retentate. The small peak at about 34 min contained hementin. This peak, designated I, was calculated from the absorbance to comprise about 3.8% of the crude extract.

Fig. 1B shows the non-reducing SDS-PAGE of samples of fibrinogen treated with aliquots of fractions obtained from IEC of the retentate as shown in Fig. 1A. Fig. 1C shows the non-reducing SDS-PAGE of fractions 13–22 and 29–44. To summarize the results shown in Fig. 1B and C, fibrinogenolytic activity elutes from the Mono Q column in seemingly distinct fractions at 31–38, 40–45, and 59–60 min. The activity in the first two of these fractions appears to be correlated with the appearance of a band at slightly above 68 000 daltons in non-reducing SDS-PAGE.

Fractions 33–38 (peak I) were pooled and concentrated to a volume of 2.0 ml on a Centricon 30. Fractions 41–45 (peak III) were similarly pooled. The principal electrophoretic band of peak I migrated at 76 000 daltons on non-reducing SDS-PAGE and 82 000 daltons on reducing SDS-PAGE. Neglecting material at the dye front, the principal band was found to be about 64% (non-reducing gel) and 57% (reducing gel) of the densitometric area. No single contaminant band represented more than about 5% of the densitometric area. Silver stain overlay, while revealing numerous trace contaminants, gave no evidence of the existence of inhomogeneity of

the principal band. Based on comparison of the CBB band areas with those of a proprietary sample of similar molecular weight, the concentration of the 76 000-dalton (non-reducing SDS-PAGE) band in peak I was calculated to be 64 μg/ml. Although RPLC subsequently demonstrated that the CBB band was inhomogeneous, the estimate of concentration was useful for the purpose of evaluating sequence data.

Reversed-phase liquid chromatography

Approximately 400 μl of peak I were further purified by RPLC. Aliquots of each fraction were assayed for composition by SDS-PAGE and for fibrinogenolytic activity. The results are shown in Fig. 2B–D. Fig. 2B shows the RPLC elution profile, Fig. 2C shows the SDS-PAGE of column fractions (10% acrylamide, silver stain) and Fig. 2D shows SDS-PAGE of 2-h digests of fibrinogen. The material that elutes in a sharp peak at 34–35 min, peak IA, is inactive. By comparison of the three panels, it can be seen that the fibrinogenolytic activity is contained largely in fraction 38, designated peak IB, characterized by an M_r of 73 000 daltons on non-reducing SDS-PAGE. The component in fractions 40–41, peak IC, is inactive, but has an M_r identical with that of IB.

RPLC of pooled peak III was also performed, and results very similar to those shown for peak I were obtained. The chromatographic trace is shown in Fig. 2A. The proteolytic activity appeared in a single peak at the same retention time as was observed for peak IB. Based on RPLC peak areas, it was calculated that only 10% of the total hementin eluted by IEC is contained in peak III.

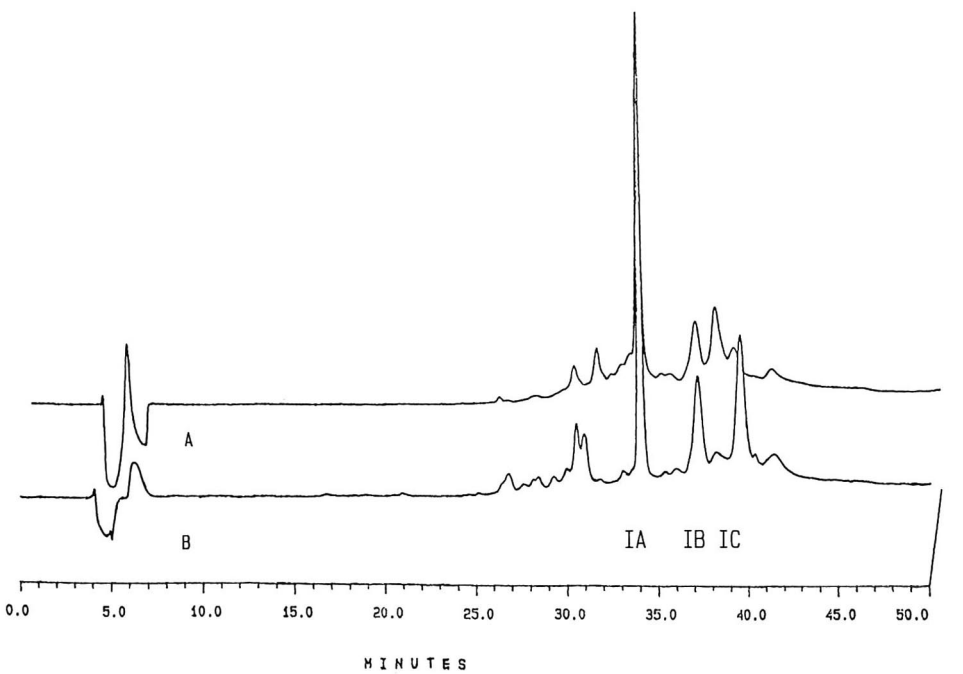

Fig. 2.

(Continued on p. 366)

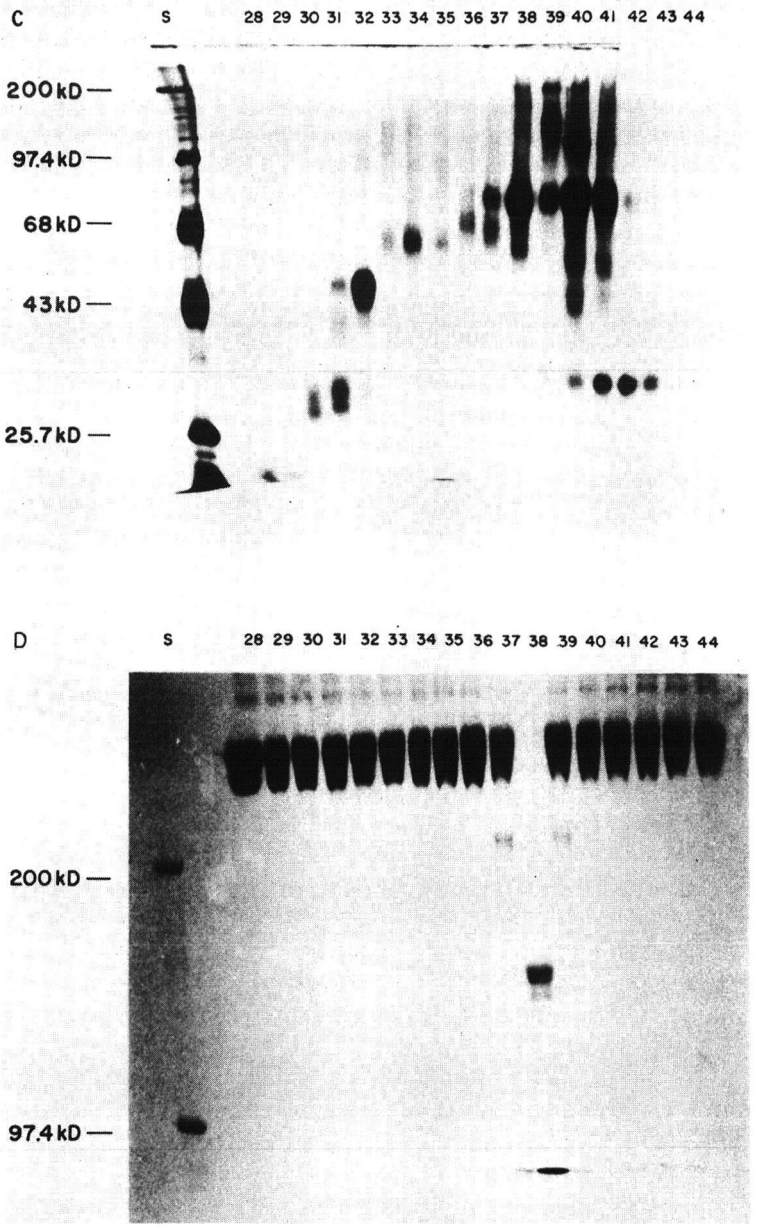

Fig. 2. Reversed-phase liquid chromatography of hementin. Fractionation was effected by applying peaks I and III of IEC-purified hementin on a C_4 column at 0.75 ml/min. The gradient was from 95% to 30% of 0.1% aqueous TFA with 0.1% TFA–iPA as the organic constituent of the mobile phase. Numerals on the horizontal axis indicate chromatographic retention times in minutes. The peak at 34–35 min is designated IA, that at 38 min is IB and that at 40–41 min is IC. (A) RPLC of IEC peak III measured at 220 nm. (B) RPLC of IEC peak I measured at 220 nm. (C) Non-reducing SDS-PAGE (10% acrylamide, silver stain) of aliquots of fractions from (B). (D) Non-reducing SDS-PAGE (5% acrylamide, CBB stain) of fibrinogen incubated at 37°C with aliquots of column fractions from (B). The symbols S and B in (C) and (D) indicate standards and blanks, respectively. On the vertical axes (C) and (D) are indicated the electrophoretic migration positions of the protein standards in kilodaltons.

Amino terminal sequencing

RPLC peak IA was found to have the sequence EVYTNYASFL[a]. Peak IB contained hementin and its sequence was TTLTEPEPDL (Table I). Of the residues other than hementin observed in sequencing this fraction, many were assigned as derived from peak IA, leaving little ambiguity in the assignment of the sequence. If one were to calculate the purity on a weight percent basis, ignoring the trace residues shown in the third row of Table I, the purity of the material in peak IB would be about 90%. Peak IC was found to have the sequence S(D)TGEEGA(K)RDV. This sequence is clearly unrelated to that observed for hementin.

DISCUSSION

The fibrinogenolytic acitivity of the posterior salivary gland of *Haementeria ghilianii* was determined to arise from a single protease migrating at an apparent M_r of 82 000 daltons on reducing SDS-PAGE, and having an amino terminal sequence TTLTEPEPDL. The principal residual impurity, proved to be inactive, was a polypeptide of M_r < 18 400 daltons, and having an amino terminal sequence EVYTNYASFL. Two minor impurities of M_r 62 000 and 67 000 daltons were also noted, but were not sufficiently abundant to sequence. Densitometric analysis indicated that these trace impurities were approximately equally divided between RPLC fractions 37 and 38, yet the fibrinogenolytic activity is clearly centered in fraction 38. Therefore, these can be excluded as sources of fibrinogenolytic activity. Several other minor impurities appear as a streak at molecular weights greater than hementin. All of these bands are far more abundant in fraction 39, so these can also be excluded as sources of fibrinogenolytic activity.

The pattern of degradation products observed on treatment of fibrinogen with purified hementin was identical with that obtained from treatment with crude extract, suggesting that the extract contains only a single protease. The fibrinogenolytic activity exhibited by IEC fractions 59–60 is believed to be due to the effects of non-specific adsorption to the Mono Q column. The digestion pattern in fractions 41–45 is consistent with extensive degradation of fibrinogen by hementin. On collecting peak III and subjecting the pool to RPLC, only about 10% of the total hementin (relative to that in peak I) was recovered; no other protease was discovered and the hementin specific activity was qualitatively consistent with the mass.

In the original attempt to isolate hementin[4], the AS and CMC steps increased the purity by a combined factor of only three. The purification scheme relied on DEAE and on non-denaturing electrophoresis to achieve the greatest increases in purity. Hementin did not bind to CMC and, therefore, probably has few exposed basic residues. The acidic residues were the principal determinants of both chromatographic (DEAE) and non-denaturing electrophoretic mobility, so these techniques were not mechanistically independent. The five-step procedure apparently did not resolve hementin from a 120 000-dalton protein. Resolution of hementin from components of M_r near 120 000 daltons was barely achieved in this work with the the high-performance techniques available today (Fig. 2C).

RPLC has become increasingly popular as a method for the purification of

[a] Throughout this article, the single-letter code for amino acids is used.

TABLE I

AMINO TERMINAL SEQUENCING OF PEAK IB

Sequence	*Cycle*									
	1	*2*	*3*	*4*	*5*	*6*	*7*	*8*	*9*	*10*
Principal sequence of hementin residues (pmol)[a]	T(9.9)	T(6.1)	*L*(9.4)	T(5.9)	*E*(7.0)	*P*(7.5)	E(6.0)	*P*(6.1)	D(4.6)	L(5.4)
Minor sequence residues (pmol)	E(5.5)	V(2.3)	Y(2.6)		N(2.7)	Y(2.3)	A(3.9)			
Other amino acid residues[b]	L,W			P	A	E	F			

[a] Residues in italics were confirmed on the Beckman 890M-2 sequence.

[b] Residues other than those derived from hementin or peak IA were present in amounts below the limits of determination.

enzymes with retention of activity, although it is known that reversible or irreversible unfolding can occur during chromatography[8–10], generating multiple or distorted peaks[10]. Therefore, it was a matter of concern that RPLC separated two components of identical molecular weight, one active and one inactive. Edman sequencing established the sequence S(D)TGEEGA(K)RDV for the inactive component, dispelling the possibility that the two might have the same primary sequence. The active and inactive species represent completely unrelated species that, by chance, co-migrate in both IEC and SDS-PAGE.

ACKNOWLEDGEMENTS

This work was supported in part by grant HL36221 from the National Heart, Lung, and Blood Institute, National Institutes of Health, Bethesda, MD, U.S.A. Thanks are due to Dr. J. E. Strickler and to J. G. Gorniak for excellent work in sequencing, to Drs. J. J. L'Italien and K. Benedek for reviewing the manuscript, to Villanova University for library services, to Dr. R. Pixley for assistance with some instrumentation and to Dr. N. E. Kirschbaum for providing posterior salivary gland extract and for independently verifying the results observed on ulrafiltration and IEC.

REFERENCES

1 A. Z. Budzynski, S. A. Olexa and R. T. Sawyer, *Proc. Soc. Exp. Biol. Med.*, 169 (1981) 259–265.
2 A. Z. Budzynski, S. A. Olexa, B. S. Brizuela, R. T. Sawyer and G. S. Stent, *Proc. Soc. Exp. Biol. Med.*, 168 (1981) 266–275.
3 F. Markwardt, *Methods Enzymol.*, 19 (1970) 924–932.
4 S. M. Malinconico, J. B. Katz and A. Z. Budzynski, *J. Lab Clin. Med.*, 103 (1984) 44–58.
5 B. R. Oakley, D. R. Kirsch and N. R. Morris, *Anal. Biochem.*, 105 (1980) 361–363.
6 D. Hawke, P. M. Yuan and J. E. Shively, *Anal Biochem.*, 120 (1982) 302–311.
7 U. K. Laemmli, *J. Mol. Biol.*, 80 (1973) 575–585.
8 M. P. Strickler and M. J. Gemski, in W. S. Hancock, (Editor), *CRC Handbook of HPLC for the Separation of Amino Acids, Peptides, and Proteins*, Vol. II, CRC Press, Boca Raton, FL, 1984, pp. 349–355.
9 K. Benedek, S. Dong and B. L. Karger, *J. Chromatogr.*, 317 (1984) 227–243.
10 X. M. Lu, K. Benedek and B. L. Karger, *J. Chromatogr.*, 359 (1986) 19–29.

Journal of Chromatography, 502 (1990) 371–378
Elsevier Science Publishers B.V., Amsterdam — Printed in The Netherlands

CHROM. 22 099

Identification and determination of sulphamethazine and N^4-acetylsulphamethazine in meat by high-performance liquid chromatography with photodiode-array detection

MASAKAZU HORIE*, KOUICHI SAITO, YOUJI HOSHINO and NORIHIDE NOSE
Saitama Prefectural Institute of Public Health, 639-1, Kamiokubo, Urawa, Saitama 338 (Japan)
NAOKI HAMADA
Applications Department, Shimadzu Corporation, 1-63-1, Shibazaki, Chofu, Tokyo 182 (Japan)
and
HIROYUKI NAKAZAWA
Department of Pharmaceutical Sciences, National Institute of Public Health, 4-6-1, Shirokanedai, Minato-ku, Tokyo 108 (Japan)
(First received May 18th, 1989; revised manuscript received September 26th, 1989)

SUMMARY

A simple and selective method for the determination of sulphamethazine (SMT) and its metabolite, N^4-acetylsulphamethazine (N^4-AcSMT), in meat by high-performance liquid chromatography (HPLC) with photodiode-array detection was developed. The drugs were extracted from meat with 0.2% metaphosphoric acid–methanol (6:4), followed by a Bond-Elut C_{18} clean-up procedure. The HPLC separation was carried out on a Supersphere RP-18e column (125 × 4.0 mm I.D.) using 0.05 *M* sodium dihydrogenphosphate (pH 4.5)–acetonitrile (8:2) as the mobile phase at a flow-rate of 0.5 ml/min, and monitored with a photodiode-array detector. The recoveries of SMT and N^4-AcSMT from meat fortified at 0.5 μg/g were 90.1–93.3 and 93.0–94.4%, respectively, with coefficients of variation of 1.9–3.2 and 1.5–2.7%. The limits of detection were 0.02 μg/g for each drug. SMT was found in ten samples of imported meat (12.5%) at levels ranging from 0.05 to 1.05 μg/g.

INTRODUCTION

Various antibiotics and synthetic antibacterials are widely used for the prevention and treatment of infectious diseases in livestock animals. According to the Japanese Food Sanitation Law, no food should contain antibiotics and, in addition, meat, poultry eggs, fish and shellfish should not contain any synthetic antibacterial substances. Therefore, a simple and reliable method is need to monitor drug residues in edible tissues of swine, cattle and chicken.

Sulphamethazine [SMT; 4-amino-N-(4,6-dimethyl-2-pyrimidinyl)benzenesulphonamide; sulphadimidine] is widely used in the rearing of food-producing animals

0021-9673/90/$03.50

to prevent and treat diseases and to promote their growth. A number of methods have been developed for the assay of SMT using spectrophotometric procedures[1], thin-layer chromatography[2–4], gas chromatography (GC)[5–7], GC–mass spectrometry (GC–MS)[7–11], enzyme immunoasay[12] and high-performance liquid chromatography (HPLC)[11,13–17].

A conventional HPLC method using a UV detector used for the determination of SMT residues in meat lacks qualitative ability. A few GC–MS methods developed for confirmation of SMT and its metabolites in animal tissues[7,11] are complicated and time consuming.

Haagsma *et al.*[18] reported an HPLC method for the simultaneous determination of SMT and its metabolites in swine tissue. However, they only measured the minor metabolite, desamino-SMT, and did not measure SMT and its major metabolite, N^4-acetyl-SMT (N^4-AcSMT), using a photodiode-array detector. According to Japanese Food Sanitation Law, the parent compound such as SMT, and its major metabolite such as N^4-AcSMT, must be measured in tissue. Hence it is important to identify the parent compound and its major metabolite.

This paper describes a simple and rapid HPLC method for the identification and determination of SMT and N^4-AcSMT using photodiode-array detection and Bond-Elut C_{18} cartridges in a clean-up step.

EXPERIMENTAL

Materials and reagents

Edible muscle tissues of swine, cattle and chicken served as samples. SMT was obtained from ICN Pharmaceuticals (Cleveland, OH, U.S.A.). Bond-Elut C_{18} cartridges (500 mg) (Waters Assoc., Milford, MA, U.S.A.) were washed with 5 ml of methanol and then 10 ml of distilled water before use. Hyflo Super-Cel was obtained from Johns-Manville (Denver, CO, U.S.A.). Other chemicals were of analytical-reagent or HPLC grade.

Synthesis of N^4-acetylsulphamethazine

N^4-AcSMT was prepared by heating SMT and acetic anhydride in glacial acetic acid according to the procedure described by Uno and Ueda[19]. The synthesized compounds were characterized by mass spectrometry (MS) and infrared (IR) spectrophotometry.

Preparation of standard solutions

Each standard (10 mg) was weighed accurately into a 100-ml flask and diluted to volume with acetonitrile. Subsequent dilutions were made with the HPLC mobile phase.

Apparatus

The HPLC system consisted of a Model LC-6A solvent-delivery pump (Shimadzu, Kyoto, Japan), a Model 7125 injector (Rheodyne, Berkeley, CA, U.S.A.) and a Model SPD-M6A photodiode array detector (Shimadzu) interfaced with an NEC PC-9801 VX-4 personal computer (Tokyo, Japan). The chromatograms were recorded on a plotter. The separation was performed on a Supersphere RP-18e column

(125 × 4.0 mm I.D.) (E. Merck, Darmstadt, F.R.G.) with 0.05 *M* sodium dihydrogenphosphate (pH 4.5)–acetonitrile (8:2) as the mobile phase at a flow-rate of 0.5 ml/min.

The other instruments used were a Model GCMS-QP 1000 mass spectometer (Shimadzu), a Model IR-435 infrared spectrophotometer (Shimadzu) and a Hiscotolon homogenizer (Nichion Irika Kikai, Tokyo, Japan).

Sample preparation

A 5-g amount of sample was homogenized with 100 ml of 0.2% metaphosphoric acid–methanol (6:4) as a deproteinizing extractant at high speed for 2 min. The homogenate was filtered through *ca.* 1 mm Hyflo Super-Cel coated on a suction funnel. The filtrate was evaporated under reduced pressure at 40°C. Evaporation was interrupted when 20 ml of solution remained in the flask. The flask contents were applied to a Bond-Elut C_{18} cartridge. After washing with 10 ml of distilled water, the cartridge was eluted with 2 ml of methanol. The eluate was evaporated to dryness under reduced pressure and the residue dissolved in 1 ml of HPLC mobile phase; 10 μl of the solution were injected for HPLC.

Calibration graphs

Standards at concentrations of 0.2, 0.5, 1.0, 2.0 and 4.0 μg/ml of SMT and N⁴-AcSMT were prepared from stock standard solutions. A 10-μl volume of these solutions was injected into the column. Calibration graphs were obtained by measurement of peak height.

RESULTS AND DISCUSSION

Chromatographic conditions

Some metabolites of drugs show biological activity and therefore, for the determination of residual drugs in animal tissues, it is desirable to establish a method that takes into consideration their major metabolites. Although several metabolites of SMT are known, the major one is N⁴-AcSMT, in which the N⁴ position of SMT has been acetylated[20,21].

In the determination of SMT by HPLC, unlike GC, no derivatization is necessary and SMT can be determined directly, and many studies[11,13–17] have been reported. However, there have been few reports[11] of the simultaneous determination of SMT and N⁴-AcSMT in animal tissues. Many of the HPLC methods for SMT employ a reversed-phase ODS column[11,13,15,16] which utilizes. Therefore, a study was made of the separation conditions using Supersphere RP-18e, LiChrospher RP-18e, Inertsil ODS, Nucleosil 5C 18 and Capcell Pak C_{18} (SG) columns and phosphate buffer–acetonitrile as the mobile phase. Although the samples were separated well with all the columns tested, the sharp peaks of SMT and N⁴-AcSMT were obtained using a Supersphere RP-18e column. Therefore we have chosen the Supersphere RP-18e column in this paper.

Based on a study with different mixing ratios of phosphate buffer and acetonitrile at various salt concentrations and pH, 0.05 *M* sodium dihydrogenphosphate (pH 4.5)–acetonitrile (8:2) without pH conditioning was chosen as the mobile phase. Fig. 1A shows the chromatogram of SMT and N⁴-AcSMT obtained under the established conditions.

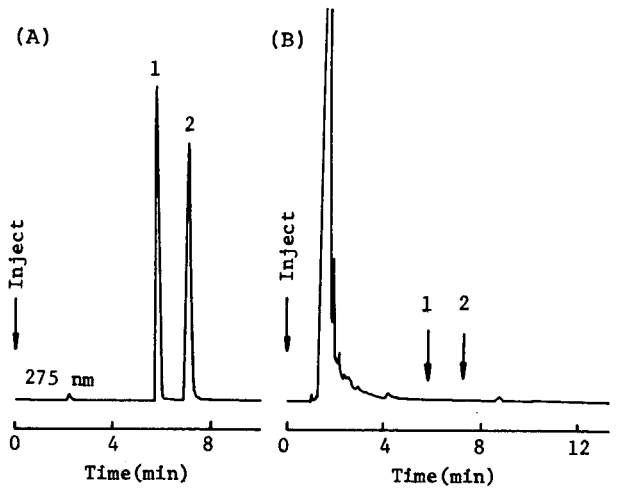

Fig. 1. Typical chromatograms of (A) standard mixture and (B) pork extract. Peaks: 1 = N^4-acetylsulphamethazine (10 ng); 2 = sulphamethazine (10 ng).

Clean-up

Liquid–liquid partition using acetone[5], acetone–chloroform[1,2,6–10,13], ethyl acetate[3,4] and ethyl acetate–chloroform[15] has been reported as a means of cleaning up meat in order to remove fatty compounds. However, these methods are complicated and time consuming, and involve problems such as emulsion formation. Haagsma *et al.*[18] used a silica cartridge for sample treatment. We used a C_{18} instead of a silica cartridge for sample clean-up, because it is important to develop a universal method that would be applicable to other antibacterials. The present method is applicable to other such compounds[22,23].

First, we tested the capacity of a commercial C_{18} cartridge to retain SMT and N^4-AcSMT. As shown in Table I, a recovery of about 90% was obtained for either

TABLE I

INFLUENCE OF EXTRACTION CARTRIDGES ON THE RECOVERY OF SULPHAMETHAZINE AND N^4-ACETYLSULPHAMETHAZINE FROM PORK MEAT

Values are means ± S.D. ($n=5$). Samples were spiked with 0.5 μg/g each of sulphamethazine and N^4-acetylsulphamethazine.

Cartridge	*Recovery (%)*	
	SMT	*N^4-AcSMT*
Bond-Elut C_{18} (200 mg)	67.9 ± 7.0	84.9 ± 3.0
Baker C_{18} (200 mg)	82.5 ± 1.7	88.9 ± 2.3
Bond-Elut C_{18} (500 mg)	93.3 ± 2.6	94.4 ± 2.7
Baker C_{18} (500 mg)	94.1 ± 2.7	94.2 ± 3.3
Easy Chromato C_{18} (500 mg)	89.2 ± 4.1	90.1 ± 3.2
Sep-Pak C_{18} (400 mg)	87.2 ± 3.9	89.1 ± 4.1

sample when 400–500 mg were packed in the column, whereas part of the SMT was not retained and leaked with a packing amount of 200 mg. Bond-Elut C_{18} (500 mg) was used as the clean-up cartridge because it gave the fewest peaks of contaminants.

An unified extraction clean-up procedure is desirable for establishing a rapid and widely applicable method for the determination of antibiotics and synthetic antibacterials in animal and fish samples. When we used 0.2% metaphosphoric acid–methanol (6:4) as the extraction solvent, which we had used previously for the determination of oxolinic acid, nalidixic acid and piromidic acid in fish culture[22]; a good recovery was obtained without any interference from coexisting substances, as shown in Fig. 1B. Similar chromatograms were obtained from chicken and beef samples.

Recovery

Linear calibration graphs were obtained from 1 to 40 ng of SMT and N⁴-AcSMT. Table II summarizes the recoveries of the drugs from commercial samples of pork, beef and chicken fortified with 0.5 μg/g of SMT and N⁴-AcSMT. Greater than 90% overall mean recoveries and 5% standard deviations were obtained with every meat sample. The detection limits were 0.02 μg/g for both SMT and N⁴-AcSMT.

TABLE II

RECOVERIES OF SULPHAMETHAZINE AND N⁴-ACETYLSULPHAMETHAZINE FROM MEATS

Values are means ± S.D. ($n=5$).

Sample	*Added (μg/g)*	*Recovery (%)*	
		SMT	*N⁴-AcSMT*
Pork	0.5	93.3 ± 2.6	94.4 ± 2.7
Beef	0.5	91.8 ± 1.9	93.0 ± 1.7
Chicken	0.5	90.1 ± 3.2	94.1 ± 1.5

Analysis of commercial samples

Using the above method, we analysed commercial samples of pork, chicken and beef for residual SMT. As shown in Table III, SMT was found in ten imported pork samples (12.5%) at levels ranging from 0.05 to 1.05 μg/g. Three samples contained about 1 μg/g of SMT. Judging from a study reported by Cox and Krzeminski[16], the pigs from which these samples were obtained are surmised to have been slaughtered almost without any interruption of the drug treatment. In all pork samples in which SMT was detected, N⁴-AcSMT was also detected at low concentrations.

HPLC using a UV detector, which is generally employed for the determination of sulpha drugs, has poor specificity, and qualitative information obtainable from this technique is limited to the retention time of the sample. Accordingly, for the analysis of meat samples that contain residual sulpha drugs, the samples are further analysed by GC–MS[7–11] to confirm the target substance. However, for GC–MS, sulpha drugs

TABLE III

DETERMINATION OF SULPHAMETHAZINE IN COMMERCIAL MEATS

Sample	*Type*[a]	*No. of samples*	*Samples with positive detection*	*Range (μg/g)*		
				Min.	*Max.*	*Av.*
Pork	I	80	10 (12.5%)	0.05	1.05	0.47
	D	40	N.D.[b]	–	–	
Beef	I	40	N.D.	–	–	
	D	15	N.D.	–	–	
Chicken	I	17	N.D.	–	–	
	D	20	N.D.	–	–	

[a] I = Imported; D = domestic.
[b] N.D. = not detected (<0.05 μg/g).

must be methylated to give suitable volatile derivatives, and thus the process is complicated and time consuming.

A photodiode-array detector, as used here, can measure both retention times and absorption spectra, and peak components can therefore be identified by comparison of the peaks with those of standards.

Figs. 2 and 3 show chromatograms of pork samples in which SMT was detected at 1.05 and 0.10 μg/g. The peak component with a retention time of 7.1 min was compared with a standard sample of SMT. The two spectra were almost identical, confirming that the peak component eluting at of 7.1 min was SMT. The similarity index given in Figs. 2, 3 and 4 represents the similarity of two spectra in terms of numbers.

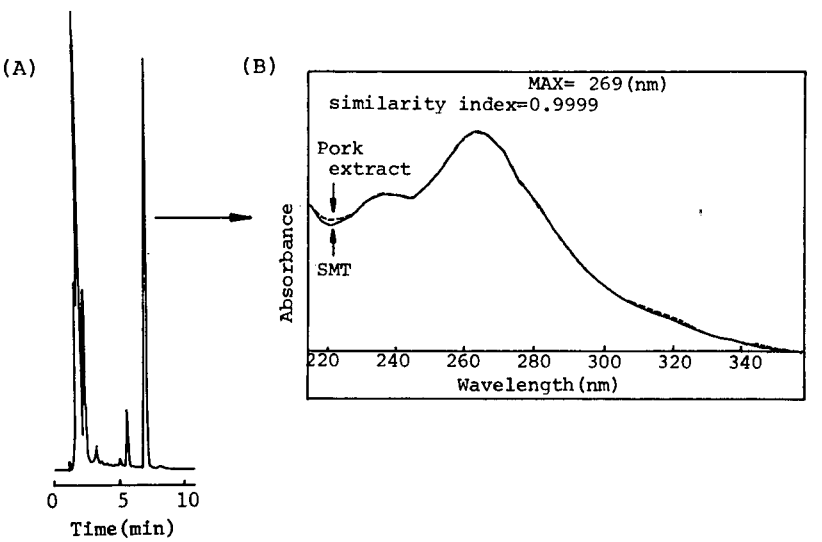

Fig. 2. (A) Chromatogram of pork sample in which sulphamethazine was detected at 1.05 μg/g, plotted at 275 nm. (B) Normalized spectra of the peak (at 7.11 min) obtained from pork extract (dashed line) and standard sulphamethazine (solid line).

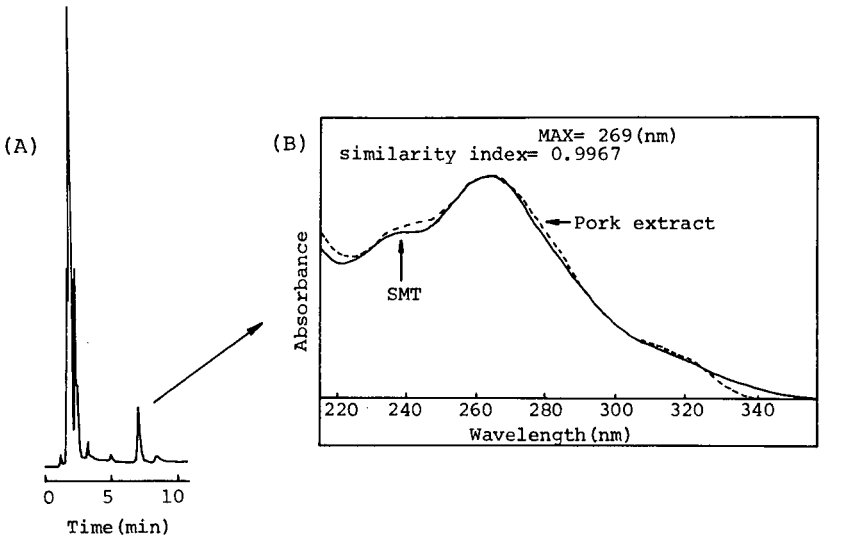

Fig. 3. (A) Chromatogram of pork sample in which sulphamethazine was detected at 0.10 μg/g, plotted at 275 nm. (B) Normalized spectra of the peak (at 7.13 min) obtained from pork extract (dashed line) and standard sulphamethazine (solid line).

In the USA, a tolerance of 0.1 μg/g for SMT[24] in edible animal tissues has been set. Consequently, our proposed method is considered to be useful as a method for the determination of residual SMT down to this level.

In general, when SMT is administered to animals, N⁴-AcSMT is also detected in tissues. The retention time of 5.8 min of the peak component in Fig. 2, for pork meat in which 1.05 μg/g of SMT was detected, is in agreement with the retention time of standard N⁴-AcSMT. The spectra of this peak and standard N⁴-AcSMT were almost identical, with a similarity index of 0.9989 (Fig. 4). Hence this peak component was confirmed as N⁴-AcSMT.

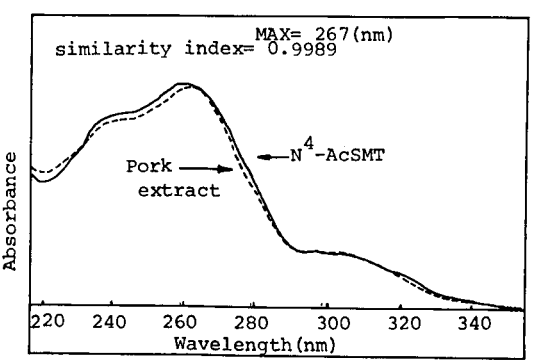

Fig. 4. Normalized spectra of the peak (at 5.80 min) obtained from pork extract (dashed line) in Fig. 3 and standard N⁴-acetylsulphamethazine (solid line).

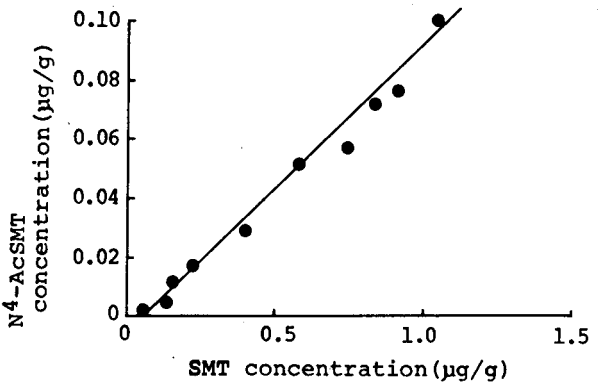

Fig. 5. Correlation between residual sulphamethazine and residual N^4-acetylsulphamethazine in pork meat. $y = 0.10x - 0.00$; $r = 0.989$; $n = 10$.

Correlation between residual SMT and residual N^4-AcSMT

Detection of SMT in meat has already been reported in the USA[15]. However, no detailed studies have been reported on the relationship between the residual concentration of SMT and that of N^4-AcSMT. We studied this relationship employing ten samples. Although this number of samples is small, a high correlation was detected between the concentrations of these two compounds, as shown in Fig. 5.

REFERENCES

1 F. Tishler, J. L. Sutter, J. N. Bathish and H. E. Hagman, *J. Agric. Food Chem.*, 16 (1968) 50.
2 W. F. Phillips and J. E. Trafton, *J. Assoc. Off. Anal. Chem.*, 58 (1975) 44.
3 M. H. Thomas, K. E. Soroka, R. M. Simpson and R. L. Epstein, *J. Agric. Food Chem.*, 29 (1981) 621.
4 M. H. Thomas, K. E. Soroka and S. H. Thomas, *J. Assoc. Off. Anal. Chem.*, 66 (1983) 881.
5 D. P. Goodspeed, R. M. Simpson, R. B. Ashworth, J. W. Shafer and H. R. Cook, *J. Assoc. Off. Anal. Chem.*, 61 (1978) 1050.
6 A. J. Manuel and W. A. Steller, *J. Assoc. Off. Anal. Chem.*, 64 (1981) 794.
7 J. E. Matusik, C. G. Guyer, J. N. Geleta and C. J. Barnes, *J. Assoc. Off. Anal. Chem.*, 70 (1987) 546.
8 F. B. Suhre, R. M. Simpson and J. W. Shafer, *J. Agric. Food Chem.*, 29 (1981) 727.
9 S. J. Stout, W. A. Steller, A. J. Manuel, M. O. Poeppel and A. R. Dacunha, *J. Assoc. Off. Anal. Chem.*, 67 (1984) 142.
10 R. M. Simpson, F. B. Suhre and J. W. Shafer, *J. Assoc. Off. Anal. Chem.*, 68 (1985) 23.
11 G. D. Paulson, A. D. Mitchell and R. G. Zaylskie, *J. Assoc. Off. Anal. Chem.*, 68 (1985) 1000.
12 D. E. Dixon-Holland and S. E. Katz, *J. Assoc. Off. Anal. Chem.*, 71 (1988) 1137.
13 K. L. Johnson, D. T. Jeter and R. C. Claiborne, *J. Pharm. Sci.*, 64 (1975) 1657.
14 A. B. Vilim, L. Larocque and A. I. MacIntosh, *J. Liq. Chromatogr.*, 3 (1980) 1725.
15 O. W. Parks, *J. Assoc. Off. Anal. Chem.*, 65 (1982) 632.
16 B. L. Cox and L. F. Krzeminki, *J. Assoc. Off. Anal. Chem.*, 65 (1982) 1311.
17 N. Haagsma and C. V. de-Water, *J. Chromatogr.*, 333 (1985) 256.
18 N. Haagsma, H. G. J. M. Pluijmakers, M. M. L. Aerts and W. M. J. Beek, *Biomed. Chromatogr.*, 2 (1987) 41.
19 T. Uno, M. Ueda, *Yakugaku Zasshi*, 80 (1960) 1785.
20 P. Nielsen, *Biochem. J.*, 136 (1973) 1039.
21 W. Horwitz, *J. Assoc. Off. Anal. Chem.*, 64 (1981) 104.
22 M. Horie, K. Saito, Y. Hoshino, N. Nose, E. Mochizuki and H. Nakazawa, *J. Chromatogr.*, 402 (1987) 301.
23 M. Horie, Y. Hoshino, N. Nose and H. Nakazawa, *Eisei Kagaku*, 31 (1985) 371.
24 *Code of Federal Regulations*, Food and Drug Administration, Superintendent of Documents, U.S. Government Printing Office, Washington, DC, 1985, Title 21, Sec. 556.670.

Journal of Chromatography, 502 (1990) 379–384
Elsevier Science Publishers B.V., Amsterdam — Printed in The Netherlands

CHROM. 22 104

High-performance liquid chromatographic determination of zinc pyrithione in antidandruff preparations based on copper chelate formation

KEIKO NAKAJIMA* and TOSHIKO YASUDA
Public Health Laboratory of Chiba Prefecture, 666-2, Nitona-cho, Chiba 280 (Japan)
and
HIROYUKI NAKAZAWA
Department of Pharmaceutical Sciences, National Institute of Public Health, 4-6-1, Shirokane-dai, Minato-ku, Tokyo 108 (Japan)
(First received April 4th, 1989; revised manuscript received August 15th, 1989)

SUMMARY

A simple and rapid method for the determination of zinc pyrithione (ZPT) in antidandruff preparations by high-performance liquid chromatography (HPLC) has been developed. ZPT in samples was converted into a stable copper(II) complex by mixing with cupric sulphate solution followed by extraction with chloroform. HPLC was carried out on a Nucleosil 5 C_{18} column (15 cm × 4.6 mm I.D.) using methanol–water (3:2) as the mobile phase with UV detection at 320 nm. The calibration graph was linear from 0.1–0.5 μg for ZPT. The recoveries from four shampoos were 98.0–100.6% with high accuracy.

INTRODUCTION

Zinc pyrithione (ZPT), the zinc chelate of 2-pyridinethiol 1-oxide is used as an antidandruff agent in shampoos, hair rinses and hair conditioners. A specific and rapid determination of ZPT is necessary for the quality control of the commercial antidandruff preparations. Several methods[1–5] have been developed for the determination of ZPT. Kondo and Takano[6] determined ZPT in commercial shampoos and the residues on human hair by high-performance liquid chromatography (HPLC) after pre-labelling with a fluorescent agent. Cheng and Gadde[7] determined ZPT in commercial shampoos directly by reversed-phase HPLC. However, direct analysis of coordination compounds is difficult owing to the interaction with reversed-phase packing materials[8] or stainless-steel components of the liquid chromatograph even if Zn^{2+} is added to the mobile phase. Fenn and Alexander[9] successfully determined ZPT in commercial products by transchelation to the Cu^{II} complex using normal-phase HPLC. The Cu^{II} complex is very stable and is considered also to be suitable for reversed-phase HPLC.

0021-9673/90/$03.50

This paper describes the reversed-phase HPLC determination of ZPT in commercial shampoos, hair rinses and hair conditioners by using the conversion of ZPT into the Cu^{II} complex.

EXPERIMENTAL

Materials

ZPT and 2-pyridinethiol 1-oxide were purchased from Tokyo Kasei Kogyo (Tokyo, Japan).

Analytical-reagent grade copper(II) sulphate pentahydrate, citric acid, disodium hydrogenphosphate dodecahydrate, disodium ethylenediaminetetraacetate (EDTA), chloroform and methanol were obtained from Wako (Osaka, Japan).

Buffer solution (pH 5.0) was prepared by mixing 0.1 *M* citric acid and 0.2 *M* disodium hydrogenphosphate (97:103).

ZPT standard solutions were prepared by dissolving ZPT in chloroform saturated with water (0.02–0.10 mg/ml).

Apparatus and chromatographic conditions

HPLC was carried out using an NSP-800-9 pump (Nihon Seimitsu Kagaku, Tokyo, Japan), a KMT-60A-II autosampler (Kyowa Seimitsu, Tokyo, Japan) and an NS-310II UV detector (Nihon Seimitsu Kagaku, Tokyo, Japan) set at 320 nm. A stainless-steel column (15 cm × 4.6 mm I.D.) packed with Nucleosil $5C_{18}$ (particle size 5 μm) (Macherey, Nagel & Co., Düren, F.R.G.) was used at 25°C.

The mobile phase was methanol–water (3:2, v/v) at a flow-rate of 1.0 ml/min. The metallic portions of the chromatographic system were prewashed with 0.1% EDTA (at 0.5 ml/min) followed by water before the chromatography.

Integration of peak areas was accomplished with a Model 7000B integrator (System Instruments, Tokyo, Japan).

Sample preparation

A sample containing 10 mg of ZPT was weighed accurately into a 100-ml volumetric flask and diluted to volume with buffer solution (pH 5.0) saturated with chloroform. If the dilution resulted in separation into liquid and solid phases, water saturated with chloroform was used instead of buffer solution. After shaking well for a few minutes and sonication in an ultrasonic bath for a few minutes, 10.0 ml of chloroform saturated with water and 2.0 ml of 1 *M* copper(II) sulphate solution were added to 10.0 ml of the above solution. The mixture was shaken vigorously for 5 min and centrifuged for 5 min at 1500 *g*. A 5-μl portion of the lower layer was injected into the chromatograph.

Calibration graph

Portions of 10.0 ml of ZPT standard solution (0.02–0.10 mg/ml) were transferred into centrifuge tubes and to each tube 10.0 ml of buffer solution (pH 5.0) saturated with chloroform and 2.0 ml of 1 *M* copper(II) sulphate solution were added. The mixture was processed as described under *Sample preparation*. A calibration graph for ZPT was constructed using peak areas.

RESULTS AND DISCUSSION

Suitability of metal complexes for chromatographic analysis

The suitability of metal complexes of ZPT was studied using 2-pyridinethiol 1-oxide (PT), which was the ligand of ZPT, and the metal ions Zn^{II}, Fe^{III}, Sn^{II}, Co^{III}, Cu^{II} and Ni^{II}.

A chloroform solution of PT was shaken with aqueous solutions of various metal ions. Fig. 1 shows the UV absorption spectra of the various metal complexes of PT. The Cu^{II} complex had the greatest absorbance at 320 nm.

The chelate formation constant of the 1:1 Cu^{II} complex of PT is much greater than those of the Zn^{II}, Ni^{II}, Co^{II} and Mn^{II} complexes[10]. The Cu^{II} complex is so stable that it is expected not to exchange for other metals during chromatographic processing.

For these reasons the copper chelate formation procedure was applied to the determination of ZPT.

Structure of the Cu^{II} complex

The structure of the Cu^{II} complex was investigated by the continuous variation method[11], as shown in Fig. 2. The structure of the Cu^{II} complex is suggested to be as Fig. 3, in agreement with the results of elemental microanalysis[12]. The conversion of ZPT into the Cu^{II} complex occurred so rapidly that the shaking time required for the formation and extraction of the Cu^{II} complex in the organic phase was less than 5 min.

Chromatography and calibration graph of ZPT

ZPT itself gave a tailing peak when methanol–water was used as the mobile phase. Conversion of ZPT into the Cu^{II} complex eliminated this problem. The Cu^{II}

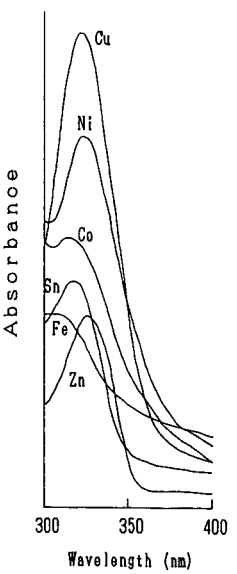

Fig. 1. UV absorption spectra of metal complexes of pyrithione.

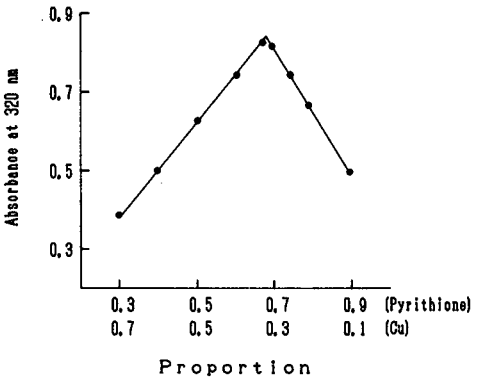

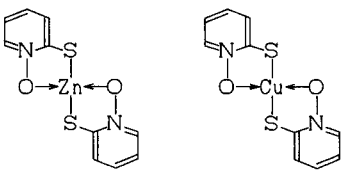

(a) (b)

Fig. 2. Composition of Cu^{II} complex of pyrithione by continuous variation method.

Fig. 3. Structures of (a) zinc pyrithione and (b) Cu^{II} complex of pyrithione.

complex gave a good peak shape (as shown in Fig. 4) with a 1.07% relative standard deviation for the peak areas of five injections. The calibration graph was linear in the range 0.1–0.5 μg of ZPT.

Suitability of diluent for sample

ZPT is not dissolved in shampoos or other products but dispersed homogeneously. ZPT is insoluble in water and soluble in 1 *M* hydrochloric acid or

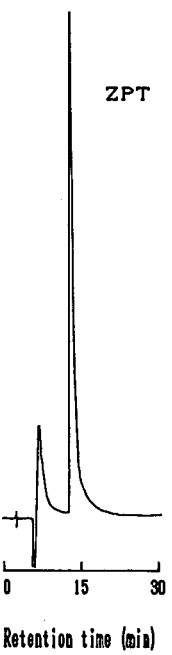

Fig. 4. Typical chromatogram obtained from shampoo. Conditions as given under Experimental.

ammonia–ammonium chloride buffer solution (pH 11.0). In 1 *M* hydrochloric acid ZPT changes to the free form which dimerizes under irradiation with UV light[5]. In our study, ZPT dissolved in 1 *M* hydrochloric acid showed a degradation of 10% immediately, 25% after 24 h and 93% after 4 days of storage at room temperature in a light-resistant container.

ZPT is stable in ammonia–ammonium chloride buffer solution (pH 11.0). However, this buffer solution, on addition of copper(II) sulphate solution, produces a deep-blue complex salt. Owing to the formation of this complex salt, the extractability of the Cu^{II} complex of ZPT in the organic phase decreased.

Based on these results, it was considered to be reasonable to dilute samples with buffer solution (pH 5.0) or water. By sonicating the aqueous sample solution, sufficient uniformity was obtained, with a 1.40% relative standard deviation for five determinations.

Validation of the method

Four commercial shampoos which were not antidandruff preparations and were

TABLE I

RECOVERY OF ZINC PYRITHIONE ADDED TO SHAMPOO

Results were obtained from five replicate analyses of shampoos containing 1.0% of zinc pyrithione.

Sample	*Recovery (%)*	*R.S.D. (%)*
A	98.0	2.0
B	99.5	0.8
C	100.6	1.3
D	98.9	1.5

TABLE II

ANALYSIS OF ZINC PYRITHIONE IN COMMERCIAL COSMETICS

Sample	*ZPT (%)*	
	Iodimetry	*Proposed method*
Shampoo 1	0.75	0.78
2	0.98	0.98
3	0.79	0.81
4	1.45	1.45
5	0.92	0.95
6	0.90	0.90
7	0.92	0.96
8	0.91	0.91
9	0.75	0.75
Hair rinse 1	0.28	0.29
2	0.45	0.46
3	0.44	0.43
Hair conditioner	0.48	0.49

spiked with 1.0% of ZPT were analysed according to the present method. The recoveries of ZPT for five determinations were 98.0–100.6% with relative standard deviations of 0.8–2.0%, as shown in Table I.

Analysis of commercial samples

Table II gives results obtained by the proposed method in comparison with those obtained by iodimetry[3]. The results agreed with each other.

REFERENCES

1 R. T. Brooks and P. D. Stemglanz, *Anal. Chem.*, 31 (1959) 561.
2 A. F. Krivis, E. S. Gazda, T. R. Supp and M. A. Robinson, *Anal. Chem.*, 35 (1963) 966.
3 *Test Method-CL-24-863*, Olin Mathieson Chem. Co., New York.
4 B. L. Kabacoff and C. M. Fairchild, *J. Soc. Cosmet. Chem.*, 26 (1975) 453.
5 M. D. Seymour and D. L. Bailey, *J. Chromatogr.*, 206 (1981) 301.
6 Y. Kondo and S. Takano, *J. Chromatogr.*, 408 (1987) 255.
7 H. Cheng and R. R. Gadde, *J. Chromatogr.*, 291 (1984) 434.
8 T. Okumura, J. Koyama, Y. Ohtsu, K. Nakamura, O. Nakata and N. Tanaka, *Proceedings of the 9th Conference on Liquid Chromatography*, Division of Liquid Chromatography of the Japan Society for Analytical Chemistry, Tokyo, 1988, p. 137.
9 R. J. Fenn and M. T. Alexander, *J. Liq. Chromatogr.*, 11 (1988) 3403.
10 P. Sun, Q. Fernando and H. Freiser, *Anal. Chem.*, 36 (1964) 2485.
11 P. Job, *Ann. Chim. (Paris)*, 10 (1928) 113.
12 M. Edrissi, A. Massoumi and J. A. W. Dalzeil, *Microchem. J.*, 16 (1971) 538.

Journal of Chromatography, 502 (1990) 385–392
Elsevier Science Publishers B.V., Amsterdam — Printed in The Netherlands

CHROM. 22 111

Behaviour of vegetable phospholipids in thin-layer chromatography

Optimization of mobile phase, detection and direct evaluation[a]

G. LENDRATH*
Department of Pharmacognosy, Hamburg University, Bundesstrasse 43, D-2000 Hamburg 13 (F.R.G.)
A. NASNER
Lucas Meyer GmbH & Co., Ausschläger Elbdeich 62, D-2000 Hamburg 28 (F.R.G.)
and
Lj. KRAUS
Department of Pharmacognosy, Hamburg University, Bundesstrasse 43, D-2000 Hamburg 13 (F.R.G.)
(First received May 29th, 1989; revised manuscript received October 17th, 1989)

SUMMARY

By systematic studies using a mobile solvent composition triangle, the optimum chloroform–methanol–water mobile phase for the separation of phospholipids by thin-layer chromatography on 5 × 5 cm silica gel was found. By using acetate buffer (pH 4) instead of water in the mobile phase and by impregnation of the silica gel layer with phosphoric acid it was possible to optimize the separation of phospholipids so that baseline separation was obtained, which is necessary for direct evaluation. Another effect of impregnation with phosphoric acid is the higher stability and intensity given with Dittmer–Lester reagent, which is specific for phosphorus. It reacts with the phosphate group common to all phospholipids so that the same signals were obtained with a measuring wavelength of 720 nm for all phosphatidylcholines of soybean, rape-seed and sunflower seed lecithin. The other phospholipids (phosphatidylethanolamines, phosphatidylinositols and phosphatidic acids) could be quantified by this procedure. The signal intensity was the same for all phospholipids as the molecular weights are very similar, although the patterns of fatty acids are different.

INTRODUCTION

Little information is available in the literature on the separation of vegetable

[a] This paper is part of the Dissertation of G. Lendrath, Hamburg University.

0021-9673/90/$03.50

phospholipids by thin-layer chromatography (TLC)[1–3]. Most papers have dealt with the separation of phospholipids of animal or human origin[4–13].

The main constituent of vegetable lecithins, such as the raw lecithins of soybean, rape-seed and sunflower seed, are phosphatidylcholine, phosphatidylethanolamine, phosphatidylinositol and phosphatidic acid. These phospholipids, isolated from raw lecithin of different origins, differ in their fatty acid patterns (Table I). Owing to these different patterns, it is necessary to quantify phospholipids by means of a standard for each plant species and to use conversion factors.

Our experience with the H-chamber[14,15] led us to carry out the separation and the densitometric evaluation of vegetable phospholipids on a 5 × 5 cm silica gel plate. Because the separation takes place over a very short distance of 3.5 cm, the mobile solvent first had to be optimized, which was done using a mobile phase composition triangel (Fig. 1).

The selection of suitable analytical reagents turned out to be difficult with regard to quantification. Detection of phospholipids on thin-layer plates has been reported by many workers using different reagents, *e.g.*, molybdophosphoric acid[16], copper(II) sulphate[16–18], copper(II) acetate[4,5,16,18,19], 2,7-dichlorofluorescein[16] and sulphuric acid[16]. Sometimes reagents are used that react with certain functional groups, *e.g.*, Dragendorff reagent[20] for the quaternary ammonium group in phosphatidylcholine, ninhydrin[20] for the ammonium group in phosphatidylethanolamine and various reagents for the phosphate group contained in all phospholipids[12,21–25].

For our purpose we used the group-specific Dittmer–Lester reagent[21], which reacts only with the phosphorus that is common to all phospholipids. In order to be able to use the reagent as an immersion reagent and thus to enhance the quantitative evaluation, we added ethanol.

TABLE I

PATTERNS OF FATTY ACIDS IN PHOSPHOLIPIDS

Phospholipid	*Source*	*Fatty acid*					
		16:0	*18:0*	*18:1*	*18:2*	*18:3*	*Others*
PC	Soybean	14.5	4.2	8.9	59.6	6.3	4.5
	Rape	9.6	1.2	44.5	28.5	4.1	8.6
	Sunflower	11.1	3.7	12.3	63.3	5.5	3.5
PE	Soybean	19.1	3.0	7.7	58.9	6.4	3.1
	Rape	9.5	0.7	45.1	37.8	4.4	2.2
	Sunflower	13.3	3.4	9.2	71.2	0.3	2.5
PI	Soybean	2.7	5.7	5.6	47.0	6.8	1.9
	Rape	17.2	1.6	37.7	35.1	5.6	2.7
	Sunflower	32.6	4.7	6.9	47.2	5.1	2.9
PA	Soybean	20.4	3.6	10.8	55.9	5.7	3.1
	Rape	9.0	0.9	48.3	35.5	4.1	1.5
	Sunflower	12.3	3.8	10.3	67.8	0.9	4.7

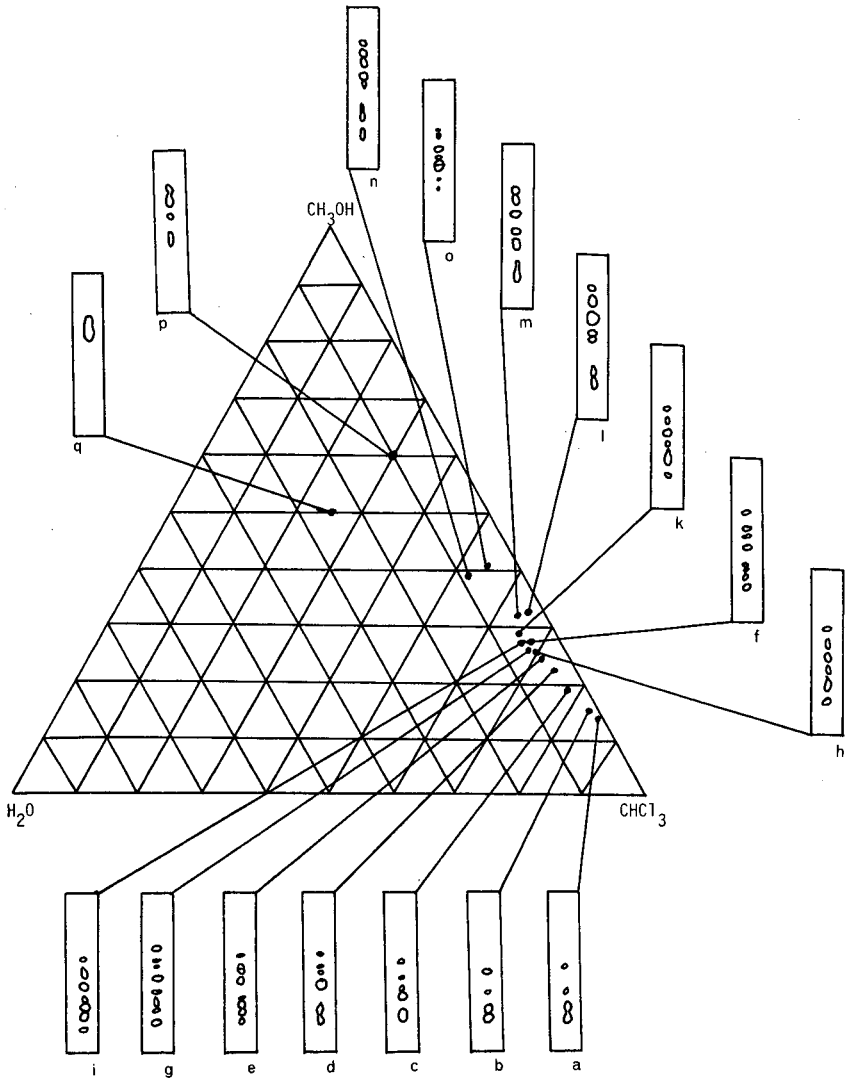

Fig. 1. Mobile phase composition triangle for chloroform–methanol–water.

EXPERIMENTAL

Standards

Phosphatidylcholine (PC), phosphatidylethanolamine (PE), phosphatidylinositol (PI) and phosphatidic acid (PA) were enriched by preparative high-performance liquid chromatography from the lecithins of soybean, rape-seed and sunflower seed and isolated by means of low-pressure column chromatography in pure form (94–98%)[26].

Thin-layer chromatography

The application solvent was 2.5 mg of phospholipid per 10 ml of chloroform. Merck silica gel 60 HPTLC plates (5 × 5 cm) were impregnated by dipping into a 0.5% solution of phosphoric acid in 70% methanol and then heated for 20 min at 120°C. The mobile phase was chloroform–methanol–0.2 *M* acetate buffer (pH 4) (65:25:4.3, v/v/v). A Desaga-H-Kammer TLC chamber was used. Detection was effected with modified Dittmer–Lester reagent (see below), with measurement at 720 nm.

Composition of the Dittmer–Lester immersion reagent. A stock solution is prepared as follows: (a) 40.11 g of molybdenum(VI) oxide were dissolved in 1 l of 12.5 *M* sulphuric acid by heating; (b) 1.78 g of molybdenum were dissolved by heating in 500 ml of solution (a); equal volumes of (a) and (b) were mixed. For the immersion solution, 1 part of the stock solution was mixed with 2 parts of water and 3 parts of ethanol.

The immersion solution must be prepared freshly when required whereas the stock solution can be kept for several months. Following the immersion, the phospholipids become visible without further treatment of the plate as blue spots on a light blue background which decolorizes almost entirely within 30 min, during which process the intensity of the blue phospholipid spots increases; 30 min after immersion, direct evaluation can be carried out.

Measuring parameters. A Zeiss PM Q II chromatogram spectrophotometer was used with a slit of dimensions 6 mm × 0.1 mm, a recorder voltage of 5 mV, plate feed at 30 mm/min and paper feed at 120 mm/min.

RESULTS AND DISCUSSION

For the separation of vegetable phospholipids on a thin layer of silica gel, we started with a known composition of the chloroform–methanol–water mobile phase and optimized the composition using the triangle shown in Fig. 1. Each corner represents 100% by volume of one of the solvents. The percentage by volume on the three connecting lines shows the compositions of binary mixtures. The surface of the triangle represents all possible percentages by volume of the three solvents.

As shown in Fig. 1, even very slight variations of the water content (chromatograms g and f) has a large influence on the separation. Other workers[15,27,28] also observed that the water conent of the mobile phase has a large effect on the R_F values of phospholipids.

By using acetate buffer (pH 4) instead of water, an even better separation of the phospholipids was obtained owing to the dependence of the phospholipid separation on pH[29,30]. In addition, by impregnation of the layer with phosphoric acid of different concentrations, we tried to obtain a baseline separation. As shown in Table II, the R_F values of all the phospholipids increase with increasing amount of phoshoric acid in the layer. This increase is particularly noticable for PA. The best separation was obtained with 0.5% phosphoric acid, as shown in Fig. 2.

As the R_F values of the phospholipids of each class from the lecithins of soybean, rape-seed and sunflower seed are almost identical, it can be assumed that the chromatographic behaviour of phospholipids depends on the groups esterified with the phosphoric acid rather than on the fatty acid pattern.

In previous studies[30] we showed that, by using the Dittmer–Lester reagent,

TABLE II

R_F VALUES OF THE PHOSPHOLIPIDS ON A PHOSPHORIC ACID-IMPREGNATED SILICA GEL LAYER

Mobile phase: chloroform–methanol–acetate buffer (pH 4) (65:25:4.3).

Phosphoric acid (%)	*PI*	*PC*	*PA*	*PE*
10	0.54	0.53	0.69	0.60
1	0.29	0.41	0.58	0.58
0.5	0.24	0.34	0.45	0.56
0.2	0.23	0.33	0.39	0.51
0	0.19	0.21	0.23	0.47

which is specific for phosphorus, the signal obtained for each class of phospholipids is independent of the origin of the soybean, rape-seed and sunflower seed, *i.e.*, independent of the fatty acid pattern. This is possibly due to the fact that all phospholipid classes have similar molecular weights. Thus each phospholipid class is characterized by a similar content of phosphorus (Table III).

By using the Dittmer–Lester immersion reagent mixed with ethanol on a non-impregnated silica gel layer, the analytical evaluation has to be carried out

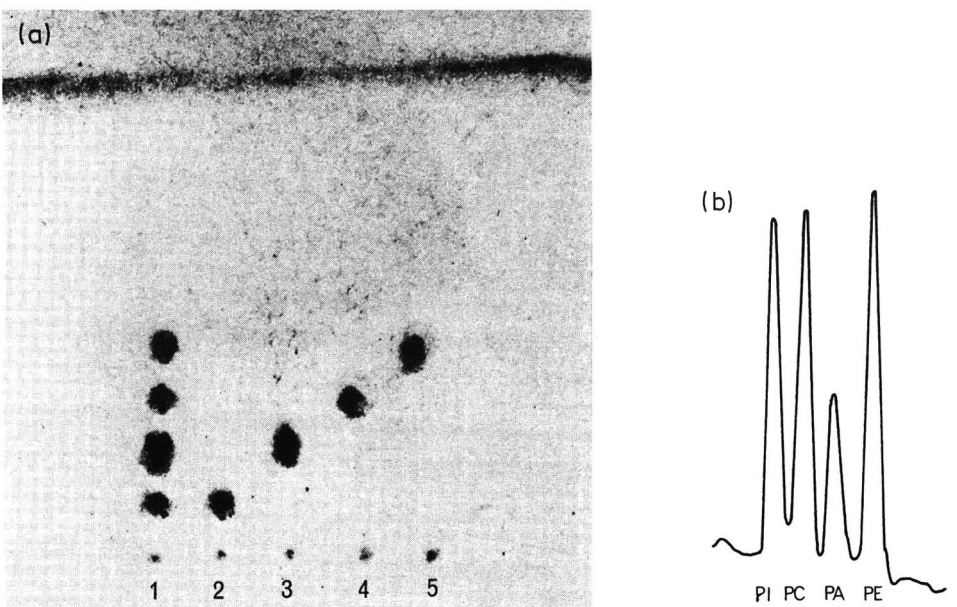

Fig. 2. Chromatograms of phospholipids. (a) Thin-layer chromatogram. 1 = Mixture of phospholipids; 2 = phosphatidyl inositol (PI); 3 = phosphatidyl choline (PC); 4 = phosphatidic acids (PA); 5 = phosphatidyl ethanolamine (PE). Stationary phase: silica gel impregnated with 0.5% phosphoric acid. Mobile phase: chloroform–methanol–acetate buffer (pH 4) (65:25:4.3). Detection: Dittmer–Lester reagent. (b) Chromatogram obtained with Zeiss PM Q II. For conditions, see Experimental.

10 min after immersion because, depending on the phospholipid class, the intensity of the spots decreased by 10–30% within 30 min after immersion and by 40–50% after 5 h (Fig. 3a). Gustavsson[12] showed that the pigmentation depends on the water content of the plate. The intensity of faded spots could be increased by using water vapour.

Impregnation of the silica gel layer with phosphoric acid turned out not only to enhance the separation of phospholipids, but also to improve the stability of the colours and the detection with Dittmer–Lester reagent. The maximum intensity of the blue spots was observed not earlier than 3 h following the detection and then remained more or less stable for about 3 h. The dependence of the measured intensities of the blue phospholipid spots on time is shown in Fig. 3b.

The quantitative measurement of the non-impregnated silica gel layer should be carried out 10 min after detection; although the signal intensity becomes relatively stable after about 1 h, by this time the signals are weak and difficult to measure. When detecting phospholipids on a phosphoric acid-impregnated layer, the intensity of the signal increases within the first 3 h and then remains almost unchanged for the next

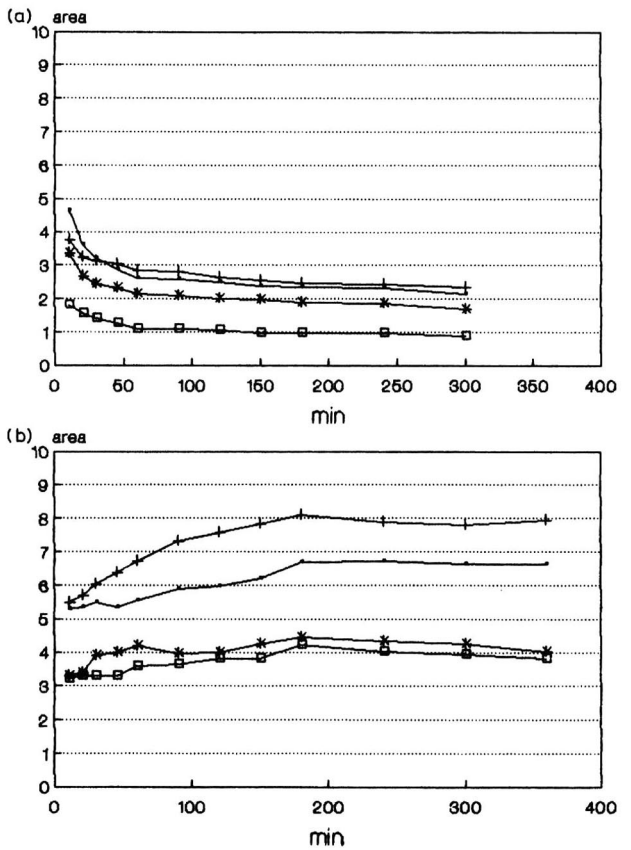

Fig. 3. Intensities of colours of phospholipids after detection with Dittmer–Lester reagent. (a) On the silica gel thin-layer surface; (b) on the phosphoric acid-impregnated silica gel thin-layer surface. ● = PC; + = PE; ∗ = PI; □ = PA.

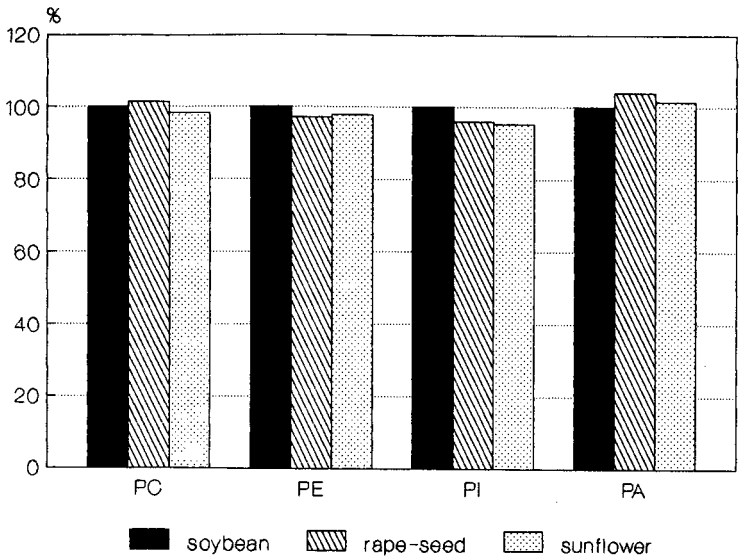

Fig. 4. Relative peak areas of the phospholipids.

TABLE III

AVERAGE MOLECULAR WEIGHTS OF PHOSPHOLIPIDS

Phospholipid class	*Soybean*	*Rape-seed*	*Sunflower seed*
PC	770	768	778
PE	724	735	736
PI	834	850	843
PA	687	691	695

TABLE IV

RELATIVE PEAK AREAS OF PHOSPHOLIPIDS

Phospholipid class	*Soybean*	*Rape-seed*	*Sunflower seed*
PC	100	101.4	98.1
PE	100	97.0	97.7
PI	100	96.0	95.4
PA	100	104.0	101.5

3 h (Fig. 3b). The quantitative evaluations can be carried out about 30 min after detection, as the intensity of the blue spots is then sufficiently stabilized. There is no need to wait before measuring until the maximum intensity of the colours has been achieved, because in spite of the higher molar absorptivity the standard deviation does not improve.

Subsequently we examined whether, after impregnation with phosphoric acid, the intensities of the colours were the same for the phospholipid classes with the Dittmer–Lester reagent irrespective of their origin. As soybean phospholipids are used as reference substances for the routine analysis, their peak areas were set as 100. The peak areas of the phospholipids of rape-seed and sunflower seed were calculated in proportion to the values for the soybean phospholipids. The results obtained for each phospholipid are shown in Table IV and Fig. 4.

There are only slight differences in the intensities of each phospholipid of one class; the differences are all within the range of the standard deviation of 4%.

By using this method of detection we were able to determine the phospholipid contents of lecithin specimens from soybean, rape-seed and sunflower seed with phospholipid standards (PC, PE, PI and PA) isolated only from the most frequently used soybean lecithin.

REFERENCES

1 M. Turelli, C. Coulomb, J. Coulomb, J. P. Roggero and M. Bounias, *Physiol. Plant Pathol.*, 24 (1984) 211–221.
2 B. Rivnay, *J. Chromatogr.*, 294 (1984) 303–315.
3 E. Martin, *Trav. Chim. Aliment. Hyg.*, 72 (1981) 402–410.
4 A. Seher, H. Spiegel, S. Könker and H. J. Oslage, *Fette-Seifen-Anstrichm.*, 85 (1983) 295–304.
5 E. Hedegaard and B. Jensen, *J. Chromatogr.*, 225 (1981) 450–454.
6 N. Robinson and B. M. Phillips, *Clin. Chim. Acta*, 8 (1963) 385–392.
7 P. R. Gentner, M. Bauer and I. Dieterich, *J. Chromatogr.*, 206 (1981) 200–204.
8 L. J. Macala, R. K. Yu and S. Ando, *J. Lipid Res.*, 24 (1983) 1243–1250.
9 H. W. Peter and H. U. Wolf, *J. Chromatogr.*, 82 (1973) 15–30.
10 H. F. Larsen and A. F. Trostmann, *J. Chromatogr.*, 226 (1981) 484–487.
11 F. M. Helmy and M. H. Hack, *J. Chromatogr.*, 374 (1986) 61–72.
12 L. Gustavsson, *J. Chromatogr.*, 375 (1986) 255–266.
13 M. Haug, D. Reinhardt and G. Harzer, *J. Chromatogr.*, 233 (1982) 349–354.
14 Lj. Kraus, E. Stahl, G. Reher and R. Richter, *Dtsch. Apoth. Ztg.*, 121 (1981) 2299–2302.
15 Lj. Kraus, *Kleines Praktikumsbuch der Dünnschichtchromatographie*, Desaga, Heidelberg, 2nd ed., 1987.
16 J. Sherma and S. Bennet, *J. Liq. Chromatogr.*, 6 (1983) 1193–1211.
17 M. Goppelt and K. Resch, *Anal. Biochem.*, 140 (1984) 152–156.
18 J. C. Touchstone, S. S. Levin, M. F. Dobbins and P. C. Beers, *J. Liq. Chromatogr.*, 6 (1983) 179–192.
19 J. Bitman and D. L. Wood, *J. Liq. Chromatogr.*, 4 (1981) 1023–1034.
20 Fortschrittsberichte, *Fette-Seifen-Anstrichm.*, 72 (1970) 1091–1103.
21 J. C. Dittmer and R. L. Lester, *J. Lipid Res.*, 5 (1964) 126–127.
22 V. E. Vaskovsky and E. Y. Kosteetsky, *J. Lipid Res.*, 9 (1968) 396.
23 S. K. Goswami and C. F. Frey, *J. Lipid Res.*, 12 (1971) 509–510.
24 S. K. Kundu, S. Chakravarty, N. Bhaduri and H. K. Saha, *J. Lipid Res.*, 18 (1977) 128–130.
25 E. K. Ryu and M. MacCoss, *J. Lipid Res.*, 20 (1979) 561–563.
26 G. Lendrath, *Dissertation*, Hamburg University, Hamburg, 1989.
27 T. R. Watkins, *J. High Resolut. Chromatogr. Chromatogr. Commun.*, 5 (1982) 104–105.
28 H. W. Peter and H. U. Wolf, *J. Chromatogr.*, 82 (1973) 15–30.
29 A. Nasner, *Dissertation*, Hamburg, 1983.
30 G. Lendrath, A. Nasner and Lj. Kraus, *Planta Med.*, Congress Issue (1988) 25.

Journal of Chromatography, 502 (1990) 393–400
Elsevier Science Publishers B.V., Amsterdam — Printed in The Netherlands

CHROM. 22 117

Note

Preliminary results on the gas chromatographic evaluation of interpenetrating polymer networks prepared from porous polymer beads

ANNA B. WÓJCIK
Faculty of Chemistry, Maria Curie-Sklodowska University, 20 - 031 Lublin (Poland)
(First received June 1st, 1989; revised manuscript received October 17th, 1989)

Chemical modification of the column packing is an attractive way to change the gas chromatographic (GC) performance of a stationary phase. This approach is still under intensive investigation even for such common materials as porous polymers. However, commercially available porous polymers often exhibit very inhomogeneous physical and chemical structures. Recent improvements in the synthesis of highly cross-linked porous polymers have led to their use as a reversed-phase liquid chromatographic packing materials. Nevertheless, efforts have been made to limit their swelling in organic solvents and to make them more water compatible. It has been reported that chemical derivatization of polystyrene beads obtained by introducing ether linkages into the polystyrene backbone makes them more suitable for the separation of biomolecules in aqueous solution[1].

This paper proposes a novel chemical derivatization technique as a means of changing the chromatographic behaviour of some porous polymer packings by producing a structure defined as an interpenetrating polymer network. This kind of derivatization may also be helpful for changing the hydrophobic properties of polymer packings and for reducing their swelling inorganic solvents.

In general, an interpenetrating polymer network is a material containing at least two polymers, each in a network form. When a cross-linked polymer I, swollen with a monomer II, is subjected to polymerization, it results in a sequential interpenetrating polymer network (IPN)[2]. A full IPN is obtained when both components are cross-linked (thermosetting polymers). If one is a linear polymer and the other is in the network form, the system is called a semi-IPN. From the point of view of such definitions, some ion-exchange resins, called "snake-cages", can be regarded as a type of sequential IPN, especially when the "snakes", *i.e.*, linear polyelectrolytes, are cross-linked[3].

Recently, sequential IPNs of both types have been prepared on the basis of porous bead copolymers, made of methyl methacrylate (MMA) and di(meth-acryloyloxymethyl)naphthalene (DMN), by swelling them with monomers and then by *in situ* polymerization[4–6]. Full IPNs have been prepared with the aim of increasing their surface area and pore volume without weakening the physical strength of the

0021-9673/90/$03.50

starting material. Usually full IPNs exhibit high densities, less swelling in organic solvents and substantial changes in specific surface area, pore size distribution and pore volume, which depend mainly on the type of monomer II used and the porous structure of the starting copolymers. For these reasons, full IPNs seem to be especially suitable for GC.

In this work, IPN-modified MMA–DMN copolymers were tested as column packings in GC and attempts were made to correlate their chromatographic behaviour with the conditions of IPN synthesis.

EXPERIMENTAL

Materials

The bead polymer sorbents used as network I in the IPN syntheses were porous bead MMA–DMN copolymers prepared under different conditions via radical suspension copolymerization of methyl methacrylate with DMN in the presence of toluene and isooctane or toluene and dodecane as diluents and 2,2′-azobisisobutyronitrile as initiator[7–9]. The characterization of these materials and their synthesis conditions are given in Table I.

TABLE I

CHARACTERIZATION OF MMA–DMN COPOLYMERS USED FOR IPN SYNTHESES

Copolymer No.	*DMN content (%, w/w)*	*Specific surface area (m^2/g)*	*Specific pore volume (cm^3/g)*	*True density (g/cm^3)*	*Pore-size distribution (Å)*	*Type*
1	50	0.1	–	1.40	–	Gel
2	50	44.3	0.40	1.42	10–243	Porous
3	50	63.8	0.25	1.42	10–730	Macroporous
4	60	124.0	0.53	1.45	10–6000	Macroporous

IPN preparation

MMA–DMN copolymer beads were swollen in a swelling agent consisting of a monomer (or monomer mixture), an initiator and a solvent. In some instances pore-forming diluents (toluene and dodecane) were used to replace the solvent. The amount of swelling agent used was such that it was completely absorbed by the polymer. After 24 h of swelling, the excess was removed by aspiration. The swollen beads were placed in an aqueous solution of poly(vinyl alcohol) (2%, w/w) at 80°C for 10 h. The beads were then washed with hot water and sequentially in a Soxhlet apparatus with acetone and then methanol.

Mixtures of MMA and DMN, ethylene glycol dimethacrylate (EGDMA) or solutions of DMN in toluene were used as monomer II. Details of the synthesis are given in Table II.

Measurements

Specific surface area, specific pore volume and pore size distributions were obtained by using BET and Barret methods. The apparatus used was a Sorptomatic 1800 (Carlo Erba, Milan, Italy).

Chromatographic measurements were carried out on a Chromatron GCHF-18.3 gas chromatograph (Chromatron, Berlin, G.D.R.) equipped with a flame ionization or thermal conductivity detector. Modified copolymer beads were packed in a glass column (1 m × 2.5 mm I.D.). Samples of 0.2 μl of test mixtures were injected; the concentration of any alcohol in the test mixture was 0.1% (v/v) and that of any alkane was 0.16% (v/v).

RESULTS AND DISCUSSION

The MMA–DMN copolymer used for the preparation of IPNs had three different porous structure: (a) gel-type structure with an unmeasurable surface area and an unmeasurable pore volume; they are recognized as empty beads of extremely low apparent density[8]; (b) porous structure with a moderately developed surface, intermediate pore sizes ($r \leqslant 400$ Å) and low pore volume; (c) macroporous structure with a well developed surface, measurable macropores and large pore volume.

These copolymers were subjected to post-polymerization according to the following procedures:

(i) Formation of a porous network II within a gel-type structure. The swelling medium consisted of a monomer mixture containing cross-linking monomer (MMA + DMN), an initiator and a pore-forming diluent (toluene + dodecane) (samples 1a and c, Table II).

(ii) Formation of a network II inside the macroporous copolymer by swelling it with liquid cross-linking monomer (EGDMA) containing an initiator (sample 2, Table II).

(iii) Formation of a network II within gel-type (empty) beads by swelling them with the liquid monomer (EGDMA) containing an initiator (sample 1b, Table II).

(iv) Formation of a porous network II inside the copolymer of developed porous structure (porous or macroporous type). The monomer mixture containing the cross-linker (DMN) and pore-forming diluent was used as a swelling medium (samples 3 and 4b, Table II).

(v) Formation of a network II within the copolymer of well developed porous structure. Cross-linking monomer (DMN) diluted with solvent and containing an initiator was used as a swelling medium (sample 4a, Table II).

All the IPNs prepared were subjected GC tests. The results obtained indicate that their chromatographic behaviour is different from that of parent copolymer (Table III).

IPNs based on copolymer I were characterized by the appearance of a certain porosity resulting in a measurable surface area and broad pore-size distribution. The results indicate that copolymer I increases its surface area after post-polymerization with or without a pore-forming diluent (first and third type of IPN procedures, samples 1a, b and c, Table II). However, this increase is insufficient to result in satisfactory efficiency of the column (Table III).

The second type of IPN synthesis, based on a macroporous copolymer, also exhibited a worse column performance in comparison with the starting copolymer (sample 2, Tables II and III).

In the fourth type of IPN synthesis, based on macroporous copolymers, the modified copolymers always exhibited a reduction in surface area and pore volume

TABLE II

EXPERIMENTAL DETAILS OF IPN SYNTHESES BASED ON MMA–DMN COPOLYMERS

Sample code	*Starting copolymer*	*Swelling mixture (w/w)*	*Specific surface area (m^2/g)*	*Specific pore volume (cm^3/g)*	*d/2[a] (Å)*	*True density (g/cm^3)*	*Description*
1a	Copolymer 1	MMA–DMN (1:1) in toluene–isooctane (4:1)	Unmeasurable	–	–	1.50	White, fragile beads with surface irregularities
1b	Copolymer 1	EGDMA	36.0	–	10–2120	1.52	White, strong, regular beads
1c	Copolymer 1	MMA–DMN (2:3) in toluene–dodecane (9:2)	40.1	1.32	10–2120	1.50	White, fragile beads with surface irregularities
2	Copolymer 2	EGDMA	43.0	1.21	10–2230	1.52	White, strong, regular beads
3	Copolymer 3	MMA–DMN (2:3) in toluene–dodecane (7:1)	30.6	0.74	10–830	1.49	White, regular beads like copolymer 3
4a	Copolymer 4	DMN in toluene (1:5)	85.0	0.49	10–500	1.55	White, regular beads like copolymer 4
4b	Copolymer 4	DMN in toluene–isooctane (4:1)	25.7	0.21	10–240	1.50	White beads with surface irregularities

[a] $d/2$ = Pore-size distribution.

TABLE III

COMPARISON OF MMA–DMN COPOLYMERS AND THEIR IPN DERIVATIVES

Column packing	*Theoretical plates for*		R_{ij}[a]	*Separation of alcohols*[b]	*Separation of n-alkanes*[c]	*Separation conditions*
	Propanol	*Heptane*				
Copolymer 1	20	10	–	No resolution	No resolution	Studied temperature range 100–200°C at flow-rate 30 ml/min
IPN 1a	62	30	–	3 peaks weakly separated	No resolution	Temp. 140°C; flow-rate 30 ml/min; time of alcohol analysis, 4.5 min
IPN 1b	50	30	–	No resolution	No resolution	Temp. 100–200°C; flow-rate 30 ml/min
IPN 1c	180	60	–	Partial resolution (3 peaks)	Partial resolution (2 peaks)	Temp. 140°C; flow-rate 30 ml/min; time of alcohol analysis, 3.5 min; time of alkane analysis, 2 min
Copolymer 2	415	110	0.35	Partial resolution (4 peaks)	Partial resolution (4 peaks)	Temp. 160°C; time for alcohol analysis, 3.5 min; time for alkane analysis, 3 min
IPN 2	150	65	–	Partial resolution (7 peaks)	Partial resolution (3 peaks)	Temp. 160°C; flow-rate, 30 ml/min; time for alcohol analysis, 6 min; time for alkane analysis, 5.3 min
Copolymer 3	360	125	0.47	10 peaks weakly separated	Partial resolution (4 peaks)	Temp. 160°C; flow-rate, 30 ml/min; time for alcohol analysis, 8.3 min; time for alkane analysis, 4 min
IPN 3	270	70	0.25	Partial resolution (7 peaks)	Partial resolution (4 peaks)	Temp. 170°C; flow-rate, 30 ml/min; time for alcohol analysis, 10 min; time for alkane analysis, 11 min
Copolymer 4	620	300	0.66	Full resolution	Full resolution	Temp. 175°C; flow-rate, 30 ml/min; time for alcohol analysis, 18.5 min; time for alkane analysis, 15 min at 195°C
IPN 4a	750	340	0.89	Full resolution	Full resolution	Flow-rate, 30 ml/min. Alcohols: temp. 175°C, 6 min. Alkanes: temp. 195°C; time, 11.5 min
IPN 4b	350	130	0.32	10 weakly separated peaks	Partial resolution (5 peaks)	Flow-rate, 30 ml/min. Alcohols: temp. 175°C; time, 18 min. Alkanes: temp. 195°C; time, 11.5 min

[a] R_{ij} = resolution for the pair of isomers 2-butanol and 2-methylpropanol. $R_{ij} = 2\,t_R(w_{p,i} + w_{p,j})$, where $t_R = t_{Rj} - t_{Ri}$, the distance between the maxima of the two peaks, and $w_{p,i}$ and $w_{p,j}$ are the widths of the peaks determined by extrapolating the points of inflection of the peaks towards the baseline.

[b] Test mixture of alcohols: methanol, ethanol, 1-propanol, 2-propanol, 2-butanol, 2-mehylpropanol, 1-butanol, 2-pentanol, 3-pentanol and 1-pentanol.

[c] Test mixture: C_5–C_{10} *n*-alkanes.

coupled with changes (usually broadening) of the pore-size distribution (samples 3 and 4b, Table II). Such a modification (interpenetration of two porous networks) resulted in a more heterogeneous pore structure with a reduction in the number of theoretical plates and the separation capability of the column (Table III).

The most promising results were obtained with the fifth type of IPN synthesis, where the swelling medium was a toluene solution of a cross-linking monomer, DMN (sample 4a, Table II). Regardless of the decrease in surface area and pore volume, there was a standardization of pore sizes combined with a lowering of the retention times and enhanced column efficiency (Table III, Figs. 1–3). Similar effects have been reported previously by Woeller and Pollock[10], who used incompletely cured styrene–divinylbenzene copolymers. They were swollen with a toluene solution of divinylbenzene and subjected to further polymerization. Such a two-stage bead preparation resulted in high performance and shortening of retention times of test mixtures was observed. Although no information about the actual structure was given, the method of modification indicates that synthesis giving rise to an interpenetrating polymer network was achieved.

The shortening of the retention times observed for IPN 4a might be a consequence of a decrease in specific surface area and its more uniform pore size distribution (Fig. 1). The higher performances observed with this copolymer might be explained by the more uniform structure expected as a result of cross-linking of the strongly inhomogeneous porous polymer network. Post-polymerization of such a system, built from more or less cross-linked units ("hard" and "soft" sites), must result in some level of interpenetration of the two-component network, *i.e.*, at least "soft" sites cross-linked by DMN[2,11,12].

Such interpenetration, for IPNs based on MMA–DMN copolymer, has been confirmed previously in studies of their glass temperatures and chromatographic behaviour[5]. Examination by scanning electron microscopy (SEM) of some selected IPNs based on MMA–DMN copolymers has been reported[5,6]. The SEM studies of

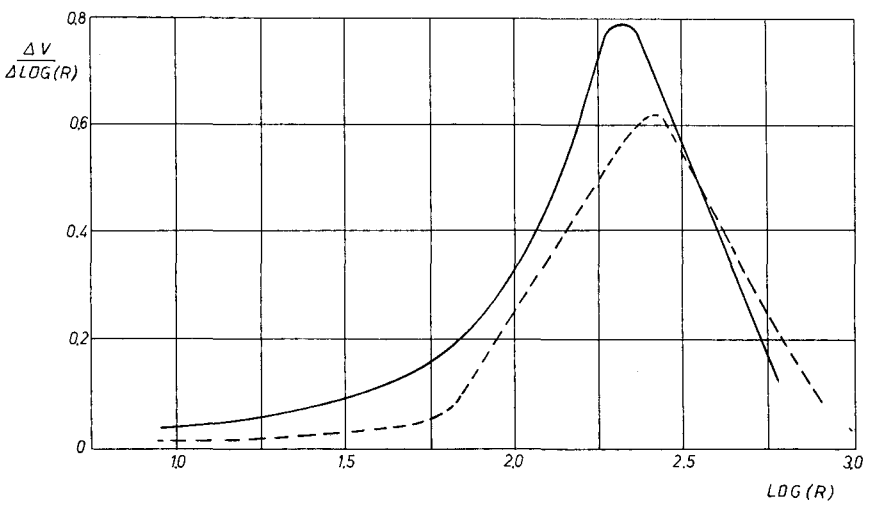

Fig. 1. Pore-size distribution for copolymer 4 (solid line) and IPN 4a (dashed line).

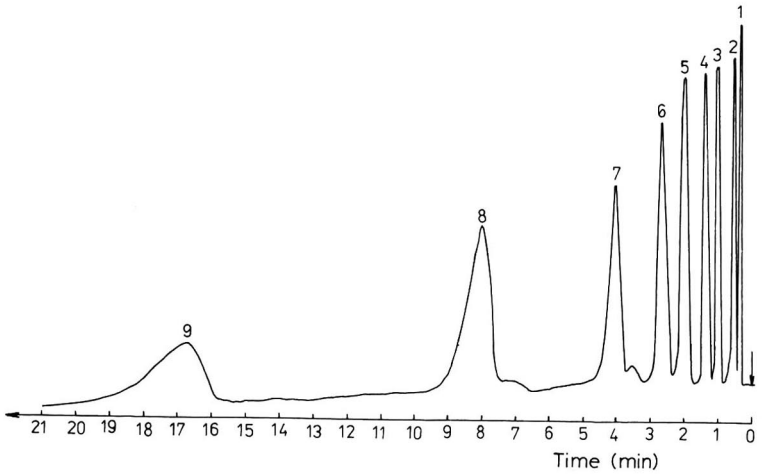

Fig. 2. Separation of alcohols using IPN 4a as a column packing: column, 1 m × 2.5 mm I.D.; temperature, 175°C; flame ionization detector; sample, 0.2 μl; hydrogen flow-rate, 30 ml/min; injector temperature, 200°C; sensitivity, $2 \cdot 10^{-10}$ a.u.f.s. Peaks: 1 = methanol; 2 = ethanol; 3 = *n*-propanol; 4 = *sec.*-butanol; 5 = *n*-butanol; 6 = *n*-pentanol; 7 = *n*-hexanol; 8 = *n*-heptanol; 9 = *n*-octanol.

sample 4a revealed impregnation of the surface copolymer shell (Fig. 4) similar to that observed previously for IPNs. This confirms some interpenetration of the two-component network for this copolymer.

To summarize, modification by formation of a porous network inside the porous copolymer proved not to be promising for GC purposes. This may be explained by an

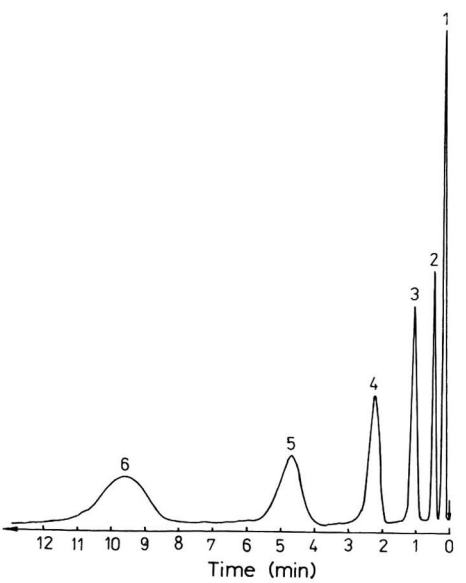

Fig. 3. Separation of *n*-alkanes. Thermal conductivity detector; other conditions as in Fig. 2. Peaks: 1 = pentane; 2 = hexane; 3 = heptane; 4 = octane; 5 = nonane; 6 = decane.

Fig. 4. SEM photograph of sample IPN 4a. Magnification ×2000.

increase in heterogeneity of the system due to post-polymerization. Post-polymerization of copolymers swollen with diluted cross-linking monomer, leading to the formation of a non-porous network interpenetrated with a porous network of the starting copolymer, seems to result in a decrease in the heterogeneity of the system. This may be useful for such purposes as shortening analysis times and improving the column performance.

REFERENCES

1 Y. Yang and M. Verzele, *J. Chromatogr.*, 391 (1987) 283.
2 L. H. Sperling, *Interpenetrating Polymer Networks and Related Materials*, Plenum Press, New York, 1981.
3 B. A. Bolto, K. H. Eppinger and M. B. Jackson, *React. Polym.*, 1 (1983) 139.
4 A. B. Wójcik, *Angew. Makromol. Chem.*, 138 (1986) 21.
5 A. B. Wójcik, in D. Klempner and K. C. Frisch (Editors), *Advances in Interpenetrating Polymer Networks*, Vol. I, Technomic, U.S.A., 1989.
6 A. B. Wójcik, *Angew. Makromol. Chem.*, 122 (1984) 43.
7 A. B. Wójcik, *Angew. Makromol. Chem.*, 119 (1983) 193.
8 A. B. Wójcik, *Angew. Makromol. Chem.*, 121 (1984) 89.
9 A. B. Wójcik, *J. Appl. Polym. Sci.*, 30 (1985) 781.
10 E. H. Woeller and G. E. Pollock, *J. Chromatogr. Sci.*, 16 (1978) 137.
11 A. B. Wójcik, *J. Appl. Polym. Sci.*, 38 (1989) in press.
12 P. V. S. Ika, H. L. Frisch, G. R. Walters, P. C. Painter and K. C. Frisch, *J. Polym. Sci., Part A*, 24 (1986) 2297.

Journal of Chromatography, 502 (1990) 401–406
Elsevier Science Publishers B.V., Amsterdam — Printed in The Netherlands

CHROM. 22 173

Note

Estimation of molecular isomer ratios of paldimycin sodium (U-70,138F) by gas chromatography

JOHN D. STODOLA* and PATRICK A. HARTMAN

The Upjohn Company, Product Control Analytical Development, 4821-259-12, Kalamazoo, MI 49001 (U.S.A.)

(First received August 2nd, 1989; revised manuscript received November 21st, 1989)

Paldimycin sodium (U-70,138F) is a mixture of trisodium salts of the N-acetyl-L-cysteine derivatives of fermentation derived paulomycin isomers (U-43,120)[1–3]. A previous report[4] described a gradient reversed-phase high-performance liquid chromatography (HPLC) method for the separation of paldimycin A (U-67,963) from paldimycin B (U-67,964) and from the corresponding paulomycins. The HPLC method is not capable of resolving paldimycin A from paldimycin A_2 (U-77,904) nor the corresponding B isomer from B_2 isomer (U-77,940) (see structures in Fig. 1). A method for determining the relative ratios of these isomers was desired to support

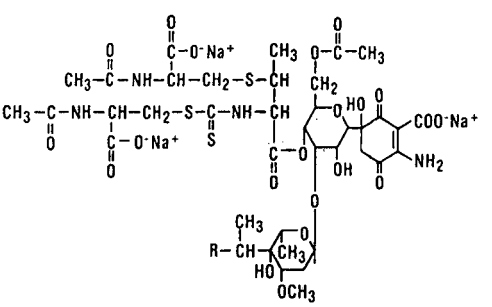

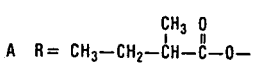

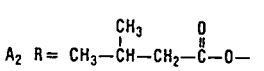

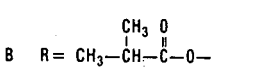

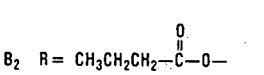

Fig. 1. Structures of isomers of paldimycin sodium. A = 2-methylbutyric acid, A_2 = 3-methylbutyric acid, B = 2-methylpropionic acid, B_2 = butyric acid.

the characterization of the bulk drug. The isomers arise[1,2] from variation in the butyric and methylbutyric acids linked via an ester bond at the C-7′ position of the sugar ring (Fig. 1). Previous reports of the separation of these and other short chain carboxylic acids include gas chromatography (GC)[5–14], HPLC[15–18], ion chromatography[17,19] and electrophoresis[20–21]. These reported methods were developed for the separation of the carboxylic acids as components which are not covalently bonded to the samples of interest however. Our goal was to develop a method which would cleave the relevant ester bonds and liberate the characteristic carboxylic acids in a medium which would allow subsequent separation by gas chromatography and indirect quantitation of the molecular isomer ratios of paldimycin sodium bulk drug.

EXPERIMENTAL

Materials

Paldimycin sodium samples were produced by Upjohn. Carboxylic acid standards and 2-vinylfuran were Gold Label quality (Aldrich, Milwaukee, WI, U.S.A.). HPLC-grade methanol and acetone (Burdick & Jackson, Muskegon, MI, U.S.A.) and Milli-Q water (Millipore, Milford, MA, U.S.A.) were used to prepare solutions. Concentrated phosphoric acid and concentrated ammonium hydroxide (Mallinckrodt, St. Louis, MO, U.S.A.) were used for adjustment of pH. High-purity compressed helium and hydrogen were delivered from gas cylinders (Welder, Kalamazoo, MI, U.S.A.) via copper tubing. Compressed air was supplied via copper tubing from an in-house system.

Instruments

A Model 5890 gas chromatograph equipped with Model 7673A robotic sampler and flame ionization detector was used (Hewlett-Packard, Palo Alto, CA, U.S.A.). Glass columns (1–2 mm × 3 mm) manually packed with Carbowax 20M and 1% phoshoric acid coated on Graphpack GC 60–80 mesh (Alltech, Rockford, IL, U.S.A.) were used for separations. A 2-cm section at the head of each column was packed with 80–100 mesh Chromosorb 101 (Alltech) to act as a guard column. Other stationary phases surveyed include Porapak Q, Porapak QS (Waters Assoc., Milford, MA, U.S.A.), Chromsorb 101 and AT 1200 with phosphoric acid (Alltech) packed in (0.6–2 m × 3 mm) glass columns. GC–mass spectrometric (MS) studies were conducted on a VG-7070F MS system (Danvers, MA, U.S.A.) using electron ionization at 70 eV and scanning a mass-to-charge ratio of 440 to 20 at 1 s/decade of mass. The mass spectrometer was interfaced via a jet separator to a Model 5790 GC system (Hewlett-Packard, Palo, Alto, CA, U.S.A.) using a 1.5-m column operated isothermally at 150°C and 30 ml/min flow.

Preparations, conditions and calculations

Samples and standards were diluted in a solution of concentrated phosphoric acid–acetone–Milli-Q water (1:10:90, v/v/v), Carboxylic acid standards were accurately prepared by serial dilutions at 0.1 mg/ml for 2-methyl propionic acid and 2-methylbutyric acid and at about 0.05 mg/ml for *n*-butyric acid and 3-methylbutyric acid. Paldimycin sodium samples (*ca.* 10 mg) were dissolved in *ca.* 200 μl of concentrated ammonium hydroxide–water (1:99, v/v) and diluted with 2 ml of the

acidic sample diluent. The sample diluent was injected as a blank solution in each run. The instrumental parameters were: column temperature 120°C, injector temperature 190°C, detector temperature 220°C, flame ionization detection (FID) hydrogen flow 50 ml/min, FID air/oxygen flow 200 ml/min, helium carrier gas flow 40 ml/min, injection volume 1 μl. The mole percent of each isomer was calculated via area percent using adjusted areas for the B isomer acids where the response factor was calculated as the ratio of the molecular weights.

Validation

Multiple injections of sample diluent blank, individual acid standards, freshly prepared samples and solution samples stored at room temperature for 16 h were injected to verify specificity, selectivity, precision and ruggedness. Accurately prepared solutions of reference standards and samples were injected to evaluate recovery, linearity and potential bias.

RESULTS AND DISCUSSION

Preparations

Initial preparation of paldimycin sodium samples in a small volume of dilute ammonium hydroxide was necessary to ensure complete dissolution before dilution with the acidic sample diluent. Acetone was included in the sample diluent to maintain solubility of the carboxylic acid reference standards. The sample preparations must be acidic (apparent pH of 2 or less), because higher pH preparations yielded poor peak shapes and poor resolution of the acids of interest. Chemical degradation of the paldimycins in solution (as determined by HPLC) did not adversely affect the recovery of the acids of interest or generate any interfering peaks in the chromatograms. The method is not applicable to paulomycins[3], because they are insoluble in the sample diluent. Attempts to use methanol as an alternative solvent for paulomycins led to very poor chromatography and apparent stripping of the stationary phase.

Specificity

The Graphpak GC Carbowax 20M phase with phosphoric acid was specifically designed for separation of short-chain carboxylic acids[22]. It was the only phase studied (see Experimental) which provided resolution of 2-methylbutyric acid and 3-methylbutyric acid from isomers A and A_2. Similar separations of these two acids on phosphoric acid-treated stationary phases have been reported elsewhere[9,14]. Separation of 2-methylpropionic acid and butyric acid from isomers B and B_2 was also obtained as demonstrated by the chromatograms of the sample solvent blank, reference standards and a paldimycin sodium bulk drug sample in Fig. 2. The acids of interest are resolved witin 18 min. No interfering peaks were detected in the blank chromatogram. An additional peak was detected in chromatograms of all preparations of paldimycin sodium (Figs. 2 and 3) however. The separation of this peak from the carboxylic acids of interest was dependent on column length, with the best resolution obtained with a 1.5-m column. GC–MS studies suggest this peak elutes with a retention time and mass spectrum matching those of 2-vinylfuran (*m/e* values of 94, 65, 39). The structure and mechanism by which this species is formed has not been rigorously established, but it is speculated that it may involve high-temperature

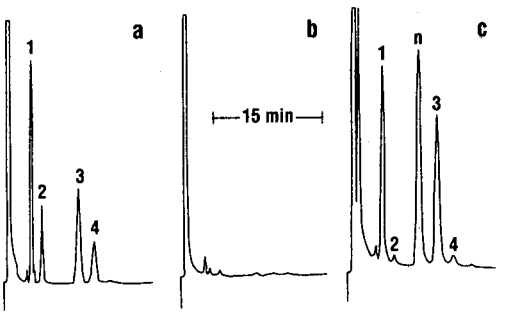

Fig. 2. Chromatograms of (a) reference standard preparation, (b) blank and (c) paldimycin sodium bulk drug sample preparation. See Experimental for conditions. Peaks: 1 = 2-methylpropionic acid; 2 = butyric acid; 3 = 2-methylbutyric acid; 4 = 3-methylbutyric acid; n = peak from paldimycin sodium preparations (matches 2-vinylfuran).

decomposition and/or dehydration of a sugar portion of the paldimycin structure. Fig. 3 shows injections of preparations of isolated paldimycin isomers to further demonstrate the specificity of the chromatography.

Paldimycins C and D derived from the corresponding paulomycins[23] would be expected to lead to observation of *n*-propionic acid and acetic acid respectively with this method. Propionic acid was not detected in any of the samples tested, however, with a detection limit of *ca.* 0.1% indicating the absence of paldimycin C. Acetic acid which may have been contributed by paldimycin D would be masked by the acetic acid liberated from the acetate esters on the other rings and N-acetyl-L-Cys (Fig. 1) and would elute near or in the solvent front and is therefore not quantitated by this method. Paldimycins E and F[23] do not contain ester side chains and are also consequently not detectable by this method.

Quantitation

The expected equivalents of each carboxylic acid were recovered from accurately weighed paldimycin sodium samples by comparison to accurately prepared carboxylic

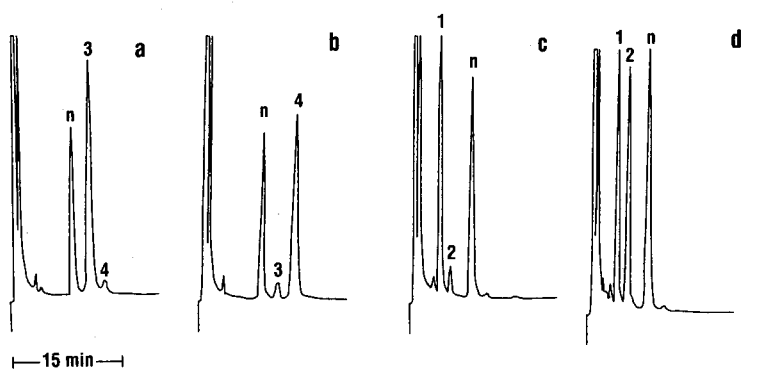

Fig. 3. Chromatograms of paldimycin sodium isomers (a) paldimycin A, (b) paldimycin A_2, (c) paldimycin B and (d) paldimycin B and B_2. See Experimental for conditions, Fig. 1 for structures and Fig. 2 for peak identification.

TABLE I

COMPARISON OF GC ISOMER AND HPLC ISOMER RESULTS FOR PALDIMYCIN SODIUM LOTS

GC results listed parenthetically are for the minor isomers. N.D. = Not detected. See Fig. 3 for chromatograms of the individual isomers listed at the bottom of this table.

Sample	*HPLC*		*GC*	
	$A+A_2$	$B+B_2$	$A+A_2$ (A_2)	$B+B_2$ (B_2)
Bulk drug U	62.3	37.7	64.6 (3.1)	35.4 (0.6)
Bulk drug V	57.5	42.5	59.5 (2.3)	40.5 (0.3)
Bulk drug W	59.7	40.3	61.7 (2.4)	38.3 (0.4)
Bulk drug X	63.8	36.2	65.9 (2.8)	34.1 (0.7)
Bulk drug Y	63.6	36.4	65.6 (2.7)	34.4 (0.6)
Bulk drug Z	56.2	43.8	58.9 (3.5)	41.1 (0.3)
Paldimycin A	100	N.D.	99.9 (4.0)	0.1 (N.D.)
Paldimycin B	1	99	0.8 (N.D.)	99.1 (5.8)
Paldimycin A_2	100	N.D.	100 (6.3)	< 0.1
Paldimycin $B+B_2$	1	99	0.9 (N.D.)	99.1 (45.9)

acid reference standard preparations. The combination of the acidic sample preparation and high temperature in the injector port is therefore adequate to ensure quantitative cleavage of the esters at C-7′. Linearity of area response was verified by injection of bulk drug prepared over a range of 25%–125% of the suggested assay concentration. Plots of amount detected *versus* amount added gave correlation coefficients of greater than 0.999. Intercepts were not significantly different from zero indicating the absence of bias.

The major isomers A and B were quantitated with a relative standard deviation (R.S.D.) of about 1% and the minor isomers A_2 and B_2 with an R.S.D. of about 10% for eight independent preparations. Table I lists results for several bulk drug lots and purified paldimycin isomers and compares the summations of $A+A_2$ and $B+B_2$ isomers determined by HPLC[4] to those determined by this method. The GC results for the minor isomer content are listed parenthetically in the table. The A_2 and B_2 isomers constitute less than 4% and 1% respectively of the isomers detected in the bulk drug lots studied.

CONCLUSIONS

A GC method for determining paldimycin sodium isomer ratios has been validated. It utilizes an acidic sample preparation and *in situ* ester cleavage within a GC system which gives linear response, good precision and is selective for carboxylic acids arising from paldimycins A, A_2, B and B_2.

ACKNOWLEDGEMENTS

We thank A. D. Argoudelis, J. M. Timko and W. J. Haak for bulk drug samples, J. DeZwaan for helpful discussions and W. K. Duholke for the GC–MS study.

REFERENCES

1 A. D. Argoudelis, L. Baczynskyj, J. A. Buege, V. P. Marshall, S. A. Mizsak and P. F. Wiley, *J. Antibiot.*, 40 (1987) 408–418.
2 A. D. Argoudelis, L. Baczynskyj, S. A. Mizsak, F. B. Shilliday, P. A. Spinelli and J. DeZwaan, *J. Antibiot.*, 40 (1987) 419–436.
3 A. D. Argoudelis, T. A. Brinkley, T. F. Brodasky, J. A. Buege, H. F. Meyer and S. A. Miszak, *J. Antibiot.*, 35 (1985) 285–294.
4 P. A. Hartman and J. D. Stodola, *J. Chromatogr.*, 385 (1985) 363–368.
5 P. G. Brotz and D. M. Schaefer, *J. Microbiol. Methods*, 6 (1987) 139–144.
6 N. P. Bole and R. K. Colwell, *J. Chromatogr.*, 410 (1987) 190–194.
7 J. L. Berdauge, *Lait*, 66 (1986) 233–246.
8 W. R. Thomann and G. B. Hill, *J. Clin. Microbiol.*, 23 (1986) 392–394.
9 M. Brazier, G. DeSmet, F. Pieri, P. Daniel, *Clin. Chim. Acta*, 148 (1985) 261–265.
10 D. N. Buchanan and J. G. Thorne, *Clin. Chim. Acta*, 145 (1985) 183–191.
11 R. J. Wiggins, M. Wilks and S. Tabaguchi, *J. Clin. Pathol.*, 38 (1985) 933–936.
12 M. J. Playne, *J. Sci. Food Agric.*, 36 (1985) 638–644.
13 I. Molnár-Perl, V. Fabian-Vonsik and M. Pinter-Szakacs, *Chromatographia*, 18 (1984) 673–676.
14 A. Tangerman, A. van Schaik, M. T. Meuwese-Arende and J. H. M. van Tongeren, *Clin. Chim. Acta*, 133 (1983) 341–348.
15 D. Tusseau and C. Benoit, *J. Chromatogr.*, 395 (1985) 323–333.
16 R. W. Gillett and G. P. Ayers, *Anal. Chim. Acta*, 177 (1985) 273–277.
17 R. Schwarzenbach, *J. Chromatogr.*, 251 (1982) 339–358.
18 R. L. Patience and J. D. Thomas, *J. Chromatogr.*, 249 (1982) 183–186.
19 K. Kihara, S. Rokushita and H. Hatano, *J. Chromatogr.*, 410 (1987) 103–110.
20 X. Huang, J. A. Luckey, M. J. Gordon and R. N. Zare, *Anal. Chem.*, 61 (1988) 766–770.
21 T. Barth, *Anal. Chem.*, 59 (1987) 2232–2237.
22 *Catalogue No. 50*, Alltech Associates, Rockford, 1983, p. 12.
23 A. D. Argoudelis, L. Baczynskyj, W. J. Haak, W. M. Knoll. S. A. Mizsak and F. B. Shilliday, *J. Antibiot.*, 41 (1988) 157–169.

Journal of Chromatography, 502 (1990) 407–415
Elsevier Science Publishers B.V., Amsterdam — Printed in The Netherlands

CHROM. 22 058

Note

Degradation and analysis of oligooxyethylene glycol mono(4-*tert.*-octylphenyl) ethers in the presence of acetyl chloride

J. SZYMANOWSKI*
Technical University of Poznań, Institute of Chemical Technology and Engineering, Pl. M. Skłowskiej-Curie 2, 60-965 Poznań (Poland)
and
P. KUSZ, E. DZIWIŃSKI and Cz. LATOCHA
Institute of Heavy Organic Synthesis "Blachownia", 47-225 Kędzierzyn-Koźle-7 (Poland)
(First received April 18th, 1989; revised manuscript received October 3rd, 1989)

Polyoxyethylene glycol mono(4-alkylphenyl) ethers, $RC_6H_4O(CH_2CH_2O)_nH$, are important non-ionic surfactants used in different fields of industry. Up to now these surfactants have been uniquely those in which the alkyl group is not straight-chain but branched. Moreover, this alkyl group is usually obtained by oligomerization of branched alkenes, usually propene or isobutene. The composition of such commercial products is very complex owing to the presence of several so far unidentified compounds in alkylphenols. For this reason, it is difficult to carry out direct analysis and it is impossible to separate and identify all components. Homologues having different numbers of the oxyethylene group can be separated but they elute in the form of broad multi-component peaks.

The aim of this work was to study the degradation of model oligooxyethylene glycol mono(4-*tert.*-octylphenyl) ethers and the application of this degradation to the determination of the average degree of ethoxylation.

EXPERIMENTAL

The following reagents were used for degradation: model oligooxyethylene glycol mono(4-*tert.*-octylphenyl) ethers (ICSO "Blachownia", Kędzierzyn-Koźle, Poland) obtained by the reaction of 4-*tert.*-octylphenol with ethylene oxide; acetyl chloride, pure for analysis (Fluka, Buchs, Switzerland); and anhydrous iron(III) chloride, pure for analysis (POCh, Gliwice, Poland).

Degradation of oligooxyethylene glycol mono(4-*tert.*-octylphenyl) ethers in the presence and obsence of iron(III) chloride was carried out according to the procedures given in previous papers[1–3], based on Waszeciak and Nadeau's method[4].

The following three different gas chromatographic (GC) columns were used: column I (0.9 m × 2.7 mm I.D.), filled with silicone resin OV-17 (3%) on Chromosorb G AW DMCS, 60–80 mesh; column II (0.9 m × 2.7 mm I.D.), filled with silicone resin

0021-9673/90/$03.50

OV-101 (3%) on Chromosorb G AW DMCS, 60–80 mesh; and column III (1.6 m × 2.7 mm I.D.), filled with Carbowax 20M–TPA (12%) on Chromosorb W AW DMCS, 80–100 mesh. The temperature of column I was 80°C for 1 min, then increased to 290°C at 6°C/min. The temperature of column II was 100°C for 1 min, then increased to 300°C ay 8°C/min. The temperature of column III was 100°C for 1 min, then increased to 220°C at 5°C/min.

The identification of the separated components was carried out by means of a mass spectrometer coupled to a gas chromatograph (GC-MS 2091; LKB, Bromma, Sweden). Columns I and II were used to identify components formed from the alkylphenyl groups and oligooxyethylene chains, respectively. The separation conditions were the same as in the GC analysis. The mass spectra were taken at the tops of the chromatographic peaks. An ionization energy of 70 eV and an ion-source temperature of 250°C were employed.

The degree of degradation (α_d) was calculated according to

$$\alpha_d = \frac{\sum_{n=1}^{m} x_n}{\sum_{n=1}^{m} x_n + \sum_{i=1}^{j} x_i} \cdot 100\% \tag{1}$$

where x_n denotes the content of component n (%, w/w) formed during degradation and x_i the content of homologue i of polyoxyethylene glycol mono(4-*tert*.-octylphenyl) ether remaining in the post-reaction mixture after degradation.

The average degree of ethoxylation (α) was calculated according to eqn. 2 and the mass of the oligooxyethylene chain (m_{EO}) in the investigated sample according to eqn. 3.

$$\alpha = \frac{m_{EO} M_H}{44(m - m_{EO})} \tag{2}$$

$$m_{EO} = \sum_{i=1}^{j} \frac{44 m_s A_i K_{s,i} n_i}{A_s M_i} \tag{3}$$

where M_H and M_i denote the average molecular mass of the hydrophobic alkylphenyl groups and the molecular mass of a component i formed by degradation of the oligooxyethylene chains, respectively, m and m_s are the mass of the analysed sample and the mass of *n*-hexadecane used as the internal standard, respectively, A_s and A_i are surface areas of peaks of the standard and a component i formed by degradation of the oligooxyethylene chains, respectively, n_i is the number of oxyethylene groups needed to form a component i and $K_{s,i}$ denotes the relative correction factor of a component i in comparison with the internal standard.

A differential microcalorimeter (TA-2000A; Mettler, Greifensee, Switzerland) was used. A sample (0.002 g) of oligooxyethylene glycol mono(4-*tert*.-octylphenyl) ether and acetyl chloride (1:15, w/w) on silicon carbide was heated in an aluminium crucible covered with a perforated lid to 350°C at 25°C/min.

A mini-autoclave of capacity 0.5 cm^3 (Mettler) was used to register differential thermal analysis (DTA) curves under isochoric conditions. Samples (0.04 g) of oligooxyethylene glycol mono(4-*tert.*-octylphenyl) ether, acetyl chloride and iron(III) chloride (1:15:1, w/w/w) were heated from 60 to 200°C at 2°C/min. Benzene was used as a standard.

RESULTS AND DISCUSSION

4-*tert.*-Octylphenol, used as a reagent to obtain polyoxyethylene glycol mono-(4-*tert.*-octylphenyl) ethers (henceforth abbreviated to E), contains about 91% (w/w) of 4-(1,1,3,3-tetramethylbutyl)phenol. Using packed chromatographic columns, three additional components were separated and identified as 4-(1,1,4-trimethylpentyl)-phenol, 4-(1,1,3-trimethylpentyl)phenol and [2-(*tert.*-butyl)-4-(1,1,3,3-tetramethyl-butyl)]phenol[5]. However, eleven components were separated as a capillary column was used. As a result, chromatograms of E, in addition to the main peaks of polyoxyethylene glycol mono[4-(1,1,3,3-tetramethylbutyl)phenyl] ethers having different numbers of oxyethylene groups, also contain polyoxyethylene derivatives of other alkylphenols[5].

Retention indices and the contents of successive homologues having different numbers of oxyethylene groups are given in Table I.

Thermograms of mixtures of E with acetyl chloride and/or without iron(III) chloride are presented in Figs. 1 and 2. Fig. 1 demonstrates that an endothermic effect is observed at temperatures of 30–110°C as a result of acetyl chloride evaporation. An exothermic effect above 110°C is caused by the acylation of E. A weak exothermic effect at 250–340°C observed for the system which do not contain iron(III) chloride is caused by slow degradation.

The DTA curve obtained under isochoric conditions (Fig. 2) demonstrates that in the presence of iron(III) chloride an exothermic effect is already observed at temperatures of 60–220°C and a significant increase in heat formed during degradation is observed above 150°C. Thus, in the presence of iron(III) chloride degradation proceeds much quicker and at lower temperatures. This is supported by chromatographic data, which demonstrates that complete degradation is impossible without the

TABLE I

RETENTION INDICES AND CONTENTS OF SEPARATED HOMOLOGUES IN OLIGOOXYETHYLENE GLYCOL MONO(4-*tert.*-OCTYLPHENYL) ETHERS

No. of oxyethylene groups	*Retention index, I_p*			*Content (%, w/w)*[a]
	OV-101	*OV-17*	*Carbowax 20M–TPA*	
0	1215–1638	1730–2114	2100–2592	2.75 ± 2.99
1	1759[b]–1843	2248[b]–2407	2668[b]–2835	90.25 ± 2.97
2	1991–2074	2549–2698	3062	7.00 ± 2.42
3	2237–2302	–	–	0.00

[a] Confidence limits for a significance level of 0.05 and 5 analyses.
[b] Main component, $(CH_3)_3CCH_2C(CH_3)_2$-*p*-$C_6H_4OCH_2CH_2OH$.

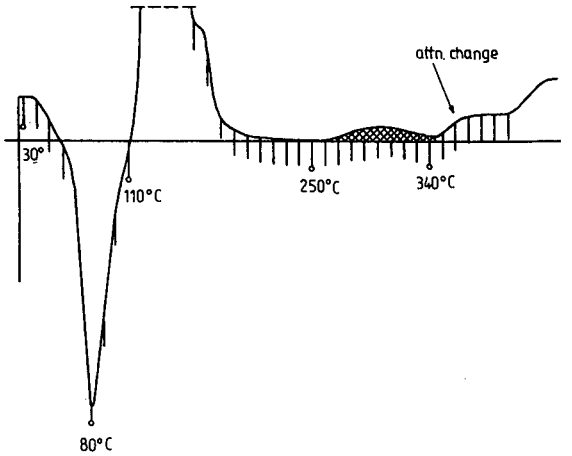

Fig. 1. DTA curve for a mixture of oligooxyethylene glycol mono(4-*tert.*-octylphenyl) ethers and acetyl chloride.

catalyst (Figs. 3 and 4). At 250°C the degradation of E is only about 45%. The degradation of polyoxyethylene glycol mono(4-nonylphenyl) ethers having an average degree of ethoxylation of 8 is even lower (30%). However, although the degradation is not complete, the products formed can be easily separated and identified. The degradation of the polyoxyethylene chain proceeds in the same way as was previously

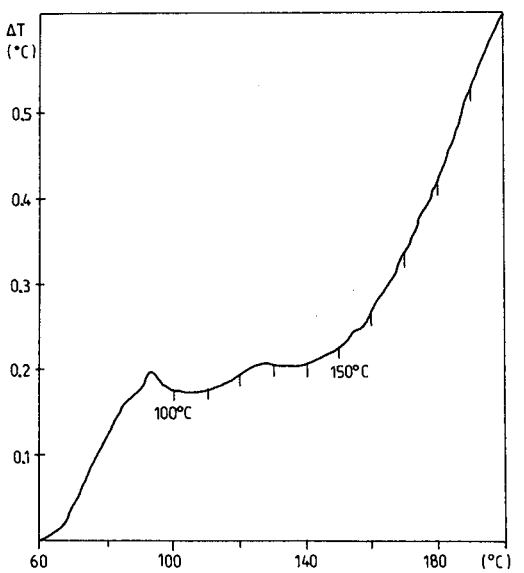

Fig. 2. DTA curve for a mixture of oligooxyethylene glycol mono(4-*tert.*-octylphenyl) ethers, acetyl chloride and iron(III)chloride (isochoric conditions).

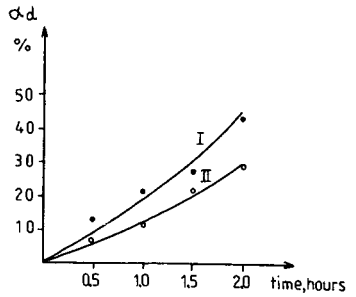

Fig. 3. Effect of time on the degradation of polyoxyethylene glycol mono(4-alkylphenyl) ethers in the absence of iron(III) chloride. (I) Oligooxyethylene glycol mono(4-*tert.*-octylphenyl) ethers; (II) polyoxyethylene glycol mono(4-nonylphenyl) ethers having an average degree of ethoxylation of 8. α_d = Degree of degradation calculated from eqn. 1.

demonstrated for polyoxyethylene glycols and their monoalkyl ethers[1–3]. 2-Chloroethyl acetate (retention index I_p = 1318) is the main degradation product and 1,2-dichloroethane (I_p = 1065), bis(2-chloroethyl)ether (I_p = 1536), 5-chloro-3-oxapentyl acetate (I_p = 1757) and dioxyethylene glycol diacetate (I_p = 1970) are formed in small amounts. Their mass spectra are similar to those reported previously[1].

In the presence of iron(III) chloride the degradation of E is complete at 150°C in 30 min (Figs. 5 and 6). Only three compounds formed from the polyoxyethylene chain were identified: 2-chloroethyl acetate (I_p = 1318 and 926 on Carbowax 20M–TPA and OV-17, respectively), bis(2-chloroethyl)ether (I_p = 1536 and 1220 on Carbowax 20 M–TPA and OV-17, respectively) and dioxyethylene glycol diacetate (I_p = 1970

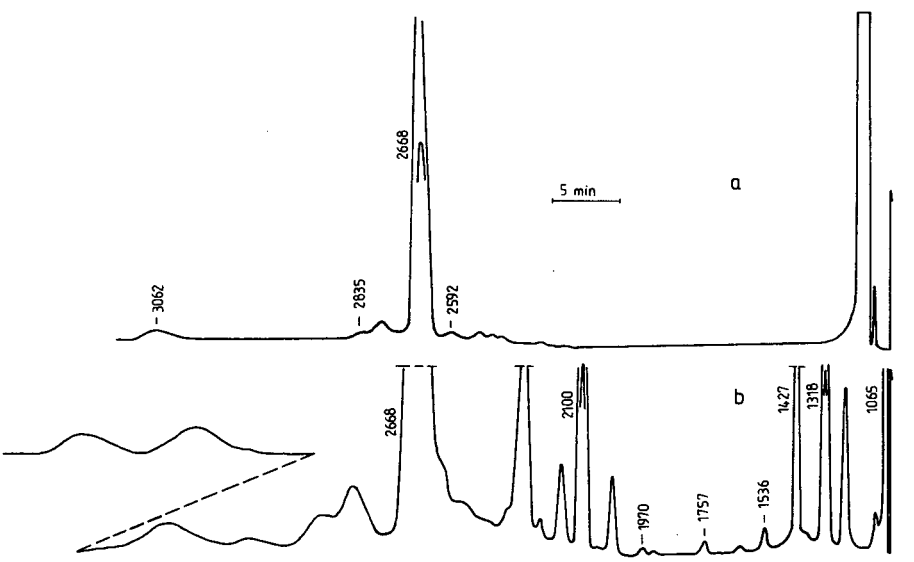

Fig. 4. Chromatogram of oligooxyethylene glycol mono-(4-*tert.*octylphenyl) ethers, (a) before and (b) after degradation without iron(III)chloride (column III, Carbowax 20M–TPA).

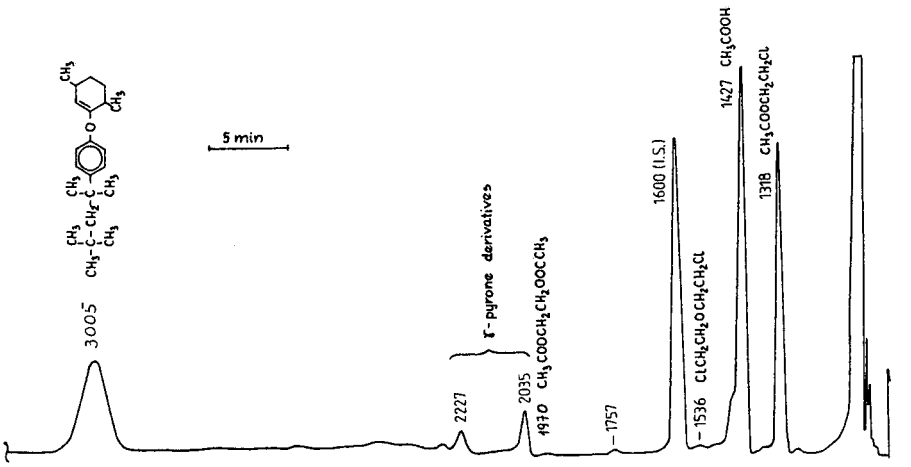

Fig. 5. Chromatogram of the degradation products with column III, Carbowax 20M-TPA.

and 1491 on Carbowax 20M–TPA and OV-17, respectively). As in previous work[1–3], peaks of acetic acid (I_p = 1427 on Carbowax 20 M–TPA) and of γ-pyrone derivatives (I_p = 2035 and 2227 on Carbowax 20 M–TPA) were observed. Acetic acid was formed from acetyl chloride, whereas γ-pyrone derivatives were formed from acetic acid. Hexadecane was used as the internal standard. All other peaks separated on OV-17 correspond to compounds obtained from alkyl phenyl groups (I_p = 2035, 2180, 2494, 2574, 2661, 2830, 3032 and 3085). Some of them were identified by their mass spectra (Fig. 7), which have lines of molecular ions and those formed by typical splitting of alkyl groups. Structures of other components were suggested taking into account their

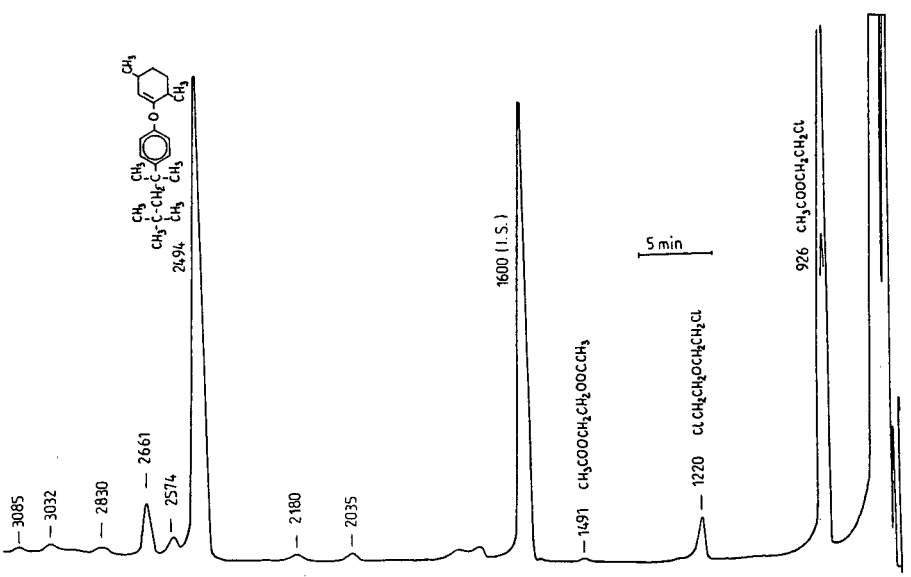

Fig. 6. Chromatogram of the degradation products with column I, OV-17.

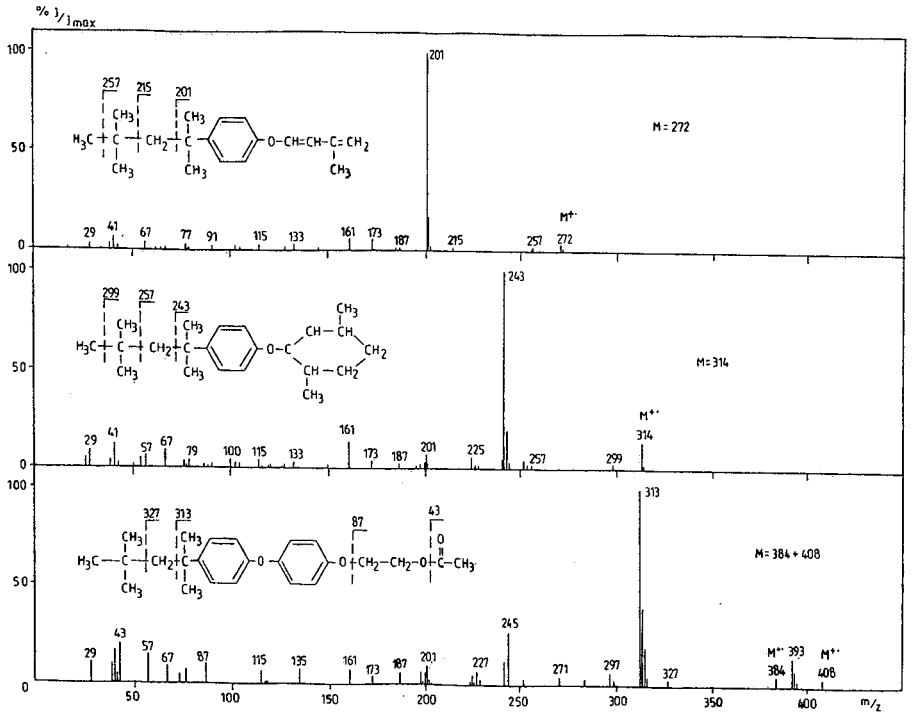

Fig. 7. Mass spectra of the products formed from alkylphenyl groups.

retention indices and those predicted from the group increments determined previously[6].

The compositions of the degradation products and their retention indices are given in Table II. The results demonstrate that 4-(1,1,3,3-tetramethylbutyl)phenyl-3,6-dimethyl-1-cyclohexenyl ether is the main compound formed from alkylphenyl groups. However, most of the alkylphenyl groups react towards unidentified resins which do not elute from the column.

Values of the average degree of ethoxylation calculated from the direct chromatographic analysis, *i.e.*, without degradation and by means of degradation, are presented in Table III. Good agreement between the results obtained by means of these two methods is observed, the average difference being only about 4%. Hence, the proposed method of degradation can be used to determine the average degree of ethoxylation of oligooxyethylene glycol mono(4-alkylphenyl) ethers. Its application to complex industrial preparations will be considered in the near future.

CONCLUSIONS

Oligooxyethylene glycol mono-(4-alkylphenyl) ethers can be degraded with an excess of acetyl chloride in the presence of anhydrous ion(III) chloride at 150°C in 0.5 h. Oligooxyethylene chains are degraded mainly to 2-chloroethyl acetate, while unidentified resins are mainly formed from alkylphenyl groups. 4-(1,1,3,3-Tetra-

TABLE II

COMPOSITION OF PRODUCTS OBTAINED BY DEGRADATION OF OLIGOOXYETHYLENE GLYCOL MONO(4-*tert.*-OCTYLPHENYL) ETHERS

Type of product[a]	*Component*	*Retention index*		*Content (%, w/w)*
		OV-17	*Carbowax 20M–TPA*	
I	2-Chloroethyl acetate	926	1318	16.21
	Bis(2-chloroethyl)ether	1220	1536	0.46
	Dioxyethylene glycol diacetate	1491	1970	0.19
II	4-(1,1,3,3-Tetramethylbutyl)phenyl-3-methyl-1,3-butadienyl ether	2035	2546	0.20
	4-(1,1,3,3-Tetramethylbutyl)phenyl-3-methyl-1-cyclobutenyl ether	2180	2726	0.45
	4-(1,1,3,3-Tetramethylbutyl)phenyl-3,6-dimethyl-1-cyclohexenyl ether	2494	3005	22.31
	4-Octylphenyl-3,6-dimethyl-1-cyclohexenyl ether	2574	3107	1.23
	4-(1,1,3,3-Tetramethylbutyl)phenyl-2-(3,6-dimethyl-1-cyclohexenyl)ethyl ether	2661	3206	2.70
	4,4′-Di(1,1,3,3-tetramethylbutyl)biphenyl	2830	–	0.49
	4-(1,1,3,3-Tetramethylbutyl)phenyl-4′-(1,1,3,3-tetramethylbutyl)methylphenyl ether	3032	–	0.20
		3032	–	0.20
	4-(1,1,3,3-Tetramethylbutyl)phenyl-4′-(2-acetoxyoxyethyl)phenyl ether	3085	–	0.15
	High-boiling resins	–	–	55.11

[a] I and II denote components obtained from the polyoxyethylene chains and alkylphenyl groups, respectively.

TABLE III

AVERAGE DEGREE OF ETHOXYLATION OF OLIGOOXYETHYLENE GLYCOL MONO-(4-*tert.*-OCTYLPHENYL) ETHERS

Parameter	*Direct chromatographic analysis (a)*	*Analysis after degradation (b)*	$b - a$	$\Delta(\%) = \frac{b-a}{a} \cdot 100$
Degree of ethoxylation (individual values)	0.98	0.96	−0.02	−2.04
	0.98	0.93	−0.05	−5.10
	0.98	0.90	−0.08	−8.16
	0.98	1.03	+0.05	5.10
	1.01	0.92	−0.09	−8.91
Average degree of ethoxylation	0.99	0.95	−0.04	−3.82
Standard deviation	0.01342	0.05070		
Confidence limits[a]	±0.02	±0.07		

[a] For a significance level of 0.05 and 5 analyses.

methylbutyl)phenyl-3,6-dimethyl-1-cyclohexenyl ether is the main low-molar-mass component formed from alkylphenyl groups. The contents of the compounds obtained by degradation of oligooxyethylene chains can be precisely determined and used to calculate the average degree of ethoxylation. Good agreement is observed between the average degree of ethoxylation determined by direct chromatographic analysis and after degradation.

REFERENCES

1 J. Szymanowski, P. Kusz and E. Dziwiński, *J. Chromatogr.*, 456 (1988) 131.
2 J. Szymanowski, P. Kusz, E. Dziwiński and Cz. Latocha, *J. Chromatogr.*, 455 (1988) 119.
3 J. Szymanowski, P. Kusz, E. Dziwiński, H. Szewczyk and K. Pyżalski, *J. Chromatogr.*, 469 (1989) 197.
4 P. Waszeciak and H. G. Nadeau, *Anal. Chem.*, 36 (1964) 1454.
5 J. Szymanowski, H. Szewczyk and J. Hepter, *Tenside Detergents*, 18 (1981) 333.
6 J. Szymanowski, A. Voelkel and H. Szewczyk, *J. Chromatogr.*, 360 (1986) 43.

Journal of Chromatography, 502 (1990) 416–422
Elsevier Science Publishers B.V., Amsterdam — Printed in The Netherlands

CHROM. 22 102

Note

Reversed-phase high-performance liquid chromatography of proteins and peptides on a pellicular support based on hydrophilic resin

YOSHIO KATO*, SHIGERU NAKATANI, TAKASHI KITAMURA, YOSUKE YAMASAKI and TSUTOMU HASHIMOTO

Central Research Laboratory, Tosoh Corporation, Tonda, Shinnanyo, Yamaguchi 746 (Japan)

(First received June 13th, 1989; revised manuscript received September 8th, 1989)

Totally porous supports have commonly been employed in high-performance liquid chromatography (HPLC). On the other hand, pellicular supports, which were once explored in the early stages of HPLC but did not come into general use, have been attracting attention during the last few years particularly in the separation of biopolymers. Since Unger and co-workers[1–3] showed that pellicular supports of small particle diameter (1.5 μm) are very useful for rapid separations of proteins, various types of pellicular supports have been prepared and some of them have become commercially available. TSKgel Octadecyl-NPR is one such support for reversed-phase chromatography. It was prepared by chemically bonding octadecyl groups on the surface of non-porous spherical hydrophilic resin of diameter 2.5 μm and has become commercially available recently (Tosoh, Tokyo, Japan). We have evaluated it for the separation of proteins and peptides and the results are presented in this paper.

EXPERIMENTAL

Chromatographic measurements were performed at 25°C on a 35 mm × 4.6 mm I.D. stainless-steel column with a system consisting of a Model CCPM double plunger pump and a Model UV-8000 variable-wavelength UV detector (Tosoh). Proteins were usually separated with a 10-min linear gradient of acetonitrile from 15 to 80% in 0.05% trifluoroacetic acid (TFA) at a flow-rate of 1.5 ml/min and detected at 220 nm. Peptides were usually separated with a 10-min linear gradient of acetonitrile from 0 to 80% in 100 m*M* perchloric acid at a flow-rate of 1.5 ml/min and detected at 215 nm. Some separations, however, were performed under slightly different conditions. In the study of operational variables, the type and concentration of acid component, flow-rate and gradient of acetonitrile were varied over a wide range. (Acids were always added at the same concentrations to both initial and final eluents in our experiments. Therefore, the acid concentrations mentioned in this paper are those in mixtures of water and acetonitrile.)

All proteins were purchased from Sigma (St. Louis, MO, U.S.A.): bovine serum

0021-9673/90/$03.50

albumin, cytochrome C, α-lactoalbumin, lysozyme, myoglobin, ovalbumin, ribonuclease, transferrin and trypsin, product numbers A-0281, C-2506, L-5385, L-6876, M-0630, A-5378, R-5125, T-2252 and T-8642, respectively. Insulin was also obtained from Sigma (product number I-5500). All other peptides were purchased from the Peptide Institute (Osaka, Japan).

RESULTS AND DISCUSSION

Fig. 1 shows the separation of a protein mixture. As exemplified here, proteins were separated rapidly, in 5–6 min, with high resolution. The same protein mixture was also separated on a totally porous support, TSKgel Phenyl-5PW RP[4], and the result was compared with that in Fig. 1. Octadecyl-NPR provided a higher resolution in a much shorter time (*ca.* 20%) than the totally porous support. The peak of ovalbumin in Fig. 1 is broader than the peaks of other proteins and some shoulders are observed. Similar patterns were observed for ovalbumin even under different conditions (see Fig. 4). Although the reason for this is not clear, one possibility is that some components existed in the ovalbumin sample that were partially separated. If this is so, it is also an indication of very high resolution in the separation of proteins on Octadecyl-NPR because such a partial separation of ovalbumin components by reversed-phase chromatography has not been reported previously.

Fig. 2 shows the separation of a peptide mixture. It was also possible to separate peptides, except small ones, in about 5 min with high resolution. However, small peptides with molecular weights below *ca.* 1000 were eluted as slightly broad peaks, probably because the support of Octadecyl-NPR is resin-based and has very small pores, although it is stated to be non-porous. If small molecules enter such very small pores, the diffusion rate there should be slow, which results in broad peaks. Such broad peaks have also been observed in the separation of other types of small molecules such as nucleotides on non-porous resin-based supports[5].

The recovery from the Octadecyl-NPR column was examined for some proteins and peptides. The recovery was estimated from the areas of the eluted peaks. As controls, we used peak areas observed when the column was replaced with an empty

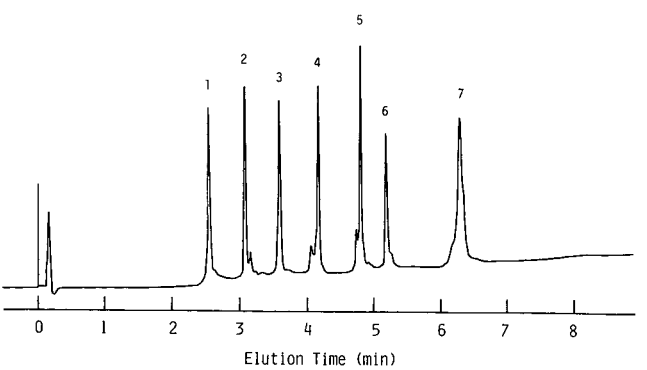

Fig. 1. Separation of a protein mixture on TSKgel Octadecyl-NPR. A mixture of (1) ribonuclease, (2) insulin, (3) cytochrome C, (4) lysozyme, (5) α-lactoalbumin, (6) myoglobin and (7) ovalbumin was separated with a 10-min linear gradient of acetonitrile from 15 to 80% in 0.05% TFA at a flow-rate of 1.5 ml/min.

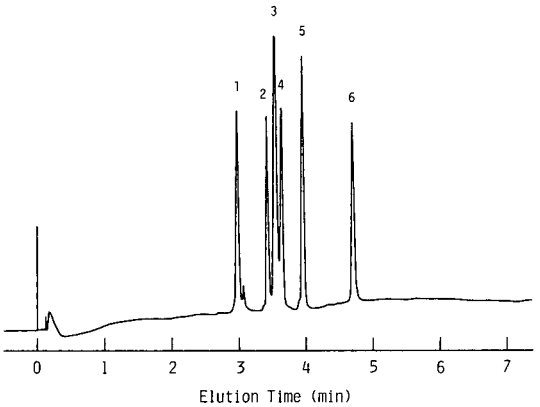

Fig. 2. Separation of a peptide mixture on TSKgel Octadecyl-NPR. A mixture of (1) α-endorphin, (2) bombesin, (3) γ-endorphin, (4) angiotensin, (5) somatostatin and (6) calcitonin was separated with a 10-min linear gradient of acetonitrile from 0 to 80% in 0.2% TFA at a flow-rate of 1.5 ml/min.

1 mm I.D. stainless-steel tube of 1 ml total inner volume. The results obtained with sample injections of 0.5 μg are summarized in Table I. Most proteins and peptides were recovered almost quantitatively. A recovery of more than 85% was achieved even with sample injections of 50 ng, as shown in Table II. The recovery of myoglobin and somatostatin was investigated with sample injections of 12.5–400 ng. Both were recovered quantitatively even with the smallest sample injection (12.5 ng). In addition, the peak volumes were usually very small (50–100 μl) in the separations on Octadecyl-NPR, as can be seen from Figs. 1 and 2. Accordingly, Octadecyl-NPR should be useful for the separation of small amounts of proteins and peptides. Such high recoveries are considered to be due to the small surface area of the support of Octadecyl-NPR. This is one of the advantages of pellicular supports.

TABLE I

RECOVERY OF PROTEINS AND PEPTIDES FROM TSKgel Octadecyl-NPR WITH A SAMPLE INJECTION OF 0.5 μg

Proteins were separated with an 8-min linear gradient of acetonitrile from 20 to 80% in 0.05% TFA at a flow-rate of 1.5 ml/min. Peptides were separated with a 10-min linear gradient of acetonitrile from 0 to 80% in 100 m*M* perchloric acid at a flow-rate of 1.5 ml/min.

Protein	*Recovery (%)*	*Peptide*	*Recovery (%)*
Cytochrome C	95	Leu-enkephalin	99
Ribonuclease	94	Oxytocin	92
Lysozyme	104	Bradykinin	89
Myoglobin	97	Angiotensin I	103
Ovalbumin	74	Bombesin	95
Bovine serum albumin	96	Somatostatin	103
Transferrin	101	γ-Endorphin	102
		Glucagon	98
		Insulin	102

TABLE II

RECOVERY OF PROTEINS AND PEPTIDES FROM TSKgel Octadecyl-NPR WITH A SAMPLE INJECTION OF 50 ng

Proteins were separated with a 10-min linear gradient of acetonitrile from 15 to 80% in 5 m*M* perchloric acid at a flow-rate of 1.5 ml/min. Peptides were separated under the conditions in Table I.

Protein	*Recovery (%)*	*Peptide*	*Recovery (%)*
Cytochrome C	96	Leu-enkephalin	94
Ribonuclease	92	Oxytocin	88
Lysozyme	94	Angiotensin I	90
Ovalbumin	89	γ-Endorphin	85
Bovine serum albumin	104		

Ovalbumin is a typical sample whose recovery is low in reversed-phase chromatography, and it was recovered in a slightly low yield (74%) also on Octadecyl-NPR, as shown in Table I. However, the recovery of ovalbumin depended considerably on the elution conditions and it was possible to attain a higher recovery by manipulating the elution conditions. For example, the recovery of ovalbumin increased on decreasing the concentration of the acid component in the eluent, by using phosphoric acid in place of TFA or by employing a steeper gradient of acetonitrile.

The loading capacity was evaluated by separating some pure and crude samples with various sample loads. The peak width remained constant at sample loads up to 0.5–1 μg and then increased with further increase in sample load in the separation of pure samples. Consequently, the maximum sample load resulting in the highest resolution is only 0.5–1 μg for pure samples. On the other hand, the maximum sample load for crude samples was higher. Such samples could be applied in amounts up to tens of micrograms with little decrease in resolution. These maximum sample loads are significantly lower (*ca.* 1–5%), than those on totally porous supports. This is the greatest disadvantage of pellicular supports. Accordingly, Octadecyl-NPR does not seem suitable for large-scale separations.

Octadecyl-NPR is chemically stable and hence it can be operated over a wide pH range. This is advantageous because separations of proteins and peptides are sometimes improved by changing the eluent pH, owing to the different selectivities at different pH. Fig. 3 shows separations of peptides at acidic, neutral and alkaline pH. The best separation was achieved at akaline pH for this sample, although alkaline pH is not always optimum. All five components were separated at pH 9.3, whereas angiotesin III, angiotensin II and α-endorphin were eluted together at pH 1.0 and γ-endorphin and angiotensin I were not separated well at pH 7.0.

The effects of the type and concentration of the acid component of eluent, flow-rate and gradient of organic solvent (acetonitrile) were studied.

Proteins were separated at various concentrations of TFA, perchloric acid or phosphoric acid. The peaks of the proteins became broader as the acid concentration decreased in the ranges below 0.02% (TFA), 2 m*M* (perchloric acid) or 50 m*M* (phosphoric acid). In addition, lysozyme was eluted as two peaks at such low acid concentrations. In contrast, the recovery of ovalbumin decreased greatly as the acid

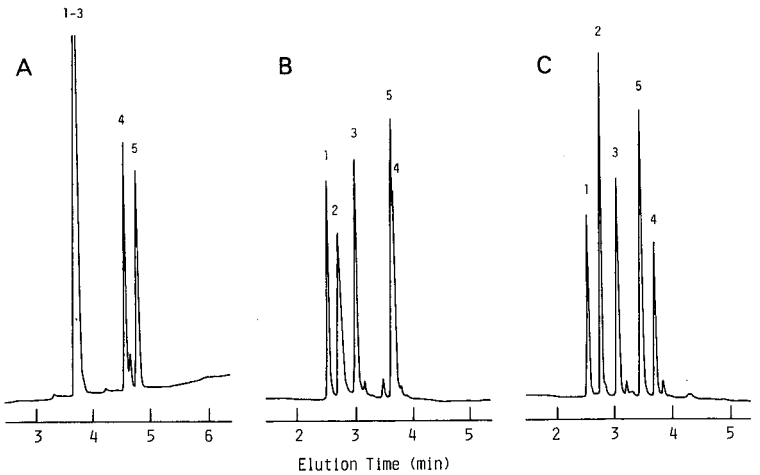

Fig. 3. Separation of a peptide mixture on TSKgel Octadecyl-NPR at acidic, neutral and alkaline pH. A mixture of (1) angiotensin II, (2) angiotensin III, (3) α-endorphin, (4) γ-endorphin and (5) angiotensin I was separated with 10-min linear gradient of acetonitrile from 0 to 60% in (A) 100 m*M* perchloric acid of pH 1.0, (B) sodium phosphate of pH 7.0 and (C) sodium phosphate of pH 9.3 at a flow-rate of 1.5 ml/min. In B and C, the initial eluent was 10 m*M* sodium phosphate and the final eluent was 0.5 m*M* sodium phosphate–acetonitrile (40:60).

concentration increased in the ranges above 0.1% (TFA), 10 m*M* (perchloric acid) or 300 m*M* (phosphoric acid). Therefore, concentrations of around 0.05%, 5 m*M* and 100–200 m*M* seem to be the best compromise for TFA, perchloric acid and phosphoric acid, respectively, in the separation of proteins. However, when some proteins are recovered in low yield, lower concentrations of acids may be better in order to obtain higher recoveries.

TFA provided the narrowest peaks for proteins among the three types of acids at their optimum concentrations, as exemplified in Fig. 4. In contrast, perchloric acid and phosphoric acid provided more stable baselines than TFA. Consequently, TFA is better than perchloric acid or phosphoric acid for achieving high resolution, whereas perchloric acid or phosphoric acid is better than TFA when a high sensitivity of detection is required in the separation of small amounts of proteins.

TFA, perchloric acid and heptafluorobutyric acid (HFBA) were explored for the separation of peptides. The peaks became broader and the resolution decreased as the acid concentration decreased in the ranges below 0.1% (TFA), 50 m*M* (perchloric acid) and 0.02% (HFBA) also in the separation of peptides, in particular for peptides that were eluted early. At higher acid concentrations, the peak widths and resolution were almost constant and the recovery was also unchanged. However, because there is no benefit in employing unnecessarily high acid concentrations, concentrations of *ca.* 0.2%, 100 m*M* and 0.05% seem to be the best choice for TFA, perchloric acid and HFBA, respectively, in the separation of peptides.

The peak widths observed with the three types of acids were very similar, but the selectivity differed to some extent with the three types of acids. Accordingly, the best acid to obtain the highest resolution varies depending on the sample to be separated.

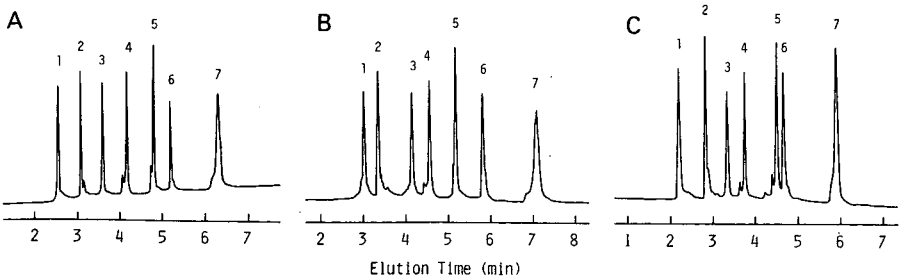

Fig. 4. Effect of type of acid component of the eluent on the separation of proteins on TSKgel Octadecyl-NPR. The same protein mixture as in Fig. 1 was separated with 10-min linear gradients of acetonitrile from 15 to 80% in (A) 0.05% TFA, (B) 5 m*M* perchloric acid and (C) 100 m*M* phosphoric acid at a flow-rate of 1.5 ml/min.

However, perchloric acid is better than TFA or HFBA for obtaining a stable baseline, just as in the separation of proteins.

The effect of flow-rate on resolution was similar in the separation of proteins and peptides with a constant gradient time. The resolution increased with increasing flow-rate up to 1.0–1.5 ml/min, then became almost constant at higher flow-rates. Although the separation time becomes slightly shorter as the flow-rate increases, the samples are more diluted and the pressure drop becomes higher almost proportionally with the increase in flow-rate. Accordingly, flow-rates of 1.0–1.5 ml/min seem to be a good compromise.

A similar tendency was also observed for the effect of the gradient of acetonitrile on resolution in the separation of proteins and peptides. A higher resolution was achieved with decreasing gradient of acetonitrile down to about 5%/min, whereas the resolution was almost constant at gradients shallower than about 5%/min. Because the shallower gradient results in a longer separation time and greater dilution of the sample, gradients of acetonitrile of *ca.* 5%/min seem to be a good compromise.

Fig. 5 shows an example of the application of reversed-phase chromatography

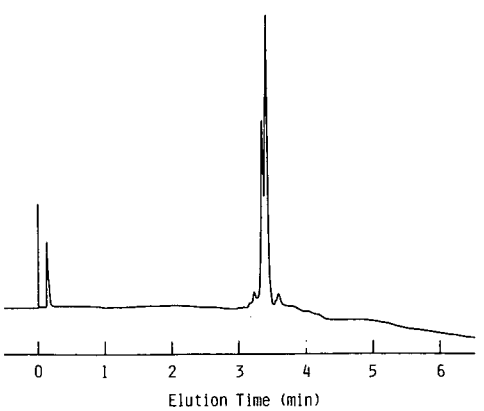

Fig. 5. Separation of trypsin (1 μg) on TSKgel Octadecyl-NPR with a 10-min linear gradient of acetonitrile from 25 to 80% in 0.05% TFA at a flow-rate of 1.5 ml/min.

on Octadecyl-NPR. A commercial sample of trypsin was separated. Two peaks appeared on the chromatogram and were collected and subjected to sodium dodecyl sulphate–polyacrylamide gel electrophoresis after reduction. Two bands were seen at positions corresponding to molecular weights of *ca.* 10 000 and 13 000 in the gel electrophoresis pattern of the first fraction, whereas a single band was seen at a position corresponding to a molecular weight of *ca.* 23 000 in the pattern of the second fraction. Accordingly, the two peaks are assumed to be α-trypsin (first peak) and β-trypsin (second peak). When this sample was separated on a totally porous support, only a single peak appeared on the chromatogram.

As demonstrated, proteins and peptides can be separated very rapidly with high resolution by reversed-phase chromatography on Octadecyl-NPR. The separation time is typically *ca.* 5 min. Consequently, Octadecyl-NPR should be very useful in particular for applications that require rapid separations such as clinical analysis and monitoring of purification or reaction (such as tryptic digest) processes. It is also useful for general analyses of proteins and peptides such as laboratory purity tests. However, the loading capacity of Octadecyl-NPR is fairly low because its surface area is small. Therefore, it does not seem suitable for large-scale separations. In contrast, proteins and peptides are recovered in high yield even with sample injections of very small amounts (low- and sub-microgram levels) owing to the small surface area. Accordingly, Octadecyl-NPR is also useful for micropreparative separations of proteins and peptides. Some pellicular supports for the reversed-phase chromatography of proteins and peptides have been reported during the last few years[2,6–11]. However, they were all laboratory-made and were not commercially available. In contrast, Octadecyl-NPR is commercially available and therefore there is no difficulty in its practical application.

REFERENCES

1 B. Anspach, K. K. Unger, H. Giesche and M. T. W. Hearn, *4th International Symposium on HPLC of Proteins, Peptides and Polynucleotides*, Baltimore, December 1984, paper 103.
2 K. K. Unger, G. Jilge, J. N. Kinkel and M. T. W. Hearn, *J. Chromatogr.*, 359 (1986) 61.
3 K. K. Unger, G. Jilge, R. Janzen, H. Giesche and J. N. Kinkel, *Chromatographia*, 22 (1986) 379.
4 Y. Kato, T. Kitamura and T. Hashimoto, *J. Chromatogr.*, 333 (1985) 93.
5 Y. Kato, T. Kitamura, A. Mitsui, Y. Yamasaki, T. Hashimoto, T. Murotsu, S. Fukushige and K. Matsubara, *J. Chromatogr.*, 447 (1988) 212.
6 G. Jilge, R. Janzen, H. Giesche, K. K. Unger, J. N. Kinkel and M. T. W. Hearn, *J. Chromatogr.*, 397 (1987) 71.
7 R. Janzen, K. K. Unger, H. Giesche, J. N. Kinkel and M. T. W. Hearn, *J. Chromatogr.*, 397 (1987) 81.
8 K. Kalghatgi and Cs. Horváth, *J. Chromatogr.*, 398 (1987) 335.
9 L. F. Colwell and R. A. Hartwick. *J. Liq. Chromatogr.*, 10 (1987) 2721.
10 K. Kalghatgi and Cs. Horváth, *J. Chromatogr.*, 443 (1988) 343.
11 Y.-F. Maa and Cs. Horváth, *J. Chromatogr.*, 445 (1988) 71.

Journal of Chromatography, 502 (1990) 423–430
Elsevier Science Publishers B.V., Amsterdam — Printed in The Netherlands

CHROM. 22 098

Note

Improved automated precolumn derivatization reaction of fatty acids with bromomethylmethoxycoumarin as label

J. H. WOLF and J. KORF*
Department of Biological Psychiatry, University of Groningen, Oostersingel 59, 9713 EZ Groningen (The Netherlands)
(Received August 2nd, 1989)

Derivatization and automation in high-performance liquid chromatographic (HPLC) analysis is very profitable for biomedical and clinical purposes, because of the gain in sensitivity and selectivity of the derivatization combined with a higher sample throughput. The most often used automated precolumn derivatization procedure is the analysis of amino acids and biogenic amines with *o*-phthalaldehyde[1]. The automation of this procedure is relatively simple as the agents and reagents are predominantly water soluble and the reaction kinetics are fast at room temperature.

Difficulties encountered by the automation of precolumn derivatization procedures in HPLC may include the use of elevated temperatures, the addition of two reagents at different time intervals, the addition of solid compounds, solvent extraction and the use of organic solvents as reaction media, which may result in peak distortion after direct injection in reversed-phase (RP)-HPLC[2].

In the HPLC of acidic compounds, bromomethylmethoxycoumarin (BrMMC) and its analogues have been extensively used as labels for derivatization[3–22]. Recently, we published a general method for the automated precolumn derivatization of fatty acids in serum and rat brain homogenates[23] for labels with a bromomethyl group, including BrMMC. In the manual procedure the label in coupled to the acid in an aprotic medium such as acetone or acetonitrile and this coupling is catalysed by the addition of solid potassium carbonate at 60°C. For the automation the following modifications were explored (see also ref. 23): lowering of the reaction temperature, replacement of the solid potassium carbonate and injection of a pure organic solvent. A satisfactory procedure was achieved by using a suspension of potassium carbonate in a solution of a crown ether and relatively high reagent concentrations. Peak distortion was reduced with a minimum decrease in peak height by using acetonitrile as solvent and acetonitrile–water mixtures as the mobile phase.

In our previous study the emphasis was more on the principle of the automation and solutions found for the indicated problems. The equipment used there had some drawbacks such as high blanks and clotting of the tubing by the suspension. With the use of a newer type of autosampler, the technical problems were solved. With the current modifications a very versatile system is obtained. Another disadvantage of our previous procedure was the formation of double peaks for every fatty acid.

0021-9673/90/$03.50

Investigations were made on the origin of this double labelling. In this paper we present an improved automated derivatization procedure for acidic compounds with BrMMC as label. The system can be used for a greater variety of reactions. As an example of the current procedure in biomedical research, we report the determination of fatty acids derived from small samples of rat blood taken during a stress procedure. The usefulness of this improved method has also been shown in drug studies[24,25].

EXPERIMENTAL

Reagents and chemicals

Analytical-reagent grade solvents were obtained from either Merck (Darmstadt, F.R.G.) or Baker (Deventer, The Netherlands) and were used without further purification except that methanol and acetonitrile were distilled. 4-Bromomethyl-7-methoxycoumarin, potassium carbonate (anhydrous) and 18-crown-6 were purchased from Aldrich (Beerse, Belgium) and the fatty acids from Sigma (St. Louis, MO, U.S.A.). 4-Bromomethyl-7-methoxycoumarin was dissolved in acetonitrile to give a working solution of 1 mg/ml. The suspension was prepared as follows: to 5 ml of a 20 m*M* solution of 18-crown-6 in acetonitrile were added 100 mg of potassium carbonte and 50 μl of water. After sonification for 30 min, the mixture was diluted with 5 ml of acetonitrile; the supernatant was separated from the solid potassium carbonate on the bottom of the vial.

Autosampler

The PROMIS autosampler (Spark, Emmen, The Netherlands) is equipped with a digital dispenser system, a miniaturized "finger pump". A coaxial pair of needles is inserted into the sample vial. Nitrogen pressure applied through the outer needle ensures that no air or vapour bubbles are formed during sample withdrawal. In our setup we used a commercially available two-way dispenser system, one line for the sample–suspension mixture and the other for the BrMMC solution. The coaxial needle is extended to approximately 1 mm above the hole in the side-port injection needle so that the needle is sufficiently under the liquid surface to ensure thorough mixing of the sample–suspension solvent.

HPLC equipment

Two Kratos SF400 pumps and a Kratos SF450 gradient mixer were used for solvent delivery. The samples were detected by a Kratos SF980 fluorescence detector equipped with a 5-μl cell, using an excitation wavelength of 325 nm and a cut-off filter of 398 nm. Data were collected with either a Kipp & Zonen (Delft, The Netherlands) BD8 recorder or an LDC CI-10 (Interscience, Breda, The Netherlands) integrator. The labelled fatty acids were separated on a Chrompack (Middelburg, The Netherlands) Chromspher C_{18} column (200 × 3 mm I.D.). The sample loop had a volume of 20 μl. All the chromatographic studies were performed at ambient temperature. A gradient of acetonitrile–water (80:20, v/v) to acetonitrile–methanol (50:50, v/v) in 45 min was used. Phosphoric acid was added to a final concentration of 25 m*M*. Elution was performed at 0.5 ml/min.

Blood samples

To 20 μl of rat blood 1 ml of acetonitrile containing margaric acid as internal standard was added. The precipitated protein was centrifuged. The supernatant is mixed 1:1 with the suspension in the vial of the autosampler.

RESULT AND DISCUSSION

Automation

In the published procedure[23], the reagents were delivered through a peristaltic pump, a standard option of the Spark SPH 125 PCD autosampler. The suspension is first mixed with the sample and subsequently with the BrMMC solution. Although all the analytical requirements were fulfilled, the system has some technical drawbacks. The choice of the tubing for the peristaltic pump is important. Acidic components from the plasticizers of the tubing can easily result in high blanks, whereas other tubing material slowly dissolves in the organic solvents. Clotting of the tubing by the suspension sometimes occurs.

In view of these problems, experiments were carried out with the newer PROMIS type of autosampler. This autosampler makes use of a dispenser to deliver the sample from the sample vial to the injection loop. Fig. 1 shows the original design (left) and the modified set-up used in this study (right). A double channel dispenser is used for adding the reagent BrMMC to the contents of the sample vial. In the sample vial the acid to be derivatized is added to the suspension. The outer needle is extended under the liquid surface. During sample withdrawal nitrogen is led through the outer needle, which ensures continuous agitation of the suspension, providing thorough mixing of the suspension–sample with the label. The dispenser is accurate and allows 20–50 μl out of a sample volume of 80 μl to be injected. With this system we determined valproic acid in human serum, rat blood and rat brain homogenates[24,25].

Investigations of the nature of the double labelling

In the automated reaction of fatty acids with BrMMC and the suspension every fatty acid showed two peaks (Fig. 2). The double labelling may be used for positive identification of the acids. Occasionally, depending on the state of the separation column, myristic acid and palmitoleic acid are not separated, but their second peaks are always separated. Accordingly, we use the second peak for the calculations. The longer the chain length, the larger is the second peak compared with the first (Fig. 2). The concentration of BrMMC does not influence the ratio for each doublet, whereas an increase in fatty acid concentration results in a relative decrease in the formation of the second peak.

No reports of double labelling were found in the literature. Therefore, we investigated whether other published procedures result in double labelling. For this, myristic acid was reacted with BrMMC under various conditions. Using our suspension[23], a ratio for the first to the second peak of 3.32 was found, whereas the frequently used manual procedure of Lam and Grushka[26] gave a ratio of 3.48. When the first peaks were compared with the internal standard, ratios of 0.61 and 0.58 were found. In their procedure, Lam and Grushka used a slight molar excess of 10% of BrMMC over the fatty acid. In our system, a much higher concentration of BrMMC is used to perform the reaction at room temperature. To establish the influenc of the

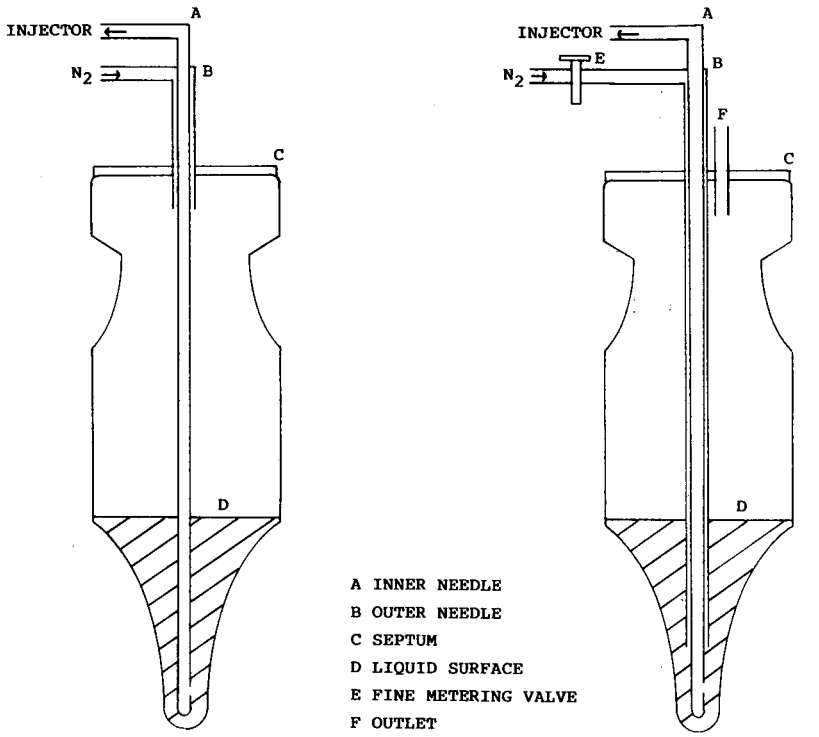

Fig. 1. (Left) the original and (right) the modified injection systems. Through the outer needle (B) nitrogen regulated with a fine metering valve (E) is led through the liquid. The extra outlet (F) prevents over-pressure.

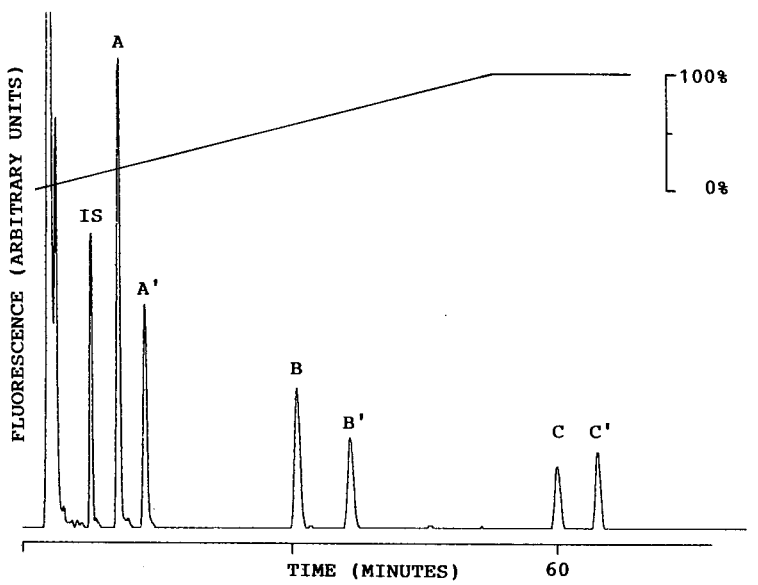

Fig. 2. Typical example of the double labelling found with BrMMC. Peaks: A = decanoic acid; B = myristic acid; C = stearic acid; IS = anthracene (internal standard). For separation conditions, see Experimental.

suspension with a high BrMMC concentration, solid potassium carbonate was used to replace the suspension. Now a ratio of 4.11 was found, so that these changes cannot explain the double labelling. Also, replacement of the suspension by tetraethylamine[13,18] gave similar results. The BrMMC concentration in the experiments was kept constant and a reaction temperature of 60°C and a reaction time of 30 min were used for the literature experiments. We conclude that the double labelling is not specific for our procedure.

In the automated procedure, the reaction mixture is injected directly onto the column, whereas in the non-automated procedure the reaction mixture is normally diluted with water to lower the solvent strengths to a composition compatible with the mobile phase. To establish whether direct injection is connected with the formation of the double labelling, the reaction mixture was diluted with water to the same composition as the mobile phase composition. Repetitive injection of this mixture for 24 h resulted in a slight decrease in the peak ratio within 3 h after the addition of the water. This reduction is due to a decrease in the second peak. The ratio of the first peak to internal standard was constant over a period of 24 h whereas the ratio of the second peak to internal standard decreased.

Three explanations can be given for the production of the double peaks: (a) impurity Y in the BrMMC reacts with fatty acid, FA, to form a product FA–Y; (b) FA–MMC, the methylmethoxy ester of a fatty acid, reacts with BrMMC via, for intance, an enol-keto tautomerization to form product FA–MMC–MMC or a structurally similar compound; (c) FA–MMC reacts under the influence of the base to give a product FA–X. By measuring the reaction constants, a discrimination between b on the one hand and a and c on the other can be made; reaction b is of second order whereas the other are of first order.

The kinetics of the derivatization reaction were investigated as a function of BrMMC concentration. The apparent rate of the reaction was evaluated by a simplex-optimized non-linear, least-squares curve fitting of first-order reaction kinetics to the time course data. The formation of the derivatives was first order with respect to BrMMC in both instances ([FA] = 3 pmol/μl; correlation coefficients >0.98).

As the rate of formation is first order with respect to BrMMC for both reactions, the second peak is not likely to be a degradative by-product of the primary reaction. Therefore, the second peak is produced in a competitive reaction with an impurity in the BrMMC. If the double labelling is caused by an impurity in the BrMMC, two explanations can be given for the relatively high signal of the second peak: the claim by the manufacturer that their chemicals are purer than 99% is not true, which is not very likely, or the relative fluorescenc efficiency for the second peak in much higher than that of the first. Because an increase in the ratio of the first to the second peak with a longer fatty acid chain is found, owing to an increase in the second peak, the relative molar fluorescence efficiency of the second peak is not dependent on the mobile phase composition as the BrMMC derivative is[17]. Recrystallization and column chromatography over silica reduced slightly the production of the second peak, but so far no cleaning procedure has given the desired results. Hopefully the structure of the impurity will be elucidated in the near future because it has a high potential as a fluorescence label for acidic ompounds. It possesses better fluorescence than BrMMC, and the relative molar fluorescence is not dependent on the mobile phase composition.

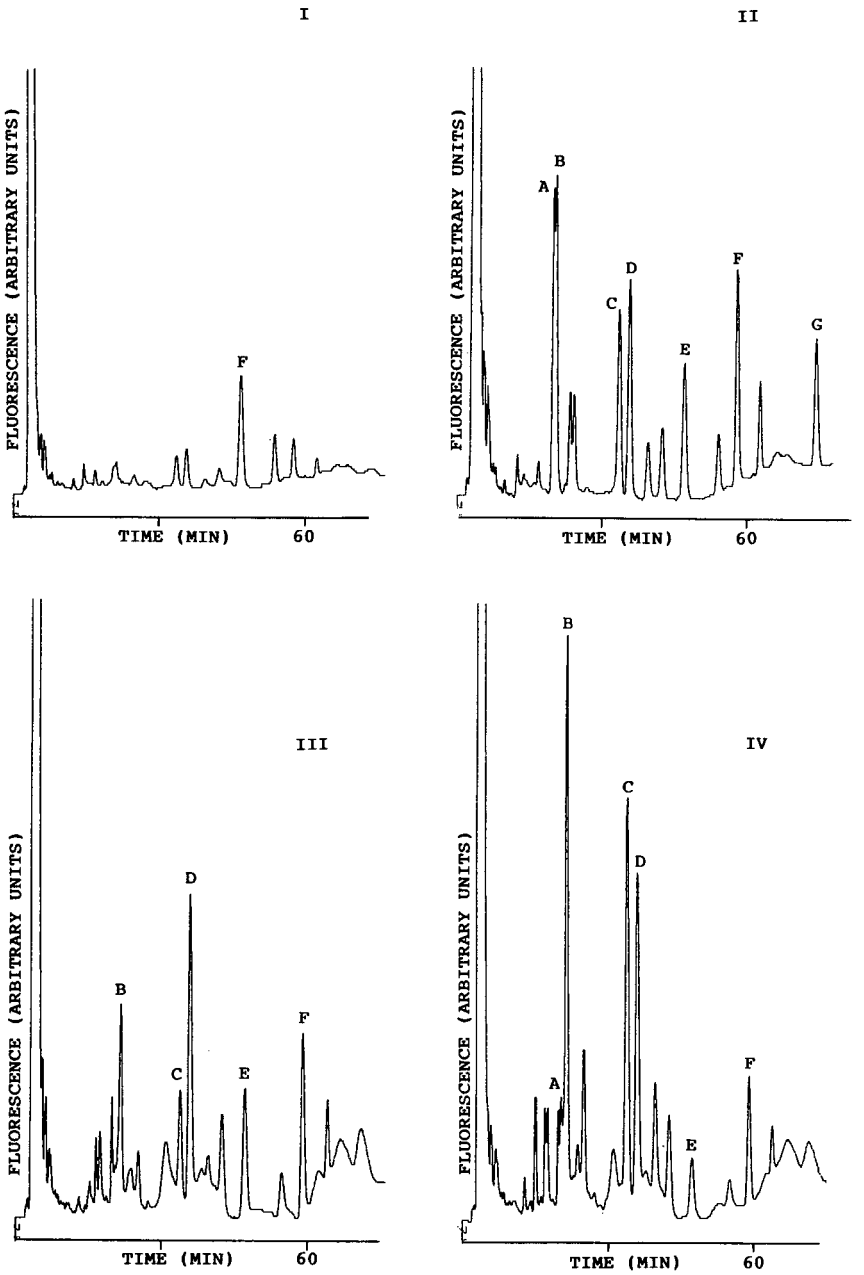

Fig. 3. Chromatograms of derivatized fatty acids taken from a rat during swimming and following rest. (I) Blank; (II) standards; (III) rat after 5 min of swimming; (IV) rat after 20 min of swimming and 10 min of rest. Peaks: A = palmitoleic acid; B = myristic acid; C = oleic acid; D = palmitic acid; E = margaric acid (internal standard); F = stearic acid; G = arachidonic acid. The differences in fatty acid composition and the pharmacological consequences will be discussed in detail elsewhere. The double labelling is not indicated here; for separation conditions, see Experimental.

Application

In Fig. 3 an example of the results of a study of the determination of fatty acids in rat blood in a stress model are shown. In this model rats were initially placed on a platform, which after about 30 min was slowly lowered into a water-bath about 3 m long: the water temperature was 33°C. After lowering of the platform, the rat was forced to swim to the other side of the bath against a water current. After the swim the rat could rest on another platform for 30 min, before being replaced in the home cage. This stress procedure was developed by Scheurink *et al.*[27]. At different time intervals 20 μl of blood were taken for the determination of, among others, fatty acids. The results of these analyses will be published in more detail elsewhere.

CONCLUSION

In bioanalysis, derivatization, either pre- or post-column, is often necessary to achieve better sensitivity; automation could enhance the reproducibility and sample throughput. In a previous paper a general principle for the automated analysis of fatty acids with bromomethylmethoxycoumarin as label was presented[23]. The problems faced are discussed there. In this paper, the optimization of that principle is discussed. By using the Spark PROMIS autosampler, a system could be constructed in which the sample and suspension are placed in the sample vial avoiding contact with tubing other than PTFE, while reducing blanks to a great extent. The application of the procedure has been illustrated by the analysis of rat blood during stress. Previously the usefulness of the automated precolumn derivatization technique for valproic acid has been shown[24].

ACKNOWLEDGEMENTS

This study was supported by the Netherlands Technology Foundation (STW). Spark Holland is thanked for providing the autosampler, Mrs. Veenma-van der Duin for technical assistance and Dr. W. Kuhr for calculations of the reaction kinetics.

REFERENCES

1 N. D. Danielson, M. A. Targove and B. E. Miller, *J. Chromatogr. Sci.*, 26 (1988) 362.
2 N. E. Hoffman, S.-L. Pan and A. M. Rustum, *J. Chromatogr.*, 465 (1989) 189.
3 W. Dünges, *Anal. Chem.*, 49 (1977) 442.
4 W. Voelter, R. Huber and K. Zech, *J. Chromatogr.*, 17 (1981) 491.
5 K. Hayashi, J. Kawase, K. Yoshimura, K. Ara and K. Tsuji, *Anal. Biochem.*, 136 (1984) 314.
6 W. Dünges and N. Seiler, *J. Chromatogr.*, 145 (1978) 483.
7 W. Dünges, *Chromatographia*, 9 (1976) 624.
8 S. G. Zelenski and J. W. Huber, *Chromatographia*, 11 (1978) 645.
9 H. Tsuchiya, T. Hayashi, H. Naruse and N. Takagi, *J. Chromatogr.*, 234 (1982) 121.
10 E. Grushka, S. Lam and J. Chassin, *Anal. Chem.*, 50 (1978) 1398.
11 K.-E. Karlsson, D. Wiesler, M. Alasandro and M. Novotny, *Anal. Chem.*, 229 (1985) 229.
12 W. Dünges, A. Meyer, K.-E. Müller, M. Müller, R. Pietschmann, C. Plachetta, R. Sehr and H. Tuss, *Fresenius Z. Anal. Chem.*, 288 (1977) 361.
13 E. Bousquet, G. Romeo and L. I. Giannola, *J. Chromatogr.*, 344 (1985) 325.
14 C. Hamada, M. Iwasaki, N. Kuroda and Y. Ohkura, *J. Chromatogr.*, 341 (1985) 426.
15 M. Yamaguchi, S. Hara, R. Matsunaga, M. Nakamura and Y. Ohkura, *J. Chromatogr.*, 346 (1985) 227.
16 M. Yamaguchi, R. Matsunaga, S. Hara, M. Nakamura and Y. Ohkura, *J. Chromatogr.*, 375 (1986) 27.

17 J. B. F. Lloyd, *J. Chromatogr.*, 178 (1979) 249.
18 W. Elbert, S. Breitenbach, A. Neftel and J. Hahn, *J. Chromatogr.*, 328 (1985) 111.
19 R. Farionotti, Ph. Siard, J. Bourson, S. Kirkiacharian, B. Valeur and G. Mahuzier, *J. Chromatogr.*, 269 (1983) 81.
20 C. Gonnet, M. Marichy and N. Philippe, *Analysis*, 7 (1979) 370.
21 M. Yamaguchi, R. Matsunaga, K. Fukunda and M. Nakamura, *J. Chromatogr.*, 414 (1987) 275.
22 R. A. Kelly. D. S. O'Hara and V. Kelley, *J. Chromatogr.*, 416 (1987) 247.
23 J. H. Wolf and J. Korf, *J. Chromatogr.*, 436 (1988) 437.
24 J. H. Wolf, L. Veenma-van der Duin and J. Korf, *J. Chromatogr.*, 487 (1989) 496.
25 J. H. Wolf and J. Korf, *J. Pharm. Pharmacol.*, in press.
26 S. Lam and E. Grushka, *J. Chromatogr.*, 158 (1978) 207.
27 A. Scheurink, A. B. Steffens, G. H. Dreteler, L. Benthem and R. Bruntink, *Am. J. Physiol.*, 256 (1989) R169.

Journal of Chromatography, 502 (1990) 431–436
Elsevier Science Publishers B.V., Amsterdam — Printed in The Netherlands

CHROM. 22 148

Note

Rapid extraction and high speed liquid chromatography of *Nicotiana tabacum* leaf pigments

DAVID A. DANEHOWER* and WILLIAM T. KELLEY[a]
Department of Crop Science, North Carolina State University, Box 7620, Raleigh, NC 27695-7620 (U.S.A.)
(First received July 25th, 1989; revised manuscript received November 14th, 1989)

The analysis of plant pigments using column liquid chromatography lies at the foundation of the chromatographic sciences. Since the classic work of Tswett[1,2], the separation and analysis of chlorophylls, carotenoids, xanthophylls and related pigments have undergone considerable refinement. Today, numerous methods exist for the analysis of plant pigments[3–8]. Prime criteria for modern methods of plant pigment analysis are that they be rapid, avoid degradation of the pigments, and be amenable to automation. This paper reports a method which we have found to meet these criteria for the isolation and rapid analysis of pigments from leaf tissues.

The isolation of pigments from plant tissues usually involves maceration of the tissue followed by repeated extractions with organic solvents such as acetone, methanol, ethanol, dimethyl sulfoxide or aqueous solutions of these solvents. More recently, N,N-dimethylformamide has been applied to the extraction of plant leaf materials without the need for maceration of the tissues[3,9–11]. This technique presents obvious advantages when it is necessary to extract large numbers of samples. Of equal significance, Bergweiler and Lutz[3] have observed that pigments extracted and stored in this solvent remain stable for extended periods.

Following extraction, the other critical step in the determination of plant pigment samples is that of quantitative analysis. A number of recent papers have reported methods for quantitative chromatographic analysis of plant pigments (for a review see Schwartz and von Elbe[12]). Typically, these methods require an analysis time of approximately 30 min or more, including the time required for re-equilibration of the initial mobile phase. The advent of 'high speed' liquid chromatographic techniques[13] has led to considerable savings in time and solvent consumption in analyses of a wide range of materials. We report here the application of this approach to the analysis of *Nicotiana tabacum* green leaf pigments.

[a] Present address: Department of Plant and Soil Science, University of Tennessee, Box 1071, Knoxville, TN 37901-1071, U.S.A.

0021-9673/90/$03.50

EXPERIMENTAL

General

Samples were kept on ice and exposed to a minimum of light and oxygen (air) during field sampling, transport, and storage prior to and after extraction. Low actinic glass volumetric flasks were used as containers for the extracted pigments which were stored at −78°C under nitrogen until analysed.

All solvents used were high-performance liquid chromatography (HPLC) grade obtained from Fisher Scientific (Pittsburgh, PA, U.S.A.). Solvents, standard solutions, and samples for HPLC were filtered through 0.45-μm nylon 66 membrane filters prior to use. Authentic standards were obtained from the following sources: chlorophyll *a*, chlorophyll *b*, β-carotene —Sigma (St. Louis, MO, U.S.A.); xanthophyll and lutein —Atomergic (Farmington, NY, U.S.A.); β-apo-8′-carotenal —Fluka (Ronkonkoma, NY, U.S.A.).

Pigment extraction and storage

Twenty disks (1.7 cm diameter) were removed from leaves of tobacco at a point approximately two-thirds of the way from the base of the leaf and approximately half the distance from the midvein to the leaf margin. Disks were transferred immediately to plastic bags, sealed, and stored on dry ice in a darkened container for transport to the laboratory.

At the laboratory, ten frozen disks were taken from the total of twenty and placed in scintillation vials, 4.0 ml of N,N-dimethylformamide (DMF) [containing 0.1% (v/v) butylated hydroxytoluene (BHT) as an antioxidant] were added, and a nitrogen atmosphere introduced. The vials were then capped, covered with aluminum foil, and placed on a reciprocating shaker operated at 120 cycles per min. The samples were extracted for 24 h at the end of which time the pigment extracts were pipetted into 10.00-ml low-actinic glass volumetric flasks. The volumetric flasks were then stored at −78°C under nitrogen. An additional 4.0 ml of fresh DMF were added to the scintillation vials containing the samples, the vials were recapped under nitrogen and extracted as before for a second 24-h period. The second solvent extract was transferred to the corresponding 10.00-ml volumetric flask and the vial was then rinsed with a small (approximately 1 ml) amount of fresh solvent. A 1.00-ml volume of an internal standard solution of β-apo-8′-carotenal (containing 0.1%, v/v, of BHT) was added to each volumetric and the volume was then adjusted to 10.0 ml with DMF as needed.

Samples were stored at −78°C under a nitrogen atmosphere and removed as needed for analysis by HPLC. During analysis, samples were maintained at 0°C in the dark by immersion in an ice bath equipped with an opaque cover.

The remaining ten leaf disks from each sample were transferred to a tared scintillation vial and weighed in order to obtain fresh weight of leaf tissue per sample. The vials and disks were then lyophilized, reweighed in order to determine dry weights of the leaf tissue samples, and discarded.

HPLC analysis

Pigment analyses were carried out on a Perkin-Elmer Series 4 liquid chromatograph equipped with an LC 85B variable-wavelength detector set at 440 nm. The

column was a Supelcosil C_{18}-DB (3.3 × 0.46 cm I.D.) high-speed analytical column (Supelco, Bellefonte, PA, U.S.A.) containing 3-μm particles. The sample was applied to the column using a Rheodyne 7125 injector equipped with a 50-μl sample loop. Flow-rate was 2.0 ml/min. The mobile phase consisted of a 4-min linear gradient from 70% aqueous methanol (solvent A) to a 40:60 mixture of solvent A and ethyl acetate (solvent B) followed by a 4-min isocratic elution at the final solvent composition. The solvent program was returned to initial conditions over 2 min and re-equilibrated for 4 min prior to injection of the next sample.

Chromatographic resolution of complex samples was improved by dilution of the DMF-sample aliquot 1:1 with HPLC-grade water. Such measures were, however, typically not needed for the majority of samples analysed.

Date analysis was carried out using an IBM System 9000 computer running the CAP 2.0 version of the chromatographic data analysis software. An internal standard method was used throughout the experiment with β-apo-8′-carotenal as internal standard. Standards were prepared and calibration curves were determined routinely for the following components: chlorophyll *a*, chlorophyll *b*, β-carotene, lutein, and β-apo-8′-carotenal.

RESULTS AND DISCUSSION

Leaf disk samples were removed from the leaf lamina of fully expanded tobacco leaves in such a way that the disks were representative of the whole leaf sample. Prior work in our laboratory and elsewhere has shown that a number of leaf constituents vary as a function of position within the leaf[14,15].

The solvent extraction procedure utilizing DMF proved to be an efficient and reproducible method for the extraction of pigments from large numbers of samples. Extraction of leaf disks was complete after 48 h in all cases (data not shown). The method employed allowed the efficient workup of fifty samples a day. Larger numbers of samples could readily be accommodated without excessive increases in time. Work in our laboratories with other plants (soybean, peanut and barley leaves) indicates that this extraction technique is applicable to these plant materials as well.

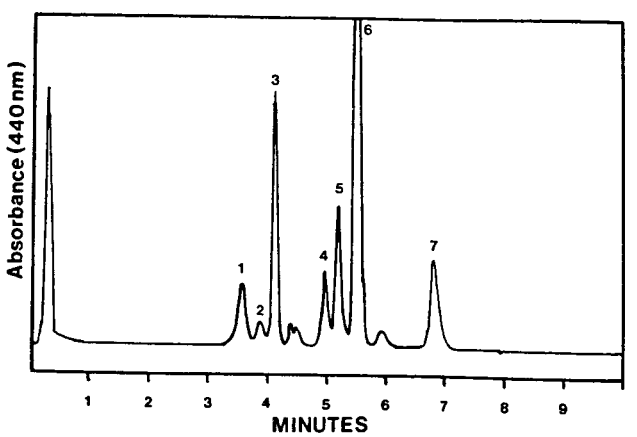

Fig. 1. A typical chromatogram of the analysis of *Nicotiana tabacum* green leaf pigments. For peak identification, see Table I.

TABLE I

IDENTIFICATION AND RELATIVE RETENTION TIMES OF *NICOTIANA TABACUM* LEAF PIGMENTS

Average of five determinations selected at random.

Peak No.	*Compound*	*Average retention time (min)*	*Relative retention time*
1	Neoxanthin	3.45 ± 0.03	0.72
2	Violoxanthin	3.83 ± 0.03	0.78
3	Lutein	4.09 ± 0.03	0.83
4	β-Apocarotenal[a]	4.94 ± 0.03	1.00
5	Chlorophyll *b*	5.15 ± 0.03	1.04
6	Chlorophyll *a*	5.44 ± 0.03	1.10
7	β-Carotene	6.80 ± 0.09	1.38

[a] Internal standard.

The use of sub-samples for fresh and dry weight determinations allows the expression of results to be made on either a leaf area, fresh weight or a dry weight basis. These determinations add to the overall time of analysis, but the actual time required is small and inclusion of these steps is required only if results are to be expressed on a weight basis. The use of leaf punches of known area eliminates the need to measure leaf area directly.

A typical chromatogram obtained in the course of these experiments is shown in Fig. 1. The time of analysis was 14 min from injection to injection. The use of a high-speed column proved to be of great value in improving the speed of the analysis. Prior attempts in our laboratory to optimize analysis time using normal analytical columns (*i.e.* 25 × 0.46 cm I.D. C_{18} columns) resulted in analysis times of approximately 25 min at best, with little increase in resolution. Thus, the use of the high-speed column allows roughly a two-fold increase in sample through-put with virtually no loss in efficiency and also results in savings in solvent and column costs.

Table I gives the identification and relative retention data for the peaks identified in Fig. 1. Identification was based on comparison with known standards, known

TABLE II

RELATIVE ERROR OF QUANTITATION OF *NICOTIANA TABACUM* LEAF PIGMENTS

Pigment	*Relative error (%) (n = 3)*				
	Mass of pigment injected (μg)				
	0.25	*0.50*	*1.25*	*2.50*	*25.0*
Lutein	2.3	1.7	0.4	0.4	0.3
β-Apocarotenal	5.3	0.9	0.6	0.3	0.7
Chlorophyll *a*	9.8	1.7	1.3	1.0	0.7
Chlorophyll *b*	1.2	1.9	0.9	0.6	0.2
β-Carotene	6.2	0.8	1.1	1.9	0.4

elution order from C_{18} columns, and spectral analysis of eluting peaks. Apocarotenal proved to be good choice for internal standard as it eluted in a time window which was devoid of other peaks. In addition, apocarotenal has not been reported to be a component of tobacco pigments.

Table II presents data on the reproducibility of the analytical method. These results indicate that the method yields quantitative results for most pigments analysed at most masses. Data were semi-quantitative for β-apo-8'-carotenal, chlorophyll *b*, and β-carotene at the lowest mass tested, 0.25 μg. This was well below the mass range normally encountered during our analyses.

CONCLUSION

The combination of the DMF-extraction technique and the high-speed HPLC method results in a system which is particularly amenable to the analysis of large numbers of samples. The use of DMF as an extracting solvent has proven to be a reliable and efficient means for the isolation of plant pigments. The stability of the DMF-pigment solution is particularly advantageous when samples cannot be immediately analysed. Samples in DMF stored for up to a week showed no sign of degradation, in agreement with the earlier report of Bergweiler and Lutz[3]. The addition of a small amount of antioxidant (0.1% BHT) to the extracting solvent and internal standard solutions may have enhanced this stability further. Storage of the solutions at -78°C under an inert atmosphere (nitrogen) also is advisable for maximal sample stability.

The high-speed HPLC method reported results in a least a two-fold improvement in time of analysis compared with existing pigment methods. The column in these experiments has been used for the analysis of over 300 samples with no significant loss of resolution.

In conclusion the overall method described here results in a significant savings in time and labor over existing techniques. The method should be of interest to researchers involved in repetitive analyses of large numbers of plant pigment samples. The savings derived from use of the less expensive high-speed liquid chromatography columns and the reduction in solvent consumption and resulting wastes are also positive considerations.

ACKNOWLEDGEMENTS

The authors would like to thank Mr. A. R. Butler for his able technical assistance. This work was, in part, supported by the North Carolina Tobacco Foundation to whom the authors are indebted.

Paper No. 12211 of the Journal Series of the North Carolina Agricultural Research Service, Raleigh, NC 27695-7643, U.S.A. The use of trade names in this publication does not imply endorsement by the North Carolina Agricultural Research Service of the products named, nor criticism of similar ones not mentioned.

REFERENCES

1 M. S. Tswett, *Ber. Dtsch Bot. Ges.*, 24 (1906) 316.
2 M. S. Tswett, *Ber. Dtsch Bot. Ges.*, 24 (1906) 384.

3 P. Bergweiler and C. Lutz, *Environ. Exp. Bot.*, 26 (1986) 207.
4 Y. Shioi, R. Fukae and T. Sasa, *Biochim. Biophys. Acta*, 722 (1983) 72.
5 K. Eskins, C. R. Scholfield and H. J. Dutton, *J. Chromatogr.*, 135 (1977) 217.
6 P. S. Stewart. P. A. Bailey and J. L. Beven, *J. Chromatogr.*, 282 (1983) 589.
7 S. Takagi, *Agric. Biol. Chem.*, 49 (1985) 211.
8 W. A. Court and J. G. Hendel, *Tob. Sci.*, 26 (1982) 103.
9 R. Moran and D. Porath, *Plant Physiol.*, 65 (1980) 478.
10 R. Moran, *Plant Physiol.*, 69 (1982) 1376-1381.
11 J. D. Hiscox and G. F. Israelstam, *Can. J. Bot.*, 57 (1979) 1332.
12 S. J. Schwartz and J. H. von Elbe, *J. Liq. Chromatogr.*, 5, (1982) Suppl. 1, 43.
13 J. L. DiCesare, M. W. Dong and L. S. Ettre, *Introduction to High Speed Liquid Chromatography*, Perkin-Elmer, Norwalk, CT, 1981, p. 106.
14 D. A. Danehower, *Tob. Sci.*, 31 (1987) 32.
15 R. W. Jenkins, H. J. Grubbs, R. H. Newman, R. T. Bass, J. S. Brenizer, D. C. Jones, T. G. Williamson, D. A. Danehower and R. C. Long. *J. Radioanal. Nucl. Chem.*, 113 (1987) 477.

Journal of Chromatography, 502 (1990) 437–442
Elsevier Science Publishers B.V., Amsterdam — Printed in The Netherlands

CHROM. 22 100

Note

Rapid identification and determination of herbicolin A and B by high-performance liquid chromatography

M. GREINER* and G. WINKELMANN

Institut für Biologie I, Mikrobiologie I, Universität Tübingen, Auf der Morgenstelle 1, D-7400 Tübingen (F.R.G.)

(First received July 18th, 1989; revised manuscript received September 26th, 1989)

Herbicolin A and B are antifungal antibiotics produced by a strain A 111 which was identified as *Erwinia herbicola* (Enterobacteriaceae)[1]. *Erwinia herbicola* is commonly found as a saprophyte on plants, in water and in soil. The structures of the antibiotics were determined as nonapeptides[2]. Herbicolin B is a lipodepsinonapeptide with the sequence DH–Abu–L–Thr–D–Thr–D–Leu–Gly–D–Gln–Gly–N–Me–L–aThr–L–Arg (DH-Abu = 2,3-dehydro-α-aminobutyric acid). The C-terminal Arg residue forms a lactone ring with the hydroxy group of L-Thr, while the N-terminus is acylated by an (*R*)-3-hydroxytetradecanoic acid residue. The main component, herbicolin A, differs from herbicolin B in having an additional D-glucose moiety linked as a 1-α-glycosidic bond to the 3-hydroxytetradecanoic acid residue. Thus herbicolin A constitutes a glycolipodepsinonapeptide antibiotic. Herbicolin A strongly inhibits yeasts, filamentous fungi[3] and sterol-requiring mycoplasmas[4,5], but not other bacteria[1].

For optimization of the fermentation of herbicolins, a high-performance liquid chromatographic (HPLC) method was developed which allows the concentration produced to be followed in a rapid and quantitative manner. Previous HPLC separations using LiChrosorb-NH_2 columns[2] were found to be inadequate for the present purpose and could be significantly improved using a C_8 column.

EXPERIMENTAL

Materials

Columns (125 × 4.6 mm I.D., metal) were obtained by Grom (Ammerbuch, F.R.G.) and octyl reversed-phase material (C_8 Nucleosil, 5 μm) was purchased from Macherey, Nagel & Co. (Düren, F.R.G.). All HPLC-grade organic solvents were purchased from Baker (Deventer, The Netherlands) and Merck (Darmstadt, F.R.G.). Sep-Pak C_{18} octadecyl cartridges for sample preparation were obtained from Waters Assoc. (Milford, MA, U.S.A.). Thin-layer chromatography (TLC) was performed in saturated glass chambers on precoated silica gel 60 (0.25 mm) F_{254}, 5 × 10 cm, purchased from Merck.

0021-9673/90/$03.50

Equipment

For all HPLC procedures the following apparatus were used: a Model 7125 valve for injection (Rheodyne, Cotati, CA, U.S.A.), a type 64 HPLC pump (Knauer, Bad Homburg, F.R.G.), a Model SP-2A UV detector (Shimadzu, Kyoto, Japan) and a Model CR-3A integrator (Shimadzu). Centrifugation was performed with a Minifuge GL centrifuge (Heraeus Christ, Osterode, F.R.G.).

Sample preparation

From the culture broth 10 ml were taken, the cells were removed by centrifugation for 15 min at 4000 *g* and 4–10 ml of the supernatant were passed through Sep-Pak cartridges. The Sep-Pak cartridges were conditioned by rinsing with 5 ml of methanol followed by 10 ml of water. After the supernatant had passed through, salts and hydrophilic components were removed with 10 ml of water. Elution was carried out with 2 ml of methanol. After appropriate dilution with methanol, this solution was used for HPLC.

HPLC procedure

The samples were injected onto the HPLC column, using a 20-μl sample loop. As the mobile phase for isocratic elution, was used acetonitrile–phosphoric acid (0.1%)–methanol (7:3:4, v/v/v) at a flow-rate of 1.5 ml/min. The herbicolins were detected by measuring the UV absorbance at 215 nm and 0.04 a.u.f.s. Integration of the peak area was performed with a CR-3A integrator.

Other chromatographic procedures

For TLC on precoated silica gel 60 F_{254} the solvent system was chloroform–methanol–water–acetic acid (65:25:4:3, v/v). The R_F values in this system are 0.12 for herbicolin A and 0.38 for herbicolin B. Other TLC systems are given in ref. 6. Herbicolins were detected using the tetramethyldiaminodiphenylmethane (TDM) method[7]. Spots of herbicolin A could also be detected with orcin reagent[8], owing the glucose moiety.

Enzymatic cleavage of herbicolin A

For enzymatic cleavage of the glucose residue of herbicolin A a solution of 0.5 mg/ml containing both herbicolin A and herbicolin B was used. Hydrolysis was performed in 0.1 *M* potassium phosphate buffer (pH 6.8) at room temperature. A 1-ml volume of buffered herbicolin solution was incubated for 1 h with 0.5 ml of buffer containing 6 units of α-glucosidase from yeast (Serva, Heidelberg, F.R.G.). The herbicolins were separated from the enzyme and desalted using the sample preparation procedure described above.

RESULTS

The chromatogram in Fig. 1 shows two main peaks designated 1 (herbicolin A) and 2 (herbicolin B) at 3.85 min, representing purified herbicolin A and B, separated by the method described under Experimental. Samples used for comparison purposes originated from an earlier batch, which represented a mixture of herbicolin A and B, purified according to the counter-current distribution method described previously[2].

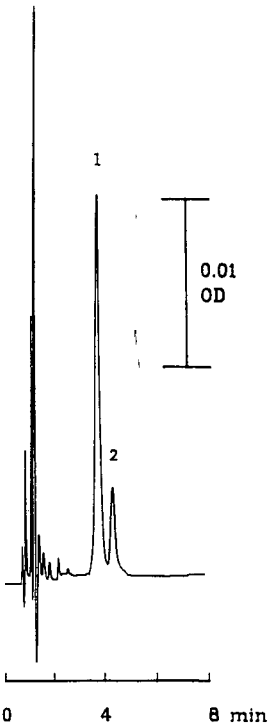

Fig. 1. High-performance liquid chromatogram of the purified forms of herbicolin A and B, detected at 215 nm using a C_8 reversed-phase column run with the isocratic solvent system acetonitrile–phosphoric acid (0.1%)–methanol (7:3:4, v/v/v). A 20-μl sample of concentration 10 μg/ml in methanol was injected. Peaks: 1 = herbicolin A; 2 = herbicolin B.

The ratio of herbicolin A to herbicolin B was approximately 4:1. This value varied depending on the fermentation conditions.

The proportions of herbicolin A and B could also be changed by using enzymatic splitting of the glucose residue of herbicolin A by commercial α-glucosidases (yeast). As shown in Fig. 2, the enzymatic treatment resulted in a reduction of the herbicolin A peak area whereas the herbicolin B peak area was increased. As herbicolin B has the same structure as the A form except for the 1-α linked glucose, splitting of this glucose should lead to herbicolin B. Further work is intended to optimize and analyse the enzymatic cleavage of the glucose moiety of herbicolin A.

In addition to identification with purified references (by HPLC and TLC), samples were scraped off from TLC and used as an additional proof that peak 1 corresponded to the glucose-containing herbicolin A whereas peak 2 corresponded to herbicolin B. Removal of the salts added to the enzyme assay was done using the Sep-Pak procedure described above. The main purpose of the present investigation, however, was to determine the content of herbicolin A in the fermentation broth. Fig. 3 shows a sample of culture broth measured according to the procedure described above. There are only a few other compounds remaining which do not interfere with quantification. Quantification was effected using pure herbicolin A as a reference.

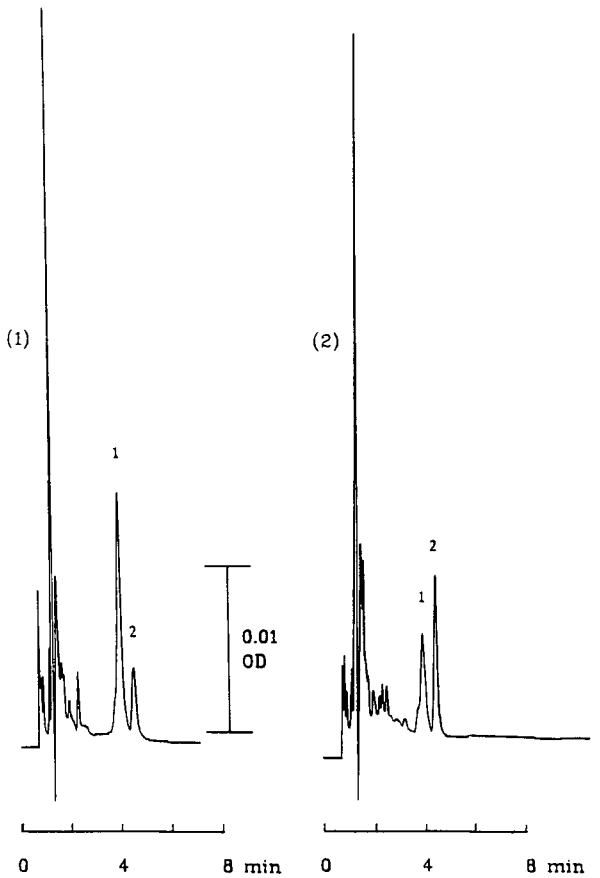

Fig. 2. HPLC of a sample of herbicolin A and B, (1) before and (2) after partial enzymatic hydrolysis of the glucose moiety from herbicolin A by α-glucosidase. Owing to the splitting off of the glucose residue from herbicolin A, the amount of herbicolin B is increased. Peaks: 1 = herbicolin A; 2 = herbicolin B.

Linearity was observed between 1 and 500 μg/ml with measurement of peak area. Fig. 4 shows the calibration graph obtained with herbicolin A, prepared as described previously[2]. The detection limit of herbicolin A was 0.1 μg/ml, at a signal-to-noise ratio of 3:1.

DISCUSSION

The HPLC method for the determination of herbicolin described here is a significant improvement over the TLC and other HPLC methods we have used previously in terms of sensitivity and time required. Attempts with C_{18} and C_4 columns were not as successful as with C_8 columns because of a higher retention time together with peak broadening or poorer resolution. Phosphoric acid (0.1%) and methanol were not suitable solvents to resolve all components. The described system of acetonitrile–phosphoric acid (0.1%)–methanol yielded the best separation properties.

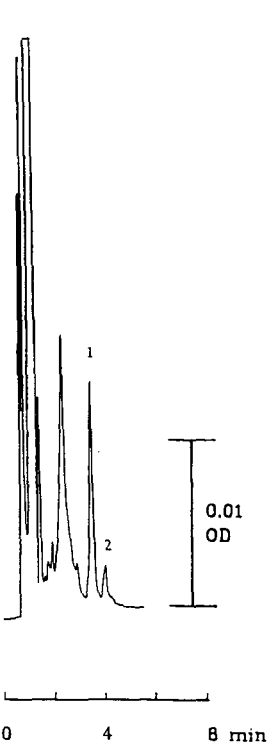

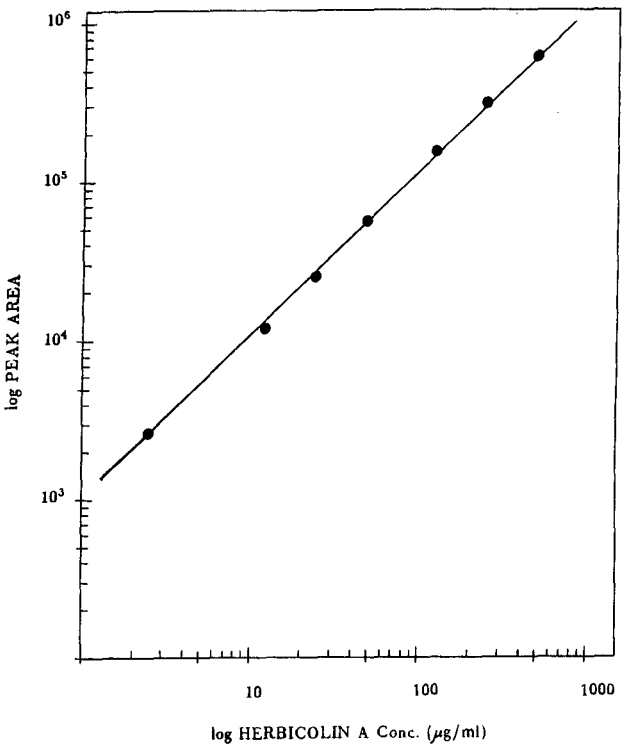

Fig. 3. HPLC of culture broth during the fermentation process after sample preparation with a Sep-Pak C_{18} cartridge. Detection at 215 nm; isocratic conditions as described. Peaks: 1 = herbicolin A; 2 = herbicolin B.

Fig. 4. Calibration graph for herbicolin A. Herbicolin A obtained from counter-current distribution according to ref. 2.

The isocratic system was found to be superior to the gradient system using phosphoric acid (0.1%)–methanol owing to easier handling, lower solvent consumption and shorter analysis time. Combined with sample preparation on Sep-Pak cartridges, the method is suitable for rapid control of fermentation and for monitoring the different fractions during the purification process.

Lipopeptides are widespread among microbial products. The diversity of molecular variations in bacterial surfactants has been described[9]. Most of these compounds, such as surfactin[10], bacillomycins[11], mycosubtilin[12], mycobacillin[13] and iturin A[14] possess antifungal activity. We have recently described the occurrence of long-chain iturin AL, which differs from iturin A by its predominant C_{16} β-amino acid[15]. Whereas the iturins have been shown to be separated by HPLC according to the chain length, the herbicolins represent compounds of constant chain length (C_{14}) but differ in the presence of a glucose residue. Hence the different polarities of the herbicolins allow their separation on reversed-phase materials. The biosynthetic origin of the herbicolins is still unresolved. They are obviously not secondary metabolic products of the stationary growth phase as is the case with peptide antibiotics of the bacillus group. As herbicolins are produced by strains of the non-spore-forming family

Enterobacteriaceae, a role in spore formation can be excluded. According to our observations, herbicolins are produced during the exponential growth phase, suggesting that herbicolins might be involved in membrane formation. The hydrophobic chain in the herbicolins represents β-hydroxymyristic acid, which is a common constituent of lipopolysaccharides of Enterobacteriaceae. Determination of herbicolins and its biosynthetic precursors by chromatographic analysis will possibly help in elucidating the biological role of herbicolins.

HPLC will be a very important tool for further investigation of lipopeptides and glycolipopeptides that are attaining not only scientific, but also therapeutic and biotechnological interest.

ACKNOWLEDGEMENT

This work was supported by a grant from Dechema (BMFT-Forschungsstipendium "Angewandte Biologie und Biotechnologie").

REFERENCES

1 G. Winkelmann, R. Lupp and G. Jung, *J. Antibiot.*, 33 (1980) 353.
2 M. Aydin, N. Lucht, W. A. König, R. Lupp, G. Jung and G. Winkelmann, *Justus Liebigs Ann. Chem.*, (1985) 2285.
3 G. Winkelmann and W. Adam, *Mycoses*, 23 (1980) 290.
4 E. A. Freundt and G. Winkelmann, *Antimicrob. Agents Chemother.*, 26 (1984) 112.
5 S. Birkelund-Anderson, E. A. Freundt and G. Christiansen, *Antimicrob. Agents Chemother.*, 29 (1986) 371.
6 R. Lupp, *Ph.D. Thesis*, Universität Tübingen, Tübingen, 1983.
7 E. von Arx, M. Faupel and M. Brugger, *J. Chromatogr.*, 120 (1976) 224.
8 J. Chrastil, *Anal. Chem.*, 47 (1975) 2293.
9 J. Vater, *Prog. Colloid Polym. Sci.*, 72 (1986) 12.
10 K. Arima, A. Kakinuma and G. Tamura, *Biochem. Biophys. Res. Commun.*, 31 (1968) 488.
11 F. Besson, F. Peypoux, G. Michel and L. Delcambe, *Eur. J. Biochem.*, 77 (1977) 61.
12 F. Peypoux, G. Michel and L. Delcambe, *Eur. J. Biochem.*, 63 (1976) 391.
13 S. Sengupta and S. K. Bose, *Biochim. Biophys. Acta*, 237 (1971) 120.
14 F. Peypoux, M. Guinand, G. Michel, L. Delcambe, B. C. Das and E. Lederer, *Biochemistry*, 17 (1978) 3992.
15 G. Winkelmann, H. Allgaier, R. Lupp and G. Jung, *J. Antibiot.*, 36 (1983) 1451.

Journal of Chromatography, 502 (1990) 443–446
Elsevier Science Publishers B.V., Amsterdam — Printed in The Netherlands

CHROM. 22 166

Note

High-performance liquid chromatographic determination of humic acid in sodium aluminate solution[a]

MICHAEL SUSIC*
Australian Institute of Marine Scienve, P.M.B. No. 3, Townsville M.C., Queensland 4810 (Australia)
and
LYNDON G. ARMSTRONG
Queensland Alumina Limited, Parson's Point, Gladstone, Queensland 4680 (Australia)
(First received January 27th, 1989; revised manuscript received November 21st, 1989)

Humic acid is derived from plant matter and is present in soils. Bauxites can contain up to 0.6% of organic carbon, part of which is derived from humic acid. The Bayer process is the main industrial process for producing alumina (aluminium oxide) from bauxite ore. Bauxite is digested under pressure with hot sodium hydroxide solution to give a sodium aluminate solution. This is clarified and aluminium trihydroxide is precipitated by cooling and seeding. Aluminium trihydroxide is then calcined to produce alumina.

Organic matter, including humic acid, enters the process with the bauxite. With recycling of the liquor, the concentration of organics and their degradation products increases until an equilibrium concentration is reached. The presence of a significant amount of organic matter in Bayer liquor causes numerous process problems that include a lower alumina yield, generation of excessive fine aluminium trihydroxide particles, decreased alumina purity and colored liquor.

Attempts have been made to characterize and quantify the organics present in Bayer liquor[1,2]. Many components such as formic acid, acetic acid, propanetricarboxylic acid and benzenetetracarboxylic acid have been successfully measured by gas chromatographic–mass spectral analysis. The analysis of humic acid has been far less successful. Yet, a knowledge of humic acid concentration is important for monitoring and planning process control.

Recently a quantitative high-performance liquid chromatography (HPLC) assay for humic acid in environmental samples, including soils, was developed[3]. We decided to investigate its applicability to the analysis of humic acid in Bayer liquor. In this report we describe a new HPLC procedure with fluorometric detection. The method is simple and rapid, results for a single sample can be obtained within 10 min. Selectivity of this method is superior to that obtained by visible absorption measurement, an in-house method sometimes used.

[a] Contribution No. 492 from the Australian Institute of Marine Science.

0021-9673/90/$03.50

EXPERIMENTAL

The HPLC system consisted of a Waters Assoc. (Milford, MA, U.S.A.) M6000 pump and U6K injector, a Schoeffel (Westwood, NJ, U.S.A.) FS970 fluorometer and a Hewlett-Packard (Palo Alto, CA, U.S.A.) 3392A computing integrator. A Hitachi (Tokyo, Japan) F-4000 fluorescence spectrophotometer was used to scan HPLC-purified humic acids by using the flow cell attachment. Wherever possible, PTFE capillary tubing obtained from SGE (Ringwood, Australia) was used for the chromatographic lines. An SGE ODS 5-μm, glass-lined (250 × 4 mm I.D.) analytical column (plus guard column) was used for the chromatographic separation.

The mobile phase was prepared by mixing analytical-reagent grade ammonia purchased from Ajax Chemicals (Auburn, Australia) with Super-Q water prepared with a Millipore (Bedford, MA, U.S.A.) purification system. The ammonia concentration was 0.003% (w/v). The mobile phase flow-rate was 1 ml/min.

Technical-grade humic acid (sodium salt) was purchased from Aldrich (Gillingham, U.K.) and purified by dissolving in ammonia solution (pH 8), decanting and precipitating with Aristar-grade concentrated hydrochloric acid purchased from BDH (Poole, U.K.). The precipitate was filtered, air-dried at 22°C for 24 h and heat-dried at 80°C for 16 h. The procedure was repeated twice.

HPLC-purified humic acid that remained in the flow cell after diversion of the mobile phase was scanned for fluorescence excitation (240–380 nm; emission 440 nm) and emission (400–600 nm; excitation 340 nm). Since the retention times of the Aldrich and Bayer liquor humic acids and their fluorescence excitation and emission spectra were almost identical, purified Aldrich humic acid was considered to be a suitable standard.

Analytical-reagent grade sodium chloride purchased from Ajax Chemicals was heated at 550°C for 16 h to remove humic acid impurities. Bayer liquor samples were diluted 2000-fold in 0.5 *M* sodium chloride solution. An aliquot of 50 μl was injected into the HPLC system.

Humic acid fluorescence was detected at >418 nm with an excitation wavelength of 340 nm. Visible absorbance measurements were performed at 691 nm with a Pye-Unicam (Cambridge, U.K.) PU8600 absorbance spectrophotometer.

To quantify the humic acid concentration of Bayer liquor, a standard addition curve was constructed by spiking 500 μl of the diluted Bayer liquor with purified Aldrich humic acid (0.20–0.95 μg). Linear regression analysis confirmed the suitability of this technique ($r^2 = 0.998$).

RESULTS AND DISCUSSION

Prior to the development of an HPLC method, the fluorescence excitation and emission spectra and absorbance spectra of unchromatographed Bayer liquor and Aldrich humic acid were compared. Below about 500 nm the absorbance spectra were very different, obviously reflecting the mixture of organic components in Bayer liquor. Above this wavelength the spectra were similar (Fig. 1). Absorbance measurements of 19 Bayer liquor samples (measured at 691 nm) were compared with results obtained by HPLC. The correlation obtained by linear regression analysis was poor ($r^2 = 0.33$). This indicates that even at this wavelength visible absorbance is a poor analytical

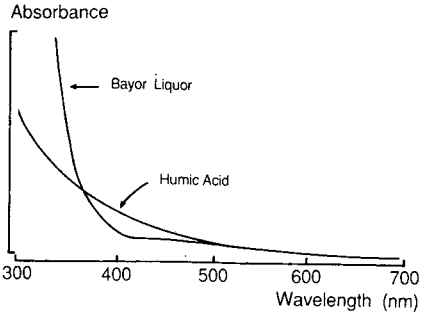

Fig. 1. Absorbance spectra of a purified Aldrich humic acid and a spent Bayer liquor.

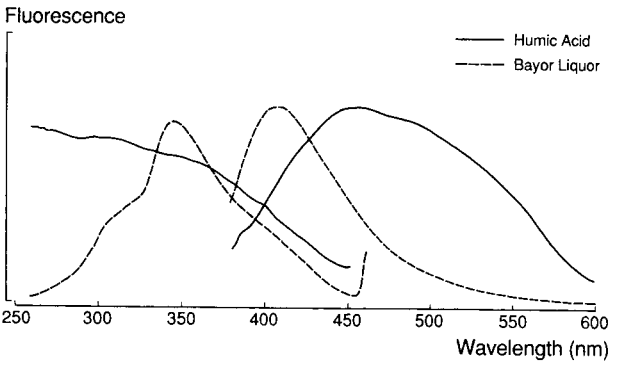

Fig. 2. Fluorescence spectra of a purified Aldrich humic acid and a spent Bayer liquor.

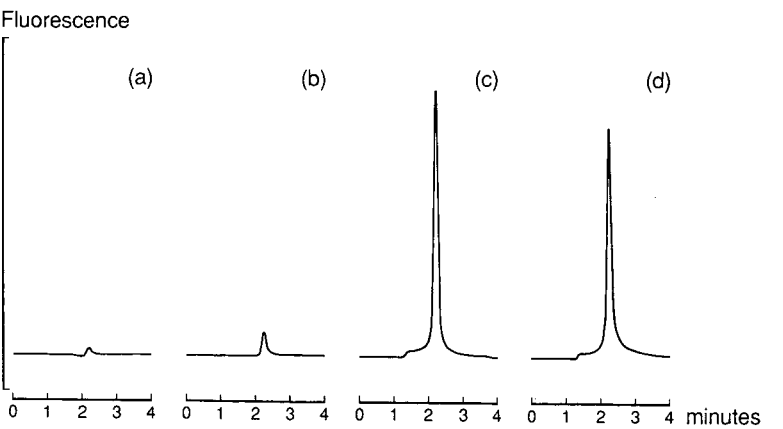

Fig. 3. Typical HPLC traces: (a) solvent blank; (b) Bayer liquor prior to extraction (0.23% humic acid); (c) Bayer liquor after extraction (3.51% humic acid); (d) standard humic acid (1.71 μg injected).

method due to the presence of a complex mixture of organics. Both the fluorescence excitation and emission spectra of the unchromatographed Bayer liquor were very different to the Aldrich humic acid (Fig. 2). Hence fluorescence measurements without chromatography were not further investigated as an analytical technique.

HPLC chromatograms were similar to those obtained in a previous study[3]. Typical chromatograms are shown in Fig. 3. The fluorescence ratio for excitation at 340 nm relative to 270 nm was 0.26 for both Aldrich humic acid and a plant liquor sample, indicating the absence of interfering components. We investigated the suitability of peak height measurement for quantification. Varying volumes of diluted Bayer liquor were injected. Linear regression analysis confirmed the suitability of peak height measurement for injection volumes between 10 μl and 75 μl ($r^2 = 0.998$). This enables a simple, low-cost HPLC system to be used for routine quality control monitoring. We chose an injection volume of 50 μl so that peak height measurement could be used without sacrificing accuracy. The relative standard deviation was 0.83% ($n = 10$). The limit of detection was 15 ng ($2 \times$ noise).

We found that humic acid comprised up to 5.27% (w/v) of a spent Bayer liquor. Such high levels underscore the desirability of having access to a rapid yet accurate analytical technique, given the many process problems encountered due to the presence of humic acid and its degradation products. This is the first report of a quantitative humic acid analysis of Bayer liquor by HPLC. The technique should prove to be a boon to process and production control in the alumina industry.

REFERENCES

1 G. Lever, *Light Met. N.Y.*, (1978) 71.
2 J. D. Guthrie, P. J. The and W. D. Imbrogno, *Light Met. N.Y.*, (1984) 127.
3 M. Susic and K. G. Boto, *J. Chromatogr.*, 482 (1989) 175.

Author Index

Request for manuscripts

Y. Ito, W.D. Conway, M. Knight and Y.-W. Lee will edit a special, thematic issue of the *Journal of Chromatography*, entitled **"Counter-current Chromatography"**. Both reviews and research articles will be included.

Topics such as the following will be covered:

- theoretical aspects
- instruments
- solvent systems
- applications
- any other topics relating to counter-current chromatography.

Potential authors of reviews should contact Yoichiro Ito, National Institutes of Health, Bldg. 10, Rm. 7N 322, Bethesda, MD 20892, U.S.A. (Tel. 301-496-3237 or -2557, Fax: 301-402-0013).

The deadline for receipt of submissions is **May 1, 1990**. Manuscripts submitted after this date can still be published in the Journal, but then there is no guarantee that an accepted article will appear in this special thematic issue. **Five** copies of the manuscript should be submitted to Y. Ito. All manuscripts will be reviewed and acceptance will be based on the usual criteria for publishing in the *Journal of Chromatography*.

Request for manuscripts

R. Majors, F. Regnier and K. Unger will edit a special, thematic issue of the *Journal of Chromatography* entitled **"LC Column Packings"**. Both reviews and research articles will be included.

Topics such as the following will be covered:

- organic packings
- inorganic packings
- non-porous particles
- macroporous particles
- restricted access media
- functionalized membranes
- solid-phase extraction materials
- commercially available packings
- physical-chemical characterization
- relative performance of packings
- packing procedures and hardware
- column care.

Only minor coverage of topics such as affinity chromatography and chiral separations is planned since these will be the topics of other thematic issues.

Potential authors of reviews should contact Roger Giese, Editor, prior to any submission. Address: 110 Mugar Building, Northeastern University, Boston, MA 02115, U.S.A.; tel.: (617) 437-3227; fax: (617) 437-2855.

The deadline for receipt of submissions is **June 1, 1990**. Manuscripts submitted after this date can still be published in the Journal, but then there is no guarantee that an accepted article will appear in this special, thematic issue. **Five** copies of the manuscript should be submitted to R. Giese. All manuscripts will be reviewed and acceptance will be based on the usual criteria for publishing in the *Journal of Chromatography*.

Vol. 502, No. 2

journal of chromatography news section

OBITUARY

PROFESSOR ARTHUR SINCLAIR RITCHIE (1911–1989)

Professor A.S. Ritchie died on September 27th 1989, after a long illness.

He was one of the group of outstanding geologists that Australia has brought forth over the last hundred years. He started his career as a teacher and when the great depression overtook Australia in the thirties he became interested in gold washing, which was the beginning of his interest in geology.

In 1938 he became a lecturer in geology and mineralogy at the Newcastle Technical College, his interests covering a broad field that ranged from the geology of the river estuary in Newcastle to evidence of previous glacier formation in the Mount Kosciusco area. He travelled widely and held visiting professional appointments in France, the U.S.A., Canada and Italy.

Professor Ritchie won international recognition for his work on the application of paper chromatography to the identification of minerals and to geochemical prospecting. He published a book on this topic in 1964, which was received with great interest by the scientific community and was translated into Russian in 1967. In connection with this work he also pioneered the use of chromatographic development on thin layers consisting of powdered rock in the study of ore deposition and concentration by the percolation of geothermal liquids.

Of note were his enduring love of mountains and bush walking, his enjoyment of music and his keen interest in his students. He founded the Hunter Valley Branch of the Geological Society of Australia, the Hunter Valley Amateur Geological Society and was a Foundation member of the Newcastle Technical College Bushwalking Club, as well as Foundation President of the Newcastle University Rugby Club, Ski Club and Swimming Club.

The present writer fondly remembers Arthur Ritchie as the leader of geological excursions, which became unforgetable due to his unusual energy and were an inspiration to his students and colleagues.

He is survived by his wife, Jean, who carried the burden of his care during his long illness, a daughter and two sons.

MICHAEL LEDERER

ANNOUNCEMENTS OF MEETINGS

11th INTERNATIONAL SYMPOSIUM ON CHROMATOGRAPHY, MONTEREY, CA, U.S.A., MAY 14–17, 1990

The 11th International Symposium on Chromatography will be held at the Conference Center in Monterey, CA, U.S.A., May 14–17, 1990.

The scientific program will feature the latest developments in:

— micro separation techniques: capillary gas chromatography (CGC); capillary GC–MS, capillary GC–FTIR and capillary GC–AES; micro-HPLC; supercritical fluid chromatography (SFC); capillary zone electrophoresis; sample preparation techniques; new columns and instrumentations; and
— new methods and applications: environmental analysis; organic chemicals; pharmaceutical analysis; drug testing; petroleum and petrochemicals; flavors and fragrances; food and beverages; proteins and peptides; biochemical separations; trace analysis.

The symposium will consist of: review papers by leading scientists in the field on the latest developments in column technology, sampling, applications, instrumentation, etc.; invited papers by young scientists; submitted papers presented in poster sessions in order to achieve intensive discussion. Plenary and parallel discussion sessions on special topics will serve to augment the formal presentation. In workshop type seminars scientists of the instrument manufacturers will present and discuss the latest developments in capillary instrumentation.

In conjuction with the Symposium there will be an exhibition of capillary chromatography instruments and accessories.

The registration fee (including the Symposium Proceedings and the Social Program) will be: prior to April 1, 1990: US$ 350; after April 1, 1990: US$ 395; students: 50% reduction of above fees.

For further details, contact: Dr. Pat Sandra, Laboratory of Organic Chemistry, University of Ghent, Krijgslaan 281 (S4), B-9000 Ghent, Belgium. Tel.: (91) 225715, ext. 2279; FAX (91) 228321.

9th INTERNATIONAL CONFERENCE ON FUNDAMENTAL ASPECTS, ANALYTICAL TECHNIQUES, PROCESSES AND APPLICATIONS OF PYROLYSIS, NOORDWIJKERHOUT, THE NETHERLANDS, JUNE 11–15, 1990

This biennual conference marks the multidisciplinarity of the analytical and applied pyrolysis field. It encompasses:
— energy distribution in macromolecular systems, reaction mechanisms and kinetics of pyrolysis reactions, computer modelling of the flash thermal dissociation of solids;
— molecular spectroscopic and mass spectrometric methods for analysis of explosive pyrolytic reactions in the 10^{-3} to 10^{-9} s time domain;
— advances in analytical techniques: on- and off-line pyrolysis (PY) in combination with GC, HPLC and SFC, microwave pyrolysis, hyphenated techniques such as PY–MS, PY–FTIR, PY–GC–(FTIR)–MS, PY–MS–MS, PY–SFC–MS, TG–FTIR, TG–MS;
— thermal reactions on surfaces: laser desorption, surface ablation, sputtering;
— fundamental studies on the pyrolysis and pyrolysis product composition of natural and synthetic polymers and their derivatives;
— bulk scale pyrolysis for biomass conversion, waste disposal: the evaluation of environmental effects (clean technology);
— applications in geochemistry, soil science, oceanography, agriculture, biological fingerprinting and medical science, food, tobacco, archaeology and forensic sciences.

Plenary sessions with oral presentations, invited review lectures and poster sessions will be scheduled. A number of posters will be selected by the attendees for short oral presentation. There will be two panel discussions.

A book of abstracts will be available to the registrants upon arrival. The proceedings of the conference will be published as a refereed volume in the *Journal of Analytical and Applied Pyrolysis*. Posters can be included as full papers or extended abstracts.

During the conference there will be space for exhibition of scientific equipment, journals and books.

For further details, contact: Louise Roos, Conference Coordinator Pyrolysis '90, FOM-Institute for Atomic and Molecular Physics, Kruislaan 407, 1098 SJ Amsterdam, The Netherlands.

8th INTERNATIONAL SYMPOSIUM ON MASS SPECTROMETRY IN LIFE SCIENCES, GHENT, BELGIUM, AUGUST 19–23, 1990

The above symposium is being sponsored by the Faculty of Pharmaceutical Sciences of the State University of Ghent, the National Foundation of Scientific Research (N.F.W.O.–F.N.R.S.) and the Ministry of National Education of Belgium. Contributed papers and posters will cover the following topics: fundamental aspects and applications of mass spectrometry in biological, environmental and health sciences; new developments in instrumentation and techniques of analysis; qualitative and quantitative applications in drug analysis, pharmacokinetics, clinical chemistry, biochemistry, toxicology, environmental and ecological research. All papers must be presented in English and no simultaneous translations will be provided. The deadline for receipt of abstracts is May 15, 1990.

Further information may be obtained from: Professor Dr. A. De Leenheer, Laboratoria voor Medische Biochemie en voor Klinische Analyse, Harelbekestraat 72, B-9000 Ghent, Belgium. Tel.: (091) 218951, ext. 324; Fax: (091) 217902.

2nd INTERNATIONAL SYMPOSIUM ON MICROCOLUMN SEPARATION METHODS, ARONSBORG, SWEDEN, AUGUST 20–22, 1990

The second International Symposium on Microcolumn Separation Methods will be arranged by the Analytical Division of the Swedish Chemical Society at Aronsborg Conference Hotel, 40 kilometers north of Stockholm, on August 20–22, 1990.

The increasing demand for analytical services in society, especially regarding the environmental, medical, biotechnological and pharmaceutical areas inspire research activities in separation sciences. The necessity to analyse more complicated matrices, to study even more potent pharmaceutical, herbicidal and related compounds puts increasingly higher demands on the analytical methodologies used. The strive for higher separation efficiencies, lower detection limits and more advanced analyses makes the ramification of miniaturized systems the currently most dynamically developing fields in the separation sciences.

The symposium will highlight developments in capillary electrophoresis, microcolumn liquid chromatography, supercritical fluid chromatography and capillary gas chromatography. New detection strategies, column technology, coupled column systems, sample introduction systems, novel solid phases and new demanding applications will have priority in the program.

Leading scientists are invited to give keynote lectures, and the scientific program will further comprise short lectures, poster and discussion sessions.

A one-day workshop preceding the symposium introduces newcomers in the field. Review lectures on the state of the art will be delivered by leading scientists in capillary electrophoresis, microcolumn LC and SFC. Demonstrations of the performance of current instrumentation as well as new application strategies will be an essential part of the program.

All correspondence concerning the symposium should be addressed to: Eva Mattsson, The Swedish Chemical Society, the Analytical Division, Wallingatan 26 B, S-111 24 Stockholm, Sweden.

10th INTERNATIONAL SYMPOSIUM ON HPLC OF PROTEINS, PEPTIDES AND POLYNUCLEOTIDES, WIESBADEN, F.R.G., OCTOBER 29–31, 1990

The 10th International Symposium on HPLC of Proteins, Peptides and Polynucleotides (ISPPD) will be held in the Kurhaus of Wiesbaden, F.R.G., October 29–31, 1990.

The need for an annual international meeting on the concepts and practice of modern and innovative techniques for the resolution of biopolymers at the analytical and preparative level led to the 1st ISPPP, held in Baltimore in 1981. Researchers from all disciplines of life science active in academia and industry have had ample opportunity to discuss new developments and applications in the area

of HPLC and other high resolution techniques for the analysis and purification of proteins, peptides and polynucleotides.

A special scientific and social program is being planned in order to highlight the tenth anniversary of ISPPP and a decade of achievements in research in HPLC of proteins, peptides and polynucleotides. Topics to be covered will foreshadow the trends for the next decades. The Organizing Committee welcomes your specific suggestions and comments.

You are invited to submit your latest research results for presentation at this meeting. Submission deadline is July 1st, 1990.

The registration fee covering all scientific and social programs, including a copy of the collected proceedings is DEM 720 (Students at DEM 360). A selected number of student scholarships will be available.

For further information, contact: Secretariat 10th ISPPP, P.O. Box 28, S-751 03 Uppsala, Sweden.

XXVII CSI, XXVII COLLOQUIUM SPECTROCOPICUM INTERNATIONALE, BERGEN, NORWAY, JUNE 9–14, 1991

The XXVII CSI organized by the Norwegian Chemical Society, will be held in the Grieg Hall, Bergen, Norway, June 9–14, 1991.

This traditional biennal conference in analytical spectroscopy will once again provide a forum for atomic nuclear and molecular spectroscopists worldwide to encourage personal contact and the exchange of experience. participants are invited to submit papers for presentation at the XXVII CSI, dealing with the following topics:

— Basic theory and instrumentation of atomic spectroscopy (emission, absorption, fluerescence), molecular spectroscopy (UV, VIS and IR), X-ray spectroscopy, gamma spectroscopy, mass spectrometry (inorganic and organic), electron spectroscopy, Raman spectroscopy, Mössbauer spectroscopy, nuclear magnetic resonance spectrometry, methods of surface analysis and depth profiling, photoacoustic spectroscopy.

— Application of spectroscopy in the analysis of: metals and alloys, geological materials, industrial products, biological samples, food and agricultural products. Special emphasis will be given to the topics trace analysis, environmental pollutants and standard reference materials.

The scientific program will comprise both plenary lectures and parallel sessions of oral presentations. Specific times will be reserved for poster sessions.

For further details contact: Secretariat XXVII CSI, HSD Congress-Conference, P.O. Box 1721 Nordnes, N-50224 Bergen, Norway. Tel: (475) 318414; Telex: 42607 hsd n; Fax: (475) 324555.

8th DANUBE SYMPOSIUM ON CHROMATOGRAPHY, WARSAW, POLAND, SEPTEMBER 2–6, 1991

The symposium will be organized by: the Institute of Physical Chemistry of the Polish Academy of Sciences, the Institute of Chemistry of the Military Technical Academy, the Department of Chemistry of Warsaw University and the Comission of Chromatography Analysis of the Scientific Committee of Analytical Chemistry of the Polish Academy of Sciences.

The scientific programme will comprise invited lectures, as well as submitted papers (oral and poster presentations, and discussion sessions dealing with all aspects of chromatography and related techniques. The proceedings of the symposium will be published in a special issue of the *Journal of Chromatography*.

In connection with the symposium an exhibition of chromatographic instruments, accessories and chromatographic literature is planned.

The conference language will be English; no translation facilities will be supplied.

For accompanying persons an attractive social programme will be arranged with tours and visits to places of interest.

Persons planning to attend the Symposium are requested to contact the organizers as soon as possible, preferably before August 1990. The second circular including more detailed information about the symposium will be distributed in November 1990.

For further details, contact: 8th Danube Symposium on Chromatography, Janusz Lipkowski, Institute of Physical Chemistry of the Polish Academy of Sciences, Kasprzaka 44/52 01-224 Warsaw, Poland.

SOFTWARE

THE REVISED AUTOSCAN PROGRAM FOR SPECTRA-PHYSICS DETECTORS, 8400 SERIES

In 1982, Spectra-Physics released the AUTOSCAN software program so that spectra, in the UV and visible regions, could be obtained automatically as sample components were eluted in liquid chromatography. A Spectra-Physics, 8400 series, detector and a 4200 (or 4400) series integrator were required. In 1985, they released the AUTOSCAN program on an EPROM chip with a slower scan rate in order to improve the signal-to-noise ratio.

With permission of Spectra-Physics, the original program has been rewritten to include the improvements found on the EPROM chip and, in addition, the following features: the length has been reduced from 7000 to 5250 bytes; the automatic peak detector is activated by the "go" time function and is tripped by peak maxima; the dialog has been extended; and the initial back-ground scan can be re-used with a series of samples.

The revised AUTOSCAN program is available, without charge, on a "floppy disk", with instructions, to those with the necessary instrumentation. If you have current need for this program, please contact: Bruce Flann, Pharmaceutical Chemistry Division, Bureau of Drug Research, H.P.B., Health and Welfare Canada, Ottawa, Ontario, Canada K1A 0L2.

Announcements are included free of charge. Information on planned events should be sent well in advance (preferably 6 months or more) to: Journal of Chromatography, News Section, P.O. Box 330, 1000 AH Amsterdam, The Netherlands, Fax: (31) 20-5862845.

CALENDAR OF FORTHCOMING EVENTS

April 3–5, 1990
Noordwijkerhout,
The Netherlands

ANATECH '90, 2nd International Symposium on Applications of Analytical Chemical Techniques to Industrial Process Control
Contact: Professor Dr. Willem E. van der Linden, Laboratory for Chemical Analysis-CT, University of Twente, P.O. Box 217, 7500 AE Enschede, The Netherlands. (Further details published in Vol. 477, No. 2.)

April 4–7, 1990
York, U.K.

2nd International Symposium on Pharmaceutical and Biomedical Analysis
Contact: Mrs. J.A. Challis, Executive Secretary, The Chromatographic Society, Trent Polytechnic, Burton Street, Nottingham NG1 4BU, U.K. Tel.: (602) 418418, ext. 2187; Fax: (602) 484266. (Further details published in Vol. 483.)

April 8–11, 1990
Ghent, Belgium

7th International Symposium on Preparative Chromatography
Contact: Professor M. Verzele, RUG-LOS, Krijgslaan 281 (S4), B-9000. Ghent, Belgium. Tel.: (091) 225715; fax: (091) 228321. (Further details published in Vol. 477, No. 2.)

April 17–20, 1990
Barcelona, Spain

2nd International Symposium on Applied Mass Spectrometry in the Health Sciences
Contact: Professor Emilio Gelpí, Palau de Congressos, Dept. de Convensions, Av. Reina Ma. Cristina s/n, 08004 Barcelona, Spain. (Further details published in Vol. 472, No. 2.)

April 17–20, 1990
Strasbourg, France

20th International Roland W. Frei Memorial Symposium on Environmental Analytical Chemistry
Contact: Mrs. Marianne Frei-Häusler, P.O. Box 46, CH-2123 Allschwil, Switzerland. Tel.: (41) 61-632789. (Further details published in Vol. 472, No. 2.)

April 19–21, 1990
Strasbourg, France

4th Workshop on the Chemistry and Analysis of Environmental Hydrocarbons
Contact: Mrs. Marianne Frei-Häusler, P.O. Box 46, CH-2123 Allschwil, Switzerland. Tel.: (41) 61-632789. (Further details published in Vol. 472, No. 2.)

April 24–26, 1990
Pécs, Hungary

4th Symposium on the Analysis of Steroids
Contact: Professor S. Görög, c/o Chemical Works of Gedeon Richter Ltd., P.O. Box 27, H-1475 Budapest, Hungary. Tel.: (361) 574566, telex: 22-5067 RICH H, fax: (361) 473973. (Further details published in Vol. 472, No. 2.)

April 24–28, 1990
Tallinn, U.S.S.R.

11th International Symposium on Biomedical Applications of Chromatography and Electrophoresis
Contact: Dr. Ljudmila Kolomiets, Scientific Council of Chromatography, Institute of Physical Chemistry, Leninskii Prospect 31, 117915 Moscow, U.S.S.R. (Further details published in Vol. 477, No. 2.)

May 8–11, 1990
München, F.R.G.

Biochemische Analytik 90, 12th International Conference on Biochemical Analysis
Contact: Ulrike Arnold, Anneli Höhnke, Nymphenburgerstrasse 70, D-8000 München, F.R.G. Tel.: (089) 1234500; fax: (089) 183258. (Further details published in Vol. 475.)

May 14–17, 1990
Monterey, CA,
U.S.A.

* **11th International Symposium on Capillary Chromatography**
Contact: Dr. Pat Sandra, Laboratory of Organic Chemistry, University of Ghent, Krijgslaan 281 (S4), B-9000 Ghent, Belgium. Tel.: 91-225 715, ext. 2279; Fax: 91-228 321.

May 20–25, 1990
Boston, MA, U.S.A.

HPLC '90, 14th International Symposium on Column Liquid Chromatography
Contact: Ms. Shirley E. Schlessinger, Symposium Manager HPLC '90, 400 East Randolph Drive, Chicago, IL 60601, U.S.A. Tel.: (312) 527 2011. (Further details published in Vol. 472, No. 2.)

May 21–23, 1990
Noordwijkerhout, The Netherlands

EuroResidue, Conference on Residues of Veterinary Drugs in Food
Contact: EuroResidue, c/o Department of Food of Animal Origin, Faculty of Veterinary Medicine, University of Utrecht, P.O. Box 80.175, 3508 TD Utrecht, The Netherlands. (Further details published in Vol. 483.)

May 22–25, 1990
Dijon, France

3rd European Meeting on Bio-Chromatography and Molecular Affinity
Contact: J.-P. Dandeu, Groupe Français de Bio-Chromatographie, Institut Pasteur, Unité d'Immuno-Allergie, 28 rue du Docteur Roux, 75724 Paris Cedex 15, France. Tel.: (1) 45688000. (Further details published in Vol. 477, No. 2 and Vol. 472, No. 2.)

June 6–8, 1990
Snowbird, UT, U.S.A.

3rd Symposium on Computer-Enhanced Analytical Spectroscopy
Contact: Peter C. Jurs, Department of Chemistry, Penn State University, University Park, PA 16802, U.S.A.

June 7–9, 1990
Cancun, Mexico

International Conference on Chirality
Contact: Mary Jo Richards, University of Missouri-Rolla, Chemistry Department, 341 Schrenk Hall, Rolla, MO 65401, U.S.A. Tel.: (314) 341-4429. (Further details published in Vol. 477, No. 2.)

June 11–15, 1990
Noordwijkerhout, The Netherlands

***9th International Conference on Fundamental Aspects, Analytical Techniques, Processes and Applications of Pyrolysis**
Contact: Louise Roos, Conference Coordinator Pyrolysis '90, FOM-Institute for Atomic and Molecular Physics, Kruislaan 407, 1098 SJ Amsterdam, The Netherlands.

June 12–15, 1990
Maastricht, The Netherlands

SCA, 2nd Scientific Computing and Automation (Europe) Conference
Contact: SCA (Europe), c/o Reunion International, WG Plein 475, 1054 SH Amsterdam, The Netherlands. (020) 165151; fax: (020) 890981. (Further details published in Vol. 475.)

June 25–30, 1990
Umeå, Sweden

***EUCHEMConference on Statistical Design of Chemical Experiments**
Contact: Rolf Carlson, Associate Professor, Department of Organic Chemistry, Umeå University, S-901 87 Umeå, Sweden. Tel: (4690) 165529; fax: (4690) 136310.

July 9–11, 1990 Wrexham, U.K.	**Ion-Ex 90, International Conference and Industrial Exhibition on Industrial, Analytical and Preparative Applications of Ion-Exchange Processes** Contact: Ion-Ex 90, Conference Secretariat, Faculty of Research and Innovation, The North East Wales Institute, Connah's Quay, Deeside, Clwyd CH5 4BR, U.K. Tel.: (0244) 817531, ext. 276 or 234, telex: 61629 NEWI G, fax: (0244) 822002. (Further details published in Vol. 464, No. 2.)
July 23–25, 1990 Brno, Czechoslovakia	**International Symposium on Polymer Analysis and Characterization** Contact: Dr. Howard G. Barth, ISPAC Chairman, DuPont Company, Experimentalo Station E228/238, P.O. Box 80228, Wilmington, DE 19880-0228, U.S.A. Tel.: (302) 695-4354. (Further details published in Vol. 483.)
Aug. 7–11, 1990 Changchun, China	**1st Changchun International Symposium on Analytical Chemistry** Contact: Professor Qinhan Jin, Department of Chemistry, Jilin University, Changchun, Jilin 130021, China. (Further details published in Vol. 477, No. 2.)
Aug. 14–17, 1990 Budapest, Hungary	**Budapest Chromatography Conference** Contact: Intercongress IPV, Dózsa Gy. út 84/a, Budapest, H-1068 Hungary. (Further details published in Vol. 477, No. 2.)
Aug. 19–22, 1990 Aronsborg, Sweden	* **2nd International Symposium on Microcolumn Separation Methods** Contact: The Swedish Chemical Society, The Analytical Division, Wallingatan 26B, S-111 24 Stockholm, Sweden. Tel.: 08-115260.
Aug. 19–23, 1990 Ghent, Belgium	* **8th International Symposium on Mass Spectrometry in Life Sciences** Contact: Professor Dr. A. De Leenheer, Laboratoria voor Medische Biochenie en voor Klinische Analyse, Harelbekestraat 72, B-9000 Ghent, Belgium. Tel.: (091) 218951, ext. 324; Fax: (091) 217902.
Aug. 20–22, 1990 Stockholm, Sweden	**2nd International Symposium on Microcolumn Separation Methods** Contact: The Swedish Chemical Society, The Analytical Division, Wallingatan 26B, S-111 24 Stockholm, Sweden. (Further details published in Vol. 477, No. 2.)
Aug. 26–31, 1990 Vienna, Austria	**Euroanalysis VII, 7th European Conference on Analytical Chemistry** Contact: Professor Dr. M. Grasserbauer, c/o Interconvention, Austria Center Vienna, A-1450 Vienna, Austria. Tel.: (43) 222-2369/647; telex: 111803 icos a, Fax: (43) 222-2369/648. (Further details published in Vol. 445, No. 1.)
Aug. 26–31, 1990 Prague, Czechoslovakia	**10th International Congress on Chemical Engineering, Chemical Equipment Design and Automation** Contact: Congress CHISA '90, P.O. Box 857, 111 21 Prague 1, Czechoslovakia. Telex: 121114 chp c.

Sept. 3–7, 1990 Balatonfüred, Hungary	**6th International Symposium on Ion Exchange** Contact: Professor J. Inczédy, Department of Analytical Chemistry, University of Veszprém, P.O. Box 158, H-8201 Veszprém, Hungary. Tel.: (3680) 22022; fax: (3680) 26016; telex: 32297. (Further details published in Vol. 477, No. 2.)
Sept. 4–7, 1990 Prague, Czechoslovakia	**Symposium on Bioanalytical Methods** Contact: Symposium on Bioanalytical Methods, House of Technology, Ing. Jirina Kostalova, Gorkeho nam 23, 111 28 Prague 1, Czechoslovakia. Tel.: (422) 236485; Telex: 121024 roh. (Further details published in Vol 483.)
Sept. 10–13, 1990 Cambridge, U.K.,	***6th International Symposium on Bioluminescence and Chemiluminescence** Contact: Professor L.J. Kricka, Department of Pathology and Laboratory Medicine, 3400 Spruce Street, 784 Founders Pavilion, Philadelphia, PA 19104-4283, U.S.A.
Sept. 11–14, 1990 Kobe, Japan	**12th International Symposium on Capillary Chromatography** Contact: Dr. K. Jinno, School of Materials Science, Toyohashi University of Technology, Toyohashi 440, Japan. (Further details published in Vol 483.)
Sept. 18–21, 1990 Verona, Italy	**1st International Symposium on Applications of HPLC in Enzyme Chemistry** Contact: Dr. F. Tagliaro, Istituto di Medicina Legale, Università di Verona, Policlinico di Borgo Roma, 37134 Verona, Italy. Tel.: +39 45 504073; Fax: +39 45 58212.
Sept. 23–28, 1990 Amsterdam, The Netherlands	**18th International Symposium on Chromatography** Contact: 18th International Symposium on Chromatography, RAI Organisatie Bureau Amsterdam bv, Europaplein 12, 1078 GZ Amsterdam, The Netherlands. Tel.: (31-20) 549 1212; telex: 13499 raico nl; Fax: (31-20) 464469. (Further details published in Vol. 464, No. 2 and Vol. 483.)
Oct. 2–4, 1990 High Tatras, Czechoslovakia	**7th International Symposium on Capillary Electrophoresis and Isotachophoresis** Contact: 7th International Symposium on CE and ITP, Dr. D. Kaniansky, Institute of Chemistry, Comenius University, Mlynská, Dolina CH-2, CS-84215 Bratislava, Czechoslovakia. Tel.: (70) 320003. (Further details published in Vol. 483.)
Oct. 19–23, 1990 Adelaide, Australia	**27th Meeting of the International Association of Forensic Toxicologists** Contact: V.J. McLinden, Chemistry Center (WA), 125 Hay Street, Perth, Western Australia 6000, Australia. (Further details published in Vol. 467, No. 2.)

Oct. 22–24, 1990 San Francisco, CA, U.S.A.	**ANABIOTEC '90, 3rd International Symposium on Analytical Methods in Biotechnology** Contact: Shirley Schlessinger, ANABIOTEC '90, 400 E. Randolph Drive, Chicago, IL 60601, U.S.A. (Further details published in Vol. 448, No. 3.)
Oct. 29–31, 1990 Wiesbaden, F.R.G.	* **10th International Symposium on HPLC of Proteins, Peptides and Polynucleotides** Contact: Secretariat 10th ISPPP, P.O. Box 28, S-751 03 Uppsala, Sweden.
Oct. 31–Nov. 2, 1990 Montreux, Switzerland	**7th Symposium on Liquid Chromatography–Mass Spectroscopy (LC–MS, MS–MS, SFC–MS)** Contact: M. Frei-Häusler, Strengigässli 20, CH-4123 Allschwil, Switzerland. (Further details published in Vol. 475.)
Feb. 10–15, 1991 Melbourne, Australia	**POLYMER '91, Polymer Materials: Preparation, Characterization and Properties** Contact: POLYMER '91 Secretary, P.O. Box 224, Belmont, Vic. 3216, Australia.
March 4–7, 1991 Les Diablerets, Switzerland	**4th Hans Wolfgang Nürnberg Memorial Workshop on Toxic Metal Compounds (Interrelation Between Chemistry and Biology)** Contact: Dr. Ernest Merian, Im Kirsgarten 22, CH-4106 Therwil, Switzerland.
March 11–13, 1991 Lausanne, Switzerland	**2nd Soil Residue Analysis Workshop** Contact: Professor J. Tarradellas, IGE-EPFL, 1015 Lausanne, Switzerland.
May 27–31, 1991 Rome, Italy	**2nd International Symposium on Chiral Discrimination** Contact: Professor D. Misiti or Professor F. Gasparrini, Laboratori di Chimica Organica, Facoltà di Farmicia, Università "La Sapienza", Piazzale Aldo Moro 5, 00185 Rome, Italy. Tel.: (06) 4452900; fax: (06) 49912780. (Further details published in Vol. 477, No. 2.)
May, 27–31, 1991 Ghent, Belgium	* **IVth International Symposium on Quantitative Luminescence Spectrometry in Biomedical Sciences** Contact: Dr. Willy R.G. Baeyens, Symposium chairman, State University of Ghent, Pharmaceutical Institute, Harelbekestraat 72, B-9000 Ghent, Belgium. (Further details published in Vol. 483.)
June 3–7, 1991 Basel, Switzerland	**HPLC '91, 15th International Symposium on Column Liquid Chromatography** Contact: Secretariat HPLC '91, Convention Center Basel, Congress Department, P.O. Box, CH-4021 Basel, Switzerland. (Further details published in Vol. 477, No. 2.)

June 9–14, 1991
Bergen, Norway

***XXVII Colloquium Spectroscopicum Internationale**
Contact: Secretariat XXVII CSI, HSD Congress-Conference, P.O. Box 1721 Nordnes, N-5024 Bergen, Norway. Tel.: (475) 318414; Telex: 42607 hsd n, Fax: (475) 324555.

Aug. 21–24, 1991
Kumamoto, Japan

5th International Conference on Flow Analysis
Contact: Professor Ishibashi, Department of Applied Analytical Chemistry, Faculty of Engineering 36, Kyushu University, Hokazaki, Higashiku, Fukuoka 812, Japan. (Further details published in Vol. 475.)

Aug. 25–31, 1991
Makuhari, Japan

ICAS '91, IUPAC International Congress on Analytical Sciences
Contact: ICAS '91 Secretariat, The Japan Society for Analytical Chemistry, 1-26-2 Nishigotande, Shinagawa, Tokyo 141, Japan. Tel.: (813) 490-3351; fax: (813) 490-3572. (Further details published in Vol. 483.)

Sept. 1–6, 1991
Lubeck-Travemunde, F.R.G.

8th International Conference on Fourier Transform Spectroscopy
Contact: Gesellschaft Deutscher Chemiker, Abt. Tagungen, P.O. Box 900440, D-6000 Frankfurt 90, F.R.G. Tel.: 17-366/360; Fax: (79) 17475; Telex: 4170497 gdch d.

Sept. 2–6, 1991
Warsaw, Poland

***8th Danube Symposium on Chromatography**
Contact: 8th Danube Symposium on Chromatography, Janusz Lipkowski, Institute of Physical Chemistry of the Polish Academy of Sciences, Kasprzaka 44/52, 01-224 Warsaw, Poland.

Sept. 4–6, 1991
Bilthoven, The Netherlands

3rd Workshop on Chemistry and Fate of Modern Pesticides
Contact: Pesticides Workshop Office Dr. P. van Zoonen, RIVM, P.O. Box 1, 3720 Bilthoven, The Netherlands. (Further details published in Vol. 472, No. 2.)

Sept. 24–28, 1991
Yokohama, Japan

***9th International Symposium on Affinity Chromatography and Biological Recognition**
Contact: Professor Ken-ichi Kasai, Faculty of Pharmaceutical Sciences, Teikyo University, Sagamiko, Tsukui, Kanagawa 199-01, Japan.

*Indicates new or amended entry

PUBLICATION SCHEDULE FOR 1990

Journal of Chromatography and Journal of Chromatography, Biomedical Applications

MONTH	J	F	M	A	M	
Journal of Chromatography	498/1 498/2 499	500 502/1	502/2 503/1 503/2 504/1	504/2 505/1	505/2 506 507	The publication schedule for further issues will be published later
Cumulative Indexes, Vols. 451–500		501				
Bibliography Section		524/1		524/2		
Biomedical Applications	525/1	525/2	526/1	526/2 527/1	527/2	

INFORMATION FOR AUTHORS

(Detailed *Instructions to Authors* were published in Vol. 478, pp. 453–456. A free reprint can be obtained by application to the publisher, Elsevier Science Publishers B.V., P.O. Box 330, 1000 AH Amsterdam, The Netherlands.)

Types of Contributions. The following types of papers are published in the *Journal of Chromatography* and the section on *Biomedical Applications:* Regular research papers (Full-length papers), Notes, Review articles and Letters to the Editor. Notes are usually descriptions of short investigations and reflect the same quality of research as Full-length papers, but should preferably not exceed six printed pages. Letters to the Editor can comment on (parts of) previously published articles, or they can report minor technical improvements of previously published procedures; they should preferably not exceed two printed pages. For review articles, see inside front cover under Submission of Papers.

Submission. Every paper must be accompanied by a letter from the senior author, stating that he is submitting the paper for publication in the *Journal of Chromatography*. Please do not send a letter signed by the director of the institute or the professor unless he is one of the authors.

Manuscripts. Manuscripts should be typed in double spacing on consecutively numbered pages of uniform size. The manuscript should be preceded by a sheet of manuscript paper carrying the title of the paper and the name and full postal address of the person to whom the proofs are to be sent. Authors of papers in French or German are requested to supply an English translation of the title of the paper. As a rule, papers should be divided into sections, headed by a caption (*e.g.*, Summary, Introduction, Experimental, Results, Discussion, etc.). All illustrations, photographs, tables, etc., should be on separate sheets.

Introduction. Every paper must have a concise introduction mentioning what has been done before on the topic described, and stating clearly what is new in the paper now submitted.

Summary. Full-length papers and Review articles should have a summary of 50–100 words which clearly and briefly indicates what is new, different and significant. In the case of French or German articles an additional summary in English, headed by an English translation of the title, should also be provided. (Notes and Letters to the Editor are published without a summary.)

Illustrations. The figures should be submitted in a form suitable for reproduction, drawn in Indian ink on drawing or tracing paper. Each illustration should have a legend, all the *legends* being typed (with double spacing) together on a *separate sheet*. If structures are given in the text, the original drawings should be supplied. Coloured illustrations are reproduced at the author's expense, the cost being determined by the number of pages and by the number of colours needed. The written permission of the author and publisher must be obtained for the use of any figure already published. Its source must be indicated in the legend.

References. References should be numbered in the order in which they are cited in the text, and listed in numerical sequence on a separate sheet at the end of the article. Please check a recent issue for the layout of the reference list. Abbreviations for the titles of journals should follow the system used by *Chemical Abstracts*. Articles not yet published should be given as "in press" (journal should be specified), "submitted for publication" (journal should be specified), "in preparation" or "personal communication".

Dispatch. Before sending the manuscript to the Editor please check that the envelope contains three copies of the paper complete with references, legends and figures. One of the sets of figures must be the originals suitable for direct reproduction. Please also ensure that permission to publish has been obtained from your institute.

Proofs. One set of proofs will be sent to the author to be carefully checked for printer's errors. Corrections must be restricted to instances in which the proof is at variance with the manuscript. "Extra corrections" will be inserted at the author's expense.

Reprints. Fifty reprints of Full-length papers, Notes and Letters to the Editor will be supplied free of charge. Additional reprints can be ordered by the authors. An order form containing price quotations will be sent to the authors together with the proofs of their article.

Advertisements. Advertisement rates are available from the publisher on request. The Editors of the journal accept no responsibility for the contents of the advertisements.

For Superior Chiral Separation

CHIRALCEL, CHIRALPAK and CROWNPAK are now available from DAICEL and include 15types of HPLC columns which provide superior resolution of racemic compounds.

Drugs directly resolved on our DAICEL columns are given as follows;

SUBSTANCE	α	column
Alprenolol	3.87	OD
Amphetamine	1.2	CR
Atenoloi	1.58	OD
Atropine	1.62	OD
Baclofen	1.39	CR
Carbinoxamine	1.39	OD
Carteolol	1.86	OD
Chlophedianol	2.82	OJ
Chlormezanone	1.47	OJ
Cyclopentolate	2.47	OJ
Diltiazem	1.46	OD
	2.36	OF
	1.75	OG
Disopyramide	2.46	OF
Ethiazide	1.54	OF
Ethotoin	1.40	OJ
Fenoprofen	1.35	OJ
Glutethimide	2.48	OJ

SUBSTANCE	α	column
Gauifenesin	2.40	OD
Hexobarbital	1.7	CA-1
Homatropine	3.13	OD
Hydroxyzine	1.17	OD
Indapamide	1.58	OJ
Ketamine	complete resolution	CA-1
Ketoprofen	1.46	OJ
Mephobarbital	5.9	OJ
	2.3	CA-1
Methaqualone	2.8	CA-1
	7.3	OJ
Methsuximide	2.68	OJ
Metoprolol	complete resolution	OD
Mianserin	1.75	OJ
Nilvadipine	complete resolution	OT

SUBSTANCE	α	column
Oxapadol	complete resolution	CA-1
Oxazepan	4.36	OC
Oxazolam	1.67	OF
Oxprenolol	6.03	OD
Perisoxal	1.33	OF
	1.27	OD
Pindolol	5.07	OD
Piprozolin	1.7	CA-1
Praziquantal	complete resolution	CA-1
Propranolol	2.29	OD
Rolipram	complete resolution	CA-1
Sulconazole	1.68	OJ
Suprofen	1.6	OJ
Trimebutine	1.81	OJ
Warfarin	1.96	OC

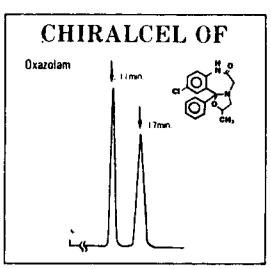

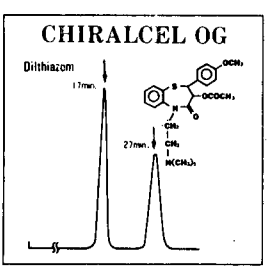

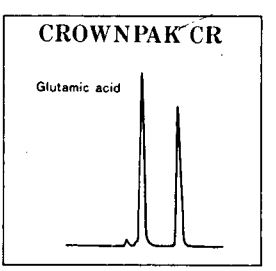

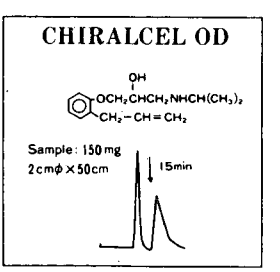

In addition to the drugs listed above, our chiral columns permit resolution also of the following: FMOC amino acids and Carboxylic acids, and Pesticides, for example Isofenfos, EPN and Acephate, and Synthetic intermediate 4-hydroxy cyclophentenone etc, Many other compounds besides these can be readily resolved.

▷ *Separation Service*

- A pure enantiomer separation in the amount of 100g~10kg is now available.
- Please contact us for additional information regarding the manner of use and application of our chiral columns and how to procure our separation service.

For more information about our Chiral Separation Service and Columns, please contact us!

DAICEL CHEMICAL INDUSTRIES, LTD.
8-1, Kasumigaseki 3-chome, Chiyoda-ku, Tokyo 100, Japan Phone: 03(507)3151 FAX: 03(507)3193

DAICEL (U.S.A.), INC.
Fort Lee Executive Park
Two Executive Drive, Fort Lee,
New Jersey 07024
Phone: (201)461-4466
FAX: (201)461-2776

DAICEL (U.S.A.), INC.
23456 Hawthorne Blvd.
Bldg. 5, Suite 130
Torrance, California. 90505.
Phone: 213-791-2030
FAX: 213-791-2031

DAICEL (EUROPA) GmbH
Oststrasse 22
4000 Düsseldorf 1, F.R.Germany
Phone: (0211) 369848
Telex: (41) 8588042 DCEL D
FAX: (0211) 364429

DAICEL CHEMICAL (ASIA) PTE.LTD.
65 Chulia Street #40-07
OCBC Centre, Singapore 0104.
Phone: 5332511
FAX: 5326454